# ROLE OF THE PROTEIN QUALITY CONTROL SYSTEM IN MOTOR NEURON DISEASES: THE CASE OF MUSCLE CELLS


MARIA ELENA CICARDI

**PhD THESIS**

Matr: R10889

Program: Integrated Biomedical Research

Year: 2016/2017

Internal relator: Chiar.mo Prof. Angelo Poletti

Coordinator: Chiar.ma Prof. Chiarella Sforza

“Sempre vi è stato detto che il lavoro è una maledizione

e la fatica è una sventura.

Ma io vi dico che quando voi lavorate portate a compimento una parte del sogno remoto della terra,

assegnato a voi quando quel sogno fu generato,

e nel mantenere voi stessi con fatica, voi in verità state amando la vita,

e amare la vita attraverso la fatica significa essere in intimità con il segreto più intimo della vita.”

Khalil Gibran “Il Profeta”

Ad Angelo, Paola, Vale

Richi, Vero, Giulia, Barbara

E alla mia famiglia

## Summary

# INTRODUCTION

## PROTEIN QUALITY CONTROL SYSTEM IN NEURODEGENERATION

### Neurodegenerative diseases: a clinical overview

Neurodegenerative diseases (NDs) are the third cause of mortality among the world population according to the World Health Organization after cardiovascular diseases and cancer (Rowinska-Zyrek et al. 2015). Approximately 30 million individuals are affected by a ND (Sheikh et al. 2013). NDs are a heterogeneous group of diseases that affect the central nervous system (CNS), and each disease is characterized by the progressive loss of a different subset of neurons. Among these diseases the most represented are Parkinson disease (PD), Alzheimer diseases (AD), Huntington's diseases (HD), amyotrophic lateral sclerosis (ALS); another NDs characterized by a lower incidence is spinal and bulbar muscular atrophy (SBMA). All NDs differ from each other by the central nervous region affected, and consequently by clinical outcomes and signs.

PD was initially described as "shaking palsy" by a physician named Parkinson. Nevertheless, reports on this disease appeared already in before Christ population, as documented by some Chinese medical texts (Rowinska-Zyrek et al. 2015). Nowadays, PD is affecting the 1% of the over sixties world population (Elbaz et al. 2016). Clinical symptoms of PD are bradykinesia, shuffling gait, micrographia, memory lapses, a 'masked', expressionless face, trembling in the hands and forearms, loss of spontaneous movement, difficulty swallowing, and impaired coordination. A considerable fraction of PD patients also develop depression and dementia (Jankovic 2008). The most affected part of the brain is substantia nigra and the dopaminergic neurons present in this part of the brain (Davie 2008). The histopathological hallmark is the presence of Lewy bodies (LBs) inside neurons. The major component of these LBs is α-synuclein protein whose function has not yet been elucidate (Spillantini et al. 1998).

AD is a debilitating disease first described by Alois Alzheimer, a German psychiatric in 1906 (Berchtold & Cotman 1998). Nowadays, AD is affecting about 26 million people worldwide. Usually, AD is diagnosed in people that are in their sixties, but in literature are also described juvenile case of AD (Brookmeyer et al. 2007). The first clinical sign of AD is forgetfulness. Eventually, signs become more severe leading to confusion, personality changes, anxiousness, irritability, memory loss, and intellectual disturbances (Oddo et al. 2003). The most affected neural population are cholinergic neurons. Histologically, this disease is characterized by deposition of β amyloid deposition around neurons (amyloid plaques) (Oddo et al. 2003). Usually, in these patients death come after 8-12 years post diagnosis (Brookmeyer et al. 2007).

HD had been always classified as chorea since George Huntington in the 19$^{th}$ (Yerbury et al. 2016; Novak & Tabrizi 2010) century firstly vividly described the hereditary character of this pathology. HD affects people at every age, but most frequently the age of onset is in middle age (Walker 2007; Novak & Tabrizi 2010). The spreading of this pathology leads to change of personality, impairment in cognition and of motor control. The most affected regions are striatal nuclei, basal ganglia and cerebral cortex (Novak & Tabrizi 2010). HD is caused by a CAG repeat expansion in the huntingtin (htt) gene (Novak & Tabrizi 2010).

SBMA and ALS are neurodegenerative diseases in which motor neurons are mainly affected. Motor neurons (MNs) degeneration lead to paralysis, and death come for respiratory failure. ALS appears as sporadic or familial, but in both cases there are proteinaceous accumulations in affected motor neurons (Neumann et al. 2006; Rosen et al. 1993; Vance et al. 2009)

SBMA in caused by a mutation (CAG repeat expansion) present in the androgen receptor (AR) gene that is translated into a polyglutamine tract in the AR protein (ARpolyQ) (Katsuno et al. 2006).

ALS and SBMA will be discussed more in detail in the sections below as the main diseases studied in this thesis.

Even if NDs do not share common clinical signs, morphological and pathological features, and aetiology, many studies have evidenced some common toxic events that lead to pathogenic manifestations of all NDs. One of the most

important factors of neurotoxicity is the presence of misfolded and aggregating proteins. Other factors involved in the pathogenesis are mitochondrial dysfunction, free radical formation, ER stress; RNA metabolism abnormalities etc... (Sheikh et al. 2013).

Another common feature of NDs is the absence of a cure that may slow down, stop or even revert the disease progression (Rowinska-Zyrek et al. 2015). This lack of therapeutic strategy is, mostly, due to the fact that the molecular mechanisms are still largely unknown, but also because the region affected are very difficult to target due to the brain blood barrier.

### Protein misfolding diseases

Correct protein activity is essential for cell life, and protein functions are strictly correlated to protein folding. Protein folding is a process that enables proteins to reach the secondary structure from the polypeptides chain, and the tertiary structure from the secondary structure. There are millions of possible structures in which a protein can be folded, but there is only one (or few more) structure in which the protein is biochemically and functionally active (Dobson 2003; Dobson et al. 1998). Since folding process of proteins is vital for cells, several systems assist polypeptides maturation when they are produced from polyribosomes (these systems will be discussed below) (Dobson 2003). There is large fraction of polypeptides that do not reach the native fold but they are promptly degraded and removed from the cell environment.

Misfolded proteins are proteins that have a different conformation from the native and correct one and can be present in cytoplasm, nucleus, ER and many other cellular compartments (Ciechanover & Kwon 2015).

Several reasons have been postulated for the generation of excessive amounts of misfolded proteins in cells: i) somatic mutation leading to a different primary structure, ii) errors in the transcription or translation processes, iii) failure of the folding systems, iv) mistakes of the post-translational modifications and in proteins trafficking, v) environmental changes and vi) mechanisms of seeding or cross seeding that lead to the loss of conformation, (Prusiner 1998; Soto 2001; Mastrianni & Roos 2000; Duyckaerts et al. 2007). Misfolded proteins are a serious treat for cell function and viability (Taylor et al. 2002).

When a protein looses the correct conformation, some hydrophobic sites that normally are buried inside the protein are exposed to cell hydrophilic environment (Ines Moreno-Gonzalez & soto 2012). β-sheets structures are highly hydrophobic structures and, when exposed, they try to self-dimerized with other hydrophobic structures. This process may starts to recruit a large number of polypeptides and it is called aggregation; depending on their size and structural conformation, the products of this aggregation are called oligomers, proto-fibrils and fibrils (Soto 2003; Soto & Estrada 2008). Initially, protein misfolding and nucleation are processes thermodynamically unfavourable and they start slowly. The rate of progression increases when few oligomers are formed acting as seeding nuclei. This process is mediated by prion like ability of misfolded proteins that drives other proteins to assume a pathogenic conformation and aggregate (Sweeney et al. 2017).

The elongation phase, in which aggregates are formed, is much more rapid than the initial lag-phase and the growing of aggregates is faster. In addition, this process is accelerated by high protein concentration. The resulting membrane-less structures can be more or less well organized, but are more thermodynamically stable than misfolded proteins, due to the high number of hydrophobic contacts between misfolded monomers (Soto et al. 2006; Link et al. 2008). Moreover, these aggregates can propagate from the affected cells to neighbours ones (Sweeney et al. 2017). It has been shown that covalent binding induces the formation of aggregates. Oxidative modifications as well as phosphorylation and SUMOylation are known to increase the rate of aggregation of misfolded proteins (Conway 2001).

Oligomers and misfolded species are the basis for the development of more structured and bigger formations but they are also the most toxic forms (Caughey & Lansbury 2003; Glabe 2006).

The exact mechanism by which different misfolded proteins exert toxicity and cause different neurodegenerative disease is still unclear (Sweeney et al. 2017). A minor part of the toxicity is linked to the previous function of the protein (that is generally lost when protein is misfolded), but protein toxicity is mainly exerted by a gain-of-function of the misfolded protein or by a dominant-negative effect of these species on the functional protein (Sweeney et al. 2017). The presence of misfolded proteins also causes other signs of stress that are believed to be both cause and consequence of NDs. Indeed, cellular distress and protein misfolding and aggregation are bidirectional and mutually exacerbating (Sweeney et al. 2017).

Aggregates contribution to the disease is still very controversial. Many studies have shown that compromising aggregates formation leads to enhanced cell toxicity, suggesting a possible protective role of aggregates against oligomeric species (Sweeney et al. 2017). On the contrary, there are evidence that the prolonged presence of these aggregates in cells causes several deleterious events, such as sequestration of others proteins, disruption of synaptic functions and impairment of degradative systems (Olzscha et al. 2011).

The connection between NDs and protein misfolding raises from the presence of familial forms of these diseases. It has been noticed that misfolded proteins found in the aggregates, are causative of the disease in the familial cases. The fact that encoded mutated proteins misfold draws a strong link between NDs and protein misfolding. The importance of protein misfolding on NDs leads to name them "proteinopathies" (Ines Moreno-Gonzalez & soto 2012). Moreover, neurons and all CNS cells are particularly vulnerable to the presence of these toxic species. In fact, neurons are post-mitotic cells and thus they can not dilute these species by self-division (Sooyeon, Lee; Sato & Ralph 2013).

## The protein quality control system: chaperones

### *The chaperone network*

Molecular chaperones are an essential part of the protein quality control (PQC) system whose role is to monitor protein homeostasis (Ciechanover & Kwon 2017). When mutated, damaged proteins are present in the cell they may activate the PQC system. The first line of response of the PQC system is the chaperone network. Molecular chaperones constitute approximately the 10% of all the proteome (Kampinga & Craig 2010). They have important physiological functions also during stress and in presence of toxic proteins. Many chaperones are called heat shock proteins (HSPs) because they are induced by heat, but they are also upregulated during various stress stimuli including presence of misfolded proteins, oxidative damage, presence of toxic chemicals and inflammation (Garrido et al. 2001). The HSPs family is a large family of proteins in which HSPs are classified on the basis of size, functions, localization and substrates specificity (Ciechanover & Kwon 2017).

The main functions of HSPs are assisting the folding and the assembly of newly synthetized proteins and preventing/dissolving aggregates by refolding damaged proteins. HSPs act in the refolding by mean of three main mechanisms: first, they can hold protein until the folded state is spontaneously reached (Rüdiger et al. 1997; Hartl et al. 2011); second, they can use ATP to unfold stable misfolded proteins and then refold them in their correct folding; third, using ATP hydrolysis they can act as "disaggregase" by forcing substrates in an unfold state (Itoh et al. 2002). Subsequently, unfolded proteins will be refolded in the mature folding. HSPs activity can be ATP dependent or ATP independent (Mosser et al. 2004; Arimon et al. 2008). Usually when HSPs need ATP hydrolysis to work they are assisted by other proteins that are named co-chaperones (Ciechanover & Kwon 2017). On the other side, ATP-independent chaperones, especially in neurons, directly bind the client recruiting them in a complex with other chaperones (D'Andrea & Regan 2003)

HSPs can also work with proteolytic machineries that degrade proteins unable to fold. Historically, HSPs have been classified in three classes based on structures similarities (class I, class II, and class III) but this classification does not

correlate with biochemical function and mechanisms. A more recent classification has been published by Dr. Kampinga, that clarify HSPs name and function. This nomenclature system is based on gene named assigned by HUGO Gene Nomenclature Committee and has been recognized by NCBI. In this classification proteins preceded by *sc* refer to yeast and if preceded by *hs* refer to human (Figure 1) (Kampinga & Bergink 2016; Kampinga et al. 2009).

### HSP90

HSP90 family members are proteins constitutively expressed, which localized in almost all cellular compartments: nucleus, cytoplasm, mitochondria, and endoplasmic reticulum (Lindquist 2009).

There is also an inducible HSP90, called HSP90α, that differently from constitutively expressed HSP90β is induced upon certain conditions (Lackie et al. 2017). There have been identified more than 2000 HSP90's interactors belonging to very different protein families such as steroid receptors, transcription factors and kinases (Lackie et al. 2017).

HSP90s are involved in a wide range of cellular functions such as telomerase maintenance, cell cycle progression, apoptosis, vesicles transport, innate immunity, protein target degradation. Moreover, HSP90, interacting with a wide range of co-factors, brings a large number of proteins to the correct conformation (Lackie et al. 2017). HSP90 activity is strictly related to its homo-dimerization that allows the formation of three regions with different roles: a nucleotide binding region (NBD), a middle region (MD) responsible for client binding, and a C-terminal region, that is the surface for HSP90 dimerization (Prodromou et al. 1997; Taipale et al. 2010).

The exact mechanism by which HSP90s recruit the clients is still enigmatic, but the folding cycle relies on ATP hydrolysis. HSP90 dimers have a V-shaped conformation due to the C-terminal dimerization (Figure 2). When a client is bound to the MD, ATP catalyses N-terminal HSP90 dimerization and this complex is the functional dimer (Ciechanover & Kwon 2017; Prodromou et al. 1997; Pearl & Prodromou 2006). This complex is very dynamic and each monomer twists around the others to correctly dimerize. Finally, when ATP is hydrolysed, N-terminal dimerization is lost and the client is released (Pearl & Prodromou 2006).

Each phase of HSP90 cycle is assisted and ruled by various co-chaperones and by post-translational modification of HSP90 like acetylation, nitrosylation, phosphorylation and methylation (Zuehlke & Johnson 2011; Buchner & Li 2013). There are some co-factors that stabilize the dimer such as p23 (Picard 2002; Whitesell & Lindquist 2005), others like HOP that inhibits HSP90 dimerization, by a non-competitive bound to the NBD on HSP90 (Prodromou et al. 1999). There are also co-factors that act on the ATPase activity (CDC37) (Taipale et al. 2010) or on ATP hydrolysis (AHA1) (Zuehlke & Johnson 2011)

### HSP70

The subfamily of the HSP70 comprises several types of heat shock proteins of 70 kDa (now also renamed HSPA). There are several HSP70 isoforms localized in nucleus, cytoplasm and organelles such as mitochondria (Kampinga & Bergink 2016). HSC70 localize in the cytosol, while the Bip/GRP78 localize in the ER. HSP70 is composed of two main subunits: the nucleotide binding domain (NBD) of 40 kDa and the substrates binding domain (SBD) of 25 kDa, that recognized hydrophobic structure exposed by proteins (Bukau et al. 2006).

HSP70 family carries out several functions: they assist native proteins in the correct folding, they drives proteins across the membrane and they also rule protein-protein interaction by modulating the conformational changes of proteins (Kampinga & Craig 2010). Almost every HSP70 activity is orchestrated by various members of the HSP40 family (Kampinga & Craig 2010) and their interaction is mediated by the J domain in HSP70 structure. J domain is a non-homologous region that is the first determinant of HSP70 activity (Kampinga & Bergink 2016).

The HSP70s act in the folding of new polypeptides and of misfolded proteins and it can also disaggregate already formed inclusions and drives misfolded proteins to degradation. HSP70 binds misfolded proteins in the hydrophobic

regions that they exposed (Rüdiger et al. 1997; Kampinga & Craig 2010). The refolding mechanism of HSP70 relies on the switch between open and closed conformations of the SBD (Mayer & Bukau 2005). ATP hydrolysis regulates HSP70 conformational change thanks to the action of members of the HSP40 family (see below) and thanks to other co-chaperones that are nucleotide exchange factors (NEF) (Kampinga & Craig 2010) (Figure 3). SBD is composed of several β-sheet structures and by a α-helix that acts as a lid. The lid is open when HSP70 is bound to ATP and is closed when HSP70 is bound to ADP (Hartl et al. 2011). The hydrolysis of ATP in ADP is accelerated by HSP40 leading to SBD high affinity for substrates, while the exchange between ATP and ADP is ruled by NEF leading to low affinity for the substrates. The HSP70 cycle starts with HSP70 in the open conformation (high on rates and off rates for the peptide) (Rüdiger et al. 1997; Mayer & Bukau 2005). After ATP hydrolysis the substrates is tightly bound to HSP70 and SBD is in the closed conformation. Then, when ATP is replaced by ADP, the substrate is released and, if it is a fast folding protein, the hydrophobic domain are immediately buried in the inner core of the protein. If the folding does not happen in few seconds, the protein is immediately rebound to HSP70. It is possible that the re-bounding to HSP70, not only prevents aggregation, but also facilitates the refolding of these slow-folding proteins (McCarty et al. 1995; Szabo et al. 1994; Laufen et al. 1999; Kampinga & Bergink 2016).

### HSP40

HSP40 proteins, also known as DnaJ proteins are a large group of HSP70 co-chaperone. Even if they are all grouped under the name of "HSP of 40 kDa", many components of this family do not weight 40 kDa but they all share the J domain. This domain is composed of 70 well conserved aminoacids, and it is the surface for interaction with HSP70. J domain is also crucial for the interaction of HSP70 flexible region with clients (Kampinga & Bergink 2016).

Members of HSP40 family (here called DNAJ proteins) activity is both client dependent or independent. If DNAJ does not bind any client, due to the lack of a client binding domain, it acts only as an activator of HSP70 through J domain. On the other side, DNAJs, that can bind clients targeting directly the nascent unfolded polypeptides. Moreover, some DNAJs can also prevent aggregates formation or dissolve already formed aggregates (Kampinga & Bergink 2016).

DnaJB6 and DnaJB8 are expressed in neurons and have a protective role against misfolded proteins. In fact, all HSP40s not only hydrolyse ATP on HSP70 but also binds misfolded substrates and brings them close to HSP70's SBD.

### Chaperonin

Chaperonins are a heterogeneous group of protein that usually function by forming a double ring structure that encloses protein up to 60 kDa for refolding. Chaperonins are divided into two subgroups (Hartl et al. 2011). The first are also call HSP60 and they are usually localized on mitochondria, but upon some stressful condition they can migrate in the cytoplasm (Itoh et al. 2002; Ranford et al. 2000; Tutar & Tutar 2010) . Inside double ring structure there is a pore in which unfolded substrates are enclosed for refolding. The disclosure of this cavity is regulated by a lid formed by the co-chaperone HSP10. When the lid is open peptides are released in a native conformation (Itoh et al. 2002; Ranford et al. 2000; Tutar & Tutar 2010).

The second subgroup is independent by HSP10 and proteins of this family usually form eight-membered rings. One important member of this family is TCP-1 Ring Complex (TRiC), alternatively called TCP1 complex (CCT). This protein interacts with several newly synthetized proteins, such as actin and tubulin, assisting their correct folding (Frydman 2001; Walker et al. 2009).

### Small HSPs

The small heat shock proteins (sHSPs) are also known as HSPBs. This family account for 10 members that are similar in size from each other. They all contain a conserved sequence of 80-100 aminoacids that is called α-crystallin domain and that is at the basis of sHSPs dimerization/oligomerization as well as recognition of the clients (Horwitz 1992; Kim et al.

1998). These dimers/oligomers can be formed by a various number of monomers (from 12 up to 48), but the oligomerization process starts with the formation of a dimer via the α-crystallin domain, and involves the C-terminus and the N-terminus, which stabilize the dimer (Lambert et al. 1999). Many sHSPs contain, in the C-terminal region, a triad of aminoacids (usually the triad contains proline) that are at the basis of the dimer formation. If this triad is not present chaperones can only form small oligomers and this is the case for HSP22 and HSP20 (HSPB8 and HSPB6). sHSPs differ from each other by tissue expression and by biochemical activity (Boncoraglio et al. 2012) (Figure 4). The main activities of sHSPs are: cytoskeleton stabilization (all these proteins bind elements of the cytoskeleton, thus determining their stabilization or destabilization (Boncoraglio et al. 2012; Brown 2007; Sharma et al. 2017; Iwaki et al. 1994)), chaperone activity and anti-apoptotic activity; sHSPs exert their activity in an ATP-independent fashion. The cytoskeleton activity of sHSPs is strictly dependent on the phosphorylation state of the sHSPs that then influence their oligomerization (During et al. 2007).

The chaperone activity of sHSPs prevents the formation of high oligomers or aggregates by preventing the nucleation (Rusmini et al. 2013; Crippa et al. 2010; Boncoraglio et al. 2012). In some cases, sHSPs also promote the refolding of substrates. Especially upon stress condition, sHSPs dimers are released from oligomers to promote the binding to the unfolded/misfolded substrates; sHSPs hold them in a soluble form preventing their aggregation (Rusmini et al. 2013; Crippa et al. 2010; Cristofani, Crippa, Vezzoli, et al. 2017). Then, sHSPs act with ATP-dependent chaperone allowing protein folding, when stressful condition is gone. It is also known that their chaperone ability varies between sHSPs family members and it is highly dependent also on substrate properties (Boncoraglio et al. 2012).

Lastly, some HSPBs may also act as anti-apoptotic factors. The most well studied member in this context is HSPB1. HSPB1 prevents apoptosis by acting upstream and downstream to the mitochondria inhibiting the activation or release of the pro-apoptotic signals by sequestering the released cytochrome-C during apoptotic stimuli (Chauhan et al. 2003; Arrigo 2017). It also prevents the function and the formation of the aptosome (functional structure for apoptosis).

All these sHSPs functions can co-operate during stress and their beneficial role is achieved by the co-existence between these different functions.

### The co-chaperones family of BAG

Among the large family of the nucleotide exchange factors (NEFs), there is BAG family whose members associate with HPSs to accelerate the hydrolytic ATP cycle; indeed, they promote the release of ADP and the subsequent bound of ATP (Young et al. 2003; Behl 2011; Kettern et al. 2011).

Human BAGs (Bcl-2 associated AthanoGenes) are proteins that have anti-apoptotic activity and have been initially associated with Bcl-2 family. Bcl-2 family is a heterogeneous group of proteins that can have anti- or pro-apoptotic function. Since some of BAG proteins act in complex with HSP70, that is a chaperone, they are usually called co-chaperones (Behl 2016).

The first BAG protein discovered was BAG1 and subsequently other 5 members were described in humans (BAG2, BAG3, BAG4, BAG5, and BAG6). All BAGs share a conserved aminoacids sequence of 40-50 aminoacids, named the BAG domain and differ from the N-terminus structure (later studies say that this domain span for 110-120 aminoacids). BAG domain is responsible for BAG interaction with other proteins such as HSP70 (Figure 5). These six proteins greatly differ from each other by structure and function (Takayama et al. 1999).

BAG1 exists in four different isoforms depending on the initiation of translation (Takayama et al. 1999). Through its BAG domain BAG1 interacts with HSP70, and exerts its NEF activity driving ADP exchange into ATP, thus allowing the release of the substrates from HSP70 (Bukau et al. 2006; Sondermann 2001; Höhfeld & Jentsch 1997). BAG1 also possesses an ubiquitin binding domain, that allows the delivery of HSP70-bound substrate to proteasome (Luders et al. 2000). BAG1

also interacts with steroids receptors, particularly the glucocorticoid receptor, influencing their activities. It has been shown that BAG1 has a role in the developing nervous system (Behl 2016).

BAG2 function is strictly correlated with its interaction with CHIP. CHIP (carboxyl-terminus of HSP70-interacting protein) is also known as STUB3 and acts both in protein folding and in protein degradation by proteasome, since it is an E3 ubiquitin ligase. There are also evidence that link CHIP to CASA-complex involved in autophagy selective routing (Crippa et al. 2010). BAG2 is known as a CHIP inhibitor and through this function it rules some processes (Arndt et al. 2005; Dai et al. 2005). The main role of BAG2 is ruling the switch between foldase activity on pro-degradative activity of HSP70. It was also shown that BAG2, positively regulates ubiquitin independent degradation by proteasome (Carrettiero et al. 2009).

BAG3 exists in two isoforms: a full-length form (70 kDa) and a shorter form of 40 kDa (Bruno et al. 2008). The shorter form is expressed only in synaptosome where the full-length form is poorly expressed. Full-length BAG3 is mainly expressed in transformed cells such as myoblast, tumour cells etc..(Gentilella & Khalili 2011; Felzen et al. 2015; Sherman & Gabai 2015; Rosati et al. 2007; Liao et al. 2001) In non-transformed cells, BAG3 is expressed upon stressful signals like oxidative stress or proteasome inhibition. BAG3 interacts with a wide range of proteins thanks to the presence of many different domains in its structure. In addition to BAG domain (essential for the interaction with Bcl-2), BAG3 also has a PxxP domain (that interacts with the SH3 domain of phospholipaseC γ and with dynein) a WW domain (that binds proline rich domains on target structure, such as adenovirus penton base protein) and two IPV domains (designate for the interaction with HSPB8, HSPB6 and HSPB5) (Fuchs et al. 2015; Doong et al. 2003). BAG3 contains also two sites, regulated by phosphorylation, which binds to 14-3-3 proteins (Ge et al. 2010).

BAG4 mainly interacts with the tumour necrosis factor (TNF) and mainly acts as a silencer of death domains (Jiang et al. 1999).

BAG5 has 4 BAG domains (it is the only BAG with this particular structure). BAG5 is not a well-studied protein, but is seems to have a pro-apoptotic role, differently form the other BAG proteins (Kalia et al. 2004).

BAG6 is the largest member of BAG proteins (1229 aminoacids), also known as Scythe in *D. Melanogaster* or BAT3 when associated to the major histocompatibility complex (MHC) of class III (Thress et al. 1998; Spies et al. 1989). BAG6 has a BAG domain, but its action on HSP70 is not explicated through that domain and is CHIP independent. BAG6 also possesses a UBL domain that helps in driving substrates to proteasome. Through its interaction with HSP70, BAG6 also has a role in cell stress, viability and development (Behl 2016; Corduan et al. 2009).

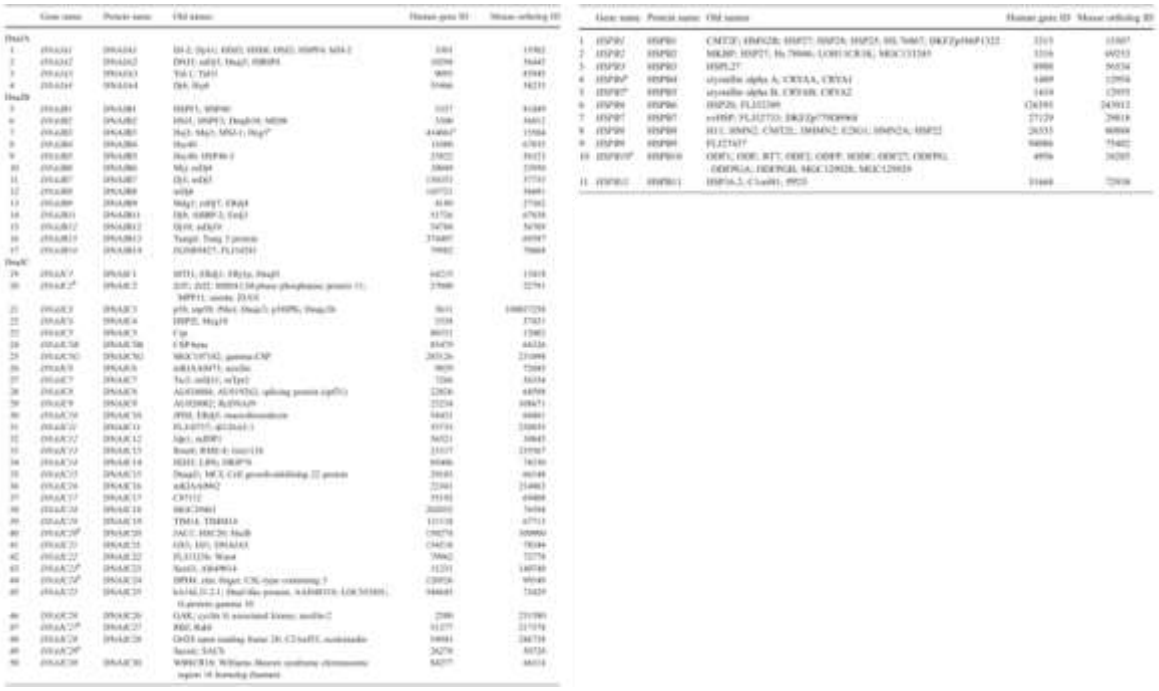

*Figura 1: HSPs nomenclature* (Kampinga et al. 2009)

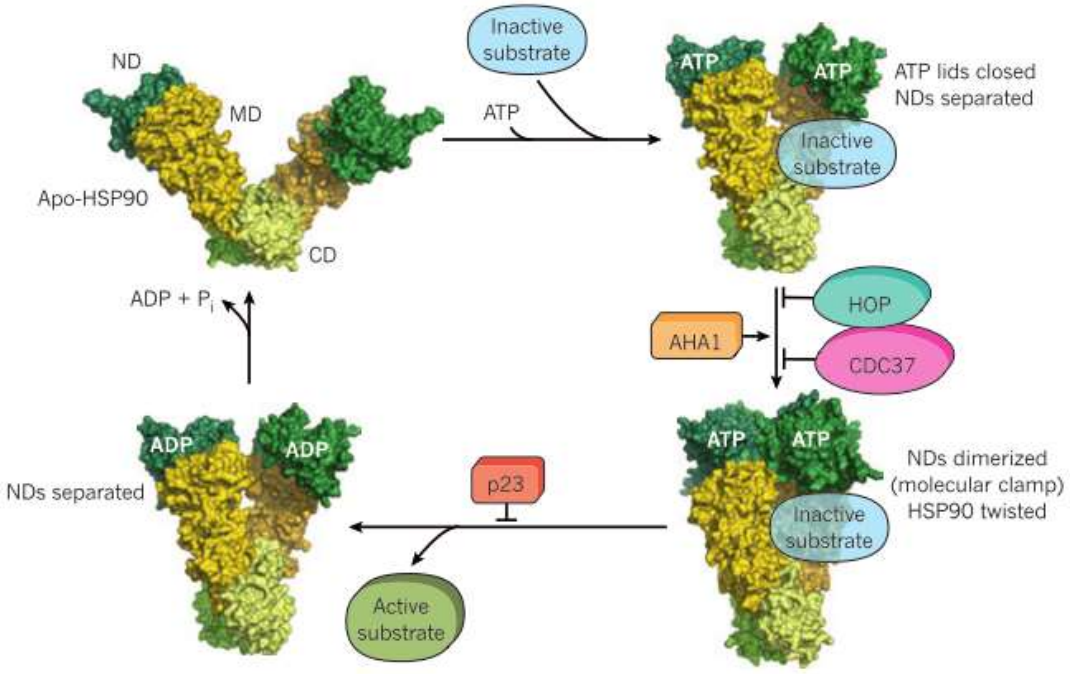


*Figure 2: HSP90 cycle* (Hartl & Hayer-Hartl 2002)

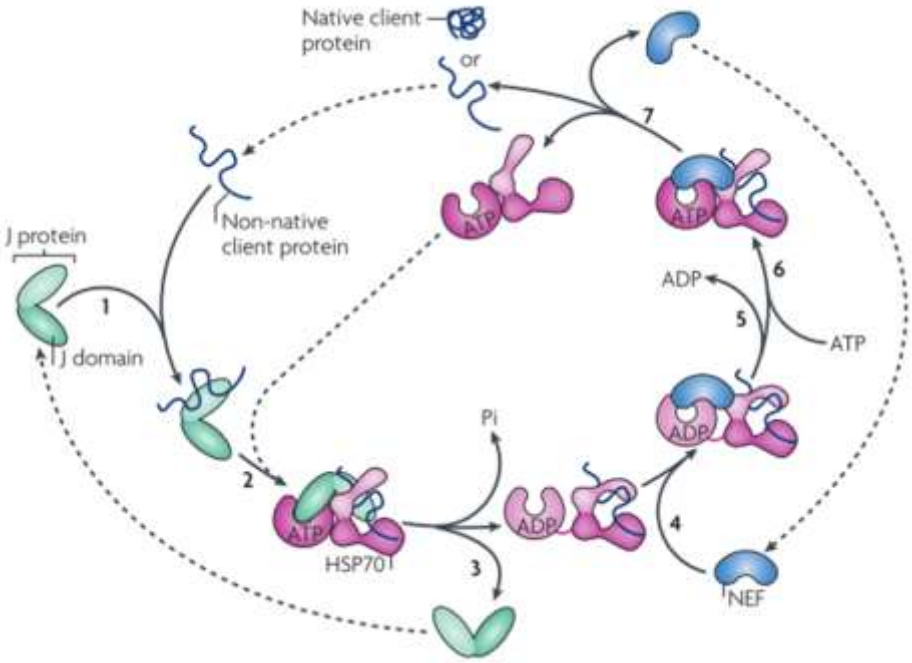


*Figure 3 HSP70 cycle* (Kampinga & Craig 2010)

| Name | Alternative names | Tissue expression profile | Function |
|---|---|---|---|
| HSPB1 | HSP27, Hsp25 (mouse) not related to *D. Melanogaster* Hsp27 | Muscles (smooth, skeletal and cardiac), brain, colon, kidney, liver, lens, lung, stomach, testis | Cytoskeleton stabilization; chaperone and pro-refolding functions; anti-apoptotic function; anti-oxidant function |
| HSPB2 | MKBP | Skeletal and cardiac muscles | Chaperone activity toward DMPK; enhance kinase activity of DMPK, maintaining myofibrillar integrity; anti-apoptotic function |
| HSPB3 | HspL27 | Muscles (smooth, skeletal and cardiac) | Maintaining myofibrillar integrity |
| HSPB4 | αA-crystallin | Lens | Chaperone and pro-refolding functions; maintaining the proper refractive index in the lens |
| HSPB5 | αB-crystallin | Muscles (smooth, skeletal and cardiac), brain, colon, kidney, liver, lens, lung, stomach, testis | Chaperone and pro-refolding functions; cytoskeleton stabilization; maintaining the proper refractive index in the lens; anti-apoptotic function |
| HSPB6 | Hsp20, p20 | Muscles (smooth, skeletal and cardiac), brain, colon, kidney, liver, lung, stomach | Smooth muscle relaxation; cardioprotection; anti-aggregation |
| HSPB7 | cvHsp | Skeletal and cardiac muscles | Maintaining myofibrillar integrity; SC35 speckle resident; anti-aggregation |
| HSPB8 | Hsp22, H11, E2IG1, not related to *D. Melanogaster* Hsp22 | Muscles (smooth, skeletal and cardiac), brain, colon, kidney, lung, placenta, skin, stomach, testis | Anti-aggregation; protein synthesis inhibition; induction of autophagy |
| HSPB9 | None | Testis | Cancer/testis antigen |
| HSPB10 | ODFP, ODF1 | Testis | Cytoskeleton stabilization |

*Figure 4 Classification of small heat shock proteins* (Boncoraglio et al. 2012)

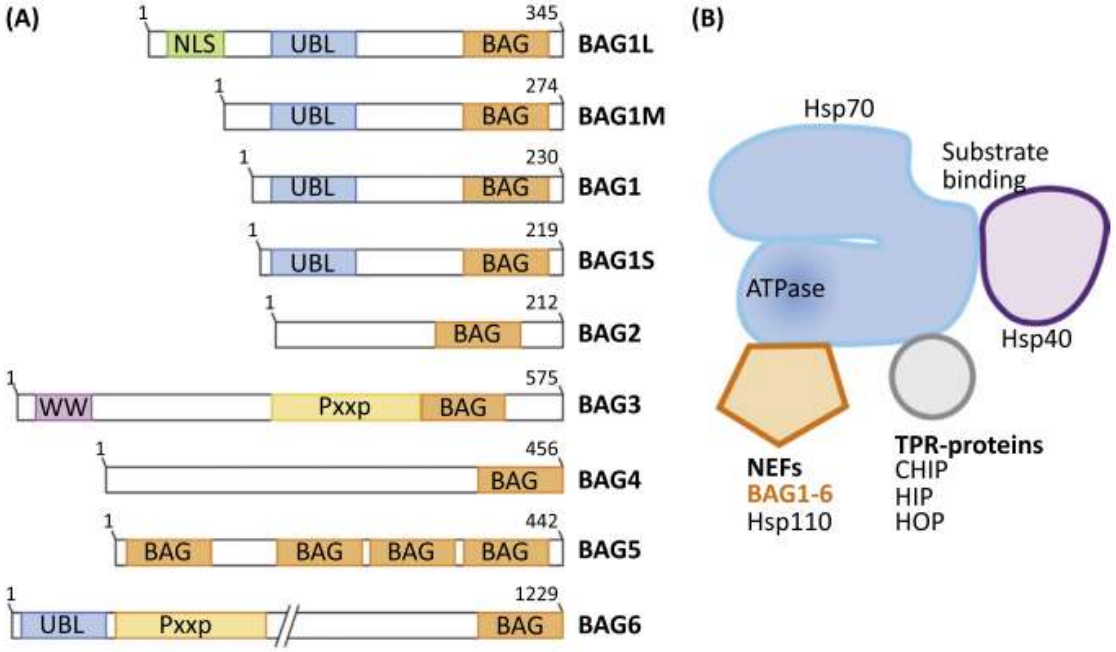


*Figure 5 BAG family* (Behl 2016)

## The protein quality control system: the degradative systems

### *The ubiquitin proteasome system*

Proteasome is the preferential route for degrading short-living proteins, and the 80% of the total amount of proteins is degraded by proteasome (Hershko & Ciechanover 1998).

The functional part responsible for enzymatic activity is a multi-heteromeric complex named "20S subunit" hereafter referred as proteasome (it is called 20S due to its sedimentation coefficient) (Hough et al. 1987). Proteasome is well conserved among eukaryotics (yeast, plant, mammalian) and also between some bacteria. The proteasome is composed of α and β subunits arranged in four rings: two rings are made of only α subunits and two rings made only of β subunits (T. Jung et al. 2009). The four rings are piled one onto the other with the two α rings outside (first and last) and the two β rings inside (α β β α structure) (T. Jung et al. 2009). Ancestral form of proteasome found in Archea have α and β subunits with only one secondary and tertiary structure; while in yeast plants and mammalians both α and β subunits display 7 different conformations present in each ring. Indeed, each ring is composed of seven different subunits whose weight spans around the 20 kDa. The whole proteasome has an overall mass of 700 kDa (T. Jung et al. 2009). Proteasome inner part is divided in three spaces: two fore chambers resulting from the space between α and β subunits and a main chamber resulting from the space between the two β rings. The main chamber is the core of the proteolytic activity of the proteasome. Subunits β1, β2 and β5 show proteolytic activity and can be replaced by β1i, β2i and β5i induced by interferon-γ under certain conditions. Proteasome with these different β subunits is called immune-proteasome and produces protein fragments of different lengths compared to the physiological proteasome (Hirano et al. 2008). Usually, the fragments lengths spans between 2-35 amino acids with an average of 8-12 aminoacids per fragment (Köhler et al. 2001; Luciani et al. 2005). β1, β2 and β5 show different kind of proteolytic activity: β1 has a peptidyl-glutamyl-peptide-hydrolysing-activity; β2 has a trypsin-like activity; β5 has a chymotrypsin-like activity (Loidl et al. 1999; Groll & Huber 2004). The catalytic centre of each subunit is the threonine residue at the N-terminal. The proteolytic activity is most important in β5 and less significant in β2 and β1 (Heinemeyer et al. 1997).

The α rings are recognition domain and regulate the access to the inner core. The N-terminal region of subunits α2 α3 and α4 form a gate that prevents the access of protein to the catalytic core (Groll et al. 2000). Each N-terminal residue involved in this gating process has its own tertiary structure adapt for closing the channel. The diameter of the pore is 13 A° enough to allow the processing of one misfolded substrate as a single chain (T. Jung et al. 2009).

When a contact between α subunits and substrates is established the N-terminal residues closing the pore, undergo a conformational change leaving the channel open. There are various cofactors that interact with α subunits to regulate the opening and the closing of the pore and the specificity for the substrate. One of these is the 19S cofactor: the binding with this cofactor increases the access to the catalytic core of 100 times and regulates substrates specificity (Adams et al. 1998; Glickman et al. 1998). The 19S is also called PA700 (proteasome activator of 700 kDa) (Figure 6A) and has a base structure made of Rpt subunits (10 different conformations with ATPase activity) and a lid structure that acts as a channel gate made of Rpn subunits (9 different conformation with no ATPase activity) (Liu et al. 2002; Tanaka 2009). Each α ring is bound with one 19S subunit (T. Jung et al. 2009). The complex between 20S and the two 19S subunits is called 26S proteasome and weights approximatively 2MDa (Glickman & Ciechanover 2002).

26S proteasome only recognizes and degrades proteins that are ubiquitinated (T. Jung et al. 2009). The 26S proteasome acts together with the enzymes responsible for the ubiquitination of substrates composed the ubiquitin proteasome system (UPS). Ubiquitin is a small protein of 76 aminoacids (8,5 kDa) highly conserved in eukaryotic and is regarded as post-translational modification. Ubiquitin acts as a signal to direct protein to proteasomal degradation (Wilkinson et al. 1980).

The ubiquitination process is composed of 3 main steps: activation, conjugation and transfer of the ubiquitin (Figure 6B). The enzymes responsible of these porcesses are E1, E2, E3 and E4 that act as single enzymes and not in a complex, even if they catalysed reactions of the same system.

E1 is an ATP dependent enzyme that activates ubiquitin. To activate ubiquitin the glycin76 at the C-terminus of ubiquitin is bound to a cysteine on the E1 enzyme (Sun 2003). Then ubiquitin is transferred on E2 enzyme on a homologous cysteine residue. The catalytic core of E2 is composed of an asparagine residue in addition to the cysteine residue. Often E2 enzyme is found in a homo-dimer complex, especially when one of the two E2 is already bound to an ubiquitin residue (Hershko & Ciechanover 1998).

After the loading of ubiquitin on E2 enzyme, both the substrates and the E2 enzyme are bound to the E3 enzyme. If E3 possesses the RING motifs, ubiquitin loaded on E2 is directly transferred to the substrate (RING E3) creating a bound between a cysteine on ubiquitin and a lysine on the substrate (Hershko & Ciechanover 1998; Hochstrasser 2006). If E3 does not possess the RING motif (HECT E3), ubiquitin is firstly transferred to E3 enzyme and then, from the E3 enzyme to the substrate. E3 enzymes are also called ubiquitin-ligase and are the most abundant proteins of the UPS (Hochstrasser 2006).

Human genome encodes for more than 500 E3s (Hershko & Ciechanover 1998), and often these ubiquitin-ligases act in collaboration with chaperones (Ciechanover & Kwon 2015). CHIP is an ubiquitin ligase and HSP70 and HSP90 co-chaperone. When is bound to HSP70, CHIP binds and ubiquitinates misfolded substrates (Demand et al. 2001). To facilitate proteasomal degradation CHIP also interacts with Rpn10 a subunit of the 19S complex (Connell et al. 2001). Proteasomal degradation of CHIP clients is further facilitated by binding with BAG1, that acts as NEF of HSP70, enhancing the releasing of the substrate from HSP70 (Takayama et al. 1997). BAG1 also has a domain for the interaction with the proteasome, thus strictly directing substrates to proteasome (Alberti et al. 2003) (Figure 7). Also HSPB1, that is a small HSP interacts directly with proteasome and modulates the ubiquitination of client (Garrido et al. 2006).

Two other important ubiquitin-ligases are UBR1 and UBR2 (that mediate the ubiquitination of misfolded cytosolic proteins) and RNF126 (that collaborates with the BAG6 family ubiquitinates proteins of the membranes) (Heck et al. 2010; Prasad et al. 1992; Eisele & Wolf 2008).

Substrates can be bound to a single moiety of ubiquitin (mono-ubiquitination), to single moieties of ubiquitin in different protein sites (poly-mono-ubiquitination) or to an ubiquitin chain (poly-ubiquitination). The polymerization of ubiquitin occurs after the attachment of the first ubiquitin to the substrates. Polymerization is based on the conjugation of single ubiquitin moieties to the growing chain: a lysine on the new ubiquitin is bound to a methionine on the last ubiquitin of the chain (Hershko & Ciechanover 1998; Ciechanover & Kwon 2015). There are several lysine residues located in the ubiquitin that can be involved in polymerization (K6, K11, K27, K29, K33, K48, or K63 (Ikeda & Dikic 2008)). The elongation of the poly-ubiquitin chain is achieved by a new cycle of E1, E2 and E3 enzymes. Occasionally also E4 mediates the attachment of ubiquitin moieties mainly through K48 linkage (Upadhya & Hegde 2007).

Now it is known that almost every ubiquitinated protein is degraded by proteasome, and that there is not a threshold for chain length: even a single ubiquitin is enough for targeting substrates to proteasome (Boutet et al. 2007).

The most common ubiquitination that leads to proteasomal degradation is in Lys48 (K48). K48 linkage are the most abundant in proteins and this modification drives most of the proteins towards proteasomal degradation; indeed, K48 linkage changes upon proteasome inhibition (Yau & Rape 2016) (Figure 10). K48 linked proteins are produced by various E3 ligases also involved in other degradative processes, such as ERAD (Yau & Rape 2016). Also K11 linkage in involved in proteasomal degradation, especially of proteins involved in cell cycle (Yau & Rape 2016; Jin et al. 2008; Song et al. 2014; Ling Song and Michael Rape 2011).

Ubiquitin is also a mediator of protein-protein interaction. Ubiquitin chains that explicit this function have different position and conformation like Lys63 (K63) (Spence et al. 1995).

Ubiquitinated substrates are recognized by 19S subunit (Thrower et al. 2000). 19S subunit plays three main different functions. First of all, it recognizes the poly-ubiquitinated substrates thanks to the action of the Rpn subunits (T. Jung et al. 2009). Once the substrate is recognized, 19S subunit unfolds it in order to let it in the central core of the 20S subunit (Ciechanover 1994). Meanwhile, 19S complex acts also as a deubiquitinase enzyme mainly through the ATPase activity of the Rpn11 . Indeed, ubiquitin is released in the cytosol as long chains. In the cytosol are present deubiquitinating enzymes (DUBs) that reduce chains into ubiquitin monomers, in order to prevent a competition between these chains and ubiquitinated substrates for the proteasome. DUBs also catalysed the shortening of ubiquitin chain on substrates modulating proteasomal degradation. Free ubiquitin moieties can deposit on aggresome where they are recognized by HDAC family and used for proteasomal routing (Hao et al. 2013).

Physiologically the UPS is involved in many cellular functions. In cell cycle progression UPS has an important role since degradation of specific cyclin rules the transition from a phase to another (Takeuchi & Toh-e 2001). In antigen processing the immune proteasome is responsible for the production of small fragments of 8-10 aminoacids of length that will be exposed on cell surface and presented as antigen to the immune cells (Osterloh et al. 2006). This process gains particular importance in presence of viral infection, when viruses produce the protein for the assembly of new viruses (Osterloh et al. 2006). Proteasome is also responsible for the degradation of newly synthetized proteins that do not reach the correct folding (Dick et al. 1996). A fraction of these proteins has to be extracted from the ER (Schmitz & Herzog 2004). There are various proteins that assist the extraction of these proteins such as p97/VCP (Valosin Containing Protein). VCP forms a channel that extracts proteins from the ER directing them to UPS degradation (DeLaBarre & Brunger 2005; Brodsky & McCracken 1999; Hampton 2002). UPS also degrades proteins that misfold due to mutations, oxidation etc...(Brégégère et al. 2006) In this context, UPS is relevant in aging, since proteasomal activity decreases in old cells compared to young cells (Chondrogianni et al. 2015). If proteasome is no longer functional, misfolded proteins may accumulate forming toxic aggregates.

### *Autophagy*

The term autophagy was created in 1963 by Christian Reneè De Duve (Nobel Prize in 1974 for his studies on lysosomes), from the greek language “auto” meaning self and “phagos” meaning eating. Autophagy was firstly identified as a cellular process whose function was to degrade part of the cell itself. Vesicles that are the basis of the autophagic process had been yet characterized in 1950, when by electron microscopy scientists observed the formation of double membrane structures surrounding other cellular components, like mitochondria (Tooze & Dikic 2016). These vesicles were called autophagosomes. During the following years research on the cellular pathway involving these vesicles was carried on only by few groups of scientists that biochemically characterized the content of this autophagy related vesicles, called autophagosomes (Tooze & Dikic 2016). During 1980s, Yoshimori Ohsumi found that autophagy was correlated with nutrient deprivation and in particular he found that autophagy was increased during starvation (Ohsumi 2013). From these first evidence Ohsumi kept on studying these process in yeasts (*Saccharomyces cerevisiae*) and characterized many proteins with a key role in autophagy that were called ATGs (AuTophagy related Genes) (Klionsky et al. 2003). Ohsumi also described an autophagy regulatory mechanism involving mTOR, and the entire process required for autophagosomes formation (Mizushima et al. 1998; Ichimura et al. 2000). In the past two decades, many studies evidenced that autophagy is not only a physiological mechanism, but that is also involved in the pathogenic mechanism of many severe diseases like cancer, NDs, metabolic disorders, inflammation, virus and bacterial infections (Mizushima et al. 2004; Liang et al. 1999). Now autophagy has gained importance and is a very widely studied pathway.

In 2016 the Royal Swedish Academy of Sciences awarded Yoshimori Ohsumi the Nobel prize, for the description and the characterization of autophagy (Tooze & Dikic 2016).

## Macro-Autophagy or "Autophagy"

### *The formation of the autophagosome*

Macro-autophagy, hereafter referred as autophagy, is a process present in yeast, plant and mammalian cells. Its main role is supplying nutrient during starvation, degrading big organelles and proteinaceous material, and eliminating infecting bacteria and viruses (Parzych & Klionsky 2014; Tanaka & Matsuda 2014). The capacity of autophagy to degrade proteinaceous formation highlight its importance in NDs.

The basic difference between autophagy and other vesicle related pathways is that autophagosomes are "de novo" formed by membrane elongation and not by membrane budding already containing cargo (Zhifen & Klionsky 2010). Autophagosomes are round shaped vesicles with a diameter of 0.4-0.9 µm in yeast, and 0.5-1.5 µm in mammals (Takeshige et al. 1992).

Autophagosomes formation is a process composed of three distinct steps: induction, nucleation and elongation (Figure 8).

Induction of autophagy involves the recruitment of factors around the phagophore assembly site (PAS). Factors that complex together for induction are ULK1/ULK2 (Unc-51-like kinase 1/2, homologs of Atg1), Atg13 and RB1-inducible coiled-coil 1 (RB1CC1/FIP200) (Hosokawa et al. 2009; C. H. Jung et al. 2009; Ganley et al. 2009; Mizushima 2010; Mizushima 2007). Atg13 also binds C12orf44/ATG101 required for a correct functioning of the complex (Noda & Mizushima 2016; Mercer et al. 2009). ULK1-Atg13-FIP2000 complex is stable and does not depend on nutrient levels (Hosokawa et al. 2009; C. H. Jung et al. 2009). ULK1 and Atg13 activity is regulated by phosphorylation. In normal conditions, MTORC (mechanistic target of rapamycin complex) maintains ULK1 and Atg13 phosphorylated and thus in an inactive status. Upon starvation or following rapamycin treatment MTORC disassociates from the ULK1-Atg13-FIP2000 complex leaving the complex available for yet unknown phosphatases. When ULK1 and Atg13 are dephosphorylated they are activated and this process induces autophagy (Hosokawa et al. 2009).

After induction, nucleation of the phagophore relies on the formation of PtdIns3K complex (ATG14-containing class III phosphatidylinositol 3-kinase). This complex is formed by PIK3C3/VPS34, PIK3R4/p150, and BECN1. If BECN1 is not associated to the complex, autophagy is inhibited. BCL-2 interaction with BECN-1 prevents its association to the complex, thus inhibiting autophagy (Itakura & Mizushima 2010). When, upon nutrient deprivation, BECN-1 is released from BCL-2, autophagy starts. There are two positive regulators of PtdIns3K complex formation that are AMBRA and SH3GLB1/Bif-1; these proteins positively regulate BECN-1 association to the complex (Kihara et al. 2001; Itakura et al. 2008; Furuya et al. 2005; Liang et al. 1999). PtdIns3K complex produces PtdIns3P (phosphatidylinositol 3-phosphate) that has a role in forming lipid raft on membrane before the recruitment at autophagosomes (Liang et al. 2006).

There are two systems required for the elongation phase. The first one is the complex formed by ATG5, ATG12 and ATG16L1, where the ubiquitin like (UBL) protein is covalently bound to ATG5, and this action is mediated by ATG7 (E1 activating enzyme) and ATG10 (E2 conjugating enzyme). Then, ATG16L1 binds not covalently ATG5 and dimerizes forming a bigger complex. There are two negative regulators of this complex. The first one is RAB33A, a Golgi protein that inhibits ATG16L1; the second one is KAT2B/p300, that acetylates ATG5, ATG7 and ATG12 resulting in their inactivation (Ohsumi 2001; Shintani et al. 1999; Mizushima et al. 2003; Lee & Finkel 2009; Kim et al. 1999).

The second system required for elongation of the phagophore is the LC3 system. LC3 (MAP1LC3B, Microtubule-associated proteins 1A/1B light chain 3B) and GABARAP (γ-aminobutyric acid receptor-associated protein) are ATG8-like

protein. These two subfamilies have different roles in phagophore maturation and elongation; LC3 is the subfamily better characterized.

Initially, LC3 undergoes to the action of the ATG4 protease that causes the exposure of a glycine residue at C-terminus of the LC3 protein (LC3-I). Subsequently, the action of the E1-like protein, ATG7 transfers LC3 on ATG3, an E2-like enzyme. Then, the ATG5-ATG12 complex, that acts as E3-like complex, conjugates LC3 with a molecule of phosphatidylethanolamine (Ichimura et al. 2000; Kirisako et al. 1999; Kirisako et al. 2000). LC3 lipidation is accelerated under starvation. Lipidated LC3 (LC3-II) is present both in the inner and in the outer side of the forming phagophore. Despite the knowledge about the activating mechanism of LC3, the exact role of this protein in phagophore maturation is still unknown (Kirisako et al. 1999). There is third system involved in phagophore formation based on ATG9 shuttling from Golgi to the phagophore in formation. This system is still largely unknown, but its role seems to involve the recruitment of membranes for the formation of the phagophore (He et al. 2008; Reggiori et al. 2004). Membrane utilized for the formation of the autophagosomes may be derived from the ER, the Golgi apparatus, the mitochondria, and even the plasma membrane (Ravikumar et al. 2011; Hayashi-Nishino et al. 2009). Lipid rafts enriched by PtdIns3P, produced by PtdIns3K, are called omegasomes and are recruited as membrane sources for autophagosome formation (Axe et al. 2008).

The process activated after closure of the phagophore is still largely unknown, but it may be dependent on GABARAP action that allows autophagosome maturation (Weidberg et al. 2010). The autophagosome can fuse to late endosome, already containing vesicles, and lastly with lysosomes forming the autolysosome (Monastyrska et al. 2010). The fusion between autophagosomes and lysosomes is not clearly understood. Recent studies show that RAB7, a GTPase protein, and VAM7 and VAM9 (Liang et al. 2008), belonging to the SNARE family, are involved in the formation of the autolysosome (Fader et al. 2009; Furuta et al. 2010).

Autophagy is primarily regulated by nutrient intracellular concentration. There are two systems that sense carbon and nitrogen that are the major regulator of autophagy. The first one is based on the action of the PKA (c-AMP dependent protein kinase A) and the second one is associated with mTOR activity (Stephan et al. 2010).

When a cell is under starvation, the concentration of AMP increases and this event activates the AMP kinase (AMPK). AMPK phosphorylates and activates TSC1/2 , which in turn phosphorylates MTORC, preventing its association to the nucleation complex, and activating autophagy. On the other side, the presence of the aminoacids positively regulates mTORC1 that prevents the formation of the nucleation complex (Inoki et al. 2003; Gwinn et al. 2009).

Since autophagy is a highly dynamic process, it is pivotal that formation and degradation of autophagosomes, called autophagic flux, is balanced. An imbalanced autophagic flux is detrimental for cells in both senses. If autophagy is excessively active, it degrades relevant cytoplasmic components involved in physiological functions, thus potentially leading to cell death. On the other side, impairment of autophagosomes formation or failure in autophagosome degradation (fusion with lysosome) are at the basis of the appearance of many diseases such as neurodegenerative diseases.

### *The CASA complex and selective autophagy*

For many years autophagy has been regarded as an unspecific process that degrades entire portion of cytoplasm in response to nutrient starvation. Recent works showing the involvement of autophagy in degradation of disease-associated proteins has evidenced the existence of selective pathways for the routing of substrates to autophagy.

The chaperone assisted selective autophagy (CASA) is a pathway of routing substrates to autophagic degradation that involved chaperones (Gamerdinger, Carra, et al. 2011; Gamerdinger, Kaya, et al. 2011).

The CASA complex is formed by HSP70, CHIP, HSPB8 and BAG3 (Figure 9). Initially, HSP70 in cooperation with HSPB8 recognizes misfolded substrates that need to be degraded. As a second step, CHIP that is an E3 enzyme associated to

HSP70, ubiquitinates these substrates (Figure 10). Finally, BAG3 that is part of the complex as HSPB8 and HSP70 co-chaperone, via its dynein interacting domain, drives HSP70-CHIP-HSPB8 complex to the autophagic receptor p62, usually localized at the microtubule organization centre (MTOC). P62 displays an ubiquitin binding domain, and is thus capable of recognizing substrates ubiquitinated by CHIP (Gamerdinger, Carra, et al. 2011; Gamerdinger, Kaya, et al. 2011). Moreover, BAG3 by its activity as NEF, allows the release of the ubiquitinated substrates from HSP70. Accumulation of ubiquitinated proteins delivered by CASA complex is called aggresome. When an aggresome is formed, p62 drives its internalization into the forming autophagosomes. Indeed, p62 also has a domain which interacts with LC3, acting as a bridge between the aggresome and the autophagic vesicles (Gamerdinger, Carra, et al. 2011; Gamerdinger, Kaya, et al. 2011).

### Microautophagy and chaperone mediated autophagy

Microautophagy and chaperone-mediated autophagy (CMA) are two processes independent of macro-autophagy (usually referred as autophagy) that involved the degradation of substrate through the lysosomes.

Microautophagy is gaining more importance in the recent year because some studies reveal its connection with some human diseases. Microautophagy is a self-eating process less known and less important than macro-autophagy. Microautophagy relies on the direct engulfment of soluble substrates into the lysosomes through invagination of the lysosome membrane (Li et al. 2012). Microautophagy can be induced by both starvation and rapamycin. There are three types of selective microautophagy: micropexophagy, piecemeal microautophagy of the nucleus, and micromitophagy (Li et al. 2012). Studies aimed to better understand the mechanisms regulating microautophagy are still ongoing.

On the other side, CMA is better characterized and more widely studied. CMA is a degradative pathway found only in mammals. Dysfunction of CMA is related to human disease especially NDs and cancer. CMA has also a relevant role in aging process (Liu et al. 2015; Cuervo & Wong 2014). If microautophagy and in some case macro-autophagy have low specificity for substrates, CMA is highly selective. Substrates of CMA must display a sequence of 5 aminoacids K-F-E-R-Q. KFERQ sequence is present on the 30% of the whole proteome and normally is hidden or is located in the internal core of the protein, sometimes on the surface of protein-protein interaction (Cuervo & Wong 2014). Therefore, to unmask the KFERQ targeting sequence, these proteins have to be unfolded. KFERQ sequence is recognized by heat shock cognate 70 (Hsc70/HSPA8) and by other co-chaperones. Hsc70 targets the proteins to lysosomes where it is recognized by the substrate receptor LAMP-2A (lysosomal-associated membrane protein 2A) (Bandyopadhyay et al. 2008). When LAMP-2A interacts with the substrates, it oligomerizes with homologous proteins forming the translocation complex. This complex is stabilized by the HSP90 present in the lumen of lysosomes. Meanwhile Hsc70 assists the unfolding of the substrate. The translocation of the unfolded substrate is assisted and partially mediated by a luminal isoform of Hsc70 (Bandyopadhyay et al. 2008). After the translocation, the LAMP-2A complex is disassembled by action of the cytosolic Hsc70, and LAMP-2A return in its monomeric form. The rate-limiting step of the whole process is LAMP-2A interaction with the substrate that modulates CMA activity and degradation power (Cuervo & Wong 2014). Regulation of CMA process is still largely unknown.

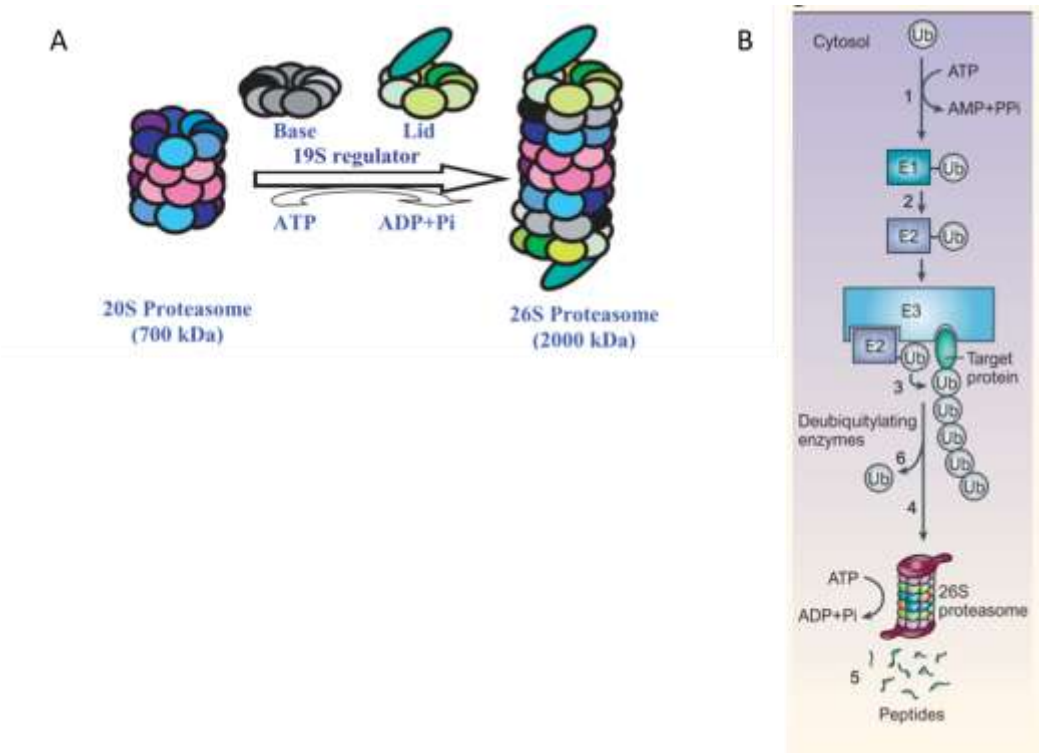


*Figure 6 A) proteasome structure B) the ubiquitin proteasome system. Adapted from* (Nandi et al. 2006; Glickman & Ciechanover 2002)

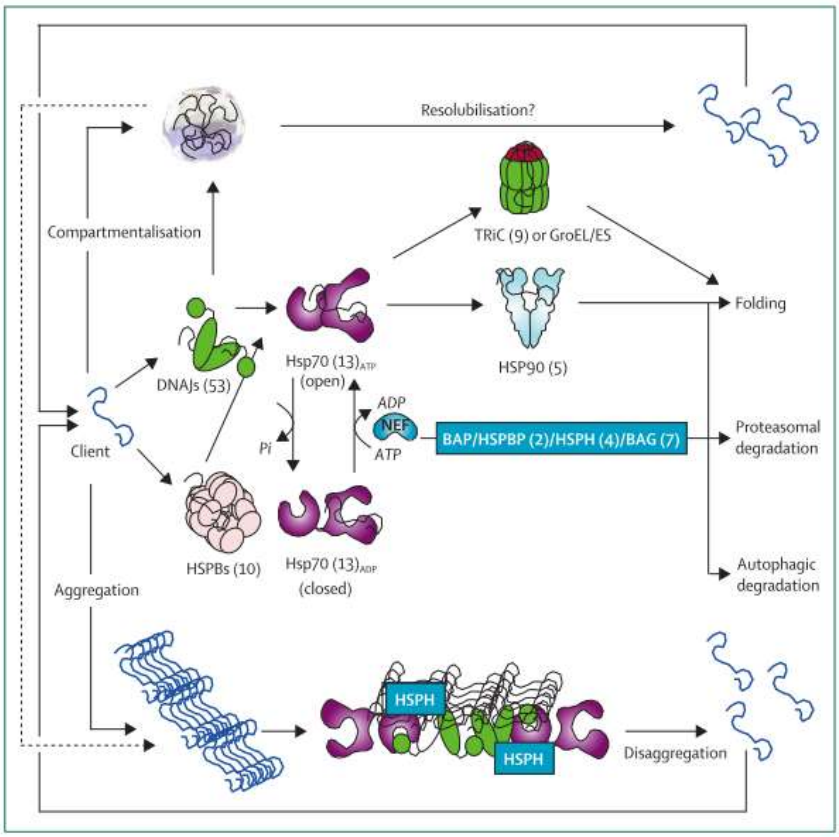


*Figure 7 Chaerone network and targeting to proteasome* (Kampinga & Bergink 2016)

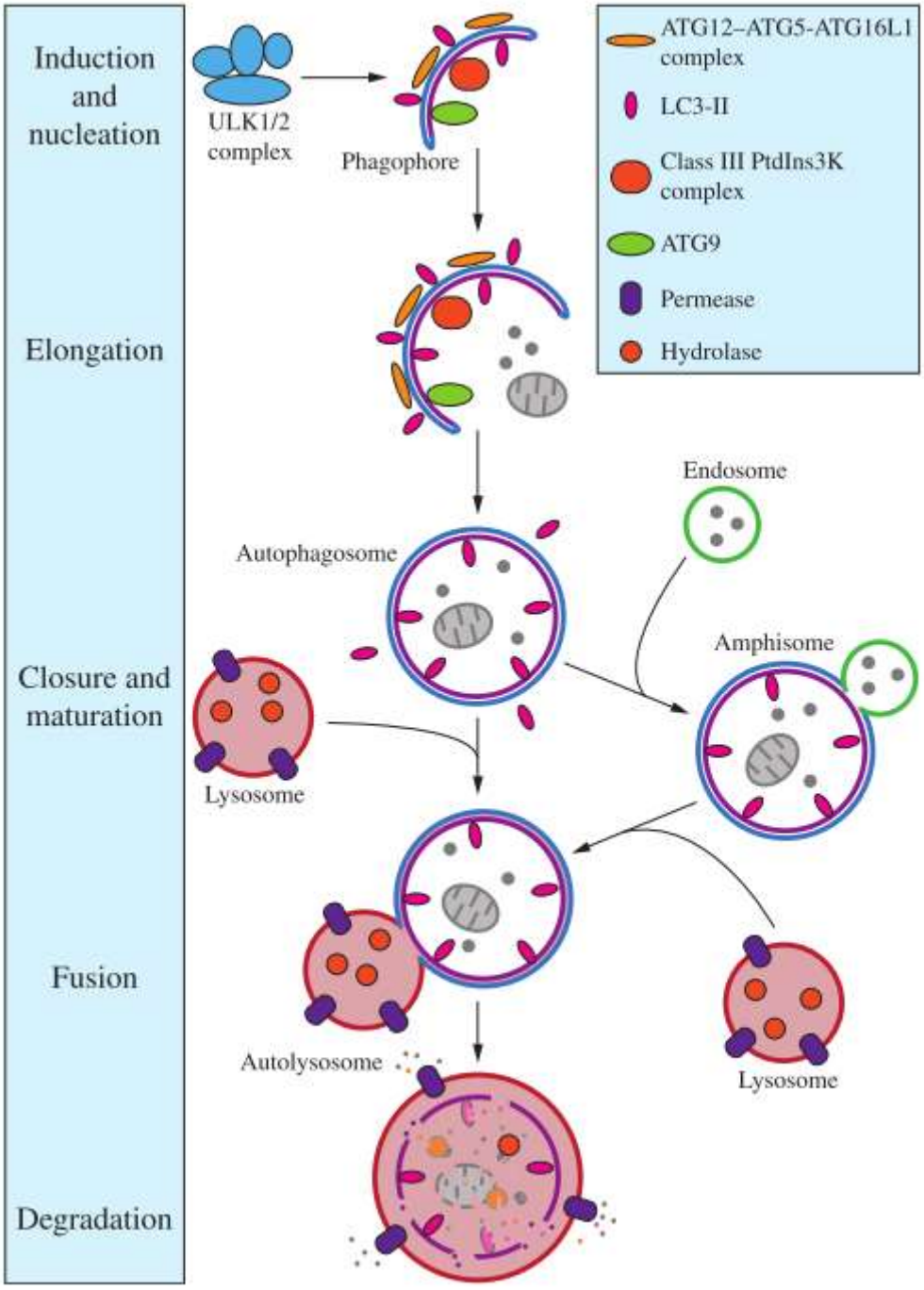


*Figure 8 The autophagic machinery* (Parzych & Klionsky 2014)

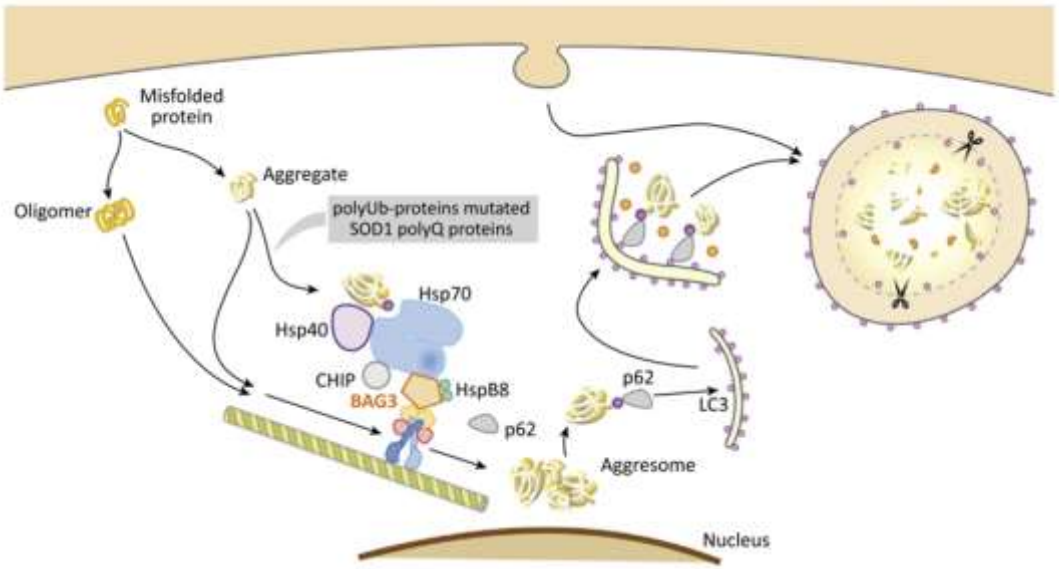


*Figure 9 Selective targeting to autophagy: the CASA complex* (Kampinga & Craig 2010)

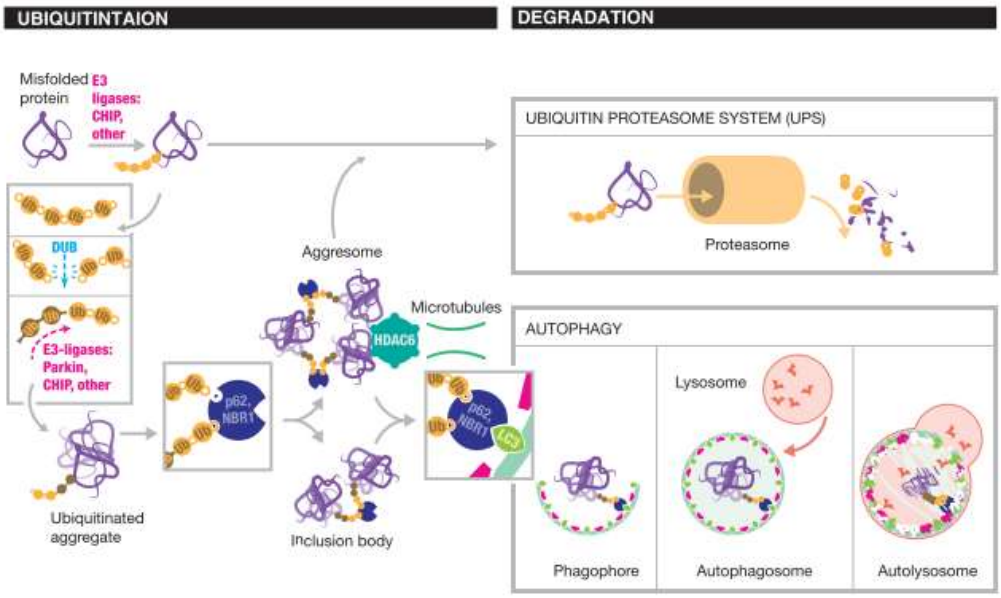


*Figure 10 The ubiquitin signaling* (Shaid et al. 2013)

## AMYOTROPHIC LATERAL SCLEROSIS

### Epidemiology and clinical signs

Amyotrophic lateral sclerosis (ALS) is a neurological disease that has gained attention in the last 30 years. Only in the last four years 5940 publications were related to ALS (almost 29% of all the papers regarding NDs) (Zufiría et al. 2016).

In USA, ALS is also known as Lou Gehrig diseases for the football player that was affected by this disease. ALS was described in 1874 by Jean-Martin Charcot who firstly started using the term "amyotrophic lateral sclerosis" to indicate the denervation and the waste of muscle that follows the degeneration of the corticospinal motor neurons in the lateral spinal cord (lateral sclerosis) (Taylor et al. 2016). Indeed, ALS is characterized by the loss of both upper and lower motor neurons.

ALS is a very heterogeneous disease that shows variability in site of onset (spinal or bulbar), age of onset, progression rate, and heritability (sporadic or familial ALS) (Robberecht & Philips 2013).

Usually, ALS leads to death in 3-5 years for respiratory failure. Some patients have shown a prolonged survival even until 20 years, but the majority of affected inviduals die in a very short period of time (Taylor et al. 2016). ALS is regard as an orphan disease, since it affects 1-2 individuals in 100,000 all over the world population. In Europe, the incidence is of 2-16 individuals among 100,000 people (Logroscino et al. 2010). The prevalence (5 individuals in 100,000) reflects the lethality of this disease (Taylor et al. 2016). ALS is generally an adult onset disease in which the first signs typically show up in the fifth decade. Indeed, the mean peak of incidence is between 57 and 60 (Zufiría et al. 2016). Nevertheless, there are some case of juvenile ALS (with an onset between the 10-20 years of age and with a longer survival (Robberecht & Philips 2013)) and some case in which ALS appears very late in life (Taylor et al. 2016). Epidemiological studies have also suggested a slighter predominance of the disease in male than in female (1,5-1,2/1) (Logroscino et al. 2010).

ALS starts focally in the CNS and then spread in the surrounding areas. Clinical features and signs are very heterogeneous depending on the CNS area affected and depending on the stadium of degeneration. Generally, ALS clinical outcomes are distinguished in two main categories: spinal-ALS and bulbar-ALS (Robberecht & Philips 2013)

- Spinal-ALS starts with painless limb weakness (two third of the affected patients) in which spinal neurons or lower motor neurons degenerate first. This form of ALS is followed by hyperreflexia and spasticity of the limb muscle. This type of ALS is often preceded by cramps.
- Bulbar-ALS (one third of the ALS population) primarily affects brainstem motor neurons. The first signs that characterize this kind of ALS are difficulty in swallowing, paralysis and atrophy of the tongue, difficulty in chewing and articulation of the tongue muscle. In this case speech is highly compromised, since the very beginning of the disease.

Less than 5-6 % of the all ALS cases show pure upper motor neurons or pure lower motor neurons involvement. In some rare cases ALS onset is anticipated by cognitive impairment, behavioural changes and respiratory failure (Taylor et al. 2016; Ajroud-Driss & Siddique 2014).

ALS diagnosis is based on the history and physical examination, followed by electrophysiological studies, neuroimaging and laboratory tests. Since ALS shares common features with frontotemporal dementia (FTD) it is very important to exclude mimickers and false positives (Brooks BR, Miller RG 2000; Chaudhuri et al. 1995).

### Familial and sporadic ALS: causative factors

There are many factors that are thought to be causative of ALS, but actually it has not been identified an absolute and unique cause of all form of ALS. ALS is a multifactorial and heterogeneous disease and there have been identified two classes of potential risk factors: environmental factors and genetic factors. Heritable genetic factors are at the basis of

familial ALS (fALS), while sporadic ALS (sALS) can be caused in some cases by gene mutations whose appearance is still largely unknown. sALS occurs without a family history of the disease and without an inherited gene mutation (Ajroud-Driss & Siddique 2014). In some cases, sALS are linked to an incomplete penetrance of a fALS or an incomplete familial history (Ajroud-Driss & Siddique 2014). Some hypothesis have been put forward suggesting that sALS may result from a mixture of genetic susceptibility and environmental risk factors (Ajroud-Driss & Siddique 2014). Various genome wide association analysis (GWAS) led to the identification of risk loci, and also brought to the possible identification of loci connected to the age of disease onset (Wills et al. 2009). Since in several cases there are many factors that occur simultaneously, it has been postulated that 6 risk factors should occur in the same patient to develop ALS (Al-Chalabi et al. 2014), and the nature of these factors determine the age of onset, the symptoms and the severity of the disease. Undoubtedly, the penetrance of a heritable mutation in causing the disease in the fALS is higher than the other factors.

***ENVIRONMENTAL FACTORS***

There are many environmental factors that different studies have identified over the years. The most studied are exposure to pesticide toxins and heavy metals, physical exercise, alcohol, viral and fungal infections (Fang & Ye 2010; Trojsi et al. 2013; Al-Chalabi & Hardiman 2013; Beghi et al. 2010).

One of the most studied and well identified toxins is β-N-methylamino-L-alanine (BMAA) that is produced by cyanobacteria (Vega & Bell 1967). This toxin has been identified in a special root used to make flavour between people in Guam. Other evidence showed that toxins produced by cyanobacteria can cause severe degeneration in the CNS, indeed there have been found cluster of patients in areas next to places where these cyanobacteria live (Masseret et al. 2013).

Another environmental risk factor is the exposure to heavy metals like lead, mercury and selenium. Lead has been found in ALS patient brain, but its real role as a risk factor is still discussed (Fang et al. 2010). On the other hand, some studies have demonstrated that mercury can deposit in both upper and lower MNs and that its presence abruptly exacerbates disease course (Arvidson 1992). Also selenium is highly toxic for MNs and for cholinergic neuron in general. Moreover, in seleniferous population (that assume selenium for example by tap water) ALS incidence is higher than in non-exposed population (Vinceti et al. 2010). Among the pesticides, the most widely used are organophosphates that are known to induce brain damage by inhibiting acetylcholinesterase (Chen 2012). Physical exercise, in particular prolonged and strenuous training, causes prolonged stress in muscle cells and sometimes this stress overflows the system capability to preserve a correct and functional neuromuscular junction. On the other hand, it has been demonstrated that mild physical exercise is beneficial. A recent study confirmed that regular physical exercise is linked to a very low risk of ALS; while extensive physical exercise can cause a continuous and severe stress on the nervous system, and in predisposed subjects this vigorous exercise could be detrimental, indeed there are many athletes in ALS cohorts. There are also studies that showed the strenuous exercise since early age is associated with two folds risk of developing ALS (Beghi et al. 2010; Gallo et al. 2016). To better understand the relationship between risk factors and the pathology, further epidemiological studies are needed.

***GENETIC FACTORS***

Genetic factors are involved in ALS at various levels. There are some genes that are directly implicated in ALS onset, and they are called causative genes (Figure 11). There is another group of genes, called susceptibility genes, which are associated to a higher risk of developing sporadic ALS. Moreover, recently epigenetics factors are gaining importance in understanding ALS genetic implications.

Causative genes

*SOD1*

Cu/Zn superoxide dismutase 1 (SOD1) was the first gene described as causative of familial ALS.(Rosen et al. 1993). SOD1 gene is localized on chromosome locus 21q22.1 and is composed of five exons separated by four introns (Figure 12). This gene encodes for a protein of 22kDa (153 aminoacids) that exerts an antioxidant function through the inactivation of the radical $O^{2-}$ (SOD1 transforms $O^{2-}$ into hydrogen peroxide and hydroxide) thanks to the presence of Cu/Zn cations. The presence of the Cu/Zn cofactors induces also a tight dimerization, since they enable an intramolecular disulphide attachment. Indeed, SOD1 regulates an important defence against oxidative stress and its importance is underlined by its high concentration in the CNS. In fact, SOD1 represents the 0,5-0,8% of all brain proteins (Pardo et al. 1995).

Nowadays, more than 155 mutations in the SOD1 gene have been identified related to fALS and the most common and widely described are D90A, A4V and G93A (Kaur et al. 2016).

D90A causes and exchange of the aspartic acid in position 90 with an alanine. Usually, this mutation is linked to a recessive form of fALS, but it can also appear as dominant heterozygous (rarely) or as homozygous (Andersen 2006).

A4V is a mutation in which alanine in position 4 is substituted by a valine. Patients bearing this mutation usually show bulbar symptoms at onset and the disease progression is aggressive and rapid (Cudkowicz et al. 1997).

G93A mutation (glycine in 93 is changed in alanine) is relatively rare, but it gained importance, since it was utilized for the production of an heterozygous mouse model in which SOD1 activity was mostly unchanged, but that developed motor neuron disease (Valentine & Hart 2003).

In general, all SOD1 mutations are divided in two groups: those in which metal binding is affected and those that leave metal binding unaffected and thus similar to that of the wild type SOD1. In both cases, SOD1 mutation lead to a change in the overall negative charge of the protein (normally protein have a net surface charge balanced to the pH of the cytosol; this prevent self-oligomerization) (Shaw & Valentine 2007). This modification of the charge and conformation eventually leads to self-oligomerization and aggregation.

Mutated SOD1 (mutSOD1) exerts its toxicity through both mechanisms of loss and gain of function. Many studies reported that mutSOD1 has a reduced antioxidant power that leads to motor neuron exposure to peroxide radicals. This reduction could be linked to a decreased half-life of mutSOD1 mRNA, but also to a decreased presence of SOD1 in the nucleus (thus causing DNA damage and altered proteins expression) (Sau et al. 2007). The nuclear deprivation of SOD1 is linked to the formation of SOD1 aggregates that prevent SOD1 from nuclear translocation (Sau et al. 2007).

On the other hand, other studies claim that mutated SOD1 can also act through both mechanisms of loss/gain of function (Sau et al. 2007). Gain of toxic function is linked to increased protein/protein interactions and increased antioxidant activity that leads to the formation of excessive hydrogen peroxide radicals, detrimental for MNs (Allen et al. 2003). Moreover, mutSOD1 directly exerts toxicity on affected motor neurons (Shefner et al. 1999), and is thus possible that the loss of function (diminished nuclear protection against free radicals) and the gain of function (increased neuronal toxicity) work in cooperation in leading to MNs degeneration.

Moreover, recent studies also sho an involvement of the endoplasmic reticulum (ER) in the SOD1 toxicity. Another site of SOD1 toxicity are mitochondria that are damaged following SOD1 aggregation (Soo et al. 2015b). In several ALS mouse models it has been reported an abnormal mitochondria transport along motor neurons axons (Ikenaka et al. 2012). These mechanisms are tightly linked since mitochondria have a role in axon maintenance. Finally, mutated SOD1 also aggregates in glial cells, leading to gliosis and immune defence aberrant response (Boillée et al. 2006).

*FUS*

Fused in sarcoma (FUS) is a gene whose mutations account for the 4% of ALS familial cases and for the 1% of sporadic cases (Mackenzie et al. 2010; Deng et al. 2014). FUS gene is located on chromosome 16 and is composed of 15 exon. This gene encodes for a DNA/RNA binding protein composed of many functional domains including two RNA binding regions and one C-terminal nuclear localization signal in which most mutations occur (Nolan et al. 2016; Mackenzie et al. 2010) (Figure 13). The exact function of this protein is still unknown (Nolan et al. 2016). It seems that it has a role in RNA processing and exporting from the nucleus, as well as in DNA repair (Wang et al. 2017; Lagier-Tourenne et al. 2013; Tan et al. 2012).

FUS mislocalization in the cytoplasm is one feature described in some ALS patients, but it also occurs in some FTD patients, enforcing the theory of a loss of function mechanism, due to nuclei deprivation of FUS. Nevertheless, it seems that FUS toxicity is exerted by a gain of toxic function of mutated FUS on RNA homeostasis, that is most affected process in presence of FUS mutations (Nolan et al. 2016). Indeed, recent studies have assessed FUS as one of the major and most important component of stress granules (SGs), and it also regulates its assembly (Bentmann et al. 2012). SGs are structures that are assembled under stress condition in order to protect mRNA from damage, allowing the translation only of necessary proteins. These SGs are formed by liquid-liquid demixing, process eased by the presence of mRNA and by the presence of low complexity domains at the C-terminus or various RNA-binding proteins such as FUS (Patel et al. 2015). It has been shown that FUS mutations alter stress granules dynamics by increasing the stability of these structures, that possibly act as seeds of aggregation. Moreover, mutant FUS can recruit wild type FUS into abnormal stress granules. Nevertheless, the exact function of these stress granules has yet to be fully assessed; indeed there are also theories that postulate that abnormal SGs production prevents irreversible FUS aggregation, giving to SGs a protective function (Shelkovnikova et al. 2013).

Since now 50 ALS related mutations on FUS have been described and the most of them are frameshift mutation or missense mutation (Deng et al. 2014). They have all dominant traits. The most common is the R521C mutation in which an arginine in 521 in changed in a cysteine. The P525L mutation (in which a proline in 525 is substituted with a leucine) sometimes occurs as sporadic and cause a juvenile ALS with a very severe phenotype (Huang et al. 2010; Nolan et al. 2016). There are no case of pure FTD clearly associated to FUS mutation, but many cases of FTD associated to FUS mutation show also ALS insurgence (Nolan et al. 2016).

Many studies also reported that no post-translational modifications affect FUS activity, and an aberrant cleavage of the protein is not described. The unique post-translational modification associated to FUS toxicity is methylation in 6 regions of the protein. These data indicate that FUS methylation is linked to FUS import into the nucleus. If methylation is inhibited FUS is transported inside the nucleus, if it is hypermethylated FUS cannot bind the protein for the nuclear import (Trasportin-1) (Du et al. 2011).

*C9ORF72*

Chromosome 9 Open Reading Frame 72 is described as the major ALS associated gene in 2011 (DeJesus-Hernandez et al. 2011; Renton et al. 2011). Abnormal expansion of $G_4C_2$ in this gene has been associated to both familial and sporadic ALS and FTD (10%–50% of familial ALS, 5%–7% of sporadic ALS, 12%–25% of familial FTD, and 6%–7% of sporadic FTD) (Majounie et al. 2012). The clinical phenotype of patients bearing these mutations is often a mixture of ALS and FTD and the age of onset and the severity of the disease vary considerably between patients (Gendron & Petrucelli 2017). A possible cause of this variability is the length of the expansion; usually, patients bear elongation of 10-100 repeats (DeJesus-Hernandez et al. 2011; Renton et al. 2011). Notably, expansion length varies also between different tissues of the same patient, owing gene instability. The presence of this expansion often causes the presence of TDP-43 pathology

(that will be discussed later in details) in frontal and temporal cortex, in hippocampus and pyramidal motor system (Beck et al. 2013; Buchman et al. 2013; Dols-Icardo et al. 2014; Blitterswijk et al. 2013).

$G_4C_2$ expansion exerts its toxicity both through a mechanism of loss of function and gain of function. $G_4C_2$ expansions are located between exon 1a and exon 1b of C9ORF27 gene that can be differently transcribed. If transcription starts from exon 1a the repeat will be transcribed, while if the transcription begins from exon 1b the repeat fall in the promotor region of the gene so it is not inserted into the C9ORF72 mRNA (DeJesus-Hernandez et al. 2011; Ciura et al. 2013). There are strong evidence of a reduction in C9ORF72 mRNA levels in many post mortem brain tissues of C9ORF72 patients (van Blitterswijk et al. 2015). The alteration in mRNA production can be linked to the presence of these repeat in the DNA. DNA regions rich in cytosine and guanosine are prone to form G-quadruplex structures. *In vitro* studies on DNA bearing this elongation demonstrate that DNA can fold in G-quadruplex structure of different shapes depending on the repeat length. Both in DNA and mRNA these structures lead to abortion of the transcription/translation (Fratta et al. 2012). This is supported by the evidence that a large amounts of transcripts of the region upstream the repeat, while regions downstream the repeat are found downregulated (van Blitterswijk et al. 2015; Haeusler et al. 2014). Moreover, there are evidence of epigenetic regulation. It has been shown that trimethylated histones (repressor of the transcription) are strongly bound to the expanded region in pathogenic cells (Belzil et al. 2014). Counterintuitively, G-quadruplex have a negative effect, since they repress C9ORF72 expression causing a loss of function, while silencing of the gene caused by trimethylated histones has beneficial effect (Belzil et al. 2014).

Even if loss of function plays a role in the pathogenesis of ALS, its role remains limited compared to gain of function contribution. Gain of function of G4C2 expansion is exerted through two main mechanisms: i) formation of RNA foci, ii) RAN-translation and production of poly-dipeptides (Gendron & Petrucelli 2017).

RNA foci are structures that arise from the transcription of the G4C2 expansion in both senses (sense and anti-sense transcripts: $r(G4C2)^{exp}$ and $r(G2C4)^{exp}$) (Belzil et al. 2013; Gendron et al. 2014) (Figure 14). These mRNA bearing these repeats are prone to sequester essential transcription factors forming these foci in cells nuclei. These foci have been found throughout the CNS, especially in neurons, and at a lower level in astrocytes, glia, and microglia (Gendron et al. 2013; DeJesus-Hernandez et al. 2011). The most abundant RNA binding proteins found in these foci are hnRNPs proteins (Donnelly et al. 2014; Mori et al. 2013). Interestingly, nucleolin is another protein highly represented in RNA foci, possibly because this protein binds G-quadruplex structures (Haeusler et al. 2014). The depletion of functional nucleolin causes nuclear stress, one of the possible mechanisms of RNA foci toxicity.

G4C2 mRNA also undergoes RAN translation. RAN translation is a non-canonical translation process that starts without the presence of an ATG start codon (Repeat-Associated Non ATG). It was first discovered studying microsatellite expansion in muscle dystrophy type 1. RAN translation can start at any point along the transcript without frameshift or truncation (Zu et al. 2010). The products of RAN translation of sense-mRNA are three poly-dipeptides: polyGA, poly GP and polyGR; on the other side the translation of antisense-mRNA produce polyPA, polyPR and polyGP (Gendron et al. 2013; Ash et al. 2013; Mori et al. 2013) (Figure 14). PolyGP dipeptides are produced from both sense and antisense RAN translation, but polyPA and polyPR are relatively less abundant than the other dipeptides (Gendron et al. 2013; Mori et al. 2013). The reasons of this difference are the minor presence of anti-sense transcript in the cytoplasm and the lower efficiency of RAN translation on the anti-sense transcript as compare to the sense transcript. These dipeptides are highly aggregation prone forming inclusions in cytoplasm and nucleus of cells, but, polyPR and polyPA have a different aggregation propensity compared to the other three dipeptides (polyGA, polyGR, polyGP), possibly because of their different biochemical properties and toxicity (Mackenzie et al. 2015; Gendron & Petrucelli 2017). It is unclear whether the DPRs coaggregate or aggregates in different inclusions, but they rarely coaggregate with TDP-43 (Davidson et al.

2014) (Figure 15). These inclusions are often detectable in the CNS, but rarely in the lower motor neurons. Since C9ORF72 ALS patients have a strong motor neuron phenotype, the contribution of these dipeptides to the pathology is still controversial (we will see some hypothesis above) (Mackenzie et al. 2015; MacKenzie et al. 2013; Proudfoot et al. 2014).

*TARDBP*

TARDBP gene is located on chromosome 1 (1p36.22) and is composed of 6 transcribed exons, which usually, are translated from exon2 to exon 6 (Pesiridis et al. 2009). Exon 6 represents the 60% of the gene and the 70% of the entire mRNA. The coded protein of 414 kDa is named TAR (transactivation response element) DNA binding protein of 43 kDa (TDP-43). TDP-43 is composed of two RNA recognition motifs (RRM), RRM1 and RRM2, a nuclear localization signal, a nuclear export signal and a glycine rich domain (Buratti et al. 2005; Hebron et al. 2013; Ignatius et al. 1995; Winton et al. 2008). TDP-43 has multiple functions both in the nucleus and in the cytoplasm. The two localization signals allow the shuttling of TDP-43 from nucleus to cytoplasm and *viceversa* (Winton et al. 2008). In the nucleus TDP-43 is a splicing regulator and a modulator of microRNA biogenesis. TDP-43 also influences the stability of various mRNA, thus regulating different cellular pathways. In addition, TDP-43 regulates the stability of its own mRNA providing a self-regulation of its own protein levels (Polymenidou et al. 2011; Ayala et al. 2011; Gregory et al. 2004; Xu 2012). A recent study has demonstrated that TDP-43 plays its role on RNA maturation by forming oligomeric structures through the interaction of the N-terminal domain. TDP-43 oligomerization depends upon RNA quantity and oligomeric forms of TDP-43 have a strong affinity to RNA compared to the monomeric form (Afroz et al. 2017).

In the cytoplasm, TDP-43 takes part in stress granules assembly and disassembly as its efflux is often a consequence of a stress. Nevertheless, TDP-43 has also a function in neuron plasticity as it takes part to RNA granules transport to dendrites extremities. This process allows the synthesis of protein *in loco* (Diaper et al. 2013; Alami et al. 2014; Liu-Yesucevitz et al. 2014; Colombrita et al. 2009).

TDP-43 was associated to ALS in 2006 and after this breakthrough discovery many mutations were described in TDP-43 (Neumann et al. 2006). Nowadays 29 ALS-associated missense mutations have been identified, 18 associated to fALS and 30 associated to sALS. They are mostly located in the C-terminal domain of TDP-43, with the exception of the D169G (Figure 16). The most frequent mutations are A382T (in which alanine in 382 is substituted with tyrosine) that is present both in fALS and in sALS and G348C (glycine in 348 is changed with cysteine) (Rutherford et al. 2008; Pesiridis et al. 2009).

TDP-43 abnormalities are found both in fALS (1-2% of total ALS cases) and in sALS (Sreedharan et al. 2008). Inclusions positive for TDP-43 have been found in cortical and spinal neurons of patients. This event is called "TDP-43 proteinopathy" and is found in 97% of ALS cases, with the exception of SOD1 and FUS associated ALS, where TDP-43 proteinopathy is absent. Either in presence and or in absence of TDP-43 mutation, these deposits are morphologically indistinguishable (Mackenzie et al. 2007; Mackenzie & Rademakers 2008; Maekawa et al. 2009) (Figure 16).

The formation of these inclusions prevents TDP-43 full length from exerting its normal and physiological function inside the nucleus. The consequence is a dysregulation of mRNA maturation and consequently alteration of cellular pathways, suggesting a loss of function of the mislocalized protein (Alami et al. 2014). Some studies demonstrated that TDP-43 mislocalization is toxic per se even in absence or prior to inclusions formation. It is still unclear if TDP-43 mislocalized in the cytoplasm is folded or misfolded and how it exerts toxicity in cell (Winton et al. 2008; Scotter et al. 2015).

TDP-43 inclusions also contain TDP-43 fragments of various size, caused by caspase cleavage. The most represented are the those of 35 and 25 kDa (Zhang et al. 2007). Inclusions containing these fragments are also found in FTD affected regions. Fragmentation of TDP-43 is a physiological process for the degradation of TDP-43, but the C-terminal fragments are highly aggregation prone being intrinsically disordered (prion-like) and owing the glycine-rich domain (Figure 19). In

addition, these fragments are mislocalization prone, since they entirely (TDP-35) or partially (TDP-25) loose the NLS. Since it is known that TDP-43 exerts its toxicity through a binding with the mRNA and aggregation is present also before fragmentation, the contribution of these fragments to TDP-43 toxicity is still controversial (Fuentealba et al. 2010; Scotter et al. 2015). It was demonstrated that TDP-35 causes defects in the splicing process (Che et al. 2011) while TDP-25 caused ubiquitinated and hyperphosphorilated inclusions of TDP-43. Phosphorylation is not a pre-requisite for TDP-25 aggregation, but TDP-25 exert a toxic gain of function on TDP-43 leading it to hyperphosphorilation and aggregation. These findings highlight TDP-25 as hallmark of the disease even if the exact mechanism of its toxicity is still unclear (Zhang et al. 2009). Caccamo et al., recently generate a mouse model homozygous for TDP-25 in which they show that this murine model shows ALS feature. Along with these findings they also demonstrate that TDP-25 forms insoluble inclusions and that in this model proteasome and autophagic power are weaker than in the control (Caccamo et al. 2015).

TDP-43 found in these inclusions often is hyper-phosphorylated and ubiquitinated (Figure 19). We still know little about the role of these post-translational modifications in the TDP-43 pathology. Phosphorylation is better studied, and it is now clear that hyper-phosphorylation is not a prerequisite for aggregation, but its presence is always associated with mislocalization and misfolding (Inukai et al. 2008; Neumann et al. 2010; Hasegawa et al. 2008).

TDP-43 inclusions also play dominant negative role recruiting other physiological and functional proteins in the cytoplasm. This gain of function further exacerbates the loss of function not only of TDP-43 proteins, but also of the other co-aggregating proteins (Scotter et al. 2015) (Figure 17).

### Other causative genes.

Other genes have been linked to fALS and are involved in various cellular functions. Only a very small group among fALS patients present these mutations. Nevertheless, the identification of these genes shade new light in understanding the mechanisms involved in ALS. Some of these genes are involved in RNA metabolism, degradative systems functioning and routing, neurofilaments dynamics, cytoskeleton assembly, stress granules formation etc.. (Figure 17) Here are reported some of the most important one.

#### *OPTINEURIN*

Optineurin (OPTN) is an adaptor receptor involved in many cellular functions that require protein-protein interaction. Among these functions OPTN acts as autophagic receptor that has a specific binding site for poly-ubiquitinated proteins and for autophagosomes. OPTN specifically recognizes the damaged cargo and drives it to the forming autophagosomes (Figure 18). The discovery of OPTN as an ALS gene suggests that the damage of a degradation systems could be as possible toxic mechanism. In 2010 there had been found 40 Japanese ALS cases, caused by mutation in OPTN (Maruyama et al. 2010). Typically, these mutations are frameshift mutations (that lead to truncated proteins) and non-sense mutations (that lead to not functional protein) which cause a dysregulation of the autophagic flux due to defects in autophagosomes maturation. Moreover, since OPTN activity regulates NF-kB functioning, mutations on OPTN lead to dysregulated NF-kB activity (Maruyama et al. 2010).

#### *VCP*

Valosin containing protein (VCP) is a multifunctional protein that is involved in various cellular functions, like proteins extraction from ER, protein routing to proteasome, stress granules dynamics, chromatin extraction etc… (Meyer & Weihl 2014; Ju & Weihl 2010; Bug & Meyer 2012). VCP exerts all these activities co-operating with a large group of co-factors (Papadopoulos et al. 2016; DeLaBarre & Brunger 2003). Mutations on this gene were firstly associated to inclusion body myopathy with Paget's disease of bones and frontotemporal dementia (IBMPFD); IBMPFD is a complex

disease that starts from muscle, in which mutations of VCP lead to the formation of not functional multivesicular bodies (Watts et al. 2004; Bayraktar et al. 2016; Guyant-Marechal et al. 2006). IBMPFD has some overlapping feature with ALS, and when VCP is present, the phenotype of the two pathologies often coexist (Koppers et al. 2012). VCP mutations do not lead to a complete loss of function of VCP. Instead they lead to the loss of one particular function. This loss of function is often connected to a loss of binding capability with one specific co-factor (Fernández-Sáiz & Buchberger 2010). Nowadays, researchers identified two major mutations associated with ALS: R155H (arginine in 155 is substituted by a histidine) and R191Q (arginine in 191 is substituted with a glutamine) (Badadani et al. 2010; Johnson et al. 2010).

*SQSTM1*

SQSTM1 is a gene that encodes for the protein of 62 kDa (p62). As already described above, P62 is a protein involved in autophagic recruitment of substrates. P62 structure comprises an ubiquitin associated (UBD) binding domain that recognises ubiquitinated proteins. P62 then drives these substrates to autophagosomes for the internalization (Rea et al. 2013; Bjorkoy et al. 2006; Johansen & Lamark 2011) (Figure 18). P62 mutations were firstly associated to Paget disease of bones (PDB) with the majority of the mutations found in the C-terminal UBA domain (Rea et al. 2014). there is a screening ongoing to found mutation also in ALS/FTD patients on p62 gene, since the relevance of this protein in neuroprotection suggest the possibility of mutation on p62 gene.

*PFN1*

Profilin 1 (PFN1) is a small protein associated to actin dynamics. It was identified as a causative ALS gene in 2010, and after that actin dynamics are regards as possible disease mechanism. Mutations in PFN1 lead to accumulation of TDP-43 in cells (Figley et al. 2014; Wu et al. 2012).

*UBQLN2*

Ubiquilin-2 (UBQLN2) is an adaptor protein that has a binding domain for ubiquitinated proteins and a binding domain for proteasome. Some recent studies also showed that UBQLN2 interacts with autophagic proteins (Lee & Brown 2012; Ko et al. 2004) (Figure 18). Initially, mutations on this gene were associated to an X-linked form of ALS and to ALS dementia (H. X. Deng et al. 2011). In 2014, UBQLN2 was assessed as causative gene of fALS, sALS and FTD-ALS, in individuals of both sexes. UBQLN-2 mutations cause accumulation of TD43 in affected cells, and this suggests a relevant role for the degradative systems in ALS pathogenesis (Majcher et al. 2015a; Williams et al. 2012; Morris et al. 2012).

There are several other genes causatives of ALS that account for a very small percentage of patients (ALSIN, SETX, VAPB, DCTN1, ANG, CHMP2B, FIG4, ATXN2, hnRNPA2B1, hnRNPA2A1). It is common that the prevalence of these rare mutations changes between populations, ethnises, etc… (Zufiría et al. 2016; Ajroud-Driss & Siddique 2014; Peters et al. 2015)

### Susceptibility genes

Studies like Genomic Wide Association Study (GWAS) also tried to identify genes associated to a higher probability of developing the disease. These susceptibility genes are very difficult to identify; indeed susceptibility genes associated to specific cohort of patients often cannot be associated to similar cohorts (Zufiría et al. 2016; Li et al. 2014; van Rheenen et al. 2013).

The protein Ataxin 2 (ATX2), causative of spinocerebellar ataxia 2 (SCA2) is a typical example of these genes. In fact, a polymorphic variant of ATX2, with polyglutamine tract in the highest normal range, but not pathologic has been found

linked to ALS in a particular cohort of ALS patients since it increases disease susceptibility. Other genes like UNC13A, ELP3, EPHA4, CYP27A1, ZNF512B, CX3CR1, KIFAP3, HTR2B, TMEM106B have been associated to different progression rate and survival time in ALS (Zufiría et al. 2016).

Epigenetic factors

DNA modifications and miRNAs expression are the most studied epigenetic factors related to ALS development.

DNA modifications lead to modulation of the expression of various genes. In many sALS patient the percentage of methylated DNA is higher than in the control cohort (Tremolizzo et al. 2014). Moreover, the activity and the expression of the histone deacetylase (an enzyme that promotes the deacetylation of histone leading to gene suppression) is higher in ALS brain and spinal cords respect to the control (Janssen et al. 2010; Valle et al. 2014). On the other hand, also miRNA are genetic modifiers involved in ALS even if their role is still controversial. Some miRNAs are reported to be protective, like miRNA-206 and miRNA-155. Indeed, mice deficient of miRNA-206 are more prone to develop ALS (Williams et al. 2009b) and miRNA-155 has been found in surviving MNs of patients dead for sporadic ALS (Koval et al. 2013). Other miRNAs are detrimental; for example miRNA-365 and miRNA-125b seem to exacerbate the disease while miRNA-1 and miRNA-206 have been also found in protein aggregates since they are bound to TDP-43 (Parisi et al. 2013; King et al. 2014; Gascon & Gao 2014).

## Pathogenic mechanisms

### *Protein misfolding and aggregation*

Protein misfolding is an important event in ALS pathogenesis. Misfolded proteins have lost their native and correct conformation and for this reason they are prone to form oligomeric structures, dimerizing with themselves and sequestering other soluble proteins (Soto & Estrada 2008; Rowinska-Zyrek et al. 2015). Oligomeric structures eventually become aggregates/inclusions that are a typical hallmark of ALS, detectable in many CNS areas such as spinal cord, cerebellum, hippocampus, thalamus, brainstem frontal and cerebral cortex (Watanabe et al. 2001; Al-Chalabi et al. 2012). As mentioned above, it is still unclear whether these inclusions are beneficial or detrimental. Some studies claim that these inclusions are not toxic, but protective in cells and acting as a sink to remove the most toxic species. These toxic species are believed to be the oligomeric forms or the misfolded protein itself (Ciechanover & Kwon 2015; Guo et al. 2010). In fALS mutated proteins encoded by the causative genes are more likely to lose their proper conformation. Indeed, they are found in inclusions either with or without the wild type counterpart. Moreover protein aggregation is poorly dependent on protein structure. For instance, mutated SOD1, TDP-43 and FUS formed skein-like inclusions in patient and animal tissues, as well as in *in vitro* models, even if they have very different structures (Parakh & Atkin 2016; Rosen et al. 1993; Neumann et al. 2006) (Figure 19).

In sALS cytoplasmic inclusions can contain wild type misfolded SOD1 as well as TDP-43 or FUS. Optineurin and ubiquilin2 are also occasionally found in sALS inclusions. TDP-43 inclusions, ubiquitinated and hyperphosphorilated are very common in almost every case of sALS, while FUS immunoreactive inclusions are found in a smaller percentage. C9ORF72 inclusions are not always positive for TDP-43, and sometimes co-aggregate with ubiquilin2 and p62 (Ajroud-Driss & Siddique 2014; H. X. Deng et al. 2011; Deng et al. 2010; D. H.-X. Deng et al. 2011).

### *Impaired protein degradation*

There are two main evidence that correlate degradative systems functionality with ALS pathogenesis: the presence of misfolded protein inclusions and the ALS associated mutation on many genes involved in the degradative pathways (Parakh & Atkin 2016).

As stated above, proteins that loose their normal conformation are targeted to the degradative pathways: proteasome and autophagy. Formation of proteinaceous aggregates means that the normal degradation of these proteins is less functional or totally abrogated (Figure 19-20). The causes of this dysfunction are different: overwhelming of the degradative pathways, dysfunction of the pathways due to presence of mutated protein linked to these pathways, that caused both haploinsufficiency of key proteins as well as dysfunctional activities. Proteins bearing ALS mutation are less functional (thus causing impaired degradation) and are also removed from the cellular environment, since they are mutated, causing haploinsufficiency. There are mutated proteins linked to proteasome activity (VCP, ubiquilin) and mutated proteins linked to autophagic pathway (p62) (Majcher et al. 2015a). The role of autophagy in ALS pathogenesis is more difficult to assess. There are some studies in which treatment with autophagic inducers rescues some of ALS phenotype such as neurite outgrowth, motor neuron loss and protein aggregation. On the other side, abnormal enhancement of autophagic flux is fatal to neurons and increases mortality in mouse models (Parakh & Atkin 2016).

***Cellular transport impairment***

Failure of the axonal transport is one of the earliest feature detected in ALS *in vivo* models, in particular in the most widely used ALS mouse model SOD1-G93A mice (Figure 20) (Williamson & Cleveland 1999). Mutated SOD1 co-aggregates with important component of the transport machinery like KAP3, causing shortening of the neurite as well as detachment and dysfunction of the axon (Tateno et al. 2009). Also, TDP-43 and FUS damage axonal transport due to the formation of resistant stress granules and the co-aggregation with neurofilaments (Li et al. 2013). In addition, supporting intracellular transport as pathogenic mechanism, there are some rare mutations of dynactin1, a component of the anterograde transport, and of profilin1, a small actin like protein (Puls et al. 2003; Wu et al. 2012). Even if the most widely studied processes regarding cellular transport are axonal dynamics, there are evidence about the impairment of the cellular transport that connect ER to Golgi apparatus. Disruption of this transport is an early event in tg ALS SOD1 mice that even precedes onset of the disease (Soo et al. 2015a; Atkin et al. 2014). Nevertheless, dysfunction of this mechanism causes ER stress, Golgi fragmentation, protein aggregation and apoptosis. For instance, TDP-43 and FUS aggregation cause disruption of ER-Golgi transport as well as aggregated dipeptide repeats associated to C9ORF72 expansions (Soo & Atkin 2015; Atkin et al. 2014; Sundaramoorthy et al. 2015).

***Oxidative stress***

Oxidative stress was firstly studied in relation to SOD1 mutation, since it was initially thought as a dysfunctional protein unable to correctly handle aberrant oxygen radicals. During years, it has emerged that mutated SOD1 exerts a toxic dominant gain of function (Akbar et al. 2016). Mutated SOD1 takes radicals form the other cellular antioxidants and gives them to the oxygen thus creating free oxygen radicals. The presence of these free radicals induces oxidative post-translational modifications of the other soluble proteins (Barber & Shaw 2010). Oxidative post-translational modifications alter proteins solubility and folding driving them to the formation of aggregates (Beckman et al. 2001; Bonafede & Mariotti 2017; Grune et al. 2004). Interestingly, the levels of glutathione are strongly reduced is brain tissue of affected patients, either fALS or sALS patients, also in those cases characterized by TDP-43 inclusions (Iguchi et al. 2012). These evidence suggest that oxidative stress is a pathogenic mechanism related both to mutated SOD1, and to other form of ALS. Oxidative stress is also present when TDP-43 and FUS are bearing mutations, and the dynamics (especially regarding stress granules formation) of these two proteins are changed in presence of oxidative stress (Colombrita et al. 2009).

***ER stress***

ER stress is not widely implicated in fALS or sALS and it is still largely discussed which is its contribution to the pathogenesis. ER stress is caused by the presence of mutated and unfolded proteins, but it is also a consequence of ER-

Golgi transport disruption (Chen et al. 2005) (Figure 20). Nevertheless. it has been demonstrated that most of ALS-related protein caused the activation of the unfolded protein response (an event downstream ER stress) and that inhibition of UPR is beneficial in many animal model of ALS (Cuanalo-Contreras et al. 2013; Parakh & Atkin 2016).

***Mitochondrial dysfunction***

Mitochondrial abnormalities have been firstly identified in muscle and in neurons innervating muscle of sALS patients. In these tissues mitochondria form large clusters and alteration in their morphology. The mechanism that drives to mitochondria dysfunctions have been studied in SOD1 cases since a fraction of SOD1 is localized in mitochondria. In these models, mitochondria appear vacuolated, the mitochondrial membrane is depolarized, and calcium storage and ATP production are disrupted (Boillée et al. 2006). Mutated SOD1 can mediate the fusion of peroxisome with mitochondria, thus forming vacuolated mitochondria. Moreover, SOD1 aggregates on the outer mitochondrial membrane impair TOM complex and thus many mitochondrial functions (Liu et al. 2004; Pasinelli et al. 2004).

***RNA metabolism and stress granules dynamics***

In the ALS field, RNA biology has gained attention after the identification of ALS related mutations in four genes that regulates RNA metabolism. RNA metabolism relies upon the formation of membrane less structure, formed via a process of liquid-liquid demixing (Taylor et al. 2016). This liquid coalescence is driven by the presence of RNA binding proteins with a low complexity domain (Molliex et al. 2015; Lin et al. 2015; Patel et al. 2015). TDP-43, FUS and hnRNPs possess this domain, and usually it is the domain that contains ALS-related mutations (Figure 20). Liquid coalescence form structures named nucleoli or stress granules (SGs); these structures are highly dynamic and are formed to preserved RNA from degradation. On the other hand, the formation of these structures brings these proteins very closed. The low complexity domain of these proteins is highly aggregation prone and tends to form amyloid like fibrils, if the phase transition is impaired. Mutations can alter this transition influencing the material properties and the function of these granules. Furthermore, the formation of these insoluble structures, not only is toxic to cells, but also sequester proteins reducing their normal activity (Molliex et al. 2015; Patel et al. 2015; Lin et al. 2015).

***Accumulation of neurofilaments***

Another important hallmark of ALS is the cytoplasmic accumulation of hyper-phosphorylated neurofilaments. Mutations on gene encoding for neurofilaments are found both in fALS and in sALS cases. Physiologically, neurofilaments regulate axon diameter and axonal transport (Yuan et al. 2006). Their activity is inversely correlated to their phosphorylation. The hyperphosphorylation of these neurofilaments lead to axonal disruption and to their accumulation in the perinuclear region or in the axon proximal region (Xiao et al. 2006). Overexpression of these neurofilaments is able to slow down the progression of the disease in animal model (Kong & Xu 2000).

***Excitotoxicity***

Glutamate is the most abundant excitatory effector of the central nervous system. Glutamate excitotoxicity was one of the first mechanism proposed for understanding ALS. Nowadays, we know that there is a state of hyper-excitability due to an increase in the concentration of glutamate in the synapses (Bendotti & Carrì 2004). This increase of glutamate is caused by the reduced levels of the excitatory amino acid transporters (EAAT2) that normally reduces glutamate concentration at synapsis after glutamate excitatory action. The reduced presence of EAAT2 at synapsis is probably caused by aberrant EAAT2 mRNA that also leads to impaired calcium permeability that is another toxic event (Lin et al. 1998; Guo et al. 2003).

***Neuroinflammation: involvement of the non-autonomous system***

The main effectors of neuroinflammation in ALS are microglia and astrocytes, they coordinates the immune response after neuron injury. It has been demonstrated that these non-autonomous cells play a pivotal role in pathogenesis fALS (Figure 20).

Microglia is the immune effector in the CNS and the cross talk between microglia and neurons is very well established. It has been demonstrated that dysfunctional microglia is determinant in ALS onset. In fact, mutated SOD1 expressed only in motor neuron is not able to induce neurodegenerative phenotype, while wild type glia is able to prevent onset and progression of ALS (Bonafede & Mariotti 2017; Clement 2003). It has been demonstrated that, in the first stage of the pathology, the M2 phenotype of glia (neuroprotective and anti-inflammatory) prevails. Then, during the progression of the disease, SOD1 is released by affected neurons in the extracellular matrix as well as other toxic factors. This event triggers the switch of M2 microglial cells into M1 microglial cells (pro-inflammatory and neurotoxic cells that secerns ROS and cytokines) (Zhao et al. 2009; Appel et al. 2011; Almer et al. 1999).

The other components of glia are astrocytes and they have a role in supporting neuron viability. They have the function of maintaining low levels of glutamate at the synapses. In fALS and sALS patients, astrocytes reduce the levels of EAAT2 thus increasing the concentration of glutamate and exacerbating the excitotoxicity (Howland et al. 2002).

**Prion like spreading of toxicity**

ALS is a pathology that starts focally in the CNS and then spreads in the surroundings areas. It has been proposed that the spreading of the pathology is linked to a prion like spreading mechanism and that ALS-associated proteins have prion-like properties (Kanouchi et al. 2012; Nonaka et al. 2013; Ravits & La Spada 2009). It has been demonstrated that aggregates of TDP-43 are able to induce aggregation in other cells. TDP-43 also possesses a prion like domain that justifies this property (Polymenidou & Cleveland 2012). Nevertheless, some studies demonstrate that also SOD1 is a prion like protein even without a prion like domain (Healy 2017).

**ALS and Fronto-temporal lombar dementia (FTLD)**

Fronto temporal lombar dementia (FTLD) is a cognitive impairment raised from degeneration of the V layer of the frontal region. Over decades, this disease has been associated with ALS. 25% of ALS patients are likely to manifest also FTLD even if often FTLD precedes motor signs and only retrospectively FTLD and ALS are associable in these patients (Swinnen & Robberecht 2014; Mioshi et al. 2014; Rippon et al. 2006). ALS and FTLD form a spectrum, a continuum in which the extremities are pure ALS (without cognitive dementia) and pure FTLD (without motor signs) (Ferrari et al. 2011; Swinnen & Robberecht 2014) (Figure 21). In the middle of this spectrum there is ALS with behavioural impairment (ALSbi, in which dementia has a mild severity), ALS with cognitive impairment (ALSci, in which patients show mild executive and language dysfunction). ALS patients that meet Neary criteria (Neary criteria is a scale of clinical signs to classify the gravity FTLD) develop ALS-FTLD. The last part of the spectrum is FTLD that develop motor signs. This is very common between FTLD patients: up to 50% develop ALS. This mixed disease is called FTLD-MND. The boundary between these categories is very blurry, but it helps in individuating which disease is the prevalent (Strong & Yang 2011). Patients belonging to these categories show different rate of progression. Patients with pure ALS have a longer prognosis compare to the ones that develop also dementia. The reason of this difference is still unclear, but one hypothesis relies on the different compliance to the therapy. In fact, patients that developed also FTD, are less compliant to the cure, due to the developing of dementia that makes them uneasy to treat (Mioshi et al. 2014).

ALS and FTLD show a significant overlap in clinical signs and this lead to the possibility that also some pathogenic mechanisms are common between the two disease. In this view understanding a feature of one of the two pathologies can help in shading light on the other.

### Evidence of muscle involvement

The role of skeletal muscle cells and of muscle tissue in ALS onset and progression is still very controversial. It very well known that a dying back mechanism from muscle to motor neuron exists due to their very strict crosstalk. Moreover, neuromuscular junction waste occurs prior to motor neuron loss and symptoms development. There are indeed several evidence of muscle damage prior to disease onset (Halter et al. 2010). In ALS mouse models, muscle are smaller and more atrophic than in controls. In addition, electrophysiological studies on neuromuscular junction show severe impairment already at week 4 (for *in vivo* model 4-6 week is pre-symptomatic stage). Moreover, in these muscles there is a decreased myogenesis due to a reduction of CDK5 activity (Park & Vincent 2009).

There are molecular mechanisms similar in motor neuron and in muscle that lead to cell toxicity and death; the most important ones are the accumulation of misfolded proteins and the excessive oxidative stress (Bhattacharya et al. 2014). Some *in vivo* studies reported that in affected muscle there is a down regulation of the heat shock proteins (protective players in motor neurons), and thus the hypothesis of protein toxicity gains relevancy. On the other hand, oxidative stress has been found before onset of the pathology and is thought to be exacerbated by an excessive oxidative metabolism. There are evidence of boosted fatty acid metabolism also in the pre-symptomatic ALS stage. Interestingly, diet with high content of fatty acid shows beneficial effects on ALS disease (Dupuis et al. 2004). Another important event in mutant muscle is mitochondrial dysfunction, revealed by biochemical abnormal activity, ultrastructural modification and alteration in mitochondrial activity. It has been shown that, in mutant SOD1 muscle, the expression of PGC-1α is enhanced, suggesting that mitochondrial biogenesis is always active to improve muscle functions also at the end stage of the disease (Cruz et al. 2013).

Importantly, since miRNA circuits are highly involved in muscle maturation and functions, it has been shown that reduction in miRNA206 expression caused an accelerated ALS progression in SOD1-G93A mice (Gascon & Gao 2014; Williams et al. 2009a).

While is evident that muscle is damaged during ALS disease, its role in the pathogenesis is still controversial. The expression of mutated SOD1 in muscle cells is able to induce atrophy and muscle weakness but does not trigger ALS disease and motor neuron death (Wong & Martin 2010). In line with these evidence the suppression of mutated SOD1 in muscle by means of antisense oligonucleotide (ASO) increases muscle growth, but does not recue the survival. Contrasting with these studies, many groups reported that restricted overexpression of SOD1 in muscle, caused muscle atrophy, destabilization of neuromuscular junction (NMJ), axonopathy and by a retrograde process motor neuron loss (Dobrowolny et al. 2008). Indeed, it has been shown that IGF-1 overexpression, alleviate all this symptoms slowing down ALS progression in mice models (Dobrowolny et al. 2005; Dobrowolny et al. 2008). Recent studies also demonstrated that restricted muscle expression of mutated SOD1, changes transcriptome of miRNAs in motor neurons (Dobrowolny et al. 2015), thus confirming role for muscle in motor neuron impairment.

Another *in vitro* evidence is that the overexpression of SOD1 in satellite cells (muscle stem cells) damages satellite cell capacity of becoming mature muscle cells that can fuse and form a functional contractile unit. It is still largely unknown if there is a type of fiber (slow- or fast-twitch) that is primarily affected in ALS.

### The protein quality control system in ALS

Many studies have evidenced the role of the protein quality control (PQC) system in ALS. Proteasome is heavily involved in the degradation of almost all ALS-associated protein. Some pharmacological approaches try to suggest an induction

of proteasome activity in order to counteract the presence of these toxic proteins. Nevertheless, increasing the proteasome activity may have devastating effects on cells, since many physiological proteins are degraded by proteasome.

*In vitro* studies demonstrated that SOD1-G93A could be specifically degraded by autophagy through the CASA complex. Indeed, the overexpression of HSPB8 caused a significant reduction of aggregated SOD1-G93A in motorneuronal model of ALS and to support this data, it has been shown that surviving motoneurons in G93A mice at the end stage, display an increased HSPB8 expression, indicating a protective role for the HSPB8, and possibly for the CASA complex (Crippa et al. 2010). Moreover it has been demonstrated that HSPB8 reduces also the aggregation of dipeptide repeats produced in presence of C9ORF72 mutation (Cristofani, Crippa, Vezzoli, et al. 2017)

Direct induction of autophagy by rapamycin is detrimental for the progression of ALS in G93A mice, since autophagy is also an unspecific process that degrades organelles, cytoplasm and proteins (Zhang et al. 2011). On the other hand, targeting of specific misfolded proteins to degradation by autophagy is promising strategy. In fact increasing selective autophagy by increasing CASA complex activity leads to the degradation only of aggregation-prone, toxic and damaged proteins. This is further confirmed by compounds that increasing the overexpression of HSPB8 counteracts the formation of aggregate in mutant TDP-43 models (Crippa, D'Agostino, et al. 2016).

In *in vivo* ALS models, some studies have also identified the difference between motor neurons and muscle regarding the protein quality control system activation. Mice G93A, at the END stage, show and an increased activation of the PQC system especially in muscle. Indeed, at the end stage the expression of HSPB8 and BAG3 (CASA complex) as well as the expression of LC3 and p62 were significantly increased. These results suggest an important role of the whole protein quality control system in development of ALS (Crippa et al. 2013).

### Therapeutic approaches

ALS is still a disease for which a cure that stops the progression is not available. All therapeutic approaches available are obviously aimed at the extension of the survival, to slowing down the progression of the disease and to ameliorate the clinical complexity of the disease. The first drug approved by US Food and Drug Administration (FDA) was Riluzole, an inhibitor of the glutamate release that reduces the excitotoxicity on neurons (Miller et al. 2012). Riluzole has also been studied in association to other drugs like Rasigiline (a MAO inhibitor) that has an antioxidant action (Waibel et al. 2004). The study demonstrated that the co-treatment of the two drugs is more efficient than the treatment of the single drug. Very recently FDA also approved edavarone (Radicava™) for the treatment of ALS. Edavarone is an antioxidant drug that brings an extension of lifespan in treated patients (Ikeda & Iwasaki 2015).

Since pharmacological approaches are not giving striking results, gene therapy and stem cells therapy are gaining attention (Bonafede & Mariotti 2017). These two strategies for the moment are mainly studied in animal models and few clinical studied are available.

Gene therapy for ALS aims at silencing mutated genes associated to toxicity. Some clinical studies in phase I are treating patients with antisense oligonucleotide (ASO) to reduce the expression of mutated SOD1. The problem associated with this strategy is mainly the compliance of the patient: the infusion of ASO should be continuous and administration must be intrathecal (Smith et al. 2006).

Stem cells are becoming a promising therapy thanks to stem cell ability to differentiate in various tissues (upon specific signals) and thanks to stem cell paracrine activity. Nowadays various type of stem cells are available and they differ for the source and for the ability to differentiate. The type of stem cell is chosen by their ability to engraft, differentiate, survive, and migrate to the damage tissue. Moreover, stem cells are neuroprotective since they secrete many trophic factors that can prevent motor neurons loss. For the moment only animal models have been treated with stem cells.

The results are promising, but there still many issues that needed to be solved before administering stem cells to patients (Faravelli et al. 2014).

| Locus | Gene | Protein | Protein function | Mutations | Proportion of ALS | | Date of discovery |
|---|---|---|---|---|---|---|---|
| | | | | | Familial | Sporadic | |
| 21q22.1 | *SOD1* | Cu–Zn superoxide dismutase | Superoxide dismutase | >150 | 20% | 2% | 1993 (ref. 2) |
| 2p13 | *DCTN1* | Dynactin subunit 1 | Component of dynein motor complex | 10 | 1% | <1% | 2003 (ref. 52) |
| 14q11 | *ANG* | Angiogenin | Ribonuclease | >10 | <1% | <1% | 2006 (ref. 141) |
| q36 | *TARDBP* | TDP-43 | RNA-binding protein | >40 | 5% | <1% | 2008 (refs 67 and 142) |
| 16p11.2 | *FUS* | FUS | RNA-binding protein | >40 | 5% | <1% | 2009 (refs 68 and 69) |
| 9p13.3 | *VCP* | Transitional endoplasmic reticulum ATPase | Ubiquitin segregase | 5 | 1–2% | <1% | 2010 (ref. 44) |
| 10p15-p14 | *OPTN* | Optineurin | Autophagy adaptor | 1 | 4% | <1% | 2010 (ref. 42) |
| 9p21-22 | *C9orf72* | C9orf72 | Possible guanine nucleotide exchange factor | Intronic GGGGCC repeat | 25% | 10% | 2011 (refs 8 and 77) |
| Xp11.23-Xp13.1 | *UBQLN2* | Ubiquilin 2 | Autophagy adaptor | 5 | <1% | <1% | 2011 (ref. 40) |
| 5q35 | *SQSTM1* | Sequestosome 1 | Autophagy adaptor | 10 | <1% | ? | 2011 (refs 41 and 143) |
| 17p13.2 | *PFN1* | Profilin-1 | Actin-binding protein | 5 | <1% | <1% | 2012 (ref. 144) |
| 12q13.1 | *HNRNPA1* | hnRNP A1 | RNA-binding protein | 3 | <1% | <1% | 2013 (refs 70 and 71) |
| 5q31.2 | *MATR3* | Matrin 3 | RNA-binding protein | 4 | <1% | <1% | 2014 (ref. 76) |
| 2q36.1 | *TUBA4A* | Tubulin α-4A chain | Microtubule subunit | 7 | <1% | <1% | 2014 (ref. 145) |
| 22q11.23 | *CHCHD10* | Coiled-coil-helix-coiled-coil-helix domain-containing protein 10 | Mitochondrial protein of unknown function | 2 | <1% | <1% | 2014 (ref. 146) |
| 12q14.1 | *TBK1* | Serine/threonine-protein kinase TBK1 | Regulates autophagy and inflammation | 10 | ? | ? | 2015 (ref. 147) |

*Figure 11 Gene involved in hereditary ALS* (Taylor et al. 2016)

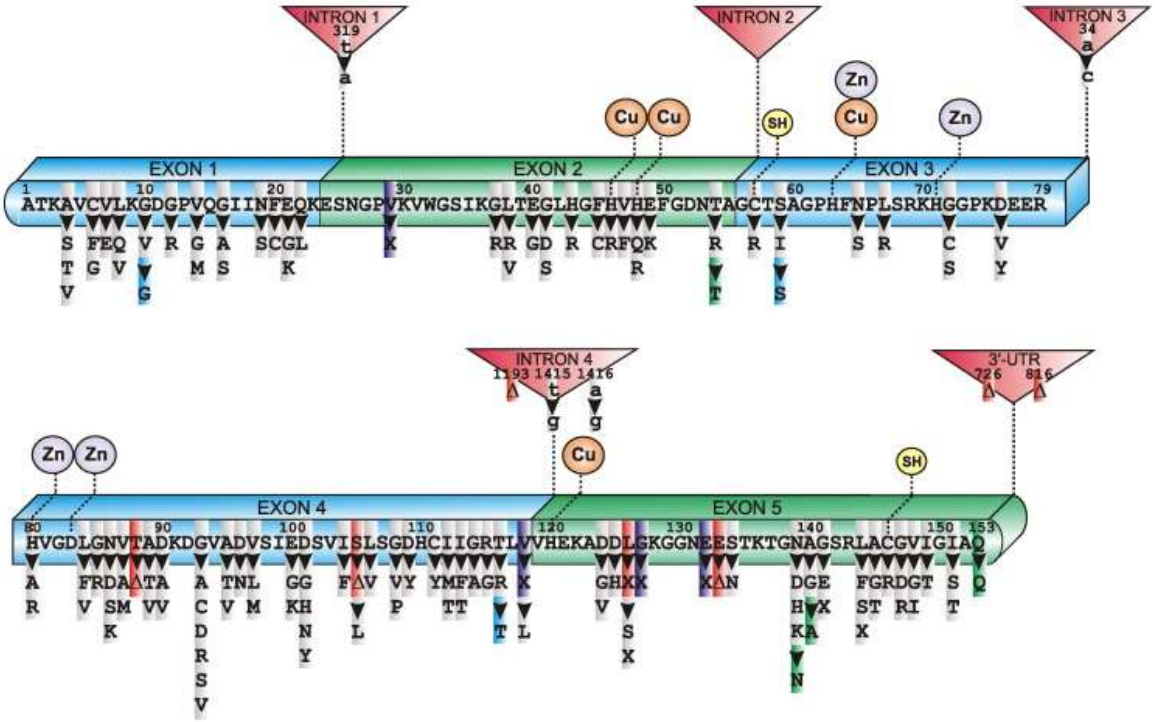


*Figure 12 Structure of SOD1 gene and ALS- associated mutations* (Turner & Talbot 2008)

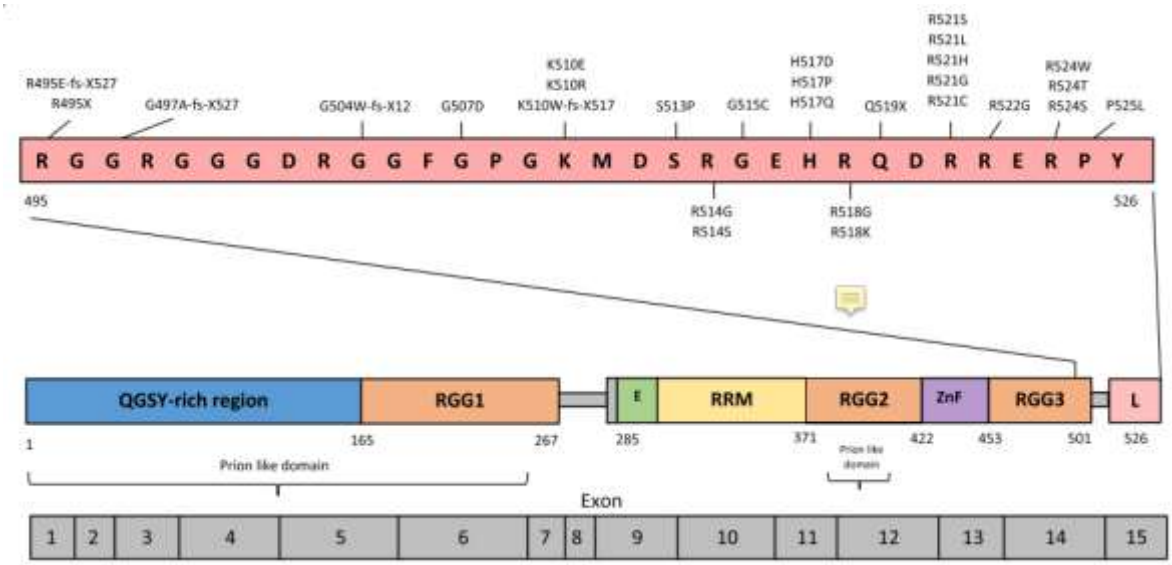


*Figure 13 Structure of FUS gene and position of ALS-related mutations* (Nolan et al. 2016)

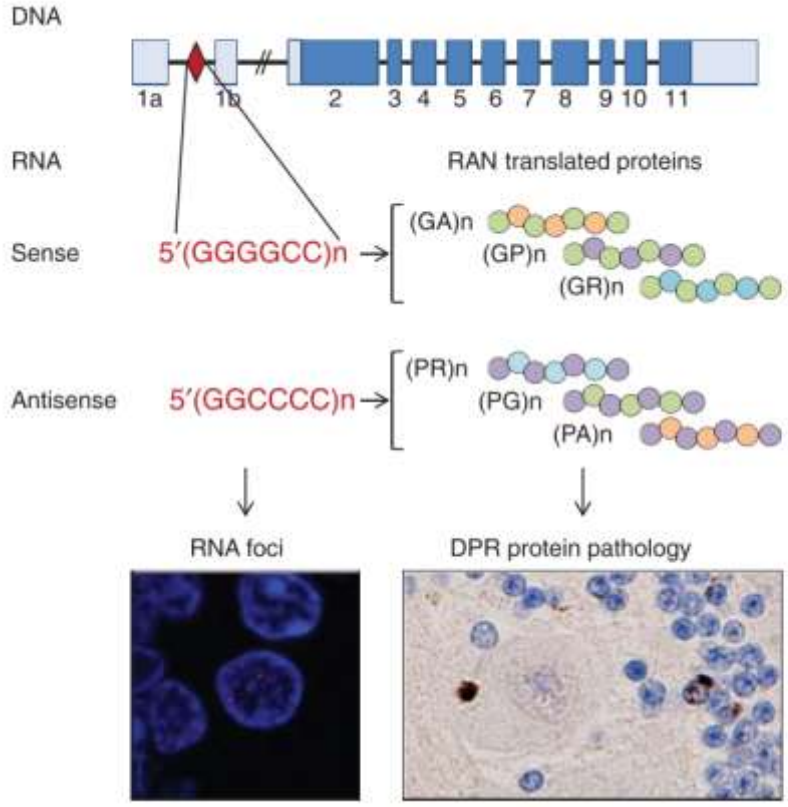


*Figure 14 DPR production by RAN-translation on sense and anti-sense transcript of $G_4C_2$ expansion* (Gendron & Petrucelli 2017)

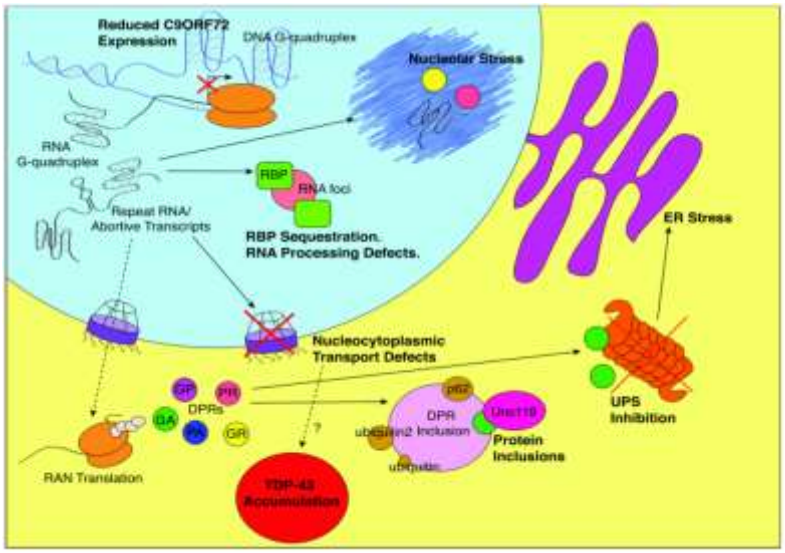


*Figure 15: C9ORF72 mechanisms of toxicity* (Todd & Petrucelli 2016)

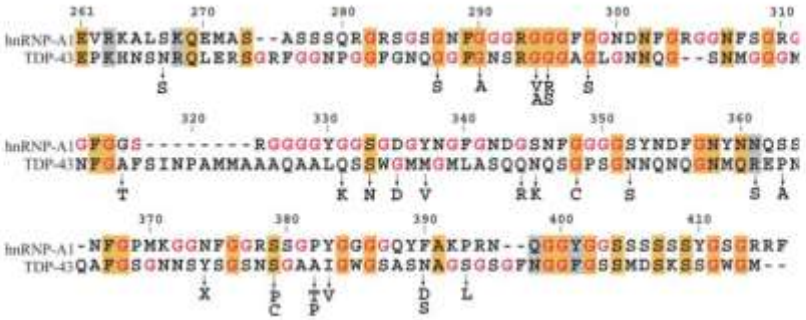


**Figure 1.** The glycine-rich domain protein sequence alignment of TDP-43 and hnRNP-A1 is shown with amino acid numbering (top) corresponding to the TDP-43 amino acid number. Identical and similar amino acid residues are boxed and colored in orange and grey, respectively. Glycines are highlighted in red and the arrows indicate missense mutations in TDP-43 with their corresponding amino acid change.

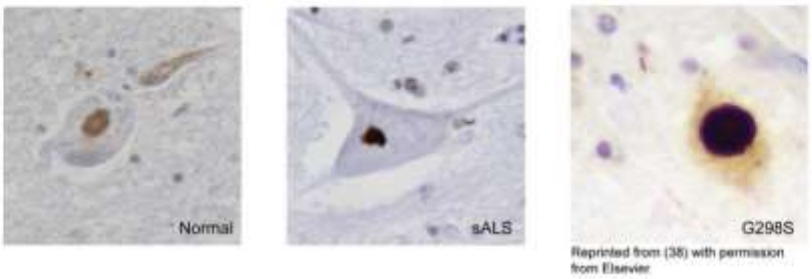


*Figure 16 TDP-43 ALS-associated mutation and TDP-43 inclusions in motor neurons of both SALS and fALS patients* (Pesiridis et al. 2009)

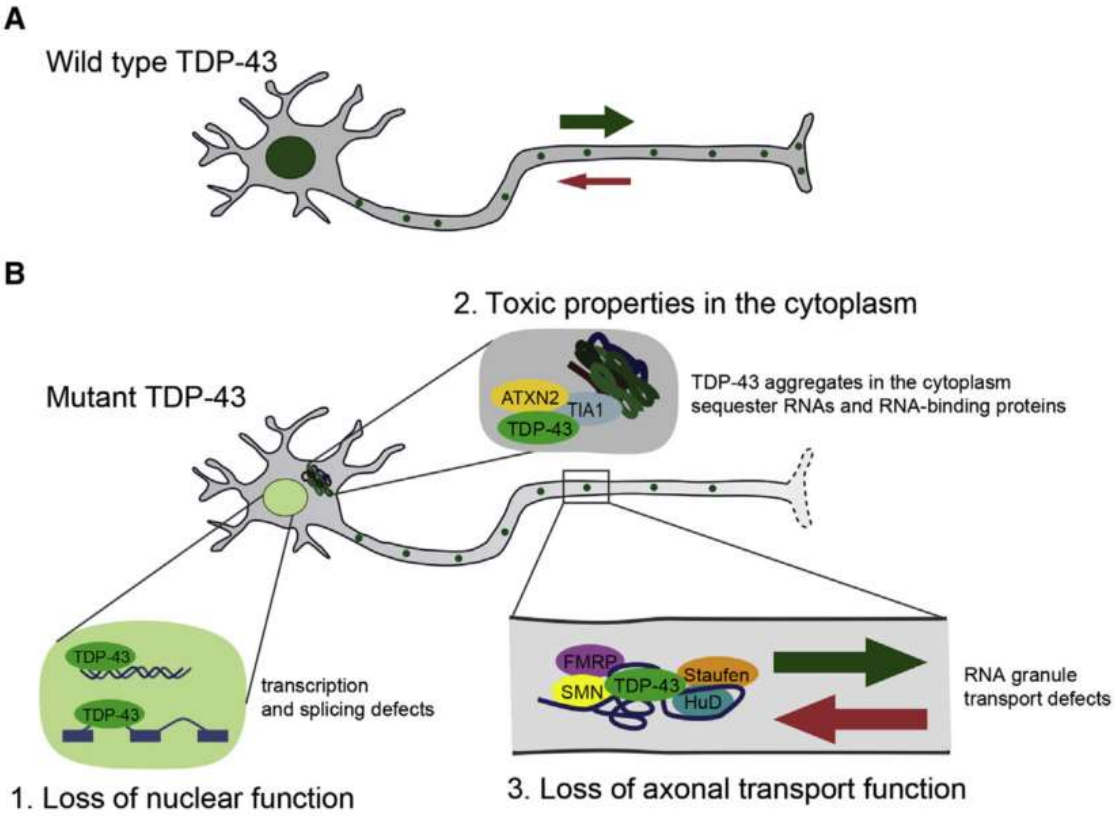


*Figure 17 pathway affected by aberrant TDP-43* (Jovicic & Gitler 2014)

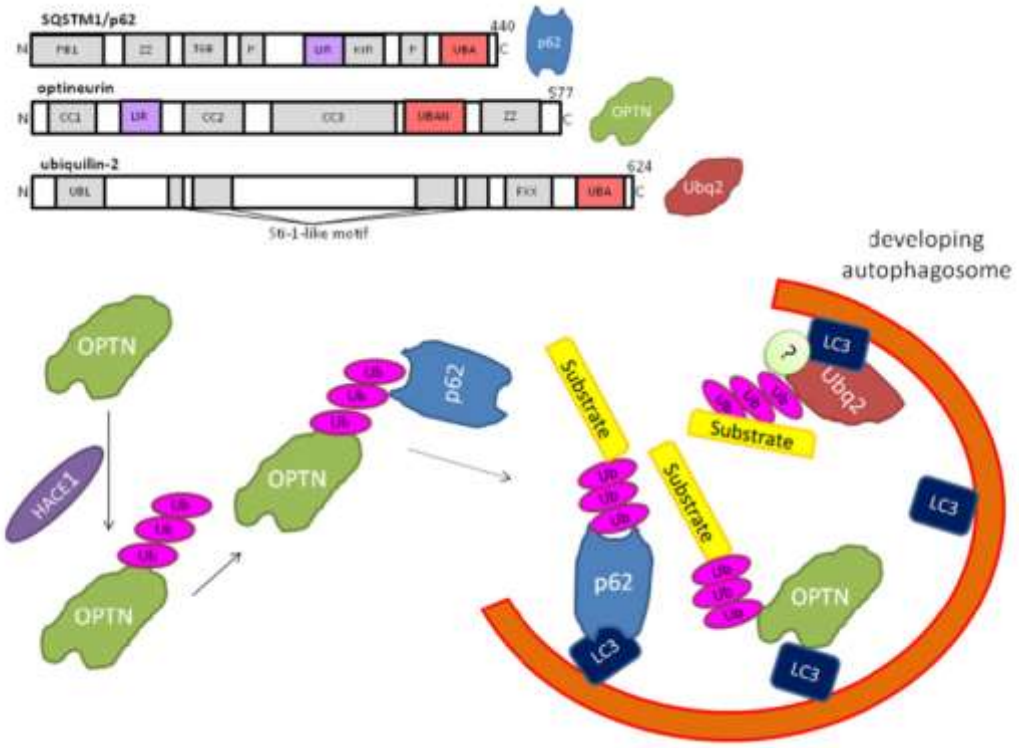


*Figure 18 Physiological role of p62, OPTN and UBQLN* (Majcher et al. 2015b)

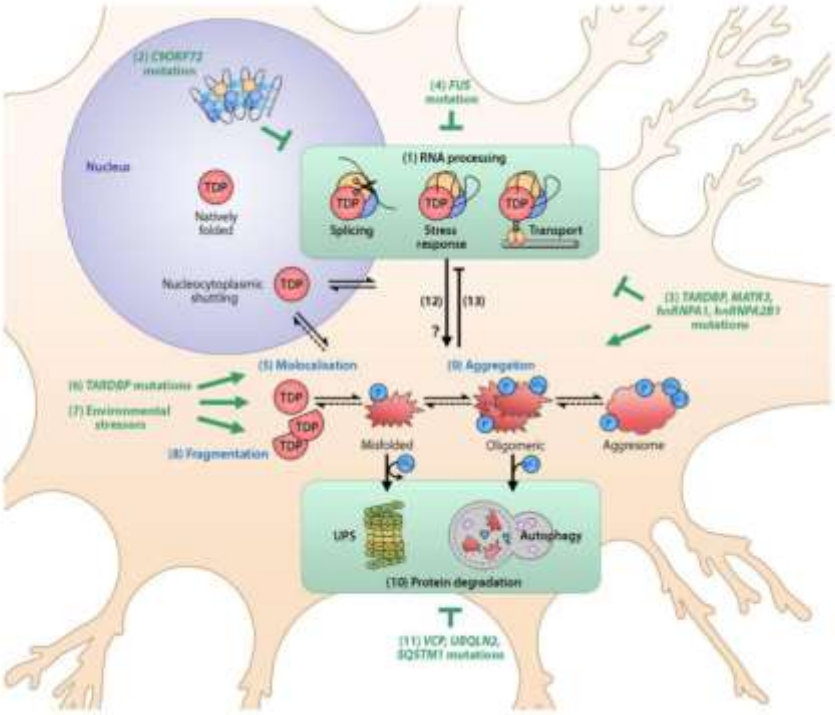


*Figure 19 TDP-43 aberrant behaviour in presence of ALS-related mutated gene* (Scotter et al. 2015)

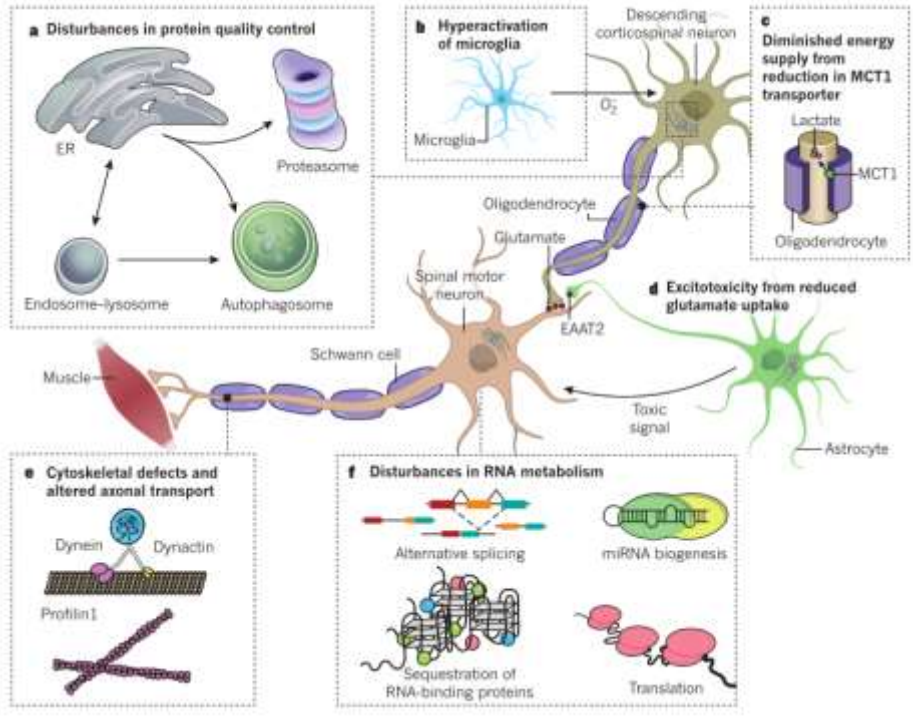


*Figure 20 ALS related pathogenic mechanisms* (Taylor et al. 2016)

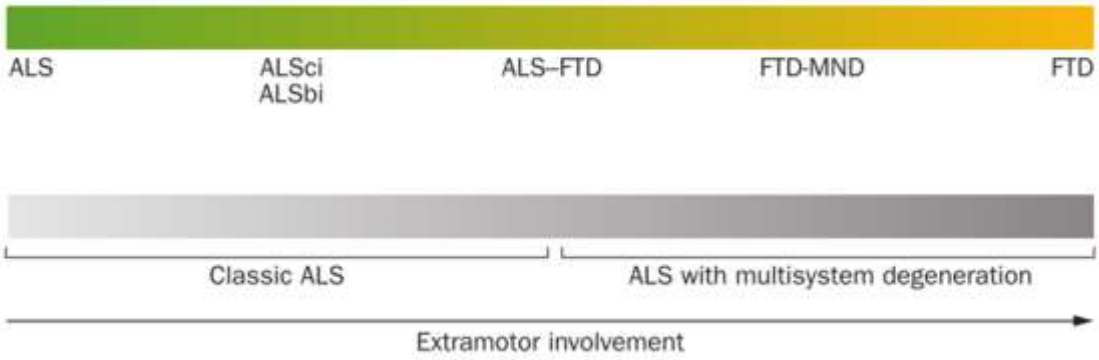


*Figure 21 ALS-FTD spectrum* (Swinnen & Robberecht 2014)

## SPINAL AND BULBAR MUSCULAR ATROPHY

Spinal and bulbar muscular atrophy (SBMA) is a MND characterized by the loss of lower motor neuron in the anterior horn of the spinal cord and in the brainstem motor nuclei. Only third, fourth and sixth cranial nerves are not target of the disease (Banno et al. 2012). It is also known as Kennedy disease, from Dr. William R. Kennedy who described clinical signs, pattern of inheritance and pathological feature of the disease. In 1989, Fischbeck and colleagues found out that the cause of the disease was linked to chromosome X and in 1991 La Spada discovered the genetic cause of the disease: the presence of a polyCAG repeat in the androgen receptor gene (La Spada AR et al. 1991). This CAG repeat is translated in a polyglutamine (polyQ) tract.

After the identification of CAG expansion in SBMA, this type of mutation has been found on other genes, unrelated to AR, that are at the cause of other NDs. This group of diseases are called polyglutamine diseases and they share not only the mutation, but also some clinical phenotype such as age of onset and rate of progression, suggesting the existence of a common mechanism between all of these pathologies (Giorgetti & Lieberman 2016a).

So far, 9 members of this family have been identified (Figure 22): Huntington's disease (HD), SBMA, DentatoRubral–PallidoLuysian Atrophy (DRPLA) and 6 spinocerebellar ataxias (SCA) (Fischbeck 2001). There are also other diseases caused by the presence of repeated triplets (100-3000 repetitions) in the untranslated region of genes. Some of these diseases are fragile X syndrome, myotonic dystrophy and Friedreich ataxia (Poletti 2004).

SBMA is affecting only male subjects and is inherited in a recessive fashion. Age of onset and severity of the disease seem to be linked to the length of the repetition. Usually, CAG repeats are from 11 to 25-27. The tract is described as pathological when it contains more than 38 repetitions. Subjects with medium CAG size (27-37) are borderline subjects (Kuhlenbäumer et al. 2001).

### Epidemiology and clinical sign

SBMA is a rare disease affecting 1/400000 patients per year (Fischbeck 1997). The prevalence of this disease varies a lot among different areas (Querin et al. 2017). Moreover, SBMA is often misdiagnosed with ALS.

SBMA is an adult onset disease (30-50 years of age) and its progression is very slow (Katsuno et al. 2012; Fratta et al. 2014). Indeed, life expectations after diagnosis are in avarage 27 years (Guidetti et al. 2016). The CAG elongation seems to not interfere with the disease progression (Fratta et al. 2014).

The main clinical manifestations can be divided in spinal signs and bulbar signs. Spinal signs, that are muscle weakness of upper and lower limbs, often appear first compare to bulbar ones and for long time they were considered as the sole onset manifestations. Affected muscles are initially and more frequently lower limb followed by upper limb. Muscle weakness is often preceded by slighter symptoms that are frequently underestimated, like hand tremor, myalgia, breast enlargement, muscle cramps and premature exhaustion after physical exercise.

Bulbar signs, due to involvement of brainstem, usually follow limb weakness and in most cases are dysphagia and dysarthria. Also jaw drop, caused by bulbar muscle weakness, is eventually present. Another important and characteristic bulbar sign is tongue fasciculation, with irregularities at the edge and deep furrowing due to wasting. Tongue atrophy is also linked to vocal cord atrophy, pharyngeal paresis (causing uncomplete bolus clearance) and palatal weakness (causing nasal voice). Even if these bulbar symptoms show up after spinal ones, they are sometimes present also in the pre-diagnostic phase (Finsterer & Soraru 2016; Harding et al. 1982; Fratta et al. 2014).

SBMA patients also show other clinical signs different from neuromuscular manifestation. Most important systemic symptom, related to endocrine dysfunctions, is gynecomastia always accompanied by testicular atrophy, azoospermia, oligospermia, erectile dysfunction and reduced libido. Some patients also show dyslipidemia abdominal obesity and liver dysfunction. Other rare systemic signs are cardiomyopathies and urological diseases that always end up with the

need of a catheter. Sometimes there are also neuropsychiatric signs such as mild form of dementia and cognitive impairment mainly affecting memory, both short and long term (Kessler et al. 2005; Dejager et al. 2002; Querin et al. 2016).

### *Diagnosis*

SBMA diagnosis is often difficult due to the similarity with other motor neuron disease. It is misdiagnosed with the spinal form of ALS that also starts with limb weakness. The first diagnostic tool is finding the polyQ elongation in the AR gene. Even if the disease sometimes shows up as sporadic it is important to perform an analysis of the family history. Another laboratory analysis that can help in identifying SBMA is measuring the levels of creatine phosphokinase, indicators of muscle sufferance. Sometimes also muscle biopsies are performed to analyze the presence of muscular neurogenic atrophy (Mariotti et al. 2000; Georgiou et al. 2001).

## Androgen receptor: structure and physiological functions

### *Gene structure*

Androgen receptor belongs to the steroid nuclear receptors superfamily.

The gene encoding for the androgen receptor is located on the long arm of the chromosome X, precisely in the Xq11–q12 position. The whole gene span for almost 54 kb and the open reading frame is composed of 8 exons (Brinkmann 2001) (Figure 23).

Exon 1 encodes for the N-terminal region of the AR protein. This region contains the transactivation domain, the polyglutamine tract and a polyglycine and a polyproline region that are poorly conserved among steroid nuclear receptor superfamily. Exon 2 and exon 3 encode each for a zinc finger domain that is a very well conserved DNA binding domain. The remaining 5 exons encode for the C-terminal region that is the ligand binding region. 5' region of the exon 4 codes for the hinge region while the 3' region contains the sequence for the nuclear localization signal (NLS). Exons 5, 6, 7 and 8 encode for the steroid binding domain. Exon 4 and exon 5 also contain 2 androgen responsive elements (ARE) that upregulates the synthesis of AR mRNA in target tissues (Brown et al. 2013).

The promoter region has a GC rich region and a SP1 binding site instead of the canonical TATA box. In this region is also present a secondary open reading frame, 1100 upstream from the transcription starting site, that encodes for a polypeptides of 9 aminoacids whose role is still obscure (Georgiou et al. 2001).

### *Protein structure*

The functional domains of the AR protein are: the N-terminal transactivation domain, the two Zinc fingers, constituting the DNA binding sites and the C-terminal steroid binding domain (Figure 23).

The N-terminal transactivation domain contains the signal for AR dimerization, for binding with other transcriptional factors, and for post-translational modification. Its capacity of binding the C-terminal domain of another AR protein is very important for forming the functional homodimer and this dimerization is testosterone dependent. The presence of the polyQ tract influences this function. In fact, when polyQ tract is abnormally elongated, dimer formation is destabilized (Figure 24). Physiologically, the polyglutamine tract (with normal length) is associated to receptor binding with AREs on other genes, while polyproline and polyglycine tract role is still unclear (He & Wilson 2002).

N-terminal region also contains strong activation function 1 (AF-1) composed of two transcription activation unit that mediates the binding with AR coactivators such as steroid receptor coactivator-1 (SRC-1) and c-AMP responsive element binding protein (CBP) belonging to the p160 superfamily. Expanded polyQ tract affects the binding of AR to its coactivator, thus influencing downstream pathway (Liu et al. 2003).

The N-terminal region also contains most of the phosphorylation, SUMOylation and acetylation sites. Phosphorylation occurs after AR activation and its role is still unclear. SUMOylation has a role in the regulation of the transcriptional AR activation. Acetylation negatively regulates Sp1 activity (Fu et al. 2002; Poukka et al. 2000; Gioeli et al. 2002).

The DNA binding domain is composed of two zinc fingers highly conserved between nuclear receptors. Zinc finger domain is formed by 4 cysteines that bound a zinc ion. These two rigid structures have the function of recognizing the ARE region and of promoting and mediating protein-DNA interaction. Immediately downstream the DNA binding domain there is a hinge region that contains a PEST sequence (proline, serine, glutamic acid, threonine), that is targeted for proteasomal degradation (Matias et al. 2000).

The C-terminal domain contains both the NLS and the steroid binding domain. The NLS interacts with α-importin to mediate AR shuttling into the nucleus (Jenster et al. 1993).

The steroid binding domain is composed of a precise number of α-helices and β-sheets structures that form a hydrophobic pocket, with high affinity for testosterone and dihydrotestosterone. Binding with agonist (and also with antagonist) changes the spatial organization of this pocket, changing the spatial distribution of the secondary structures. When pocket structure changes, AR interaction with other proteins is influenced because also the second strong activation function 2 (AF-2) is exposed. This interaction site is less strong and less active of AF-1 in the N-terminus. In fact, it has weak affinity for co-activators such as SRC-1. The hydrophobic structure of C-terminus is functional to N/C interaction (Matias et al. 2000).

### *Activation of the androgen receptor*

The activation of the androgen receptor is testosterone dependent. Testosterone is AR endogenous ligand as well as dihydrotestosterone, synthetized directly in target cells from testosterone by the 5α-reductase (Figure 24).

Unbound AR is localized in the cytoplasm of cells, bound to different chaperone proteins (HSP90, HSP40, HSP70) by its N-terminal and C-terminal domain (Cardozo et al. 2003). These proteins keep maintaining the hydrophobic pocket in the conformation that has the highest affinity with ligands. After testosterone binding these proteins are released by AR that dimerizes prior to enter the nucleus and prior to bind DNA (Jenster et al. 1993). Testosterone binding, triggering a conformational change, takes also to the exposure of the NLS in the C-terminal domain. When AR enters in the nucleus it binds several transcription activators in its N-terminal region (Figure 24). This complex recognizes the target DNA and recruits the RNA polymerase that starts the transcription (Brinkmann 2001; Wong et al. 1993). When AR activity is ended, AR is exported into the cytoplasm, rebound to the HSPs and recycled.

### *AR role in nervous tissues*

AR is differently expressed in CNS areas: while it is highly expressed in hypothalamus, in motor neuron spinal cord, in dorsal root ganglia and in hippocampus, its expression is very low in areas such as stria terminalis, medial preoptic area, dorsal and ventral zones of the periventricular nucleus. Some of these areas show sexual dimorphism in AR expression, that explains the differences between male and female in behavior, neural development and prevalence in neurological and psychiatric diseases (Fernandez-Guasti et al. 2000).

AR is highly expressed in the spinal nucleus of the bulbo-carvernosus system (SNB) and in this neurons it mediates neural development, since birth, and, in adulthood, it prevents loss of SNB neurons (Goldstein & Sengelaub 1990; Jordan et al. 2002). AR also has a role in the growth after nerve resection of peripheral nerves (Yu 1989). In spinal cord AR governs neural development, formation of neuromuscular synapsis, axonal and dendrites growth. These functions are mainly achieved by regulating structural proteins like actin and tubulin and the gap junction channel. All these proteins are highly upregulated during axonal development and growth after resection (Matsumoto 1997). Also neuritin whose function is mediating neurites growth is upregulated by AR activity (Naeve et al. 1997).

**Mechanisms of ARpolyQ toxicity**

***Loss of function or Gain of function***

Physiological function of the AR is promoting the transcription of target genes. The presence of the polyglutamine tract reduces AR transcriptional activity, probably mediating negatively AR binding with other transcription co-activators (Figure 24). Indeed, polyQ tract is contained in the transactivation region where other coactivators should bind. It is anyway well established that AR loss of function account only for endocrine phenotype, but does not explained motor neuron loss and muscle atrophy. This notion is supported by studies showing that mutations on AR, that prevent its synthesis or its whole activity, causes androgen insensitivity syndrome but not motor neuron death (Neuschmid-Kaspar et al. 1996).

Gain of function theory to explain AR mediated toxicity rises from the evidence that, when present, ARpolyQ caused death both in *in vivo* and in *in vitro* systems (Verhoef et al. 2002; Poletti 2004). Moreover, this toxicity is mediated uniquely by the binding with testosterone (Figure 24). This evidence was smartly demonstrated by Katsuno and colleagues that started investigating the importance of circulating androgens, since only males are affected by the disease. They showed that castrated SBMA male mice lose all SBMA symptoms. Compared to SBMA male mice, castrated SBMA mice show increased muscle strength, loss of tremor and increased lifespan. On the other hand, homozygous SBMA female mice do not show any phenotype. After treatment with testosterone, in SBMA female mice, starts appearing motor neuron impairment, tremor and life span is shorter than in untreated individuals. In summary, SBMA female subjects display phenotype only when treated with testosterone. This experiment shows that ARpolyQ mediates toxicity on motor neuron/muscle but only after testosterone binding. So the toxicity of the ARpolyQ is strictly dependent on the presence of testosterone (Katsuno et al. 2006; Katsuno et al. 2002).

***ARpolyQ aggregation***

An important histopathological hallmark of SBMA is the presence of ARpolyQ inclusions both in the nucleus and in the cytoplasm (Adachi et al. 2005). These inclusions are mainly found in neuronal tissue, in particular in anterior horn motoneurons, posterior horn neurons, the substantia nigra and the hypothalamus (Figure 25). Notably, these aggregates are detectable also in non-neuronal tissues such as scrotal skin, other skin, proximal tubules of the kidney, hepatocytes, Steroli cells of the testis, glandular epithelium and in fibroblasts of the interstitial connective tissue of the prostate gland (Adachi et al. 2005) (Figure 25).

The mechanism by which ARpolyQ forms these inclusions is associated with the intrinsic capability of the polyQ tract to self-associate. In fact, a stretch of 20 contiguous glutamine residues form a secondary structure that is highly unstable, when the size of the stretch becomes longer that 40 residues or more the structure is stabilized by hydrogen bounds (Perutz et al. 2002). In the early stages, this process is highly reversible and controlled by several cellular mechanisms (chaperones). In the later stages, these structures are stabilized also by the binding between polyglycine tract. This process may be exacerbated by impairments of the degradative systems that lead to an increased presence of ARpolyQ protein in the intracellular compartments, thus facilitating the nucleation process. It is noteworthy that ARpolyQ aggregation is triggered by the binding with testosterone, while in absence of AR activation no aggregates are detectable (Poletti 2004). This finding is explained firstly by the presence of chaperone the mask the presence of the polyQ tract since they are bound to AR (since AR is activated by testosterone). Moreover, when these chaperones are associated with AR, they keep the folding of the protein in the correct conformation (Ciechanover & Kwon 2015). Another reason for the absence of aggregates in absence of testosterone is that the cytoplasmic environment may prevent aggregates formation, by degrading AR via the degradative systems, if AR does not reach the correct folding. It

is possible that the capacity of these systems is exceed by the continuous presence of ARpolyQ (Becker et al. 2000; Walcott & Merry 2002; Katsuno et al. 2002). Consequently, ARpolyQ is no more degraded and it aggregates in cells. It is still very controversial defining the exact role of these aggregates. Since they are present also in not dying neurons, and thus they are not directly linked to toxicity. On the other hand, their presence may lead to alteration of many different intracellular pathways (Poletti 2004).

There are three types of intracellular aggregates: cytoplasmic aggregates, neuropil aggregates and nuclear aggregates (Figure 26).

Cytoplasmic aggregates are formed after a short time. A possible function of these inclusions is to confine the toxic monomeric form to remove it from cytoplasmic environment. Removing testosterone, cytoplasmic aggregates formation can be reverted (Simeoni 2000).

Neuropil aggregates on the other hand can play important role in SBMA pathogenesis since they block axonal transport of vesicles, organelles and polyribosomes (Poletti 2004; NAGAI et al. 1999).

Nuclear aggregates, both in patients and in artificial models, are largely enriched in the N-terminal fragment of the ARpolyQ; since there is a site of cleavage on AR protein, it is possible that in presence of polyQ there is an aberrant proteolytic cleavage of ARpolyQ; species generated by this cleavage are toxic to target cells. This kind of inclusions are found in patient brain and can be reproduced *in vitro* and *in vivo* only by using a very long polyQ tract. ARpolyQ in these aggregates also sequesters steroid receptor coactivator-1 (SRC-1) and the CRE binding protein (CREB). Moreover, aggregates prevent ARpolyQ from its normal function as transcription activator, exacerbating the loss of function process (Walcott & Merry 2002; Ellerby et al. 1999; Merry 2001; Stenoien et al. 1999).

#### *ER and mitochondria damage*

There are several downstream pathways, regulated or affected by AR activity or by pathological AR function.

ARpolyQ is able to cause a marked mitochondrial pathology associated with an increased apoptotic activity and an altered nucleolar regulation of mitochondrial DNA through PGC-1α. It has been also shown that mitochondria are found in ARpolyQ aggregates, meaning that aggregation process requires energy.

Another event associated with ARpolyQ toxicity is ER stress. It has been demonstrated that AR is able to cause an abnormal unfolded protein response (UPR), that originate from the ER. Moreover, the ablation of any mediator of these pathways (like CHOP) strongly exacerbates the phenotype.

### Neuromuscular degeneration

For decades SBMA was studied mainly as a neurological disorder, involving only motoneurons. The involvement of the nervous system is well established both by the presence of many ARpolyQ aggregates and also by clinical signs clearly associated with lower motor neurons and sensory neurons loss, even if the sensory contribution is less relevant to disease. Histologically, SBMA patients show a decreased axon number associated with decreased motor conduction velocity, compound muscle action potentials, sensory conduction velocities, and sensory nerve action potentials (Katsuno et al. 2006; Borgia et al. 2017; Querin et al. 2017).

Muscle contribution to neurodegeneration was initially suggested by pre-onset clinical manifestations, such as myalgia, tremor, cramps and elevated serum levels of creatine kinase (Katsuno et al. 2012). In 2014 two studies clearly demonstrated the central role of muscle tissue in SBMA onset.

The first study was conducted on SBMA mouse models, generated with BAC gene for AR Q 112. The exon 1 containing the polyQ tract was flanked by two loxP sites that allow the elicitation of the sequence in presence of a CRE enzyme. Transgenic mice showed decreased lifespan, body weight loss and motor neuron phenotype. Crossing BAC-ARQ112 mice with mice ubiquitously expressing CRE, it was obtained a strain of mice that do not developed all SBMA-related

features, because since polyQ tract was absent. It has also been demonstrated that the elicitation of polyQ tract only in muscle cells, by crossing BAC-ARQ112 with mice expressing CRE only in muscle cells, rescued SBMA phenotype to same extent as the ubiquitous elicitation of polyQ. These data demonstrated that the selective expression of ARpolyQ in muscle cell is able to cause the onset of SBMA. Moreover, these data also showed that presence of ARpolyQ in motor neurons (even if aggregating) is not sufficient for SBMA insurgence (Cortes et al. 2014).

The second study supporting these findings was based on the use of antisense oligo nucleotides (ASO) to suppress AR expression in muscle cells. After ASO administration mice displayed a rescue of the phenotype by life span measure, behavioral test, and histological analysis of muscle sections (Lieberman et al. 2014).

Knowing these findings, it is likely that muscle determines SBMA phenotype in the first-stage of the pathology. Then during progression, muscle atrophy influences motor neuron survival also indirectly, by not providing the necessary trophic factors (such as neurotrophin-4 (NT-4), glial-cell derived neurotrophic factor (GDNF), and brain derived neurotrophic factor (BDNF), etc.). At the end stage of the pathology motor neurons are massively dying and the progression of the disease in mainly driven by motor neurons loss (Giorgetti et al. 2016).

In conclusion SBMA could be considered a neuromuscular disease, since both muscle and motor neuron are directly involved as site of ARpolyQ toxicity (Figure 27). Muscle atrophy is especially important in the first phase of the disease, since it is highly involved in the onset of SBMA. During progression of the pathology, contribution of motor neurons gains importance determining the loss of voluntary movements and the paralysis (Giorgetti & Lieberman 2016b) (Figure 26).

### The protein quality control system in SBMA

In recent years the knowledge about the PQC system shed light also in SBMA disease mechanism, and many studies focused their attention in understanding the interaction between the PQC system and ARpolyQ, using molecules that inhibit or active key elements of the PQC system.

ASC-JM1 is a small molecule that increases overall proteostasis. Indeed, it increases the expression of proteasome subunit by interacting with the HSF-1 (heat shock factor 1). In SBMA models, both *in vitro* and *in vivo* models, ASC-JM1 treatment is beneficial against ARpolyQ toxicity (Bott et al. 2016). ASC-JM1 not only activates the heat shock response (thus counteracting protein misfolding and aggregation), but it also mediates an anti-oxidant response. Furthermore, it has been shown that the anti-oxidant response is essential for ASC-JM1 activity, while heat shock response is not. Anti-oxidant effect is mediated by two factors NRF1 and NRF2 that are highly overexpressed in presence of ASC-JM1.

Other studies investigated the role of particular heat shock proteins; HSP90 prevents ARpolyQ degradation by maintaining AR soluble in the cytoplasm. When proteins are released by HSP90 they can be substrates of the proteasome. Inhibiting HSP90 by mean of 17-DMAG (17-(dimethylaminoethylamino)-17-demethoxygeldanamycin), facilitates ARpolyQ degradation through the proteasome that is well preserved in SBMA models till the last stages. Inhibiting HSP90 activity that maintain AR in the correct conformation for testosterone binding, 17-DMAG is able to increase the degradation of AR monomeric form before ARpolyQ activation. Indeed, 17-DMAG also induces the expression of HSP70 and HSP40 (Tokui et al. 2009) thus promoting ARpolyQ degradation. 17-DMAG was also demonstrated to be effective in *in vivo* models highlighting its capacity of passing the brain blood barrier (Tokui et al. 2009). Recent studies have also shared a light on the possibility of routing misfolded protein to proteasome, by modulating BAG1. It was demonstrated that increased routing to proteasome through BAG1-HSP70 complex is beneficial in SBMA "*in vitro*" models, and resulted in a strong reduction of misfolded proteins (Cristofani, Crippa, Rusmini, et al. 2017).

Autophagic flux contribution in NDs has been widely assessed in CNS. In recent years many works highlight autophagy involvement also in muscle cells. Results show that at the end stage muscle cells overexpress autophagic markers (like

BECL1, ATG10, p62 and LC3) indicating a role for autophagy in the late event of the pathology. Moreover mice at the end stage also show increased expression of the CASA complex components (HSPB8, BAG3) in muscle cells. In motor neuron almost no differences has been observed in the expression of the same markers (Rusmini et al. 2015).

If autophagy involvement in affected cells is well-established, the possibility to target autophagy with therapeutic strategy is still very controversial, since excessive autophagy is detrimental as well as autophagic impairment. In recent years, many studies focused their attention searching approaches that aim to reduce the amount of toxic proteins by routing them to autophagy instead of directly activating the autophagic flux. For instance, the overexpression of HSPB8, a co-operator of HSP70 and part of the CASA complex, is able to reduce the amount of insoluble proteins targeting them to autophagy, without directly activating autophagic flux (P Rusmini et al. 2013).

On the other side many studies tested drugs that directly activate autophagy.

17-AAG (17-(allylamino)-17-demethoxygeldanamycin) is a compound which has been successfully tested in SBMA *in vitro* models, and was found to be able to reduce the accumulation of ARpolyQ via a mechanism mediated by autophagy activation (Rusmini et al. 2011). It was shown that 17-AAG was able to induce a specific overexpression of all heat shock protein, including HSP70 and HSP40 that drive proteins to autophagy (Rusmini et al. 2011). Another tested compound is trehalose, a well-known autophagic activator, different from rapamycin since it is mTOR independent. It is known from studies on other diseases that induction of autophagy by rapamycin has not beneficial effects in NDs, and trehalose has been investigated as a valuable alternative. Studies demonstrated that trehalose is able to reduce ARpolyQ accumulation in motor neuronal cell models of SBMA, in an autophagic dependent manner; in addition the co-treatment with anti-androgenic drugs further increases trehalose degradation of AR; indeed, anti-androgen drugs slows AR translocation in to the nucleus, thus leaving AR disposable for cytosolic degradation through autophagy. Trehalose increases AR degradation not only by activating autophagy, but also by inducing the expression of the components of the CASA complex, like HSP70, HSPB8, BAG3 and CHIP; in this way, trehalose induces the degradation only of selected proteins (Giorgetti et al. 2014). In an HD mouse models, another disease caused by polyQ expansion, it was also demonstrated that trehalose has a beneficial effect on disease progression, and studies on SBMA models are now ongoing.

### Therapeutic approaches

At present, no treatments are available to prevent or stop SBMA progression. Only some palliative treatments, that cure the symptoms (such as dysphagia, muscle weakness, infertility), but not the whole pathology, are administered to patients. Several clinical trials with very different read out have been performed or are in progress, but no one resulted in an efficient therapeutic approach for SBMA.

Strategies that are now pursued by different investigators are based on the reduction of AR expression, androgen ablation, allosteric regulation of AR, regulation of AR expression and modulation of degradative pathways.

To achieve modulation of AR expression, miRNA gained attention since they are potent gene expression modulators. It was demonstrated that miRNA 196a shows positive effects in SBMA mouse models; indeed, it reduces mRNA stability, by negatively regulating CELF2, an AR mRNA stabilizer. They also demonstrated that administration of miRNA in mouse models, exert protective effects on disease progression (Miyazaki et al. 2012).

AR expression can also be regulated by the activity of the histone deacetilase (HDAC). The HDAC inhibitor sodium butyrate shows beneficial effect on AR expression (Minamiyama et al. 2004).

Since testosterone triggers ARpolyQ toxicity another valuable strategy is androgen ablation from serum. Testosterone production is regulated by the hypothalamic–pituitary–testicular axis and the first stimulus is the gonadotropin-releasing hormone. Leuprorelin is an analog of GnRH that prevents testosterone production. Effects of this drug on motor neuron degeneration are beneficial, but patients show a very low compliance to this drug due to the

development of depression. Another strategy is targeting testosterone conversion into dihydrotestosterone (DHT) (more active metabolite of testosterone) with Dutasteride (blocker of 5 α-reductase activity) that showed no significant efficacy on disease progression nor in other parameters like muscle waist (Fernández-Rhodes et al. 2011; Baniahmad 2016). Other studies test drugs that targeted the dimerization of AR by N/C interaction. This process can be inhibited by Flutamide or others selective androgen receptor modulators (SARM) such as RTI-016 and RTI-051b. Even if Flutamide does not produce any variation in SBMA onset and progression, it seems that it exerts other positive effects in SBMA mouse model (Nedelsky et al. 2012; Orr et al. 2010). Another strategy is to target AR co-regulators in order to regulate AR gene expression. Curcumin-related compound 5-hydroxy-1,7-bis[3,4-dimethoxyphenyl]-1,4,6-heptatrien-3-one (ASC-J9) and the soybean-derived isoflavone genistein act on AR interaction with AR associated co-regulator 70 (ARA70) improving SBMA phenotype (Yang et al. 2007).

Finally, since ARpolyQ is substrates of the two main degradative pathways, activating the degrading machinery could have beneficial effect as widely reported and described previously.

| Disease | Protein involved | PolyGln size | |
|---|---|---|---|
| | | Normal | Elongated |
| SBMA or Kennedy's | Androgen receptor | 11–33 | 40–62 |
| HD | Huntingtin | 11–35 | 36–121 |
| DRPLA | Atrophin-1 | 7–35 | 49–79 |
| SCA-1 | Ataxin-1 | 9–39 | 40–81 |
| SCA-2 | Ataxin-2 | 17–29 | 37–50 |
| SCA-3/MJD | Ataxin-3 | 12–40 | 61–84 |
| SCA6 | α1A-vltg-dpt $Ca^{2+}$ channel | 4–16 | 25–30 |
| SCA-7/DCAII | Ataxin-7 | 7–35 | 37–130 |
| SCA-17 | TATAbox binding protein | 25–42 | 45–70 |

*Figure 22 Classification of polyglutamine diseases* (Poletti 2004)

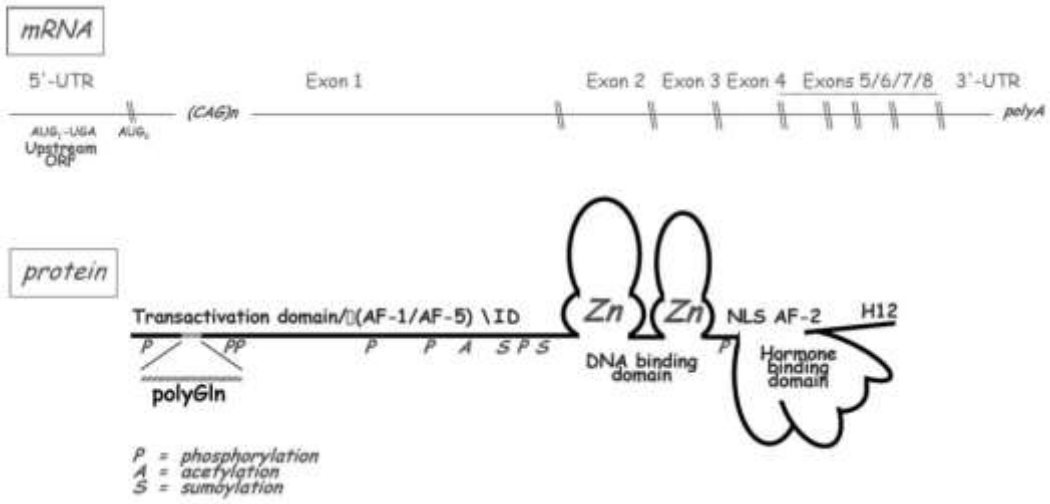


*Figure 23 Transcript and protein structure of androgen receptor* (Poletti 2004)

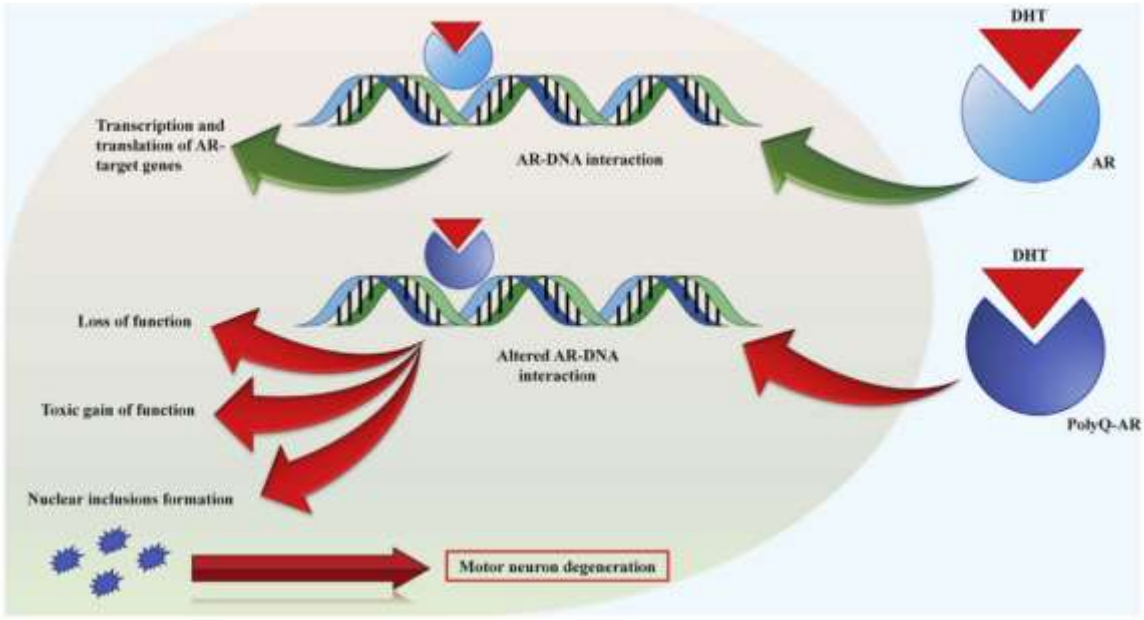


*Figure 24 Physiological and pathological functioning of AR* (Querin et al. 2017)

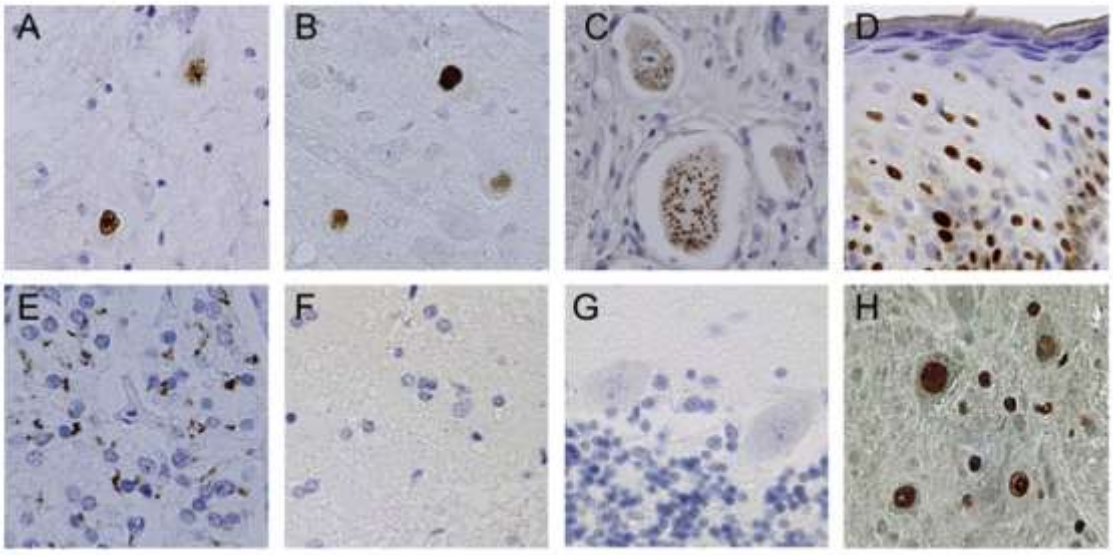


*Figure 25 Presence of AR inclusion in various tissues: A) spinal cord B) brainstem nuclei C)sensory D) nerves scrotal E) skin pancreas F) cerebral cortex G) cerebellum H) spinal cord of ARQ97 mice* (Katsuno et al. 2012)

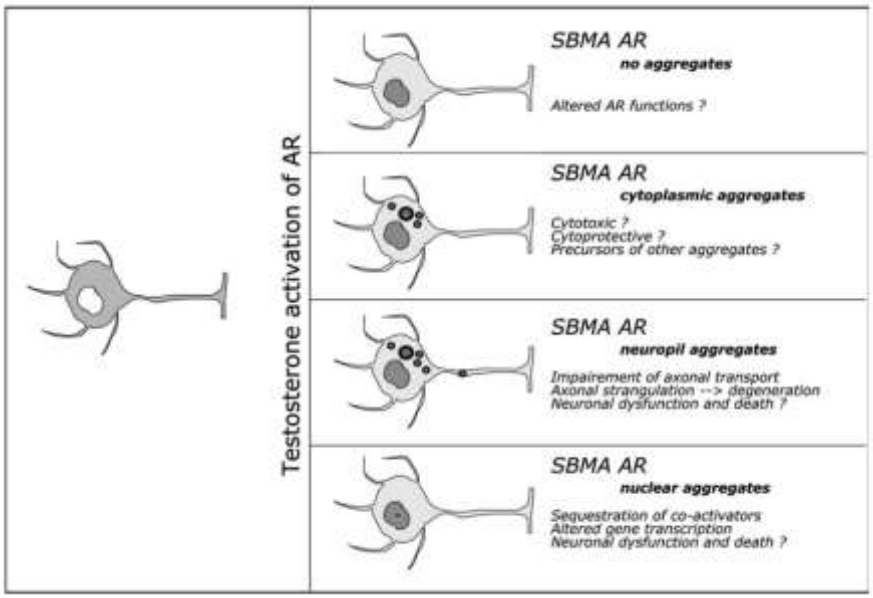


*Figure 26 AR inclusions localization in motor neurons* (Poletti 2004)

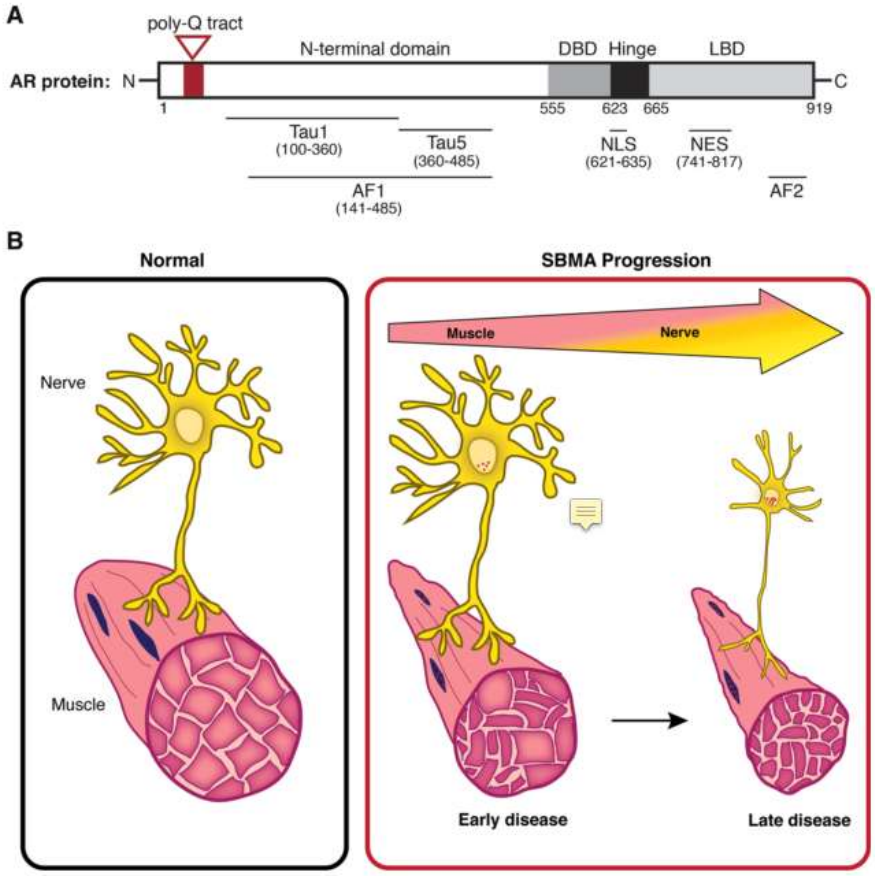


*Figure 27 Different contribution of muscle and motor neurons to SBMA onset and progression* (Giorgetti & Lieberman 2016b)

# PART ONE: PROTEIN QUALITY CONTROL SYSTEM INVOLVEMENT IN AMYOTROPHIC LATERAL SCLEROSIS

## Part One: Aims

The first part of this thesis is focused on the study of amyotrophic lateral sclerosis. As ALS is a multifactorial disease, there still many aspects that have not yet been clearly defined. In this context, some works highlight the possibility that muscle cells and muscle tissue are involved in the disease. The existence of a correlation between the onset of the pathology and muscle involvement is still under debate. One of the most important proteins in ALS is TDP43 since it is involved in both familial and sporadic ALS. Since in almost all patient motor neurons have been found inclusions of TDP43, degradative systems such as proteasome and autophagy gained importance since they should monitor the presence of misfolded and/or aggregated proteins and removed them.

The aims of the part one of this work are:

- Studying the behaviour of TDP43 and its disease associated fragments in both motor neuron and muscle cells.
- Studying the involvement of proteasome and autophagy in the removal of both monomeric and aggregated proteins
- Studying which protective systems could be enhanced in order to prevent or counteract aggregation of TDP43 and its disease associated fragments.

# CHAPTER 1: TDP-43 PATHOLOGY IN MOTOR NEURON: THE ROLE OF THE PROTEIN QUALITY CONTROL SYSTEM

**Introduction**

Amyotrophic lateral sclerosis is a fatal motorneuronal disease that caused death in about five years in affected patients. The most important clinical feature of ALS is motor neuron death that is caused by numerous factors such as excitotoxicity, presence of misfolded protein, presence of free radicals etc. TDP43 is one of the most important protein in the study of ALS: physiologically it exert its function in the nucleus or shuttling between nucleus and cytoplasm. TDP43 was found mutated in a small percentage of familial ALS but it has been found mislocalized in motor neurons of the vast majority of sporadic ALS patients. When TDP43 mislocalized in the cytoplasm it forms aggregates that often contain fragments of TDP43. The most represented fragments are the one of 35 and the one of 25 kDa (Zhang et al. 2007; Zhang et al. 2009). Once aggregates are formed they should be fast and promptly removed from cell environment by autophagy. In this first part, I analysed the aggregation propensity of TDP43 and of its disease associated fragments in mouse motor neuronal like cell line NSC34. Subsequently I analysed which degradative pathway is involved in the removal of both monomeric soluble protein (sometime the most toxic form) and aggregated protein. lastly I analysed the protective role of HspB8, a small heat shock protein, that is part of the complex that routes aggregates to autophagy (CASA complex).

These data have been already published in (Crippa, Cicardi, et al. 2016)

## Materials and methods

### CHEMICALS

Z-Leu-Leu-Leu-al or MG132 was used at 10μM for 16 hrs (Sigma Aldrich, Merck, Darmstadt, Germany). DMSO was used as control (Sigma-Aldrich). 3-methyl-adenine or 3MA was used at 10mM for 48 hrs (Selleckem, Houston, TX, USA) and it was directly diluted in medium.

### CELL CULTURES

NSC34 were used as motor neuronal model. Cells were routinely used in our lab. Briefly cells were maintained in high glucose medium (Euroclone, Pero, MI, Italy) added with glutamine (Euroclone), penicillin (SERVA, Electrophoresis GmbH, Heidelberg, Germany) and streptomycin (SERVA) and 5% fetal bovine serum (Sigma-Aldrich). Cells are growth at 37°C at 5% $CO_2$.

GFP-TDPs-NSC34 cell lines were obtained by transiently transfecting a TR4 NSC34 cell line (kindly provided by Dr. E. Garattini (Mario Negri Institute, Milan, Italy)), with pcDNA5/TO-GFP-TDPs plasmids and selecting positive clones with 200 μg/ml hygromycin for 3 weeks. GFP-TDPs-NSC34 selected clones were cultured in low-glucose DMEM (Euroclone, Pero, Milan, Italy) supplemented with 5% of tetracycline-free serum (Euroclone), 100 μg/ml hygromycin (Euroclone). GFP -TDPs expression was induced with doxycycline 1 μg/mL.

### PLASMIDS AND SIRNA

The following plasmids were used: pEGFP-TDP-43 which codes for the full-length form of TDP-43, pEGFP-TDP-35 which codes for the 35 kDa TDP-43 fragment, pEGFP-TDP-25 which codes for the 25 kDa TDP-43 fragment, that are all kindly provided by Dr. Petruccelli; pCI-neo-hHSPB8 which codes for the human form of the small heat shock protein of 22 kDa; pCDNA3 by Addgene was used as a transfection control.

Following siRNA duplex were used for silencing mHSPB8 endogenous expression: (sense: 5'-CGGAAGAGCUGAUGGUAAAUU-3'; antisense: 5'-UUU ACCAUCAGCUCUUCCGUU-3') (Dharmacon, Thermo Scientific Life Sciences Research, Waltham, MA, USA). A custom non- targeting siRNA duplex was used as a negative control (sense: 5'-GGGUAAAGCUAGAGAGAAUUU-3'; antisense: 5'-AUUCUCU CUAGCUUUACCCUU-3').

### TRANSFECTION PROCEDURE

NSC34 cells were transfected using Lipofectamine® Transfection Reagent (Invitrogen, Thermo Scientific Life Sciences Research, Waltham, MA, USA), following manufacturer protocol. Plasmid DNA was previously incubated with transferrin (Sigma-Aldrich) and then mixed with Lipofectamine.

When experiments were carried out in 12-well plates the following quantities of plasmids were used: 0.5μg of pEGFP-TDP-43, pEGFP-TDP-35 and pEGFP-TDP-25 and 0.6μg of pCI-neo-hHSPB8 and pCDNA3 as a control. Plasmids quantities were halved if experiments were carried out in 24-well plate, while are doubled if experiments are carried out in 6-well plate.

### CELL LYSIS AND FRACTIONATION

*PBS extraction*: Cells were plated in a 12-well plate (90,000 cell/mL). 48 hrs after transfection cells were harvested in culture medium and centrifuge at 100g x 5min. The supernatant was discarded and the pellet was re-suspended with PBS and slightly sonicated (3 hits at low intensity).

*NP40 soluble/insoluble extraction*: Cells were plated in a 12-well plate (90,000 cell/mL). 48 hrs after transfection cells were lysed passing each sample with 1mL syringe in the NP-40 buffer (150 mM NaCl (Sigma-Aldrich); 20mM TrisBase (Sigma-Aldrich); Nonidet P-40 (NP-40) 0.5% (Sigma Aldrich, Merck, Darmstadt, Germany); 1.5 mM MgCl2 (Sigma-Aldrich); Glycerol 3% (Sigma-Aldrich), pH 7.4) with protease inhibitor (cOmplete EDTA free Tablet 25X (Sigma-Aldrich)) and 1,4-Dithioteitol 1Mm (DTT ; Sigma-Aldrich) to get rid of S-S bond. Samples are then centrifuged at maximum speed (15 minutes at 4°) and the supernatant (the NP-40 soluble fraction) is transferred in a new tube while the pellet is rinsed in fresh NP-40 buffer, without protease inhibitor and DTT. NP-40 soluble fraction is quantified with bicinchoninic acid (BCA) assay (Euroclone). NP-40 insoluble fraction had been loaded as equal volume to NP-40 soluble fraction.

FILTER RETARDATION ASSAY

Filter retardation assay (FRA) is based on protein filtration on a cellulose acetate membrane thanks to vacuum applied at a Bio-Dot SF Microfiltration Apparatus (Bio-Rad, Hercules, CA, USA). The following quantities were loaded: NSC34 PBS extract 1.5µg; NSC34 NP-40 soluble extracts 1.5 µg; NP-40 insoluble extracts were loaded as equal volume. After vacuum filtration protein are fixed on the membrane with methanol and then the membrane is incubated for 1 hr at RT in blocking solution (5% of dried non-fat milk (Euroclone)). After two washes with TBS-T 1X the membrane is incubated with the HRP-conjugate anti-GFP antibody diluted in TBS-T 1X at RT (find incubation timing and antibody dilution above). After three washes with TBS-T 1X at RT membrane was incubated with ClarityTM Western ECL Blotting Substrate (Bio-Rad) to reveal the signal. Images were acquired using a ChemiDoc XRS System (Bio-Rad).

WESTERN BLOT

GFP-TDP-43 and its fragments proteins were visualized always by loading samples on 12% polyacrylamide gels. 15µg of PBS extracts or 15µg of NP-40 soluble extracts were loaded (insoluble NP-40 extracts were loaded as equal volume to NP-40 soluble extracts). Proteins were transferred to nitrocellulose membrane (Bio-Rad) thanks to TransBlot (Bio-Rad) following manufacturer instructions. Membrane were then incubated with blocking solution (5% of dried non-fat milk (Euroclone)) and with primary antibody at 4° overnight. After two washes, membrane were incubated with the HRP-conjugated secondary antibody diluted in TBS-T 1X for 1 hr at RT. Signal was detect with ChemiDoc XRS System (Bio-Rad) after incubation with ClarityTM Western ECL Blotting Substrate (Bio-Rad). Antibody description and dilution are described above.

ANTIBODY DILUTION

The following primary antibodies were used: HRP-conjugate anti-GFP antibody (MB-0712; Vector Laboratories, Burlingame, CA, USA) for TDPs detection in FRA and WB (1:10,000 for NSC34); home-made rabbit polyclonal anti-HSPB8 (1:2,000); goat polyclonal anti-ACTIN (Santa Cruz Biotechnology, sc-1616) (1:1,000); rabbit polyclonal anti GAPDH (Santa Cruz Biotechnology, sc-25778) (1:1,000); mouse monoclonal anti-α-tubulin (Sigma-Aldrich T6199) (1:2,000). The following secondary antibodies were used: goat anti-rabbit HRP-conjugate secondary antibody (Santa Cruz Biotechnology, sc-2004); goat anti-mouse HRP-conjugate secondary antibody (Santa Cruz Biotechnology, sc-2005); donkey anti-goat HRP-conjugate secondary antibody (Santa Cruz Biotechnology, sc-2020)

IMMUNOFLUORESCENCE

Cells were seeded on coverslips in a 24-well plate (70,000 cells/mL). 48 hrs after transfection cells were fixed using paraformaldehyde and methanol. Cells were permeabilized using a solution of TRITON X-100 diluted 1:5000 in PBS.

After the incubation of 1hrs in blocking solution cells were incubated with primary antibody overnight at 4°C. The following primary antibodies were used: home-made rabbit polyclonal anti-HspB8 (1:500 kindly provided by Dr. Landry). After two washes with PBS cell were incubated for 1 hr at RT with goat anti-rabbit 549 Alexa (1:1000, Life Technologies, Thermo Fischer, A-11012). Coverslips were then mounted on a support. Images were acquired using LSM510 Meta system confocal microscope (Zeiss, Oberkochen, Germany) and processed with the Aim 4.2 software (Zeiss).

**The biochemical behaviour of TDP-43 and its fragments in motor neuronal cells**

To visualize the intracellular localization of TDP-43 and of its fragments, I transfected motor neuronal NSC34 cells with plasmids coding for GFP-TDP-43, GFP-TDP-35 and GFP-TDP-25. NSC34 are hybrid cell line obtained by fusion of murine neuroblastoma and murine spinal cord; since they maintain various motor neuronal phenotypes they are a *bona fide* motor neuronal-like model.

As control, I use a plasmid coding for GFP only. Cells were fixed and after nuclei staining observed at microscope (Figure 28A). I observed that GFP-TDP-43 was localized in the nucleus and no cytosolic or nuclear inclusions were detectable. Cells transfected with GFP-TDP-35 showed fluorescence both in the nucleus and in the cytosol sometimes forming cytoplasmic aggregates. GFP-TDP-25 was the only protein localized exclusively in the cytosol, and its localization was not diffused, but it was present in an aggregated form, with large inclusions both in the cell body and in the neurites.

I used also filter retardation assay (FRA) to detect the insoluble forms and western blot (WB) to analyse the soluble fraction (Figure 28B) of the GFP-TDP-43 and fragments. I observed that in FRA GFP-TDP-43 was more retained than GFP-TDP-35 and GFP-TDP-25 (*** $p<0.001$ vs GFP-TDP-35 and GFP-TDP-25; (Figure 28C)). By WB I observed that GFP-TDP-25 formed more SDS-soluble species than GFP-TDP-43 and TDP-35 (equal loading was verified by tubulin blotting). To better isolate the insoluble forms of GFP-TDP-25 clearly visible in IF, I performed a NP-40 fractionation and loaded soluble and insoluble extracts both in FRA and WB (Figure 28D). I observed that GFP-TDP-43 and GFP-TDP-35 were equally represented in both fractions, both with FRA and with WB. On the other side, GFP-TDP-25 was most present in the NP-40 insoluble fraction than in the soluble one. Indeed, the insoluble/soluble ratio of the two fractions in FRA, showed a significant increase for GFP-TDP-25 (### $p<0.001$ vs GFP-TDP-35; * $p<0.05$ vs GFP-TDP-43; (Figure 28E)).

I concluded that GFP-TDP-25 and GFP-TDP-35 form aggregates in NSC34, while GFP-TDP-43 is soluble in the nucleus. To correctly visualize these aggregates with FRA and WB, NP-40 extraction is required. Probably, GFP-TDP-25 is more insoluble than GFP-TDP-43 and GFP-TDP-35, indicating that specific isolation procedure (NP-40 extraction) is required to discriminate these species.

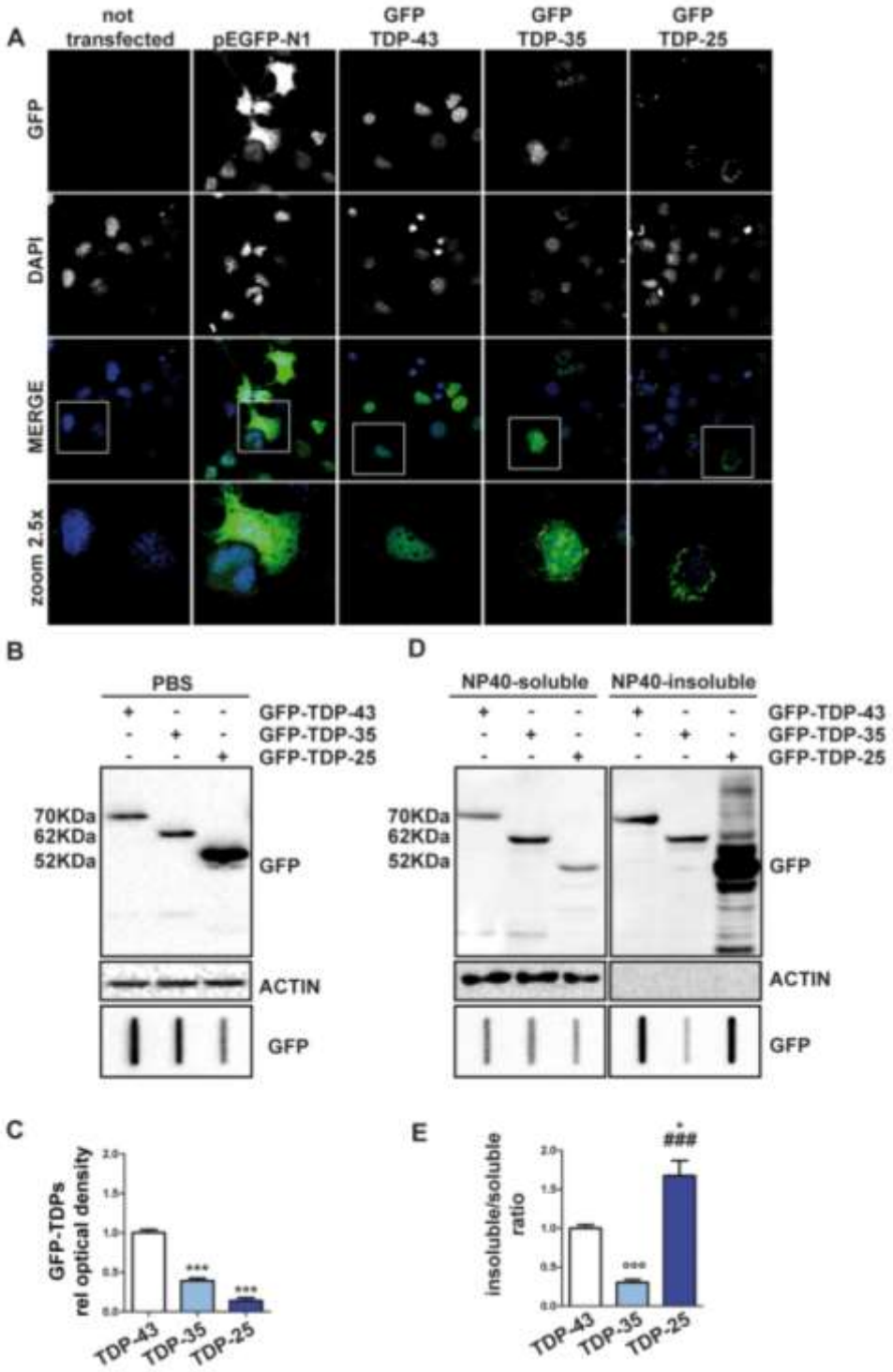


*Figure 1: GFP-tagged truncated TDP-35 and TDP-25 show different biochemical behaviour from that of full-length TDP-43. (A) Confocal microscopy analysis (63X magnification) of mouse motor neurone NSC34 cells transiently overexpressing GFP-TDP-43, GFP-TDP-35, GFP-TDP-25, or GFP alone (pEGFP-N1, used as a control). DAPI: nuclei staining. A 2.5x magnification of selected areas is shown. (B): Western Blot (WB; upper insets) and filter retardation assay (FRA, lower inset) of the PBS extracts of mouse motor neurone NSC34 cells transiently overexpressing the GFP-TDP-43, GFP-TDP-35 or GFP-TDP-25. (C) Quantification of the PBS extract by FRA (***P<0.001 vsGFP-TDP-43). The data represent in each case the mean ± sem of n=3 independent samples. (D): WB (upper insets) and FRA (lower insets) of the NP40 extracts of cells transiently overexpressing GFP-TDP-43, GFP-TDP-35 or GFP-TDP-25 (left insets, NP40-soluble fraction; right insets, NP40-insoluble fraction). (E): Quantification of FRA NP40 insoluble/soluble ratio (°°°P<0.001 vs GFP-TDP-43; * P<0.05 vs GFP-TDP-43; ### P<0.001 vs GFP-TDP-35). The data again represent the mean ± sem of n=3 independent samples.*

**Relevance of the degradative systems in TDP-43 clearance**

To investigate the degradative pathway responsible for the clearance of the various GFP-TDPs species, I blocked each degradative system in presence of TDP-43 species.

I transfected NSC34 with plasmids coding for GFP-TDP-43, GFP-TDP-35 and GFP-TDP-25 and then I inhibited the proteasome with MG132 and the autophagy with 3MA.

48 hours after transfection I collected the cells and I performed an NP-40 extraction followed by FRA and WB analyses (Figure 29).

Surprisingly, analysis by FRA showed that proteasome inhibition by MG132 treatment caused a reduction of GFP-TDPs species in the soluble NP-40 fraction compared to control condition. On the other side, when I blocked autophagy with 3MA, I observed that in FRA 3MA treatment did not produce any variation in GFP-TDPs presence in NP-40 soluble fraction (Figure 29A).

This trend was confirmed in WB analysis of the soluble fractions of the cell lysates: in fact, after MG132 treatment there was a minor presence in NP-40 soluble fraction of all the three GFP-TDPs species; after autophagy inhibition, the protein levels of the NP-40 soluble fraction in WB were comparable to the control condition (Figure 29A).

On the other hand, the analysis of the NP-40 insoluble fraction by FRA revealed that after MG132 treatment all the three GFP-TDPs species were greatly increased. Especially for GFP-TDP-35 and GFP-TDP-25, I observed the formation of species at higher molecular weight (possibly ubiquitinated forms) and at lower molecular weight (M.W.) (possibly fragments generated to increase the clearance of the two species). After 3MA treatment, the only fragment showing an increased presence in the insoluble fraction is GFP-TDP-25 (Figure 29B).

WB analysis mainly reflected FRA results showing a great increased of GFP-TDPs species protein levels following proteasome inhibition, while 3MA treatment caused a significant increase only in levels of GFP-TDP-25 NP-40 insoluble fraction (Figure 29B).

The ratio between insoluble and soluble fraction quantified after FRA showed that after proteasome inhibition all the three species were more represented in the NP-40 insoluble fraction (* $p<0.05$). On the other hand, inhibiting autophagy caused a shift toward the insoluble fraction only of the GFP-TDP-25 species (Figure 29C).

From these data, I conclude that proteasome actively degrades all TDPs species. Indeed, when proteasome activity is inhibited by MG132, all GFP-TDPs species accumulate in NP-40 insoluble fraction, meaning that the degradation of these proteins is slowed down or absent. The role of the autophagy in degrading GFP-TDPs species is different from that of the proteasome; autophagy is apparently involved in the selective degradation of only GFP-TDP-25. Based on data reported above, 3MA treatment causing defective autophagy, affects only GFP-TDP-25 levels. Compared to control condition, GFP-TDP-25 levels in NP-40 insoluble fraction increase when autophagy is inhibited by 3MA. On the contrary, GFP-TDP-43 and GFP-TDP-35 levels in NP-40 soluble and insoluble fraction do not change after inhibiting autophagy with 3MA. Collectively these data suggest that GFP-TDP-43, and GFP-TDP-35 are not normally degraded by autophagy, while GFP-TDP-25 is a substrates of autophagy at basal condition.

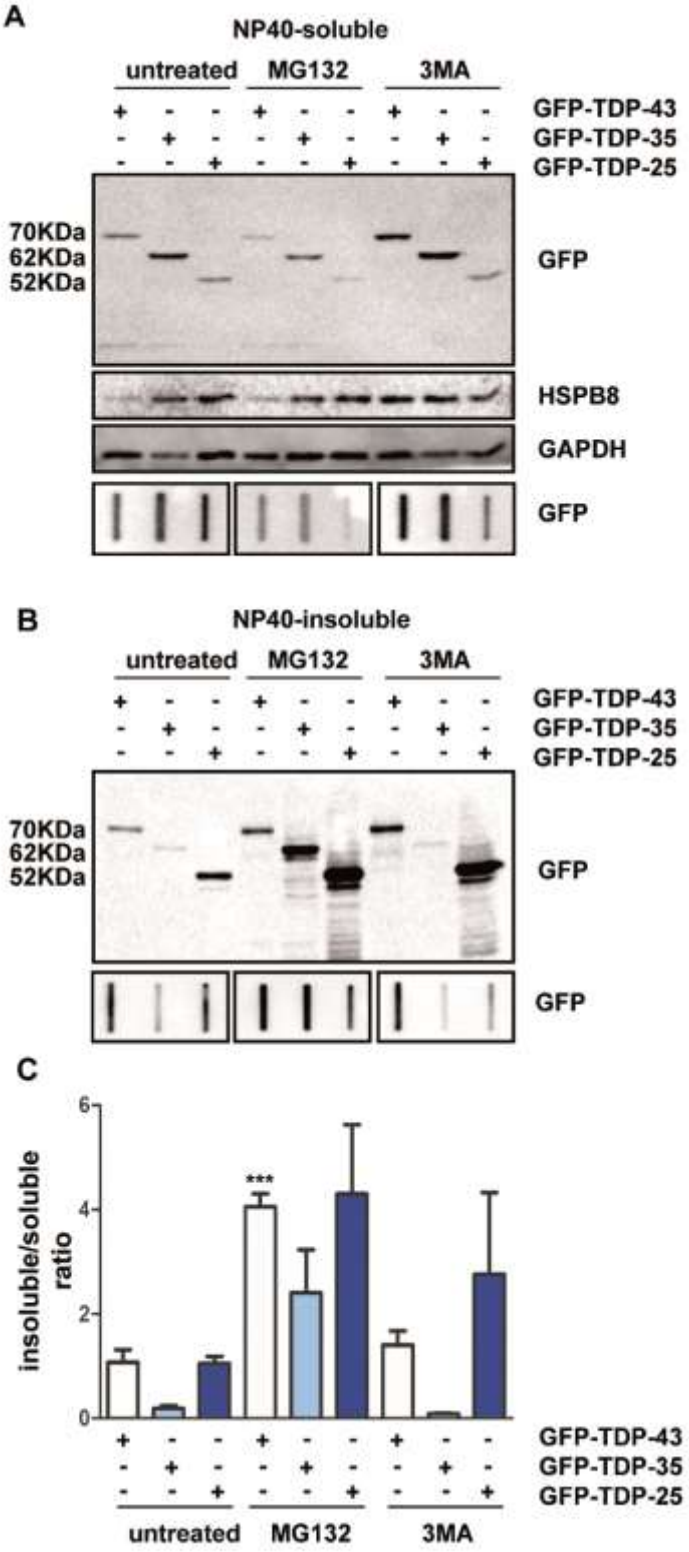


*Figure 28: GFP-TDP-35 and GFP-TDP-25 show different clearance from that of full-length GFP-TDP-43. (A) WB (upper insets) and FRA (lower insets) of the NP40-soluble extracts of mouse motor neurone NSC34 cells transiently overexpressing GFP-TDP-43, GFP-TDP-35 or GFP-TDP-25 and treated with 10mM MG132 for 16h or 10mM 3-methyladenine (3-MA) for 32 h. (B) WB (upper insets) and FRA (lower insets) of NP40-insoluble extracts. (C) Quantification of FRA NP40 insoluble/soluble ratios (***P<0.001 vs GFP-TDP-43). The data represent the mean ± sem of n¼3 independent samples.*

**HSPB8 routes TDP-43 and its fragments to autophagy**

HSPB8 is a small heat shock protein whose pro-degradative role against protein inclusions has already been demonstrated in different proteinopathies. It was demonstrated that the overexpression of HSPB8 was able to reduce aggregation of SOD1 (ALS; (Crippa et al. 2010)), ARpolyQ (SBMA; (Paola Rusmini et al. 2013)) and huntingtin (HD; (Carra et al. 2008)). To evaluate if HSPB8 protective role was effective also against TDP-43 fragments aggregation, I co-transfected HSPB8 with GFP-TDP-43, GFP-TDP-35 and GFP-TDP-25 in NSC34 and I performed an IF, detecting HSPB8 and GFP-TDPs localization. Nuclei were stained with Hoechst (Figure 30A-B). By IF I observed that the localization and the fluoresce intensity of the GFP-TDP-43 remained unchanged, while in presence of GFP-TDP-35 and GFP-TDP-25 HSPB8 greatly reduced the number and the size of the aggregates, compared to control condition (pcDNA3).

Subsequently, to better evaluate the reduction of misfolded, aggregation-prone species in presence of HSPB8 I performed NP-40 extraction, to measure protein levels in both soluble and insoluble fractions, transfecting NSC34 with GFP-TDPs and HSPB8.

By WB analysis (Figure 30C) I noted that GFP-TDPs levels in both soluble and insoluble fractions were greatly decreased in presence of HSPB8 (even detected in WB). I observed that HSPB8 exerted a pro-degradative activity of the soluble species of all the three GFP-TDPs detectable by WB analysis performed on NP-40 soluble extracts.

In parallel, the analysis of the NP-40 insoluble fraction, showed that the TDPs insoluble species detected in that fraction were greatly degreased by mean of HSPB8 activity. (Figure 30D).

After having assessed the pro-degradative role of HSPB8 against GFP-TDP-43 fragments aggregation, I wanted to evaluate if depletion of HSPB8 would results in worsened GFP-TDPs species aggregation. Since I wanted to mimic physiological condition, I used NSC34 cell lines stably expressing GFP-TDP-43, GFP-TDP-35 and GFP-TDP-25, in which the expression of GFP-TDPs species is comparable to endogenous gene expression. In these cell lines, I silenced HSPB8 with a specific siRNA and to obtain a condition of exacerbated aggregation of GFP-TDPs species, I also inhibited proteasome with MG132 and autophagy with 3MA. To analyse GFP-TDPs protein levels variation, I performed an NP-40 extraction and I analysed the fractions by FRA (Figure 30E-F-G).

I observed that, when proteasome is inhibited, GFP-TDP-43 levels in both fractions remain comparable to the untreated controls. The autophagy contribution in the GFP-TDP-43 clearance was negligible. In fact, the levels of GFP-TDP-43 in both insoluble and soluble NP-40 fractions remained unchanged after 3MA treatment.

By silencing HSPB8 endogenous expression, the Hsp70-Bag3-HSPB8 is no more formed, thus preventing the routing of protein/aggregates to autophagy. Even blocking this routing pathway by HSPB8 siRNA, did not produce any variation in GFP-TDP-43 protein levels in both NP-40 soluble and insoluble fractions analysed by FRA (Figure 30E).

Looking at the NP-40 soluble fraction, GFP-TDP-35 levels in FRA were significantly increased when autophagy (3MA treatment) and routing to autophagy (HSPB8 silencing) were inhibited (* $p< 0.05$). MG132 inhibition of proteasome did not produce any variation in NP-40 soluble levels of GFP-TDP-35. On the other side, analysing GFP-TDP-35 NP-40 insoluble fraction, I observed increased GFP-TDP-35 levels in FRA only after proteasome inhibition (** $p<0.001$), while 3MA treatment and HSPB8 silencing caused no variation in its NP-40 insoluble levels. (Figure 30F).

GFP-TDP-25 NP-40 insoluble levels were significantly increased only when proteasome was inhibited by MG132 (** $p<0.01$). 3MA treatment produced no variation both in the NP-40 soluble and NP-40 insoluble levels of GFP-TDP-25. HSPB8 silencing increased the levels of the protein retained in FRA only in the NP-40 soluble fraction (* $p<0.05$), while the insoluble fraction was comparable to the control conditions (Figure 30G).

I conclude that at basal levels HSPB8 is able to drive soluble toxic proteins, such as GFP-TDP-25, to autophagy in order to prevent their accumulation inside cell cytoplasm and thus their aggregation.

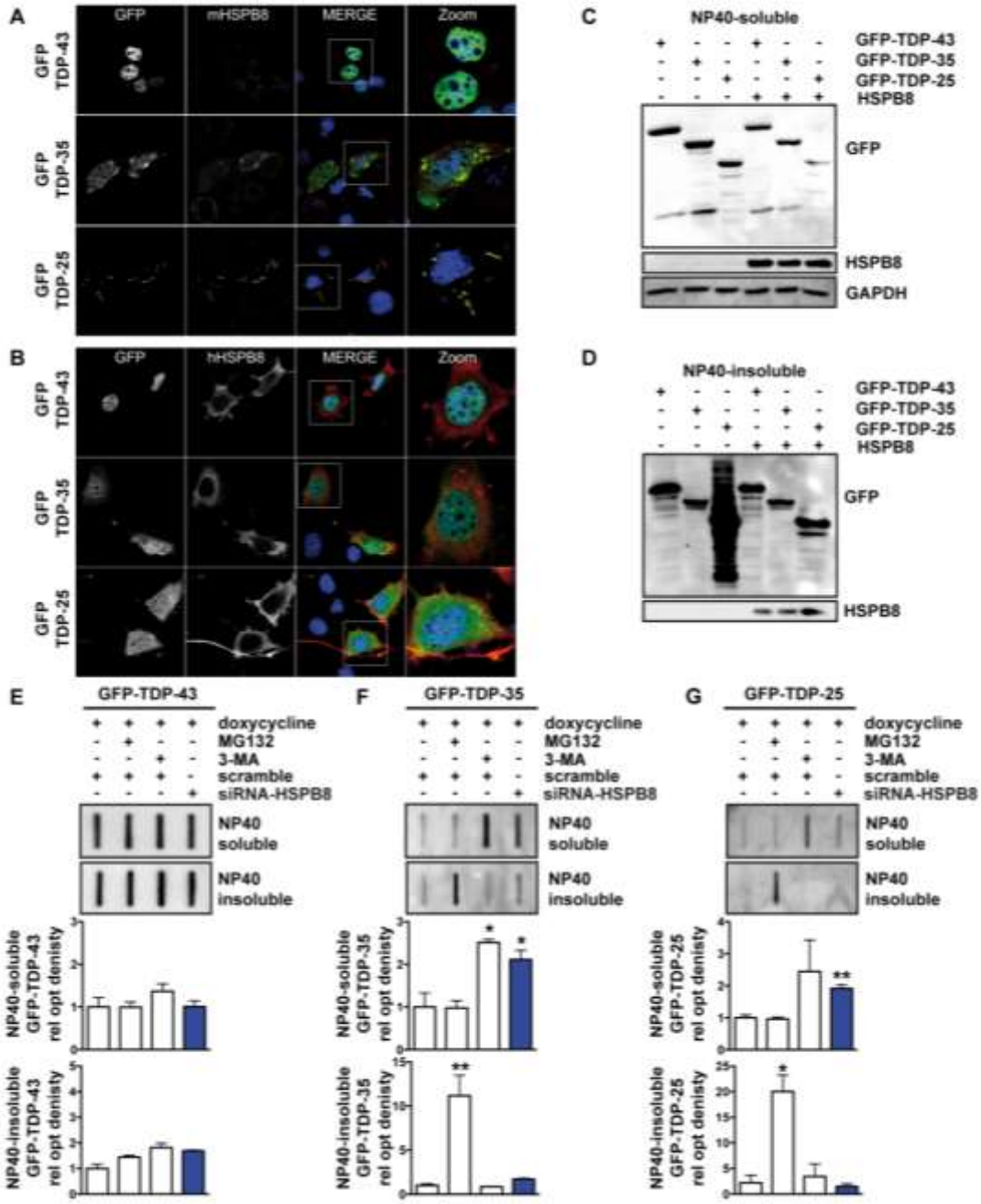


*Figure 29: HSPB8 affects the accumulation of GFP-TDP-35 and GFP-TDP-25 fragments. (A,B) Confocal microscopy analysis (63X magnification) of NSC34 cells transiently co-transfected with plasmids coding for GFP-TDP-43, GFP-TDP-35 or GFP-TDP-25 and pCDNA3 (A) or hHSPB8 plasmid (B). DAPI: nuclei staining. RED: murine endogenous HSPB8 (mHSPB8) or human transfected HSPB8 (hHSPB8). A 2.5X magnification of selected areas is shown. (C)WB of the NP40-soluble extracts of mouse motor neurone NSC34 cells transiently overexpressing GFP-TDP-43, GFP-TDP-35 or GFP-TDP-25 and human HSPB8. (D): WB of the NP40-insoluble extracts. E-G: Representative FRA (upper panels) and FRA quantification (lower panels) of the NP40-soluble and NP40-insoluble extracts of mouse motor neurone NSC34 cells stably overexpressing GFP-TDP-43 (E), GFP-TDP-35 (F) or GFP-TDP-25 (G), induced for 72h with 1 µg/ml doxycycline and transfected with scramble or siRNA-HSPB8; the cells were treated with 10lMMG132 and 10mM3-MA for the last 16h prior to extraction. The optical densities of GFP-TDPs were expressed relative to the mean optical densities of the corresponding samples treated with doxycycline and a scramble RNAi sequence, taken as internal references. The data represent the mean ± sem of n=3 independent samples. (*P<0.05 vs scramble; ** P<0.01 vs scramble).*

**TDP dynamics are not influenced by GFP-tag**

The green fluorescent protein (GFP) is a protein of 29 kDa and when is fused to endogenous protein (such as TDP-43) it might influence protein behaviour. To test if GFP tag was influencing somehow the biochemical behaviour observed for TDPs species, I produced three plasmids coding for TDP-43, TDP-35 and TDP-25 tagged with FLAG, a smaller tag than GFP. I cloned the three TDP sequences in plasmid with a tag 2xFLAG. I obtained three different plasmids coding for the three TDPs species carrying a 2xFLAG tag at the N-terminus.

I transfected NSC34 cells with 2xFLAG-TDPs plasmids and performed an (IF) against the tag-FLAG (Figure 31A). I observed that FLAG-TDP-43 was localized in the nucleus, not forming aggregates, but in a diffuse way, and this behaviour correlates with GFP-TDP-43 behaviour. FLAG-TDP-35 was partially mislocalized in the cytoplasm, but differently from the results obtained with GFP-TDP-35, it did not form aggregates in the cytoplasm. FLAG-TDP-25 is only localized in the cytoplasm, but differently from GFP-TDP-25, it did not form aggregates, but rather it was found diffuse in the cytoplasm.

Then, to check total protein levels of 2xFLAG-TDPs, I performed FRA and WB analysis on NSC34 samples transfected with FLAG-TDPs (Figure 31B). PBS extracts analysed by FRA showed that 2xFLAG-TDP-43 was heavily retained on the membrane compared with the other two proteins (** $p<0.01$ vs FLAG-TDP-35 and FLAG-TDP-25). The two fragments were barely visible in FRA, with FLAG-TDP-25 even less detectable then FLAG-TDP-35 (° $p<0.05$). The differences observed in FRA could be ascribed to different protein turnover and, to investigate FLAG-TDPs turnover, NSC34 cells were transfected with FLAG-TDPs and treated with MG132, to inhibit proteasome and 3MA to inhibit autophagy (Figure 31C-D-E) and PBS extracts were analysed by FRA and WB. FLAG-TDP-43 levels increased in FRA following proteasome and autophagy inhibition (* $p<0.01$ vs NT), while in WB I detected only a slight increase in protein levels (Figure 31C). FLAG-TDP-35 showed the same trend as FLAG-TDP-43 in FRA: the amount of protein retained in FRA was increased by MG132 and 3MA (*$p<0,05$). At variance of FLAG-TDP-43, in WB blot FLAG-TDP-35 levels were greatly increased after the inhibition of both the degradative systems (Figure 31D).

By analysing the extracts of FLAG-TDP-25 in FRA PBS, I noted that the most of the protein, that is not detectable in basal condition, is recovered after blocking the degradative pathways with MG132 and 3MA (**$p<0.01$). WB analysis on the same samples revealed that the treatment with MG132 led to the recovering of the soluble form of FLAG-TDP-25, while 3MA treatment had no effects on the soluble levels of monomeric TDP-25 (Figure 31E).

Since TDP-43 fragments are misfolded and toxic proteins, I wanted to evaluate if HSPB8 pro-degradative role was comparable to the one observed for GFP-TDPs. I co-transfected HSPB8 with FLAG-TDPs to assess HSPB8 pro-degradative role with FLAG-TDPs. When HSPB8 is overexpressed in presence of FLAG-TDPs, TDPs levels in FRA were significantly decreased in the case of TDP-43 (**$p<0.01$) and of TDP-35 (**$p<0.01$). FLAG-TDP-25 was not significantly reduced but I could detect only a slight decreased in protein levels in FRA (Figure 31 F-G-H-I). Since protein levels are very low, it is possible that a strong decrease is not detectable. By analysing the PBS extracts in WB, I observed that the total protein levels of FLAG-TDP-43 were reduced in presence of HSPB8; while in the case of FLAG-TDP-35 and FLAG-TDP-25, I only observed a little variation in total protein levels, with HSPB8 overexpression (Figure 31F).

Overall these results demonstrated that GFP tag impact on TDPs rate of aggregation; indeed, I found that TDP-25 aggregation is different if GFP is present, and it seems that GFP enhances TDP-25 aggregation. Probably its effect on TDP-25 is due to the weight of the two proteins that is almost the same. Another explanation is that GFP makes degradation of TDPs less easy than FLAG tag. Nevertheless, even if the amount of aggregation is different in presence of GFP, HSPB8 maintains it capacity of routing misfolded proteins to degradation.

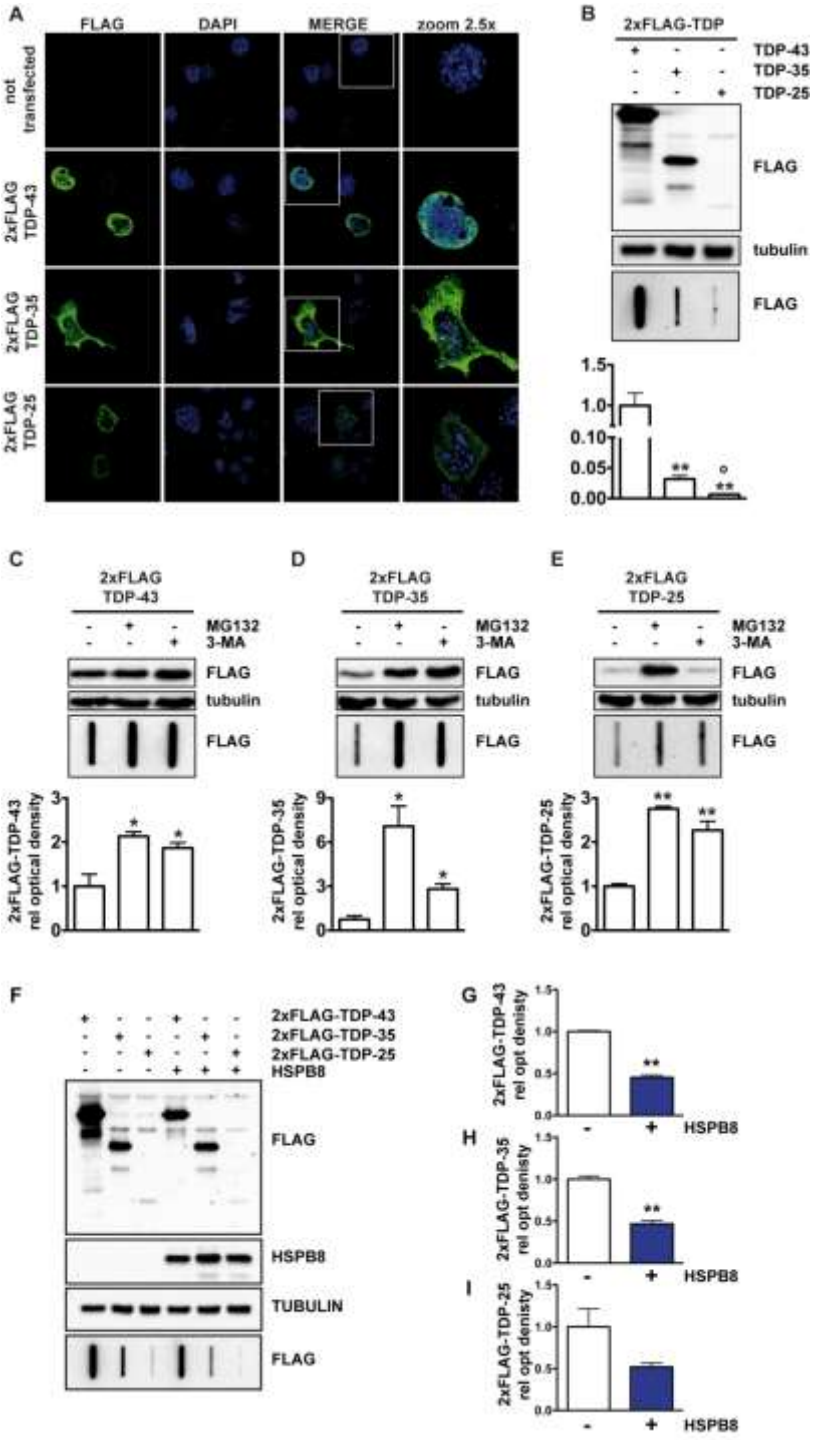


*Figure 30: Accumulation and clearance of FLAG-tagged TDP-43, TDP-35 and TDP-25. (A) Confocal microscopy analysis (63x magnification) of mouse motor neurone NSC34 control cells or cells transiently overexpressing 2xFLAG-TDP-43, 2xFLAG-TDP-35, 2xFLAG-TDP-25. DAPI: nucleic acid staining. A 2.5x magnification image of selected areas is shown. (B) WB (upper insets) and FRA (lower insets and FRA quantification, bar graph) of the PBS extracts of mouse motor neurone NSC34 cells transiently overexpressing the 2xFLAG-TDP-43, 2xFLAG-35 or 2xFLAG-TDP-25. The data represent the mean ± sem of n=3 independent samples. ** P<0.001 vs 2xFLAG- TDP-43; ° P<0.05 vs 2xFLAG-TDP-35. (C-E): WB (upper insets) and FRA (lower insets and FRA quantification, bar graph) of the PBS extracts of mouse motor neurone NSC34 cells transiently overexpressing 2xFLAG-TDP-43 (C), 2xFLAG-35 (D) or 2xFLAG-TDP-25 (E) and treated with 10mM MG132 for 16h or 10mM 3-methyladenine (3-MA) for 32h (**P<0.001 or * P<0.01 vs untreated controls). The data represent the mean ± sem of n=3 independent samples. (F-I): NSC34 cells transiently co-transfected with plasmids coding for 2xFLAG-TDP-43, 2xFLAG-TDP-35 or 2xFLAG-TDP-25 and pCDNA3 or hHSPB8. WB and representative FRA (F). FRA quantification (G, TDP-43; H, TDP-35; I, TDP-25) (**P<0.001 vs pCDNA3 transfected cells). The data represent the mean ± sem of n=3 independent samples*

**CHAPTER 2: TDP-43 PATHOLOGY IN MUSCLE CELLS: DIFFERENCES AND COMMUNALITIES WITH MOTOR NEURON TDP-43 PATHOLOGY**

**Introduction**

The role of muscle tissue in the pathogenesis of ALS has not been clearly defined. There are many works that demonstrated that during ALS, muscle tissue is damaged. On the other hand muscle importance during the onset of the pathology is very controversial. In this context many works have been carried out in SOD1 mouse model. Some studies demonstrated that SOD1 restricted expression in muscle cells, caused muscle atrophy but not ALS. On the other side there are other works that claim that overexpression of IGF-1 is able to mildly rescue ALS phenotype.

In this second chapter, I compared TDP43 and its disease associated fragments behaviour in both motor neuronal cell line NSC34 and immortalized murine myoblast C2C12. Subsequently, I analysed which degradative system degrades TDP43 species inside muscle cells. In the last part, I analysed the protective effect of HspB8 in muscle cells in presence of TDP43 species.

## Materials and methods

### CHEMICALS

NSC34 and C2C12 were treated with the same chemicals described in the previous chapter.

### CELL CULTURES

NSC34 were cultured as described in the previous chapter.
C2C12 were used a muscle model. Cells were maintained in high glucose medium completed with glutamine, penicillin, streptomycin and 10% of fetal bovine serum (GIBCO, Thermo Scientific Life Sciences Research, Waltham, MA, USA). Cells are growth at 37°C at 5% $CO_2$.

### TRASFECTION METHOD

NSC34 were transfected using Lipofectamine® Transfection Reagent as described in the previous chapter
C2C12 cells were transfected with Lipofectamine® 2000 Transfection Reagent (Invitrogen) following manufacturer instructions. Briefly DNA was incubated with Lipofectamine® 2000 reagent and the mix was added to cells directly in medium deprived of serum and antibiotics. After 5 hours medium was replaced with fresh one supplemented with serum and treatment.
For these experiments the same plasmids used in the chapter above were utilized.

### FRACTIONATION

Both cell lines were plated in 6-well plate (NSC34 100,000 cells/mL; C2C12 65,000 cells/mL). 48 hrs after transfection cells were harvested and centrifuged at 100 rcf at 4° for 5 min. Cells were then diluted in 100µL PBS (Euroclone) added with protease inhibitor cocktail (Sigma-Aldrich), sonicated (3 hits at lowest intensity) and centrifuged for at maximum speed at 4°C for 15min. Supernatant was then transferred in a new tube and pellet was rinsed in 100 µL of 1% TRITON X-100 (Sigma-Aldrich) solution in PBS. Suspension was slightly sonicated and centrifuged at maximum speed at 4°C for 15 min. The supernatant (that corresponds to TRITON X-100 soluble fraction) is placed in a new tube. Pellet was rinsed in 100µL of a solution of PBS and 5% SDS (Sigma-Aldrich) sonicated and centrifuged as previously described to obtain TRITON X-100 soluble fraction. The SDS soluble fraction is transferred in a new tube and the pellet was rinsed in 100µL of a solution of 88% formic acid (FA) (Sigma-Aldrich) in PBS, sonicated and centrifuged with same protocol used to obtain TRITON X-100 and SDS soluble fraction. The FA soluble fraction is transferred in a new tube and the remaining pellet is discarded. PBS soluble fraction and TRITON X-100 soluble fraction were quantified using bicinchoninic acid (BCA) (Euroclone) assay. SDS soluble fraction and FA soluble fraction were loaded as equal volume to PBS soluble fraction.

### NP40 EXTRACTION, FILTER RETARDATION ASSAY AND WESTERN BLOT

NP40 extraction was performed as described in chapter one. NSC34 were plated at 90,000 cell/mL and C2C12 were plated at 65,000 cell/mL in 12-well plate. Filter retardation assay (FRA) was performed as already described (see Cap. 1): NP40 extracts were loaded after BCA quantification: 1.5 µg of soluble extracts for NSC34 and 6µg for C2C12. Insoluble fraction was loaded as equal volume. For WB analysis of both NP-40 extracts 15µg of soluble fraction of both cell lines were loaded. Insoluble fraction was loaded as equal volume. For WB analysis of fractionation 15µg of PBS and TRITON

X100 extracts of both cell lines were loaded. SDS and FA extracts were loaded as equal volume counted on PBS extracts quantification.

ANTIBODY DILUTION

The following primary antibodies were used: HRP-conjugate anti-GFP antibody (MB-0712; Vector Laboratories, Burlingame, CA, USA) for TDPs detection in FRA and WB (1:10,000 for NSC34; 1:2,000 for C2C12); home-made rabbit polyclonal anti-HSPB8 (1:2,000); home-made polyclonal anti-Bag3 (1: 3,000); rabbit polyclonal anti-HA (Santa Cruz Biotechnology, sc-7392) (1:500); goat polyclonal anti-ACTIN (Santa Cruz Biotechnology, sc-1616) (1:1,000); rabbit polyclonal anti GAPDH (Santa Cruz Biotechnology, sc-25778) (1:1,000); mouse monoclonal anti-α-tubulin (Sigma-Aldrich T6199) (1:2,000). The following secondary antibodies were used: goat anti-rabbit HRP-conjugate secondary antibody (Santa Cruz Biotechnology, sc-2004); goat anti-mouse HRP-conjugate secondary antibody (Santa Cruz Biotechnology, sc-2005); donkey anti-goat HRP-conjugate secondary antibody (Santa Cruz Biotechnology, sc-2020)

IMMUNOFLUORESCENCE

Cells were seeded on coverlips in 24-well plate (NSC34 70,000 cell/mL; C2C12 55,000 cell/mL). After transfection cells were fixed in paraformaldehyde 4% and methanol. Immunofluorescence was carried out as previously described.
For aggregates counting, microscope was supported with a grind ocular. For each cells, in the field chosen, small and big aggregates were counted. 3 fields for each sample were analysed, and for each condition 3 samples were prepared.

**Muscle cells are a site for TDP-25 aggregation**

Since little is known about muscle response in presence of misfolded and aggregation prone proteins, I investigated the behaviour of misfolded proteins in C2C12 muscle cell model.

I transfected in parallel NSC34 cells and C2C12 cells with GFP-TDP-43, GFP-TDP-35 and GFP-TDP-25. Cells were fixed and nuclei stained for microscope acquisition.

As previously observed in NSC34 cells, GFP-TDP-43 in muscle cells was retained in the nucleus, and it formed no aggregates. As in NSC34 cells, GFP-TDP-35 was partially mislocalized in the cytoplasm of muscle cells (Figure 32A-C). In both cell models, few aggregates were observed in presence of GFP-TDP-35. Conversely, in both cell models GFP-TDP-25 is completely mislocalized in the cytoplasm where it was found in its aggregated form. I observed that aggregates in NSC34 cells were bigger and more numerous than in muscle C2C12 cells (Figure 32A-C). Counting aggregates per cells I found that in C2C12 cells the number of big and small aggregates was fewer than in NSC34 cells (Figure 32E).

To further investigate and to better characterize the solubility of the different GFP-TDPs species, I performed a fractionation in four buffers with increasing solubility power (PBS < TRITON X100 < SDS < FA) (Figure 32B-D). Western blot (WB) results showed that, in NSC34 cells, GFP-TDP-43 was equally found in PBS, TRITON X100, and SDS, while in C2C12 cells it is mainly solubilized by PBS and TRITON X100 and only a little fraction appear in SDS soluble fraction. GFP-TDP-35 in both cell lines was equally distributed in the PBS, TRITON X100, and SDS. GFP-TDP-25, on the other hand, is poorly present in PBS and TRITON X100 fractions compared to the other two species; the most of the GFP-TDP-25 protein was detected in the SDS fractions. Noteworthy, in NSC34 cells, GFP-TDP-25 can also be found in the FA fraction.

I also investigate the biochemical behaviour of the autophagic receptor p62; p62 is a protein that recognizes substrates and facilitates internalization of these substrates into autophagic vesicles. I observed that in NSC34 cells, p62 was found in all fractions and its expression did not change in presence of the different TDPs. However, in NSC34 cells expressing GFP-TDP-25, p62 was found also in the FA fraction (Figure 32B-D), while in C2C12 cells p62 was equally found in PBS, TRITON and SDS fractions, but not in the FA fraction, even when GFP-TDP-25 was expressed.

This first observation shows that the three GFP-TDPs species have the same localization in both cell lines: TDP-43 forms no aggregates and remains in the nucleus, GFP-TDP-35 mislocalizes in the cytoplasm where it aggregates and GFP-TDP-25 (that completely loses the NLS) is found aggregated in the cytoplasm. I also observed that all the three GFP-TDPs species have comparable biochemical behaviours in NSC34 cells and in C2C12 cells: GFP-TDP-43 and GFP-TDP-35 are more soluble than GFP-TDP-25 that is almost exclusively found in the SDS (or FA) fractions. Most importantly, I also noted a significant difference between the two models: in fact, GFP-TDP-25 aggregates are more numerous and bigger in NSC34 cells than in C2C12 cells, while GFP-TDP-25 aggregates are smaller and fewer compared to aggregates detected in NSC34 cells.

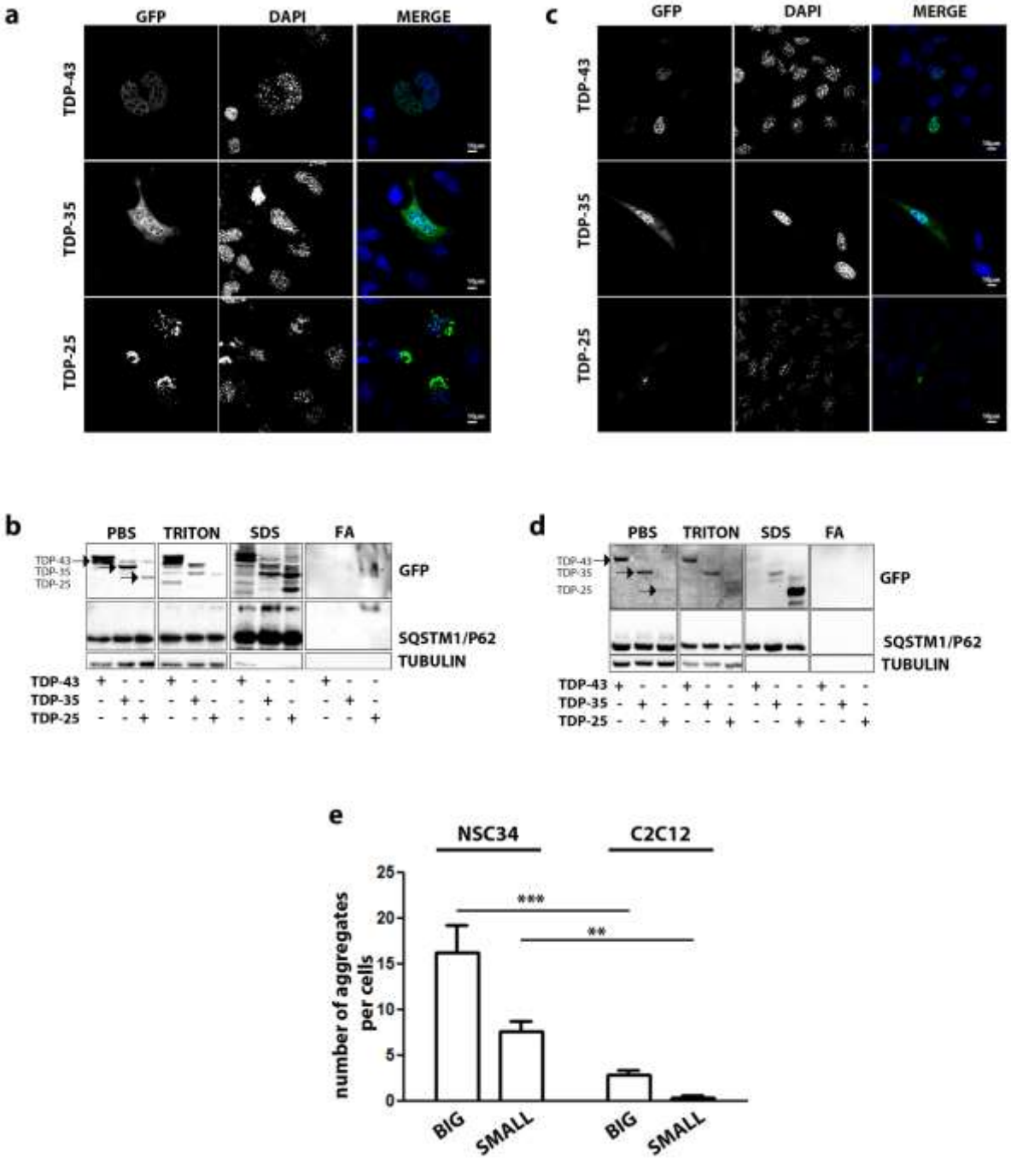


*Figure 31: TDP-43 variants show different behavior in mouse motor neurone NSC34 and C2C12 cells. (A) Confocal microscope analysis. Mouse motor neurone NSC34 cells were transiently transfected with GFP-TDP-43, GFP-TDP-35, GFP-TDP-25. Nuclei were stained with DAPI. Images were acquired using confocal microscope with 63X magnification. (B) Western blot (WB) shows PBS, TRITON X-100, SDS and formic acid (FA) extracts. Actin was used as loading control.(C) Confocal microscope analysis. Immortalized mouse myoblast C2C12 cells were transiently transfected with GFP-TDP-43, GFP-TDP-35, GFP-TDP-25. Nuclei were stained with DAPI. Images were acquired using confocal microscope with 63X magnification. (D) WB shows PBS, TRITON X-100, SDS and FA extracts.(E) Quantitation of small and big aggregates per cells was performed with ImageJ. Graph bar shows the medium number of small and big aggregates per cell in mouse motor neurone NSC34 and C2C12 transiently transfected with GFP-TDP-25. **p<0.01; ***p<0.001 vs C2C12.*

**GFP-TDP-25 aggregates are equally isolated by fractionation and NP-40 extraction**

With fractionation I set a valuable method for correctly visualizing GFP-TDP-25 aggregates. Since fractionation is a long time-requiring procedure, for routine comparison of both cell lines, I decided to adopt the fractionation method based on NP-40 extraction (Figure 33).

I transfected both cell line with GFP-TDP-25 and then I performed in parallel fractionation and NP-40 extraction. WB results on different extracts showed that the most of the GFP-TDP-25 in both cell lines was retained in the SDS soluble fraction and in the NP-40 insoluble fraction and the amount of GFP-TDP-25 was comparable in these two fractions (SDS soluble fraction and NP-40 insoluble fraction). P62 levels were also analysed and I found that in NSC34 cells, p62 levels were higher in the SDS-soluble and NP-40 insoluble fractions, following GFP-TDP-25 distribution. In C2C12 cells, p62 levels did not change among different fractions. Tubulin was used as a control for a proper extraction since it appeared in PBS, TRITON X100 and NP-40 soluble fractions, while it was absent in SDS soluble and NP-40 insoluble fractions.

I confirmed that to correctly visualize TDP-25 aggregates I can mutually use fractionation and NP-40 extraction.

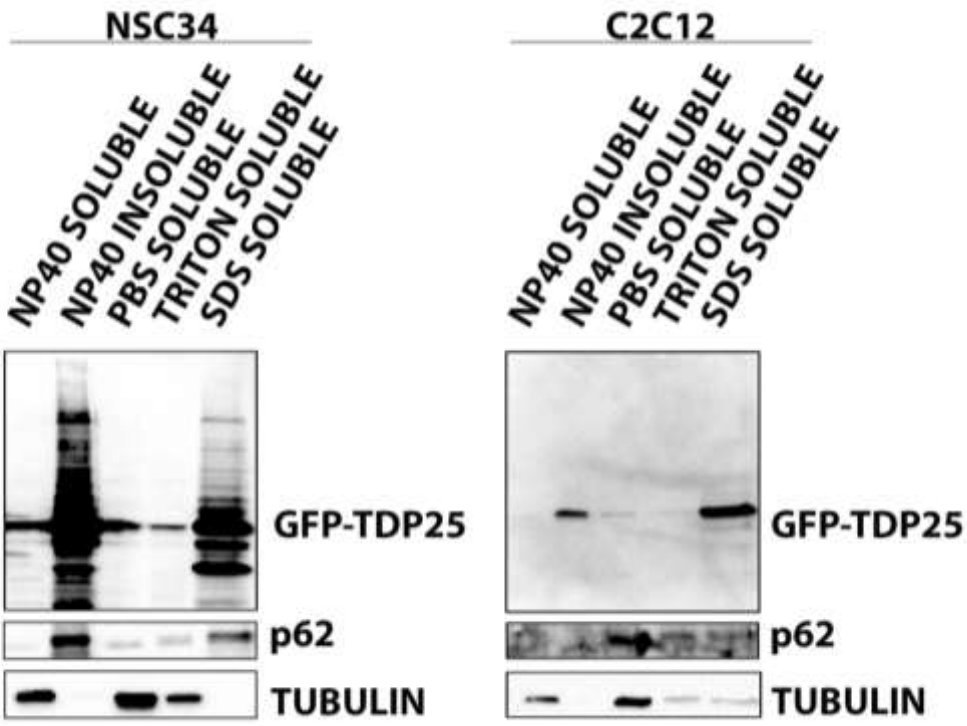


*Figure 32: Comparison between fractionation and NP-40 extraction. (A) Western Blot shows both extracts of fractionation and extracts from NP-40 extraction of mouse motor neurone NSC34 transiently overexpressing GFP-TDP-25. (B) Western Blot shows both extracts of fractionation and extracts from NP-40 extraction of immortalized mouse myoblast C2C12 transiently overexpressing GFP-TDP-25.*

**Proteasome and autophagy relevance in degradation of TDPs species in muscle cells.**

Previous experiments showed that the three GFP-TDPs species behaved differently in the two cell models. Indeed, I found that in NSC34 cells the aggregation propensity of GFP-TDP-25 was greater than in C2C12 cells. To investigate the reason of this difference, I analysed the contribution of the two degradative systems in C2C12 cells in presence of GFP-TDPs.

I transfected C2C12 cells with GFP-TDP-43, GFP-TDP-35 and GFP-TDP-25. To evaluate the contribution of each degradative system, I treated cells with MG132 overnight to inhibit the proteasome and with 3MA for 48 hrs to inhibit autophagy. Samples were analysed with FRA and WB (Figure 34) following an NP-40 extraction.

Analysing the NP-40 soluble fractions in FRA, revealed that proteasome inhibition by MG132 caused a reduction in GFP-TDP-35 and GFP-TDP-25 protein, while protein levels of GFP-TDP-43 did not change upon MG132 treatment (Figure 34A). On the other side inhibition of autophagy did not cause changes in protein amount retained in FRA related to GFP-TDP-43, GFP-TDP-35 and GFP-TDP-25. When looking at the soluble protein levels in WB, I observed that proteasome inhibition by MG132 caused an increased only in GFP-TDP-25 protein levels, while GFP-TDP-35 and GFP-TDP-43 soluble protein levels were not affected by proteasome inhibition. WB analysis of extracts after autophagy inhibition reflected FRA analysis showing no changes in protein amount after autophagy inhibition.

Analysing the NP-40 insoluble fraction by FRA I observed that following proteasome inhibition with MG132, GFP-TDP-35 and GFP-TDP-25 accumulated at higher levels compare to control conditions (*** $p<0.001$ vs control condition), while GFP-TDP-43 levels in FRA did not change upon MG132 treatment (Figure 34B). Notably, inhibition of autophagy with 3MA produced no significant effect on insoluble species retained in FRA for all the three insoluble species. WB analysis confirmed the trend observed with FRA analysis: MG132 produced an increase in GFP-TDP-25 NP-40 insoluble species, while GFP-TDP-35 and GFP-TDP-43 levels remained unaffected (Figure 34B); on the other side, autophagy inhibition did not produce changes in NP-40 insoluble protein levels analysed in WB.

The ratio between the insoluble and the soluble fractions analysed in FRA showed that, after MG132 treatment, there was a significant shift towards the insoluble species for GFP-TDP-35 and GFP-TDP-25 ($p<0.05$ vs control condition) (Figure 34C). In addition, the GFP-TDP-43 ratio suggested that there were more insoluble species, but the differences with the control were not significant. Conversely, 3MA produce no change in the solubility of GFP-TDPs; indeed, there is no shift towards the insoluble NP-40 species for all the GFP-TDPs species.

These results show that in muscle cells the proteasome is apparently more relevant in the degradation of toxic fragments of TDP-43; indeed when proteasome is pharmacologically inhibited I found the formation of more NP-40 insoluble species. On the other hand, autophagy at basal levels is poorly involved in GFP-TDPs degradation, since its inhibition with 3MA did not produce any change in GFP-TDPs protein levels.

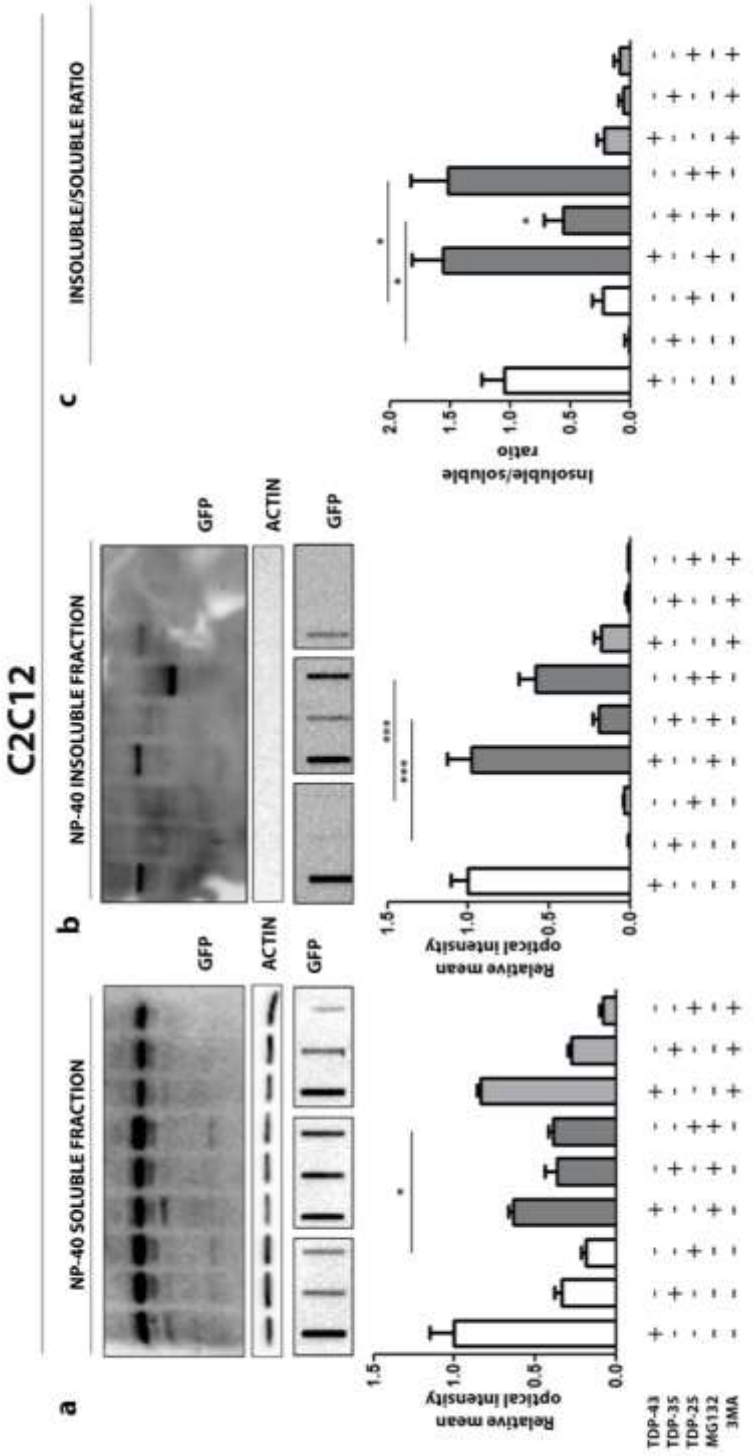


*Figure 33: Degradative systems involvement in C2C12 with GFP-TDPs species. immortalized mouse myoblast C2C12 were transiently transfected with GFP-TDP-43, GFP-TDP-35 and GFP-TDP-25. Treatments for 10 hours with MG132 (10μM) or for 36 hours with 3MA (10mM). (A) Panel shows NP-40 soluble extracts WB analysis (upper inset), NP-40 soluble extracts FRA analysis (middle inset) and quantification of NP-40 soluble extracts FRA assay (** p<0.01 vs untreated GFP-TDP-25) (lower inset); (B) Panel shows NP-40 insoluble extracts WB analysis (upper inset), NP-40 insoluble extracts FRA analysis (middle inset) and quantification of NP-40 insoluble extracts FRA assay (** p<0.01 vs corresponding untreated GFP-TDP-35 and GFP-TDP-25) (lower inset); (C) Panel shows quantification of insoluble/soluble ratio (* p<0.05 vs respective untreated GFP-TDP-35 and GFP-TDP-25).*

**Autophagic routing of TDPs fragments reduces aggregation in muscle cells.**

Since proteasome has a low capacity to degrade misfolded species and the presence of ALS related misfolded proteins can overwhelm and damage the system, I perform some experiments aimed to direct insoluble species to the more capable autophagy system, with the goal to reduce the load on proteasome and the aggregation of misfolded proteins. To achieve this aim I overexpressed HSPB8, whose role in directing misfolded species to autophagy is well assessed in motor neurons. In fact, HSPB8 is part of a complex that recognized misfolded species and brought them directly in to the autophagic vesicles. I overexpressed HSPB8 in C2C12 cells in presence of GFP-TDP-43, GFP-TDP-35 and GFP-TDP-25 and NP-40 extracts were analysed by FRA and WB.

Both in FRA and WB, GFP-TDP-43 and GFP-TDP-35 protein levels in NP-40 soluble fractions slightly changed when HSPB8 is overexpressed compared to control condition (pcDNA3) (Figure 35A). Interestingly, in FRA NP-40 soluble levels of GFP-TDP-25 were significantly decreased in presence of HSPB8 (** $p<0.01$ vs control condition) while in WB soluble levels of GFP-TDP-25 were not affected by HSPB8 activity (Figure 35A).

In FRA, GFP-TDP-43 proteins levels in NP-40 insoluble fraction were not affected by the presence of HSPB8. On the other side, HSPB8 produced a significant reduction in GFP-TDP-35 and GFP-TDP-25 species isolated in NP-40 insoluble fraction (** $p<0.01$ vs control condition; *** $p<0.001$ vs control condition) (Figure 35A). GFP-TDP-43 NP-40 insoluble levels in FRA were not change after HSPB8 overexpression. WB analysis of NP-40 insoluble fraction showed diminished levels only of the GFP-TDP-25 protein in the NP-40 insoluble fraction when HSPB8 is overexpressed (Figure 35A). Noteworthy, it seems that the levels of the overexpressed HspB8 change depending on which TDP specie is present.

I also performed an IF co-transfecting HSPB8 with GFP-TDPs. I observed that in muscle cells, GFP-TDP-43 localization and quantity was unaffected by HSPB8 overexpression. The few aggregates formed by GFP-TDP-25 were completely cleared by HSPB8 overexpression (Figure 35B).

With this experiment I observed that even if autophagy is not involved at basal level (see Figure 34), it is possible to route misfolded species to autophagy, reducing the loading of proteasome and thus increasing the clearance of misfolded proteins. Indeed, HSPB8 overexpression increased the clearance of GFP-TDPs species, directing misfolded species towards autophagy.

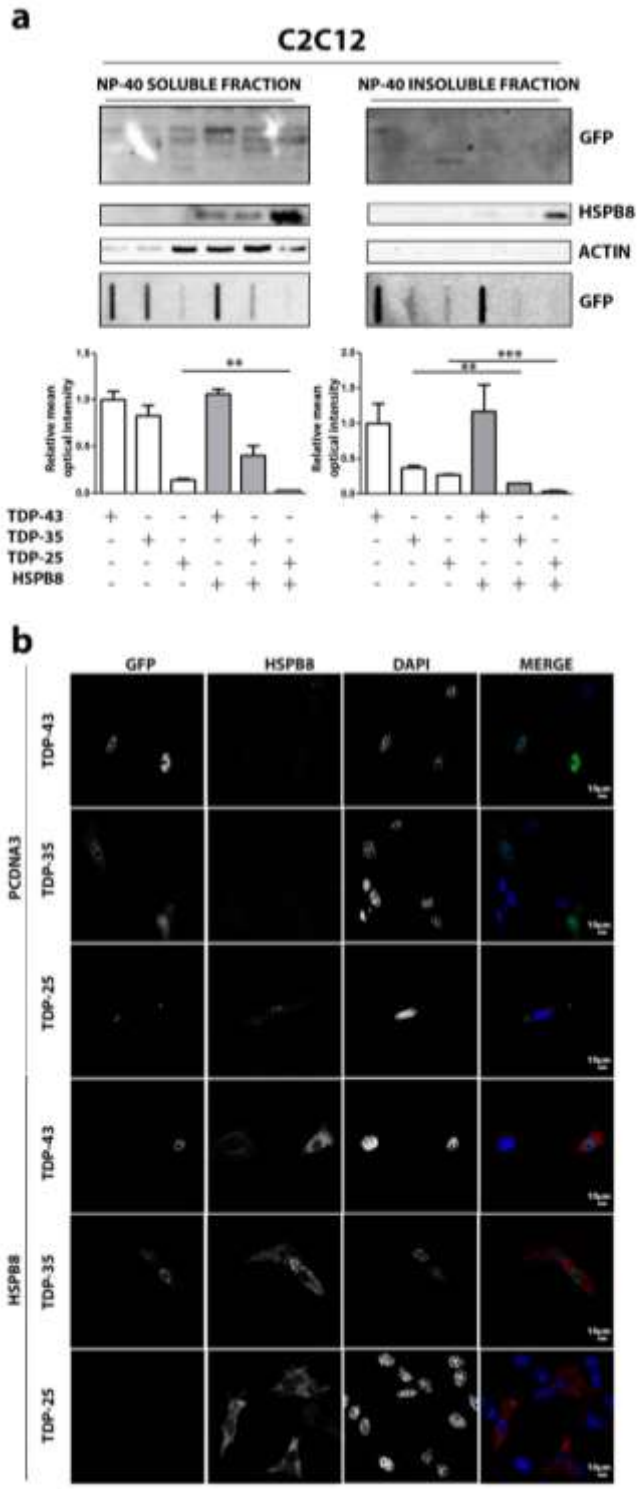


*Figure 34: HSPB8 overexpression counteracted GFP-TDP-25 accumulation in C2C12. Immortalized mouse myoblast C2C12 transiently overexpressing GFP-TDP-43, GFP-TDP-35 and GFP-TDP-25, and co-transfected with pCI- hHSPB8 or pcDNA3 as control vector. (A) NP-40 extraction: left panel NP-40 soluble extracts WB analysis (upper inset), NP-40 soluble extracts FRA analysis (middle inset) and quantification of NP-40 soluble extracts FRA analysis (** p<0.01 vs GFP-TDP-25 co-transfected with control vector) (lower inset). Right panel shows NP-40 insoluble extracts WB analysis (upper inset), NP-40 insoluble extracts FRA analysis (middle inset) and quantification of NP-40 insoluble extracts FRA analysis (**p<0.01; *** p<0.001 vs relative GFP-TDPs co-transfected with control vector).(B) Immortalized mouse myoblast C2C12 transiently overexpressing GFP-TDP-43, GFP-TDP-35 and GFP-TDP-25, and co-transfected with pCI- hHSPB8 or pcDNA3 as control vector analysed with confocal microscope. 63X magnification. Green: GFP-TDPs; Red: hHSPB8; nuclei staining: DAPI.*

**CHAPTER 3: DIFFERENTIAL ROUTE TO PROTEASOME AND AUTOPHAGY IN ALS IN MOTOR NEURON AND MUSCLE CELLS**

**Introduction**

Proteasome and autophagy are the two main degradative systems in charge of maintaining the correct protein homeostasis inside cell environment. Both misfolded protein and aggregates are toxic to cells if they are not correctly removed from cells. It has been postulated that in the last stages of ALS, degradative systems are no more functional and misfolded proteins lead to motor neuron death. Both proteasome and autophagy are able to sense the presence of misfolded, toxic proteins and the presence of aggregates and protein inclusions. The chaperone system helps the degradative systems in recognising misfolded proteins and aggregates. In particular Hsp70, which can recruits substrates to be degraded, forms a complex with an ubiquitin ligase, named CHIP, and alternatively with Bag1 or Bag3-HspB8. Bag1 directs the complex and the bound substrates to proteasome while Bag3-HspB8 drives the complex to autophagy.

In this last part, I analysed the effect of Bag1 and Bag3 on TDP43 species in both motor neurons and muscle cells.

**Materials and methods**

All the experiments were performed following protocols described in the previous chapters.
For these experiments GFP-TDPs plasmids were co-transfected with pCI-6xHis-FL-Bag3 which codes for the human form of full length BAG3 and pCDNA/HA-Bag1 which codes for the human form of BAG1, that are all kindly provided by Dr. H.H. Kampinga; pcDNA3 was used as control plasmid. To detect the proteins encoded by these antibody the following antibody were used: home-made rabbit polyclonal anti-Bag3 (1:3,000 for WB, 1:500 for IF; kindly provided by), rabbit polyclonal anti-HA (1:500 for WB, 1:250 for IF; Santa Cruz, sc-805).

**BAG3 role in autophagy routing of misfolded proteins**

BAG3 is HSPB8 co-chaperone in the HSP70-HSPB8-BAG3 complex, which has a double function: it helps HSPB8 in cargo recognition and, after association with HSP70, BAG3 regulates the release from HSP70 of the cargo at the MTOC. Since I already tested the protective of HSPB8 in motor neuronal and muscle cells in presence of misfolded proteins, I analysed BAG3 role in presence of GFP-TDPs species.

NSC34 cells and C2C12 cells were transfected with BAG3 and with GFP-TDP-43, GFP-TDP-35 and GFP-TDP-25 (pCDNA3 was taken as control) and NP-40 extracts were analysed by FRA and WB (Figure 36A-C).

In NSC34 cells, FRA performed on NP-40 soluble extracts showed that BAG3 overexpression reduced the amount of GFP-TDP-25 retained on the membrane compared to control condition (* $p<0.05$ vs control). In FRA, the levels of GFP-TDP-43 and GFP-TDP-35 were not reduced by BAG3 overexpression. WB analysis confirmed the trend observed in FRA of the NP-40 soluble GFP-TDPs species: GFP-TDP-25 monomeric form was mildly decreased in presence of BAG3 overexpression while GFP-TDP-43 and GFP-TDP-35 levels remained unaffected. BAG3 overexpression also reduced the amount of GFP-TDP-25 in NP-40 insoluble fraction analysed in FRA (* $p<0.05$ vs control). The levels of GFP-TDP-43 in NP-40 insoluble fraction were not changed with BAG3 overexpression, while GFP-TDP-35 levels were reduced, but not in a significant manner (Figure 36A); WB analysis of the NP-40 insoluble fraction showed that there was no differences in GFP-TDPs presence in this fraction, when BAG3 is overexpressed compare to control conditions. IF analysis co-expressing BAG3 and GFP-TDPs species (Figure 36B) revealed that, in presence of BAG3 (BAG3 is stained in red when overexpressed), GFP-TDP-25 aggregates were smaller and fewer in number if compared to control condition, confirming the results obtained with NP-40 extraction. In parallel, I was unable to detect changes of the presence and localization of GFP-TDP-43 and GFP-TDP-35.

In C2C12 cells, the soluble NP-40 extracts analysed in FRA showed a significant decreased of GFP-TDP-25 amount after BAG3 overexpression (*** $p<0.001$ vs control) (Figure 36C), while the amount of GFP-TDP-43 and GFP-TDP-43 in the NP-40 soluble fraction was not affected by BAG3 overexpression. WB analysis showed the same trend observed in FRA analysis. Indeed, GFP-TDP-25 levels, in presence of BAG3, changed while GFP-TDP-43 and GFP-TDP-35 protein levels remained unaffected (Figure 36C).

In order to test the effect of BAG3 on insoluble, HMW formations, insoluble NP-40 fraction was analysed. FRA showed a significant reduction of GFP-TDP-25 species (* $p<0.05$) in presence of overexpressed BAG3 while GFP-TDP-43 and GFP-TDP-35 amount in this fraction was no affected by BAG3 overexpression (Figure 36C). Also IF analysis performed C2C12 transfected with BAG3 and GFP-TDPs species showed that BAG3 overexpressing cells were completely cleared by GFP-TDP-25 aggregates, while GFP-TDP-43 and GFP-TDP-35 remained unchanged in presence of BAG3 overexpression (Figure 36D).

These results suggest that BAG3 has a pro-degradative role against GFP-TDP-25 aggregates in both cell models, indeed aggregation of GFP-TDP-25 measured by FRA on NP-40 extracts or IF is reduced by BAG3 overexpression. On the other side it has no effect on GFP-TDP-43 and GFP-TDP-35 protein levels and protein aggregation.

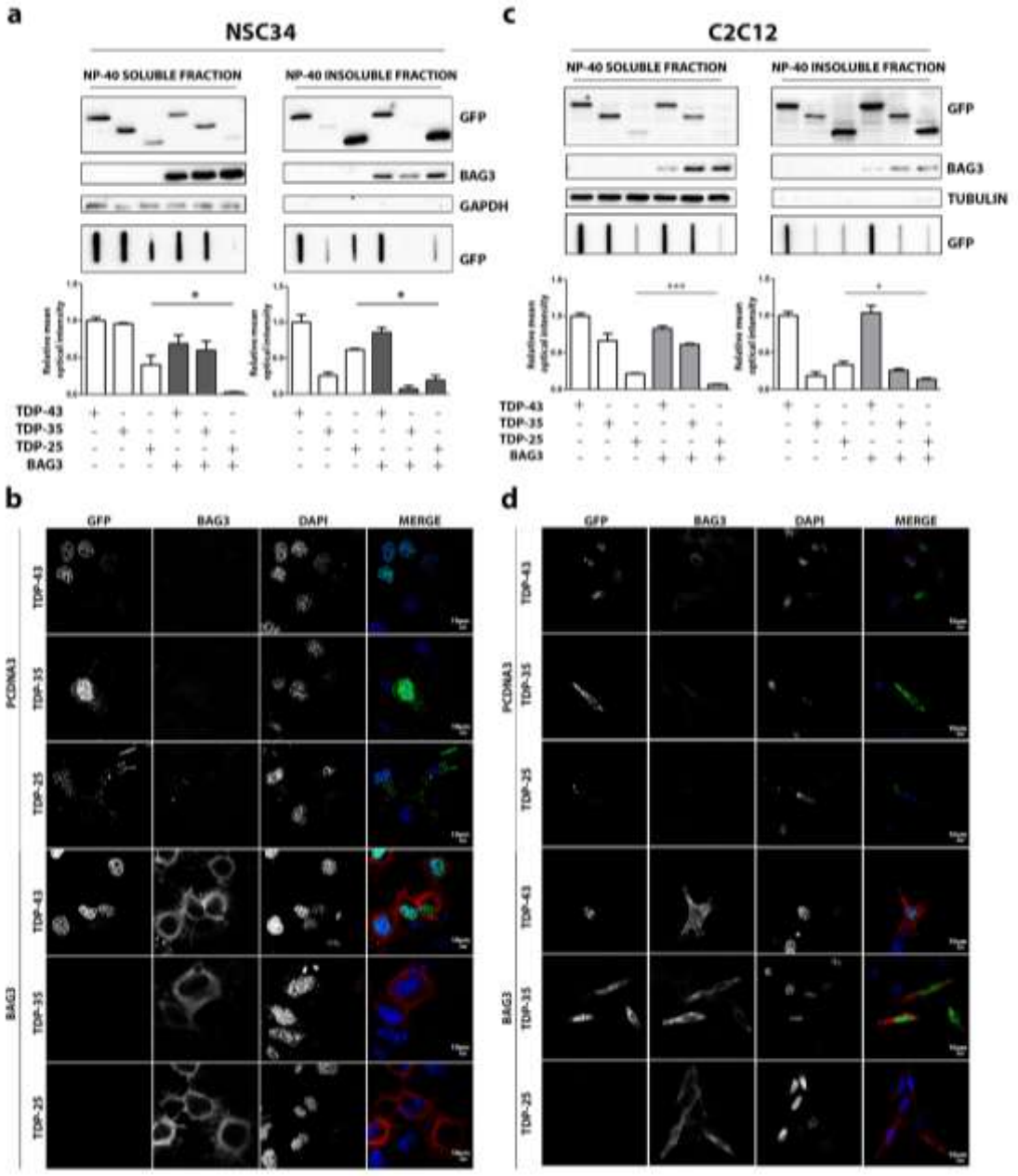


*Figure 35: Co-chaperone BAG3 counteracts GFP-TDP-25 aggregation in NSC34 and C2C12 (A) mouse motor neurone NSC34 transiently overexpressing GFP-TDP-43, GFP-TDP-35 and GFP-TDP-25, and co-transfected with pCI-6xHIS-Bag3 or pcDNA3 as control vector. Left panel shows NP-40 soluble extracts WB analysis (upper inset), NP-40 soluble extracts FRA analysis (middle inset) and quantification of NP-40 soluble extracts FRA analysis (* p<0.05 vs GFP-TDP-25 co-transfected with control vector) (lower inset). Right panel shows NP-40 insoluble extracts WB analysis (upper inset), NP-40 insoluble extracts FRA analysis (middle inset) and quantification of NP-40 insoluble extracts FRA analysis (*p<0.05 vs GFP-TDP-25 co-transfected with control vector) (lower inset). (B) mouse motor neurone NSC34 transiently overexpressing GFP-TDP-43, GFP-TDP-35 and GFP-TDP-25, and co-transfected with pCI-6xHIS-Bag3 or pcDNA3 as control vector analysed with confocal microscope. 63X magnification. Green: GFP-TDPs; Red: hBAG3; nuclei staining: DAPI.(C) Immortalized mouse myoblast C2C12 transiently overexpressing GFP-TDP-43, GFP-TDP-35 and GFP-TDP-25, and co-transfected with pCI-6xHIS-Bag3 or pcDNA3 as control vector. Left panel shows NP-40 soluble extracts WB analysis (upper inset), NP-40 soluble extracts FRA analysis (middle inset) and quantification of NP-40 soluble extracts FRA analysis (*** p<0.001 vs GFP-TDP-25 co-transfected with control vector) (lower inset). Right panel shows NP-40 insoluble extracts WB analysis (upper inset), NP-40 insoluble extracts FRA analysis (middle inset) and quantification of NP-40 insoluble extracts FRA analysis (*p<0.05 vs GFP-TDP-25 co-transfected with control vector).(D) Immortalized mouse myoblast C2C12 transiently overexpressing GFP-TDP-43, GFP-TDP-35 and GFP-TDP-25, and co-transfected with pCI-6xHIS-Bag3 or pcDNA3 as control vector analysed with confocal microscope. 63X magnification. Green: GFP-TDPs; Red: hBAG3; nuclei staining: DAPI.*

**Routing to proteasome, through Bag1 activity prevents the formation of GFP-TDPs aggregates.**

BAG1 is another member of the BAG family and its role is different from BAG3. In fact, BAG1 binds HSP70 and routes misfolded proteins to proteasome rather than to autophagy. Its potential role against misfolded proteins has been poorly assessed. Since GFP-TDPs species are substrates of the UPS, I investigate the role of BAG1 on the degradation of GFP-TDPs species.

NSC34 and C2C12 cells were transfected with BAG1 and GFP-TDP-43, GFP-TDP-35 and GFP-TDP-25; NP-40 soluble and insoluble fractions were analysed by FRA and WB.

FRA analysis of NSC34 NP-40 soluble extracts showed that levels of GFP-TDP-43 and GFP-TDP-35 remained unchanged upon BAG1 overexpression (Figure 37A). Notably, GFP-TDP-25 levels in NP-40 soluble fraction were reduced in FRA by BAG1 overexpression. WB analysis in which the monomeric form of NP-40 soluble species were detectable, showed that all the three GFP-TDPs monomers were reduced by BAG1 overexpression.

By Analysing NP-40 insoluble extracts by FRA I found a significant reduction of GFP-TDP-25 species in presence of BAG1, while GFP-TDP-43 and GFP-TDP-35 protein levels remained similar to those found in control samples. WB analysis of the same NP-40 insoluble extracts, showed that in presence of BAG1 overexpression all the three GFP-TDP species were reduced (Figure 37A).

IF analysis on NSC34 cells transfected with GFP-TDPs and BAG1 showed that this co-chaperone counteracts GFP-TDP-25 aggregation. Indeed, these aggregates appeared smaller in size and in a lower number when BAG1 is overexpressed compared to control condition. Also GFP-TDP-35 mislocalization was partially rescued (Figure 37B) by BAG1 overexpression since many GFP-TDP-35 aggregates disappeared from cell cytoplasm; while GFP-TDP-43 was not affected by BAG1 presence.

BAG1 overexpression in muscle cells reflected the observation obtained in motor neurons. Indeed, C2C12 NP-40 soluble extracts analysed in FRA showed a significant reduction of GFP-TDP-25 accumulation after BAG1 overexpression (** $p<0.01$); GFP-TDP-43 and GFP-TDP-35 amount in NP-40 soluble fraction was not affected by BAG1 overexpression. WB analysis on the same extracts showed that BAG1 overexpression produced no change in the amount of the monomeric GFP-TDPs (Figure 37C).

NP40 insoluble extracts analysed in FRA revealed that BAG1 overexpression reduced also the presence of GFP-TDP-25 in this fraction (* $p<0.05$), while the levels of GFP-TDP-43 and GFP-TDP-35 remained unchanged. Surprisingly, WB analysis of NP-40 insoluble extracts revealed that in presence of BAG1 overexpression, GFP-TDP-25 and GFP-TDP-35 levels increased, while GFP-TDP-43 levels decreased (Figure 37C).

IF analysis of C2C12 transfected with GFP-TDPs in presence of BAG1 confirmed the pro-degradative activity of BAG1 against GFP-TDP-25 aggregation. Indeed, cells that displayed high aggregation of GFP-TDP-25 in control condition, in presence of BAG1 showed no aggregates. As observed in NSC34, levels of GFP-TDP-35 were lower (Figure 37D) in presence of BAG1 while in control condition TDP-35 mislocalization and aggregation was stronger.

In conclusion, these results show that, both in motor neurons and muscle cells, routing to proteasome by BAG1 overexpression, is able to counteract/reduce GFP-TDP-25 aggregation, and also GFP-TDP-35 mislocalization/aggregation. Indeed, I observed that NP-40 insoluble levels of GFP-TDP-25 were reduced by BAG1 overexpression, while effect on GFP-TDP-35 was not detectable by NP-40 extraction. Overall, these results suggest that BAG1, probably acting in complex with HSP70, may have a protective role against the formation of TDP-25 toxic species.

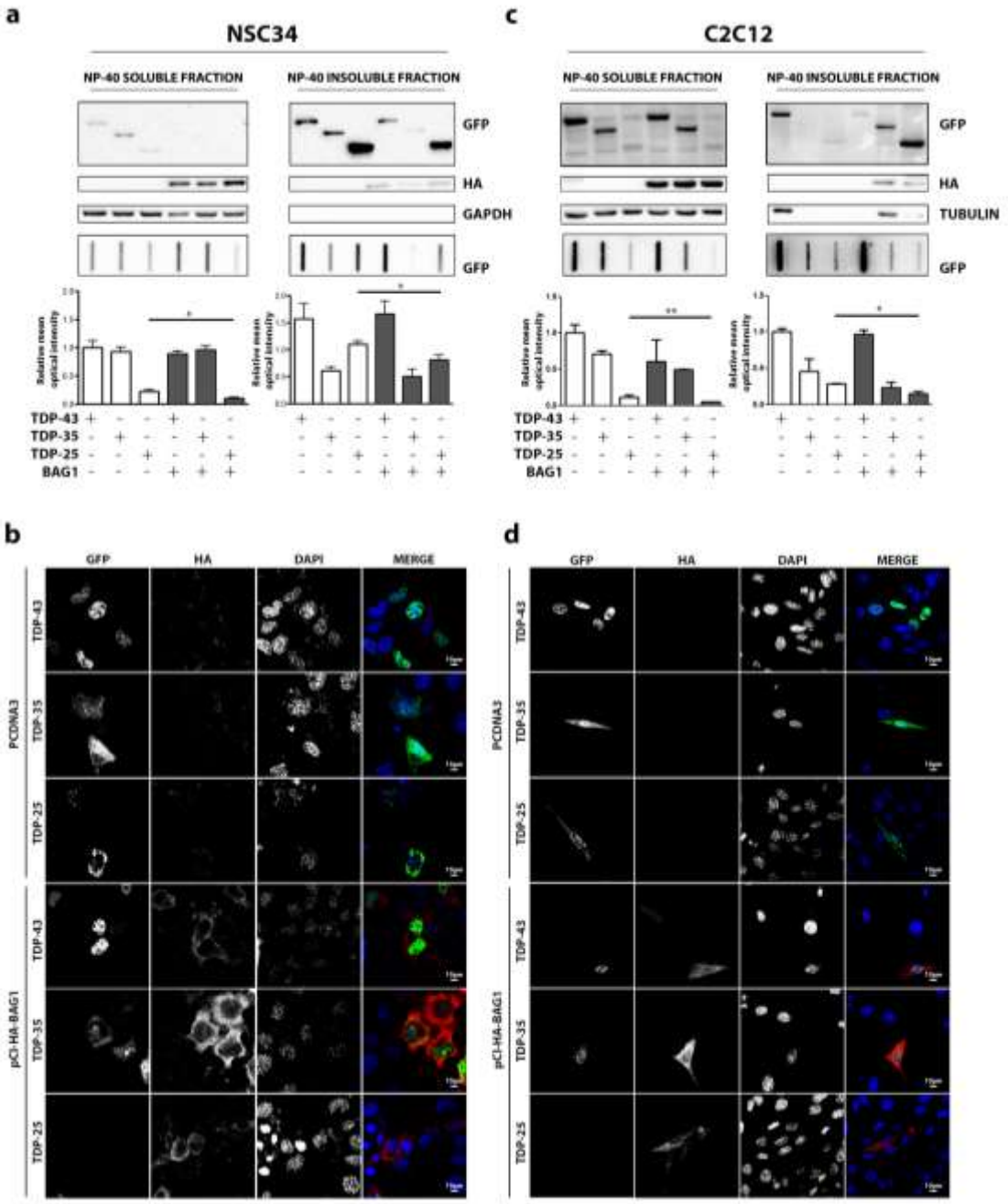


*Figure 36: Proteasome rerouting is beneficial to GFP-TDP-25 aggregation. (A) mouse motor neurone NSC34 transiently overexpressing GFP-TDP-43, GFP-TDP-35 and GFP-TDP-25, and co-transfected with pCI-HA-Bag1 or pcDNA3 as control vector. Left panel shows NP-40 soluble extracts WB analysis (upper inset), NP-40 soluble extracts FRA analysis (middle inset) and quantification of NP-40 soluble extracts FRA analysis (* p<0.05 vs GFP-TDP-25 co-transfected with control vector) (lower inset). Right panel shows NP-40 insoluble extracts WB analysis (upper inset), NP-40 insoluble extracts FRA analysis (middle inset) and quantification of NP-40 insoluble extracts FRA analysis (*p<0.05 vs GFP-TDP-25 co-transfected with control vector) (lower inset).(B) mouse motor neurone NSC34 transiently overexpressing GFP-TDP-43, GFP-TDP-35 and GFP-TDP-25, and co-transfected with pCI-HA-Bag1 or pcDNA3 as control vector analysed with confocal microscope. 63X magnification. Green: GFP-TDPs; Red: hBag1; nuclei staining: DAPI. (C) Immortalized mouse myoblast C2C12 transiently overexpressing GFP-TDP-43, GFP-TDP-35 and GFP-TDP-25, and co-transfected with pCI-HA-Bag1 or pcDNA3 as control vector. Left panel shows NP-40 soluble extracts WB analysis (upper inset), NP-40 soluble extracts FRA analysis (middle inset) and quantification of NP-40 soluble extracts FRA analysis (** p<0.05 vs GFP-TDP-35 co-transfected with control vector) (lower inset). Right panel shows NP-40 insoluble extracts WB analysis (upper inset), NP-40 insoluble extracts FRA analysis (middle inset) and quantification of NP-40 insoluble extracts FRA analysis (*p<0.05 vs GFP-TDP-25 co-transfected with control vector).(D) Immortalized mouse myoblast C2C12 transiently overexpressing GFP-TDP-43, GFP-TDP-35 and GFP-TDP-25, and co-transfected with pCI-HA-Bag1 or pcDNA3 as control vector analysed with confocal microscope. 63X magnification. Green: GFP-TDPs; Red: hBag1; nuclei staining: DAPI.*

## DISCUSSION

Amyotrophic lateral sclerosis is a fatal motor neuron disease that still lacks a proper therapy. The primary target of the pathology are motor neurons, but recent evidence suggest that also oligodendrocytes and astrocytes could be directly involved in the diseases (Taylor et al. 2016). Moreover, these cells could play a role in the onset and in the progression of the pathology. Muscle is directly connected to motor neurons and thus is the tissue more affected by motor neuronal loss, becoming atrophic and loosing strength when disease progresses. In fact, patients die for respiratory failure. Even if muscle degenerates during ALS progression, its involvement in ALS pathogenesis is still unclear (Dobrowolny et al. 2008; Pansarasa et al. 2014). There are still no evidence in favour of a muscle involvement at the beginning of the pathology; what we know till now is that muscle atrophy is a consequence of motor neuron degeneration. Motor neuron degeneration could be ascribed to several factors; one of these is the presence of proteins that lose their conformation and misfold (Gendron et al. 2014). TDP-43 is a protein found misfolded and mislocalized both in familial and sporadic case of ALS. Moreover, TDP-43 is aberrantly cleaved in two major fragments of 35 and 25 kDa (Neumann et al. 2006; Zhang et al. 2009; Yamashita et al. 2014). TDP-43 inclusions, found in almost all patient tissue (apart from SOD1 and FUS patients), are enriched by these two fragments. These fragments do not properly fold and are highly aggregation prone. Indeed, I found that these TDP-43 fragments are partially (TDP-35) or completely (TDP-25) mislocalized and aggregated in the cytoplasm of both motor neuronal and muscle cells. Obviously, the aggregation propensity of these fragments is increased when the protein are fused with eGFP protein. On the other hand, TDP-43 with both tags is completely retained in the nucleus in a soluble form in both cell line. The protein quality control (PQC) system is the first defence against the presence of misfolded proteins. PQC system exerts its action by re-folding or degrading substrates thanks to a chaperone network and the degradative systems (Ciechanover & Kwon 2015; Ciechanover & Kwon 2017). I found that TDP-43, TDP-35 and TDP-25 are mainly degraded by the proteasome system, which acts on substrates in their monomeric state. Proteins like TDP-43 and its fragments accumulate in cells when proteasome is inhibited. Proteasome degrades these proteins both in motor neuron and muscle cells, probably recruiting them when they are not yet in inclusions. It is possible that, if the load of misfolded proteins (TDP-43 fragments) saturate the proteasome, this degradative system becomes overwhelmed and loses its degrading capacity, leading to protein aggregation. The second intracellular degradative pathway is autophagy, whose role on TDP-43 fragments degradation has yet to be assessed. By investigating the involvement of autophagy in presence of misfolded proteins, I observed that in NSC34 cells autophagy is involved only in the degradation of TDP-25, while TDP-43 and TDP-35 are not degraded by autophagy. On the contrary, in muscle cells autophagy is not involved in the degradation of any of the various TDP species considered. Indeed, the inhibition of autophagic vesicles formation did not cause accumulation of the various TDPs species analysed. Routing of toxic species to the degradative systems is achieved through the formation of specific complexes that recognize misfolded protein by exposure of particular sequence or by post-translational modifications. One of the most important pathways of routing to degradation is based on HSP70 activity. HSP70 activity relies on BAG3 co-chaperone that rules the nucleotide exchange of ATP essential for HSP70 activity. HSPB8 is a chaperone that recognized misfolded proteins or substrates, with a still unknown mechanism. BAG3 has also a domain that binds HSPB8 (harbouring misfolded substrates) and another domain that binds p62 autophagic receptor to internalize substrates into autophagic vesicles in formation. This system is a way of selective autophagy and is thus called chaperone assisted selective autophagy (CASA).

Instead of directly activating degradative systems, routing the protein to degradation could be an efficient way to enhanced protein degradation. In fact, in several *in vitro* and *in vivo* models, the direct stimulation of degradative pathway produced detrimental effect (Zhang et al. 2011).

To increase misfolded proteins recognition, I enhanced the formation of CASA-complex by overexpressing HSPB8. I found that HSPB8 overexpression in motor neurons is able to decrease the accumulation of TDP-25 and TDP-35. Surprisingly, it also diminishes TDP-43 fraction, even if it is not forming aggregates. It I possible that TDP-43 is a substrate of the CASA-complex and thus I boosted a mechanism that is responsible of a correct protein homeostasis. Importantly, HspB8 pro-degradative role was confirmed also against the oligomeric form formed by TDPs tagged with FLAG.

In muscle cells, I also found that the overexpression of HSPB8 reduces the accumulation of TDP-25 and TDP-35 (NP-40 insoluble fraction in FRA), while TDP-43 levels were not affected by HSPB8. Importantly, results in muscle cells suggest that HspB8 expression could be modulate by which TDP specie is present; this difference could be a first explanation at the basis of the difference in aggregation between motor neurons and muscle cells.

I also overexpressed BAG3 and the results slightly differed from those obtained with HSPB8 overexpression. Indeed, the two proteins have different function inside the CASA-complex (Gamerdinger, Kaya, et al. 2011; Minoia et al. 2014; Behl 2011). The difference between HSPB8 and BAG3 overexpression is that BAG3 does not directly recognize the target, while HSPB8 has this ability. Moreover, BAG3 is responsible for association of HSPB8 and HSP70, and thus it enhances degradation of substrates already bound to HSPB8. I found that both in motor neuron and in muscle cells BAG3 overexpression was able to reduce the accumulation of TDP-25, but the amount of the other two species (TDP-43 and TDP-35) remained unaffected.

With this result I showed that, even if autophagy is not physiologically involved, it still has the capacity of degrading substrates when routing to autophagy is boosted (i.e. by BAG3 or HSPB8 overexpression).

Lastly, I also enhanced the routing of misfolded substrates to proteasome. To this purpose I overexpressed BAG1, which, by associating to HSP70, drives proteins to proteasome instead of autophagy. I found that BAG1 was able to reduce TDP-25 accumulation, while TDP-43 and TDP-35 protein amount does not change upon BAG1 overexpression. From data collected in these experiments, it seems that the effect of proteasome routing is less efficient than the routing to autophagy. This is probably due to the different capacity of the two systems. Proteasome could be partially overwhelmed when misfolded protein are present in the cells (transient expression of TDP-35 and TDP-25) and the capacity of the system is not very high. On the contrary, autophagy is a system with a very high capacity and routing to autophagy demonstrates to be efficient in removing highly aggregation-prone species.

In conclusion with these results I showed that also muscle cells are a site for TDP-25 aggregation, even if aggregation of misfolded species is less heavy, probably because degradative systems are more active in muscle cells.

I also showed that the PQC system is important in presence of misfolded proteins in both motor neuron and muscle cells. Indeed, degradative systems maintain a correct protein concentration preventing protein aggregation, since misfolded proteins load saturates them. Most importantly, I found that forcing the routing of misfolded substrates towards one of the degradative pathways exerts beneficial effect against protein aggregation. These strategy is particularly efficient when substrates are routed to autophagy that has the capacity of degrading large substrates.

With this work, I highlight the possibility of boosting routing systems to degrade misfolded proteins whose presence and aggregation is detrimental for cells. Even if we are far away from suggesting a cure for ALS, I showed the importance of the routing systems in order to reduce the amount of misfolded proteins, and drugs that induce these pathways could have beneficial effect in ALS developing.

# PART TWO: THE ROLE OF THE PROTEIN QUALITY CONTROL SYSTEM IN SBMA

# CHAPTER 4: ROLE OF THE PROTEIN QUALITY CONTROL SYSTEMS IN MUSCLE CELLS IN PRESENCE OF ARpolyQ

**Part Two: Aims and introduction**

Spinal and bulbar muscular atrophy (SBMA) is a neurodegenerative disease caused by a mutation on the androgen receptor (AR) gene. Normally in the exon one of AR gene there is a polyCAG tract of 23-39 repetition, that encodes for a polyglutamine (polyQ) tract whose role is not clear. In SBMA patients, the polyCAG tract spans up to 60 repetition. The AR protein bearing this elongation is toxic and is highly aggregation prone thanks to the hydrophobic polyQ tract.

SBMA has been recently defined as a neuromuscular disease. Indeed, in the first stage of the pathology muscle contribute is strikingly important even more relevant than motor neuronal contribution (Lieberman et al. 2014; Cortes et al. 2014). Indeed, it has been clearly demonstrated that the expression of ARpolyQ in muscle is able to induce onset of SBMA, while ARpolyQ expression in motor neurons is not able to cause SBMA insurgence. Motor neuron contribution increases in the later stage of the pathology, causing paralysis and then death.

In this context, in the part two of this thesis, I studied the aggregation of the androgen receptor in muscle cells and the effect of ARpolyQ on muscle cells viability. Subsequently, I studied which degradative system (proteasome or autophagy) is in charge of degrading ARpolyQ present in muscle cells. In the last part I focused on the effect of a drug, trehalose, that could enhance the activity of autophagy. I studied the effect on autophagy activation and on ARpolyQ aggregation. Lastly, I study the role of HspB8 that is a protein induce by trehalose treatment.

**Materials and methods**

CHEMICALS.

All the following treatments were obtained by Sigma-Aldrich (St. Louis, MO, USA). Cells were treated with:

- Testosterone (10nM) usually for 48 hrs (ethanol was used as control)
- Z-Leu-Leu-Leu-al or MG132 (10μM) for 16 hrs (DMSO was used as control)
- Bafilomycin A1 from *Streptomyces griseus* (100μM) for 16 hrs (DMSO was used as control)
- D-(+)-Trehalose dihydrate (100mM) for 48 hrs (diluted directly in the cell medium)

CELL CULTURES

Immortalized mouse myoblast C2C12, stably transfected respectively with ARQ24 and ARQ100, were kindly obtained from Dr. M. Pennuto (CIBIO, Trento, Italy). Briefly C2C12 were transfected with the lentiviral vector #945.PCCL.sin.cPPT.SV40ployA.eGFP.minCMV.hPGK.deltaLNGFR containing the cDNA encoding full length ARQ24 and elongated ARQ100 (Milioto et al. 2017). Green Fluorescent Protein (GFP) was cloned under the CMV promoter. After transfection cells were sorted using the fluoresce emitted by GFP to select positive cells. Sorted cells of both the two lines were cultured with D-MEM high glucose medium (Euroclone, Pero, MI, Italy) supplemented with glutamine 1mM (Euroclone), penicillin (SERVA, Electrophoresis GmbH, Heidelberg, Germany), streptomycin (SERVA), and 10% fetal bovine serum (GIBCO, Thermo Scientific Life Sciences Research, Waltham, MA, USA). Cells were maintained at 37°, with 5% $CO_2$. For splitting cells were detached using trypsin (Euroclone)

TRANSFECTION, PLASMIDS AND SIRNA.

Lipofectamine® 2000 Transfection Reagent (Invitrogen, Thermo Scientific Life Sciences Research, Waltham, MA, USA) was used to transfect cells with 1μg of plasmids DNA or with 40pmol of custom siRNA following manufacturer instruction. The following plasmids were used: pCI-neo-HSPB8, coding for human HSPB8. To silence the expression of endogenous genes, custom duplex siRNAs were used with the following sequence: siRNA_mHSPB8 (sense: 5'-CGGAAGAGCUGAUGGUAAAUU-3'; antisense: 5'-UUUACCAUCAGCUCUUCCGUU-3'). Treatments were always added during medium change after 5-6 hrs from transfection.

CELL VIABILITY ASSAY

Cells were plated at 1,500 cells/mL in a 24-well plate and treated with testosterone for 7 days (ethanol was used as a control) or at 45,000 cells/mL in a 24-well plate and treated with testosterone and trehalose for 48 hours. After treatment cells were incubated for 30 minutes at 37° C at 5% CO2 with 300μL/well of a solution of medium and 3-(4,5-dimethyl-2-thiazolyl)-2,5 diphenyl-2H-tetrazolium bromide (MTT, Sigma-Aldrich) at a concentration of 1.5 mg/mL. Medium was then removed and cells were lysated in 500μL of isopropyl alcohol. The optical density (OD) of each well was measured by Enspire (Perkin Elmer, Waltham, MA, USA) at a wavelength of 550nm.

PROPIDIUM IODIDE ASSAY

To measure cell mortality Propidium Iodide assay was performed. Cells were plated in 12-well plate at 1,500 cell/mL and treated with testosterone or ethanol for 7 days. Cells were harvested, centrifuged (100 rcf for 6 min at 4°) and diluted in a solution of PBS and 50 µM propidium iodide (Sigma-Aldrich). Cells displaying red fluorescence were analysed and counted by NovoCyte Flow Cytometer 3000 (ACEA Biosciences, San Diego, CA 92121, USA).

PREPARATION OF PBS PROTEIN EXTRACTS

Cells were plated in 12-well plate at 65,000 cell/mL. After transfection and/or treatment cells were harvested, centrifuged (100 rcf for 6 min at 4°) and diluted in 60µL of PBS (Euroclone) added of protease inhibitor cocktail (Sigma-Aldrich). After slight sonication (3 hits at 10% of intensity), the protein content of each sample was quantified by bicinchoninic acid (BCA) assay (Euroclone).

NP-40 SOLUBLE-INSOLUBLE EXTRACTION

Cells were plated in 6-well plate at 65,000 cell/mL. After treatments cells were harvested, centrifuged (100 rcf for 6 min at 4°) and diluted in 65µL of a solution made by NP-40 extraction buffer (150 mM NaCl (Sigma-Aldrich); 20mM TrisBase (Sigma-Aldrich); Nonidet P-40 (NP-40) 0.5% (Sigma-Aldrich); 1.5 mM MgCl2 (Sigma-Aldrich); Glycerol 3% (Sigma-Aldrich), pH 7,4), added of protease inhibitors (cOmplete EDTA-free Tablet 25X (Sigma-Aldrich)), and 1,4-Dithioteitol 1Mm (Sigma-Aldrich). Cells were lysated by passage in 1 mL syringe. Sample were then centrifuged (maximum speed for 15 min at 4°). Supernatant was transferred in a new tube and the pellet was rinse in 65µL of NP-40 extraction buffer. Protein content of the NP-40 soluble fraction was quantified by bicinchoninic acid (BCA) assay (Euroclone). The insoluble fraction was sonicated (3 hits at 10% of intensity).

FILTER RETARDATION ASSAY

Filter retardation assay (FRA) was carried out using Bio-Dot SF Microfiltration Apparatus (Bio-Rad, Hercules, CA, USA). 6µg of both PBS and NP-40 soluble extracts were loaded on a cellulose acetate membrane with pores of 0,22 µm. For NP-40 insoluble extracts an equal volume to NP-40 soluble extracts were loaded on the membrane. Samples were filtered on the membrane applying vacuum at the apparatus. Protein were fixed at the membrane using methanol and the membrane was incubated for 1 hr in blocking solution (5% dried non-fat milk (Euroclone) in T-BST 1X). The membrane was then incubated with rabbit polyclonal AR-H280 antibody (Santa-Cruz, sc-13162) 1:1,000 in blocking solution for at least 2 hrs. After two washes with TBS-T 1X the membrane was incubated for 1 hr with goat anti-rabbit HRP-conjugate secondary antibody (Santa Cruz Biotechnology, sc-2004) 1:5,000 in TBS-T 1X. After three washes in TBS-T 1X signal was revealed with Clarity™ Western ECL Blotting Substrate (Bio-Rad) and optical densitometry was acquired by ChemiDoc XRS System (Bio-Rad). Results were analysed using Prism 4.0 applying the two-way ANOVA test. Each result represent mean ± SEM of three biological replicates.

WESTERN BLOT

Western blot experiments were carried out using 10% acrylamide gels. To visualize androgen receptor protein, 15µg of each PBS extract or 30µg of each NP-40 soluble and insoluble extracts were loaded on gels. Following electrophoresis, proteins were transferred over night at 4° on nitrocellulose membrane. Membrane was then incubated for 1 hr at RT and then overnight at 4° with primary antibody diluted in blocking solution (5% dried non-fat milk (Euroclone) in T-BST 1X). After two washes with TBS-T 1X the membrane was incubated for 1 hr with secondary antibody diluted in TBS-T 1X.

Signal was revealed using Clarity™ Western ECL Blotting Substrate (Bio-Rad) and images were acquired by ChemiDoc XRS System (Bio-Rad). The following primary antibody were used: rabbit polyclonal AR-H280 antibody (1:1,000, Santa-Cruz Biotechnology, sc-13162), rabbit polyclonal anti-LC3-B antibody (1:1,000, Sigma-Aldrich, L8918), rabbit polyclonal anti-p62/SQSTM1 antibody (1:3,000, Abcam, Cambridge, UK, ab91526), home-made rabbit polyclonal anti-HSPB8 (1:2,000), rabbit polyclonal anti-GAPDH (1:1,000, Santa Cruz Biotechnology, sc-32233), goat polyclonal anti-ACTIN (1:1,000, Santa Cruz Biotechnology, sc1615), mouse monoclonal anti-α-tubulin (1:3,000, Sigma-Aldrich, T6199). The following secondary antibodies were used: goat anti-rabbit HRP-conjugate secondary antibody (1:10,000, Santa Cruz Biotechnology, sc-2004), goat anti-mouse HRP-conjugate secondary antibody (1:10,000, Santa Cruz Biotechnology, sc-2005), donkey anti-goat HRP-conjugate secondary antibody (1:10,000, Santa Cruz Biotechnology, sc-2020)

IMMUNOSTAINING AND CONFOCAL MICROSCOPE ANALYSIS

Cells were seeded on coverslips at 55,000 cells/mL. After treatments cells were fixed at 37° using a solution 1:1 of paraformaldehyde 4% in PB 0.2 M (Sigma-Aldrich) and sucrose 4% in PB 0.2 M (Sigma-Aldrich). After 25 min fixing solution was removed and ice methanol was added to complete the fixation. Cells were permeabilized using a solution of TRITON X100 (Sigma-Aldrich) 0.2% in PBS. Cells were than incubated for 1 hr in blocking solution (5% dried non-fat milk in T-BST 1X), and then incubated over night at 4°C with the primary antibody. After three washes with PBS cells were incubated for 1 hrs with a fluorophore-tagged secondary antibody. Nuclei were stained with Hoechst. The following primary antibodies were used: rabbit polyclonal AR-H280 antibody (1:500, Santa-Cruz Biotechnology, sc-13162), rabbit polyclonal anti-LC3-B antibody (1:500, Sigma-Aldrich, L8918), rabbit polyclonal anti-p62/SQSTM1 antibody (1:500, Abcam, ab91526). The following secondary antibodies were used: goat anti-rabbit Alexa 594 (1:1,000, Life technologies, Thermo Scientific, A-11012). All the primary and secondary antibodies were diluted in blocking solution. Coverslips were mounted on a glass support using MOWIOL. All the images were acquired using LSM510 Meta system confocal microscope (Zeiss, Oberkochen, Germany) and processed with the Aim 4.2 soft- ware (Zeiss).

REAL TIME PCR

Cells were plate in 6-well plate at 65,000 cell/mL. After treatment or transfection cells were harvested, centrifuged (100 rcf for 6 min at 4°) and lysed using TRI Reagent (Sigma-Aldrich). mRNA was extracted following manufacturer instructions and quantified using NanoDrop 2000 spectrophotometer (Thermo Scientific). After DNA decontamination using DNase I (Sigma-Aldrich) 0.5µg of the total mRNA was reverse-transcribed using High-Capacity cDNA Archive Kit (Life technologies, Thermo Scientific). mRNA levels were assayed using iTaq SYBR Green Supermix (Bio-Rad) on CFX 96 Real-Time System (Bio-Rad). All results were normalized to mRplP0 control. All the primers used were obtained by Eurofins Genomics. The following primers were used:

| Target Gene | Sequence Forward | Sequence reverse |
|---|---|---|
| hAR | 5'-AAGGATGGAAGTGCAGT-3' | 5'-GATGGGCTTGGGGAGAACCA-3' |
| mBeclin 1 | 5' -TGAAATCAATGCTGCCTGGG-3' | 5'-CCAGAACAGTATAACGGCAACTCC -3' |
| mTFEB | 5'-GCGGCAGAAGAAAGACAATC-3' | 5'-CTGCATCCTCCGGATGTAA-3' |
| mBag3 | 5'-ATGGACCTGAGCGATCTCA-3' | 5'-CACGGGGATGGGGATGTA-3' |
| mBag1 | 5'-GAAACACCGTTGTCAGCACT-3' | 5'-GCTCCACTGTGTCACACTC-3' |
| mHspB8 | 5'-ATACGTGGAAGTTTCAGGCA-3' | 5'-TCTCCAAAGGGTGAGTACGG-3' |
| mMAP-LC3-B | 5'-CGTCCTGGACAAGACCA-3' | 5'-CCATTCACCAGGAGGAA-3' |
| mSQSTM1/p62 | 5'-AGGGAACACAGCAAGCT-3' | 5'-GCCAAAGTGTCCATGTTTCA-3' |

| | | |
|---|---|---|
| mVCP | 5’-TGCCATCCTAAAAGCCAATC-3’ | 5’-TCAGCTCCAGAAAAGCCATT-3’ |
| mAchR | 5’-GTGCTGGGCTC TTTCATCTC -3’ | 5’ -TTCTGTGCGCGTTCTCATAC -3’ |
| mRplp0 | 5’-GGT GCC ACA CTC CAT CAT CA-3’ | 5’ -AGG CCT TGA CCT TTT CAG TAA GT-3’ |

**Muscle cells are a site for androgen receptor aggregation and toxicity**

C2C12_ARQ24 and C2C12_ARQ100 were plated and treated with testosterone for 48 hrs (to activate androgen receptor (AR)) and protein samples were extracted in PBS. Western blot (WB) results showed that both ARQ24 and ARQ100 were stabilized by testosterone treatment. In fact, I observed an increased amount of AR when cells were treated with testosterone respect to control condition with ethanol (Figure 38A). Interestingly, filter retardation assay (FRA) showed that ARQ100 formed high molecular weight (HMW) species only following testosterone treatment (*** p<0.001 vs control cell line; °° p<0.01 vs ethanol) (Figure 38A). On the contrary, ARQ24 did not form HMW species detectable in FRA even after activation with testosterone. Immunofluorescence (IF) analysis showed that both ARQ24 and ARQ100 translocated into the nucleus upon testosterone treatment, and levels of the soluble protein was increased both cell line (Figure 38C). In C2C12_ARQ100 cell line, I could not detect any visible aggregates or inclusions after testosterone treatment. To better characterize the HMW species observed in FRA but not visible in IF, I performed a NP-40 extraction on both cell line. By FRA analysis I found that testosterone triggered the formation of NP-40 insoluble species of ARQ100, while these species were not formed by ARQ24 (** p<0.01 vs control cell line) (Figure 38B). I also observed that WB of the NP-40 insoluble extracts showed a great amount of ARQ100 compared to the control condition (ethanol) and compared to the control cell line (C2C12_ARQ24) (Figure 38B). To assess the expression levels of AR in these cells I performed an RTq-PCR on extracts of both cell lines in presence and absence of testosterone. I found that in C2C12_ARQ100 *AR* gene expression is significantly higher than in C2C12_ARQ24 (*** p<0.001; ** p<0.01 vs same condition in the control cell line) (Figure 38D). I also investigated if the presence of the activated ARpolyQ caused mortality or atrophy in muscle cells. MTT assay was performed on both cell line treated with and without testosterone. To amplify testosterone effect for the following experiments, treatment was maintained for 7 days. I observe that the presence of ARQ100 caused a reduction in cell viability even without testosterone (*** p<0.001; ** p<0.01 vs same condition in the control cell line) (Figure 38E). To assess if this difference was linked to cell mortality, I performed an analysis by flow-cytometry, staining dying cells with propidium iodide. I found that after testosterone treatment C2C12_ARQ100 showed an increased mortality respect to the control line treated with testosterone (* p<0,05 vs control cell line in same condition) (Figure 38F). Finally, in order to characterized ARpolyQ contribution to muscle atrophy I analysed the expression of the acetyl-choline receptor (*AchR*). AchR is a denervation marker, whose expression is increased when muscle are denervated.

I found that C2C12_ARQ100 expressed these receptor at lower levels respect to C2C12_ARQ24 (*** p<0.001 vs same condition in the control cell line) (Figure 38G). I observed that in C2C12_ARQ100 treated with testosterone the expression of the *AchR* was increased compared to control condition with ethanol (*** p<0.001 vs control condition) (Figure 38G). I also noticed that levels of *mAchR* in C2C12_ARQ100 were significantly lower than in C2C12_ARQ24 (°°° p<0.001). Since in this model, muscle cells are not part of a neuromuscular junction, these results describe only what happen in muscle following testosterone treatment and in presence of the polyQ tract.

In conclusion, I observed that ARQ100 forms HMW species in presence of testosterone, that are detectable in FRA both in PBS extracts and in NP-40 insoluble extracts. These HMW species are not detectable in IF, probably because they are not yet in a fibrillary state, but still in an small oligomeric state. I also evaluated ARQ100 toxicity on muscle cells and I found that testosterone causes only a mild increased in cell mortality. On the other hand, these results suggest that ARQ100 may cause atrophy in muscle cells, even without testosterone.

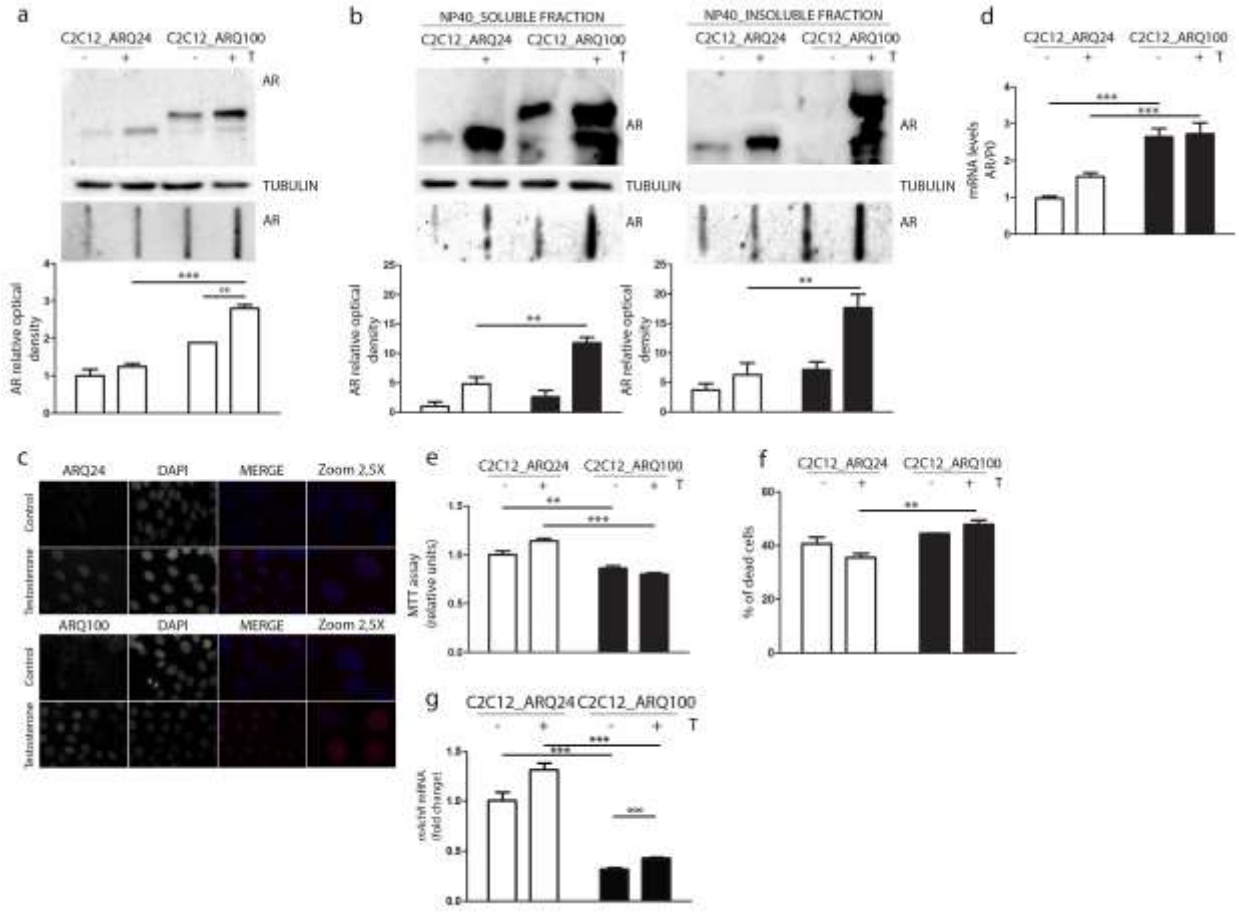


*Figure 37: Characterization of the cellular model. (A) Western blot (upper inset) and Filter retardation assay (FRA) (middle inset) of PBS extracts. Optical densitometry quantification of FRA (lower inset). *** p<0.001 vs ARQ24+T; °° p>0.01 vs ARQ100-T. (B) Western blot (upper inset) and FRA (middle inset) of NP-40 extracts. Optical densitometry quantification of FRA (lower inset). ** p<0.01 vs ARQ24+T. (D) RTqPCR quantification of hAR levels. ** p<0.01; ***p<0.001 vs ARQ24 in the same conditions. hAR expression levels were normalized on p0 expression levels (C) Immunostaining for androgen receptor. Nuclei staining: Hoechst. 63X magnification. (E) MTT assay. ** p<0.01; ***p<0.001 vs ARQ24 in the same conditions. (F) Propidium Iodide Assay. ** p<0.01 vs ARQ24+T. (G) RTqPCR quantitation of mAchR levels normalized on p0 levels. ***p<0.001 vs ARQ24 in the same conditions; °°° p<0.001 vs ARQ100-T.*

**The role of the degradative pathways in presence of ARQ100**

Misfolded proteins are substrates of the protein quality control (PQC) system. PQC system relies on a chaperone network that maintains proteins in the correct conformation or drives them to the degradative pathways: proteasome and autophagy. To investigate PQC system activation in presence of mutated ARpolyQ, I performed an RTq-PCR on mRNA samples from both cell line treated with ethanol or testosterone (Figure 39A). I analysed the expression of *Tfeb*, *Beclin1*, *Lc3* and *p62* (involved in autophagy activation), *Bag3*, *HspB8*, (part of the complex that routes aggregates to autophagy), *Bag1* (that routes misfolded proteins to proteasome), and *VCP* (involved in protein extraction from membranes). I observed that there were no differences in the expression of *Tfeb*, *Beclin1*, *Lc3* and *p62*, between the two lines (C2C12_ARQ24 vs C2C12_ARQ100) or following AR activation by testosterone. *Bag3,* but not its partner *HspB8,* was decreased in C2C12_ARQ100; *Bag1* levels did not changed between cell lines and conditions; *VCP* levels decreased in C2C12_ARQ100 with both treatments. Even if the presence of the mutated protein was not able of inducing an activation of the PQC system, I investigated which degradative pathway is responsible for ARQ24 and ARQ100 degradation. I inhibited the degradative pathway in both cell lines using MG132 (proteasome inhibitor) and bafilomycin (autophagic inhibitor) and I extracted samples in PBS. I observed that following proteasome inhibition both ARQ24 and ARQ100 accumulated in FRA (Figure 39B). The levels of FRA accumulation upon MG132 treatment were the same with or without testosterone (** $p<0.01$; *** $p<0.001$ vs same condition and cell line without testosterone). Protein levels in WB remained unchanged in presence of MG132, but in both cell lines the activation of AR following testosterone treatment was clearly detectable (Figure 39B). Upon autophagic inhibition by bafilomycin, I found that there was no increased in ARQ24 HMW species retained in FRA (Figure 39B) compared to control condition. On the contrary, inhibiting autophagy caused a significant increase of HMW species of ARQ100, following testosterone treatment. Analysis in WB did not show any increase caused by bafilomycin treatment in both cell lines (Figure 39B).

I also performed and NP-40 extraction on the same samples and, analysing samples in FRA, I found that ARQ24 was detectable mainly in the NP-40 soluble fraction even after inhibition of proteasome and autophagy (Figure 39C). WB analysis of both the NP-40 soluble and insoluble fractions showed that testosterone stabilized the receptor in any conditions, but that there was no change in the amount of ARQ24 protein even upon degradative systems inhibition (Figure 39C).

FRA performed on NP-40 soluble and insoluble extracts of C2C12_ARQ100, showed that after proteasome inhibition most of the protein was found in the NP-40 insoluble fraction (Figure 39C) and WB reflected this shift toward the insoluble fraction. When autophagy was inhibited by bafilomycin, I found that ARQ100 was mainly present in the NP-40 insoluble fraction forming HMW species clearly detectable also in WB in the upper part of the gel (Figure 39C).

IF analysis, performed after proteasome and autophagy inhibition, revealed that, in both cell lines, levels of AR were increased after MG132 treatment, but still no aggregates were detectable in cell cytoplasm and nucleus. Despite the increase of the total protein levels, there were no visible inclusions in C2C12_ARQ100 even after bafilomycin treatment (Figure 39D).

In summary, these results show that at basal levels there is no PQC system activation in presence of activated ARQ100. It is possible that, in normal condition, muscle cells have the PQC system already robustly activated and the presence of the misfolded protein is not able to cause a further activation. Indeed, when degradative systems are inhibited, ARQ100 degradation is blocked, and consequently ARQ100 accumulates in FRA. Interestingly, proteasome is involved in the degradation of both ARQ24 and ARQ100, while autophagy is involved only in presence of ARQ100.

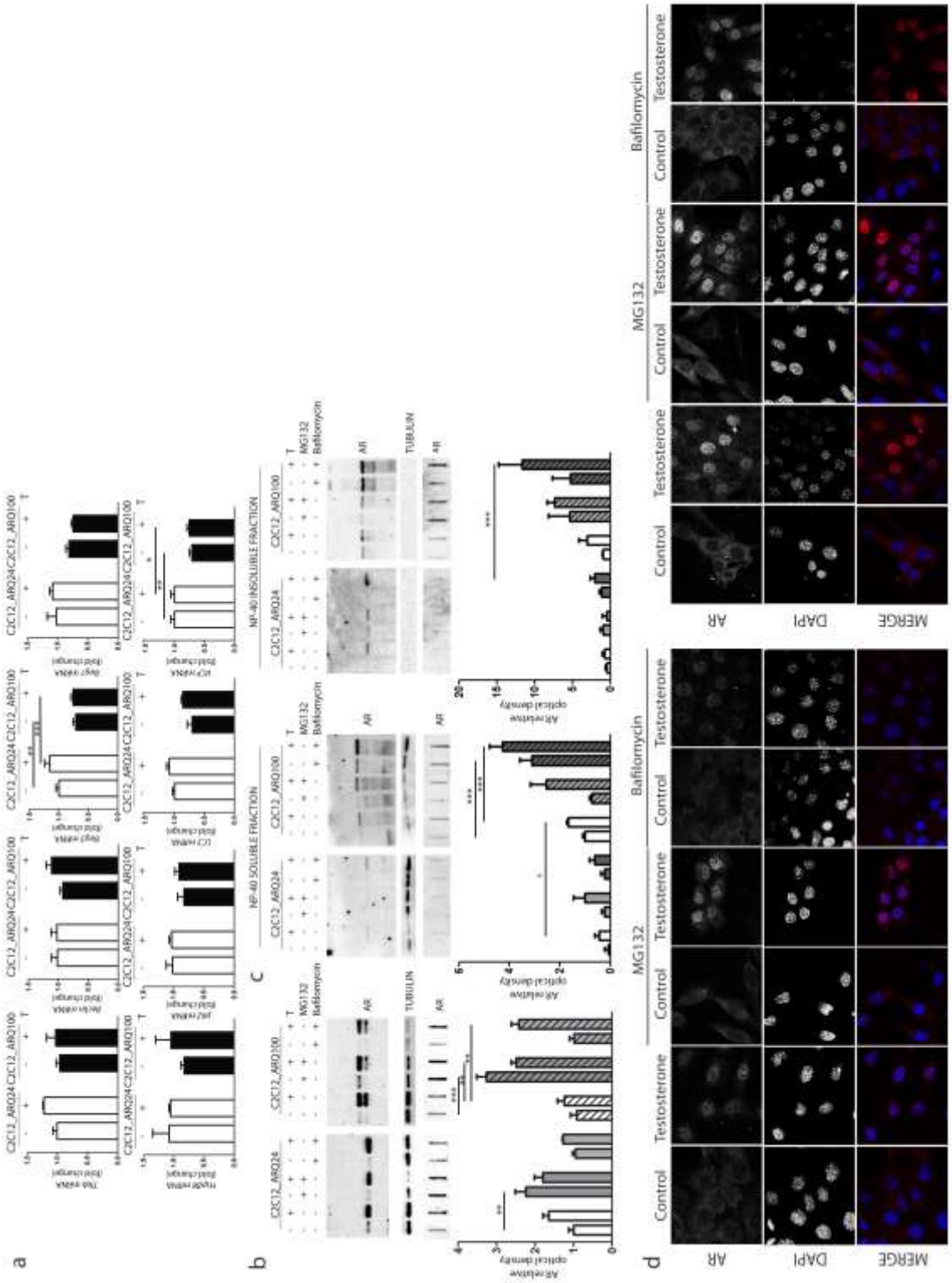


*Figure 38: Degradative systems involvement. (A) RTqPCR of PCQ system related genes. *p<0.05; ** p<0.01; *** p<0.001 vs ARQ24 in the same conditions. (B) Left Panel: Western blot (WB) (upper inset) and Filter retardation assay (FRA) (middle inset) of PBS extracts. Optical densitometry quantification of FRA (lower inset). ** p<0.01; ***p<0.001 vs relative control conditions –T/+T. Middle and right panels: WB (upper inset) and FRA (middle inset) of NP-40 extracts of C2C12_ARQ100 treated with testosterone 10nM, MG132 10μM, and Bafilomycin 100μM. Optical densitometry quantification of FRA (lower inset). ** p<0.01; ***p<0.001 vs relative control conditions –T/+T; ° p<0.05 vs control condition –T. (C) Immunostaining for androgen receptor on fixed C2C12_ARQ24 and C2C12_ARQ100 cells.*

**Autophagy induction is protective against ARQ100 aggregates.**

Since autophagy is an important player in ARQ100 degradation, compounds that target this process gained importance as therapeutic possibility. I tested a well known autophagic activator, trehalose, that is an mTOR independent autophagic activator. Trehalose was already tested in HD models and also in SBMA motor neuronal models, and it was demonstrated that trehalose has a beneficial effect against mutated proteins (Giorgetti et al. 2014; Rodrìguez-Navarro et al. 2010). I tested trehalose also in muscle C2C12 cells, expressing mutated AR.

C2C12_ARQ100 cells were treated with trehalose and autophagic activation was tested by RTq PCR. I observed that trehalose treatment increased the expression of many genes involved in the protein quality control (PQC) system (Figure 40A). *FOXO3*, *Tfeb*, *Beclin1*, *Lc3* and *p62*, genes involved in regulation of autophagy and in autophagic machinery were all increased in a significant fashion (* $p<0.05$; ** $p<0.01$; *** $p<0.001$ vs untreated samples). In addition, I found that the expression of genes involved in autophagic routing such as *Bag3* and *HspB8* were dramatically after trehalose treatment (*** $p<0.001$ vs untreated samples). Interestingly also *Bag1* and *VCP* expression increased was increased by trehalose (*** $p<0.001$ vs untreated samples), even if these genes are not directly correlated to autophagy. I also evaluated the expression of the AchR and I found that following trehalose treatment the expression of the *AchR* was greatly increased (*** $p<0.001$). As already mentioned, results obtained looking at AchR expression give as a suggestion of how trehalose affect AchR expression; since a neuromuscular junction is not present, these results are not an indication on deneravation (Tsay & Schmidt 1989; Rusmini et al. 2015).

By IF I analysed LC3 and p62 localization and distribution. I found that trehalose produced an increase in LC3 puncta indicating an increased formation of autophagic vesicles. Trehalose also caused the formation of p62 bodies, structures that rise after by p62 dimerization upon autophagy activation (Figure 40B).

C2C12 cells were then treated with trehalose and co-treated with bafilomycin. Protein samples were extracted in PBS and analysed in FRA and WB (Figure 40C). I found that trehalose treatment counteracted the formation of ARQ100 HMW species produced after testosterone activation. Furthermore, the monomeric fraction of AR in WB was reduced by trehalose. Trehalose also causes the formation of LC3-II, detectable in WB. FRA analysis also showed that co-treatment of trehalose with bafilomycin recovered ARQ100 aggregation, after testosterone treatment, at levels comparable to control samples; also ARpolyQ protein levels, detected in WB, returned comparable to untreated control, when cell were treated with trehalose and bafilomycin. In WB I detected an increased in LC3-II formation and in p62 expression in presence of the co-treatment of trehalose and bafilomycin.

These results show that trehalose enhances autophagy in C2C12 cells and that it is also able to counteract ARQ100 aggregation in an autophagic dependent-manner, as demonstrated by bafilomycin treatment that reverts trehalose effect.

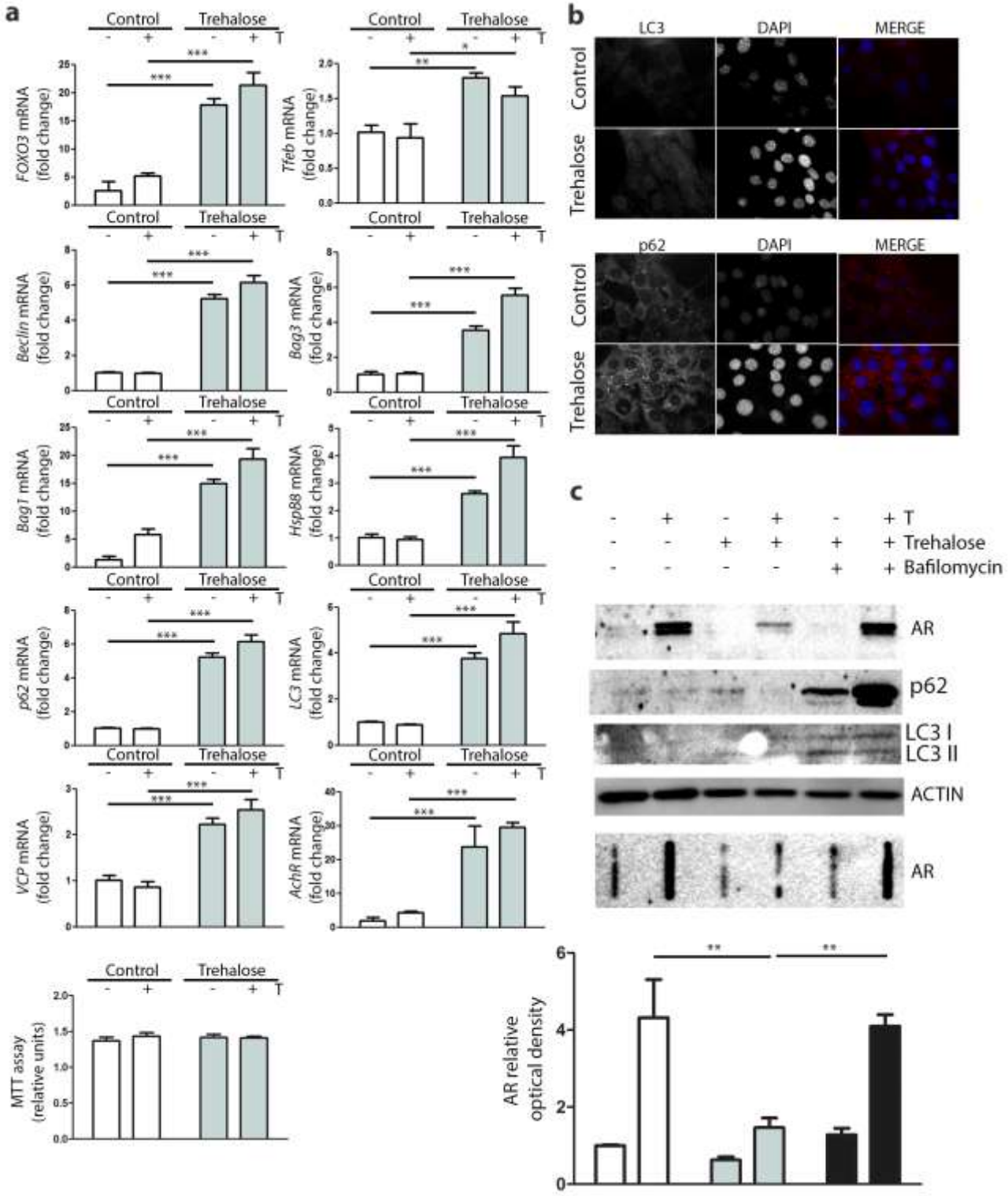


*Figure 39: Trehalose activates autophagy and reduces ARQ100 accumulation. (A) RTqPCR of PCQ system related genes. ** p<0.01; ***p<0.001 vs relative untreated control. (B) Immunostaining for LC3 (upper inset) and p62 (lower inset) of C2C12_ARQ100 in presence of trehalose. (C) MTT assay of C2C12_ARQ100 in presence of trehalose. (D) Western Blot (upper inset) Filter retardation Assay (FRA) (middle inset) of PBS extracts of C2C12_ARQ100 treated with trehalose and bafilomycin. Optical densitometry quantification of FRA (lower panel) ** p<0.01 vs relative untreated control; ***p<0.001 vs trehalose +T.*

**Autophagy routing counteract ARQ100 aggregates formation**

Previous result shows that trehalose treatment enhanced the expression of chaperones involved in the complex that routes aggregates to autophagy. HSPB8 is highly involved in autophagic routing of misfolded proteins and it has already been demonstrated that it plays a protective role in motor neuronal models of SBMA.

I overexpressed HSPB8 in C2C12_ARQ100 cells and protein samples were extracted in PBS. FRA showed that HSPB8 overexpression reverted ARQ100 aggregation caused by testosterone treatment (** $p<0.01$ vs pcDNA3) (Figure 41A). Also monomeric ARQ100 was reduced by HSPB8 overexpression.

To further test the importance of HspB8 in ARpolyQ degradation, I silenced the endogenous HspB8. C2C12_ARQ100 cells were transfected with a specific siRNA that target *HspB8* mRNA. Samples were extracted in PBS and FRA analysis showed that when HSPB8 was silenced, ARQ100 aggregation was exacerbated in a significant fashion (**$p<0.001$ vs scramble) (Figure 41B). I tested by WB that HSPB8 was silenced in presence of its specific siRNA. Monomeric AR was mildly reduced in WB by HSPB8 silencing.

With these experiments, I demonstrated that HSPB8 plays a protective role against ARQ100 aggregation also in muscle cells. I also observed that at basal levels HSPB8 in muscle cell works to maintain ARQ100 aggregation at low levels, probably directing misfolded ARQ100 species to autophagy.

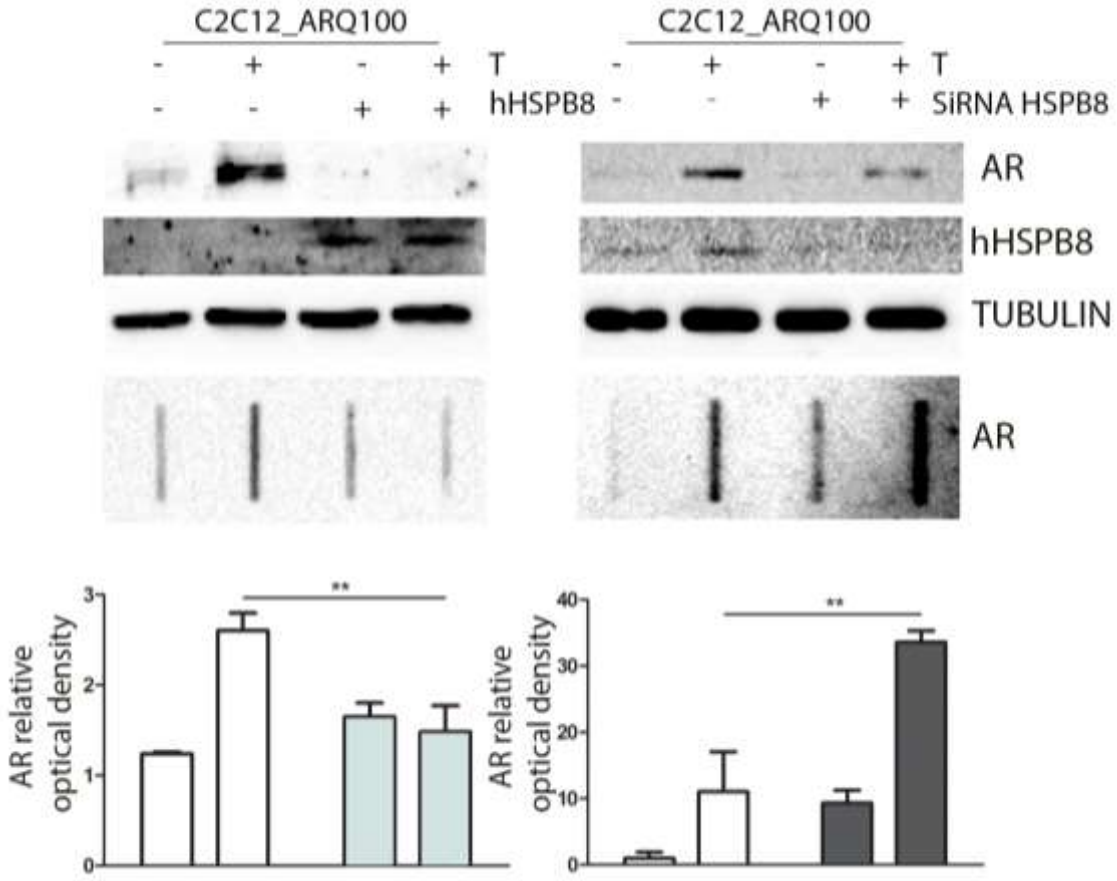


*Figure 40: Role of HspB8 in counteracting ARpolyQ aggregation. Right panel: Western Blot (WB) and Filter Retardation Assay (FRA) of PBS extracts of C2C12_ARQ100 overexpressing HspB8, upper and middle insets. Optical densitometry quantification of FRA (lower inset) ** p<0.01 vs pcDNA3 transfected control. Left panel: Western Blot (WB) and Filter Retardation Assay (FRA) of PBS extracts of C2C12_ARQ100 with silencing of endogenous mHspB8, upper and middle insets. Optical densitometry quantification of FRA (lower inset) ** p<0.01 vs SCRAMBLE transfected control*

## DISCUSSION

SBMA has been regarded for years as a motor neuron disease (Grunseich et al. 2014), but recent works have defined it a neuromuscular disease (Giorgetti & Lieberman 2016b). Indeed, it was recently demonstrated that muscle tissue is a primary site for SBMA toxicity. Muscle atrophy often precedes motor neuron loss, and the onset of the pathology could be rescued if ARpolyQ is specifically deleted in muscle cells and preserved in motor neurons (Lieberman et al. 2014; Cortes et al. 2014). Even if these studies were carried out in murine model and findings remain to be confirmed in human, there are strong evidence that support direct muscle involvement in SBMA onset and progression. I observed that muscle cells are a site for ARpolyQ aggregation. Indeed, following testosterone activation, ARQ100 was retained in FRA while ARQ24 was not, despite testosterone activation. I also observed that the presence of the ARpolyQ, even without testosterone treatment caused a mild atrophy and an increase in mortality. A possible reason that should be taken in account to correctly understand these results, is that experiments were carried out in undifferentiated muscle cells and not on mature myotubes.

As ARpolyQ is a mutated protein, it tends to misfold; misfolded soluble form of ARQ100 is the one associated to toxicity even before forming aggregates (Poletti 2004). The presence of misfolded protein is stressful to cells and, potentially, they can activate the protein quality control (PQC) system as a defense against the presence of these toxic proteins (Rusmini et al. 2016). Controversially, I observed that neither the presence of the ARpolyQ nor its activation by testosterone caused an increase in the activity of the PQC system. It is possible that activity of the degradative pathway is already sufficient for managing the presence of misfolded proteins, without a further activation of one particular degradative pathway. Indeed, I found that ARQ24 and ARQ100 are substrates of proteasome in muscle cells, and if proteasome is damaged both proteins aggregate (ARQ100 in a more massive fashion). Interestingly, autophagy, that is a system with a higher capacity, degrade only ARQ100, probably when it is yet in oligomeric status (high molecular weight (HMW) species). In fact, inhibition of autophagy caused an increased in the formation of activated ARQ100 insoluble species while levels of activated ARQ24 remain equal to control after autophagy inhibition. These results suggest that, in muscle cells, autophagy is a specific pathway for the degradation of ARQ100 insoluble species. In this context targeting autophagy could be an efficient strategy to reduce the accumulation of ARQ100, without affecting the concentration of wild type soluble proteins, thus impairing other cell functions. Trehalose activates autophagy in mTOR independent manner and, in muscle cells, it caused the reduction of ARpolyQ insoluble species. I found that trehalose also increased the expression of key factors of the CASA-complex (chaperone assisted selective autophagy), like *HspB8*, that probably helps in the recognition of selected cargo avoiding the uncontrolled degradation of every intracellular element. A possible way for the routing of ARQ100 HMW species to autophagy involved HSPB8. Indeed, when HSPB8 is silenced, ARpolyQ insoluble species increase; on the other hand, when HSPB8 is overexpressed (by trehalose treatment or by plasmid transfection), ARpolyQ aggregation upon testosterone treatment is counteracted.

Overall these results show that ARpolyQ aggregation happens also in muscle cells, and is hallmark of the disease. Targeting aggregation of ARpolyQ could play beneficial effect, since the permanence of inclusions in the cells could cause the damage of several pathways and the recruitment of other soluble proteins, impairing other pathways. Autophagy appears as a valuable pathway for the degradation of ARpolyQ HMW species; in this context, trehalose played beneficial effect on ARpolyQ aggregation. In parallel and supporting this study, there are several ongoing studies that are testing, in *in vivo* models, novel compounds that will address the protein quality control system, to reduce the presence of the misfolded toxic protein.

# CHAPTER 5: DEVELOPING OF CRISPR/CAS9 SYSTEM TO CREATE AN ISOGENIC STEM CELL LINES

**Short overview on CRSIPR/Cas9 system**

CRISPR/cas9 system is the most recent addition to genome-editing toolbox. In recent years the need of modifying genome of various and different organisms has grown, and in parallel has grown the need to find a method easy to handle and that would guarantee an high specificity (D'Agostino & D'Aniello 2017; Gaj et al. 2016).

The first system used for genome editing was Zinc Finger Nuclease (ZFN) (Figure 42). This system is based on a fusion protein made of FokI subunit, containing the restriction catalytic site, and of a zinc finger subunit; this fusion protein is called zinc finger endonuclease (Carroll 2011; Kim et al. 2009; Gaj et al. 2016). Zinc finger subunits recognize the specific DNA sequence and their dimerization is allowed by FokI cleavage domain. Zinc finger recognized the target DNA. Structural analysis reveal that the interaction site between aminoacids and DNA is composed of β-sheet and α-helix; in particular a specific combination of these secondary structures could recognize specific DNA triplets. These structures were fused together in tandem, in order to recognize a specific and desired sequence. After DNA recognition FokI produces a double strand break (DSB) on DNA 5-7 bp upstream the targeted sequence. ZFN has two main negative sides: it is difficult to realize and to use due to the complexity of the design; moreover it produces a high number of off-target effects.

The second system developed was transcription activator-like effector nucleases (TALEN) system (Figure 42). TALEN system has many commonalities with ZFN: it is composed of a DNA recognition domain that dimerizes with another thanks to the action of FokI cleavage domain (Boch et al. 2009; Gaj et al. 2016). The interaction domain of TALEN proteins with DNA is made of repeat domains that recognize only a single nucleotide. This feature makes TALEN system easier to use and more efficient compared to ZFN.

In this context, CRIPSR/Cas9 represent a great step forward in the spreading genome editing, since it does not require a specific expertise and is very efficient. It was discovered in bacteria as a defense mechanism against viruses (Figure 42-43) . When foreign DNA is integrated in CRISPR (clustered regularly interspaced short palindromic repeats) locus, all the region is transcribed and is called crRNA (crisprRNA) (Horvath & Barrangou 2010; Ratner et al. 2016; Jiang & Doudna 2015). Then, these segments of DNA associate with trans-activating crRNA (transcrRNA) to direct sequence-specific DSB mediated by Cas9 (endonuclease belonging to larger family of Cas proteins). During years it has been found that the Cas9 protein only requires the seed sequence among the crRNA (called guide RNA, gRNA) and a protospacer adjacent motif (PAM) sequence on the targeted sequence. The PAM sequence for the *Streptococcus pyogenes* Cas9 is 5'-NGG-3'. The Cas9 nuclease catalytic sites are called RuvC and HNH that recognized the hetero-duplex, positively charged, formed by the DNA and the gRNA (Jinek et al. 2012; Mojica et al. 2009).

CRISPR/Cas9 system has been further modified to reduce the number of off target genes, for example by mutating the catalytic site transforming Cas9 from a nuclease to nickase. To introduce a double strand break (DSB) two nickases will be directed on the target sequence, one cutting the plus strand and one cutting the minus strand (Ran et al. 2013; Cong et al. 2013).

After introducing DSB, by mean of one of the above described systems, DNA repair system are activated (Figure 44). During DNA repair, some nucleotide can be lost; this event can cause various effects on the target genes: knock-out, insertion of mutation (frame-shift), insertion of stop codon. This process is called non-homologous end joining (NHEJ) repair, and is often used to insert mutation, to silence a gene, to have truncated protein, etc.

There is a second mechanism that allows the insertion of a wanted sequence and is called homologous end joining repair (HDR). It relies on an exogenous DNA sequence, containing the corrected sequence, that acts as template to direct the repair systems towards the wanted correction (Gaj et al. 2016; Wiles et al. 2015).

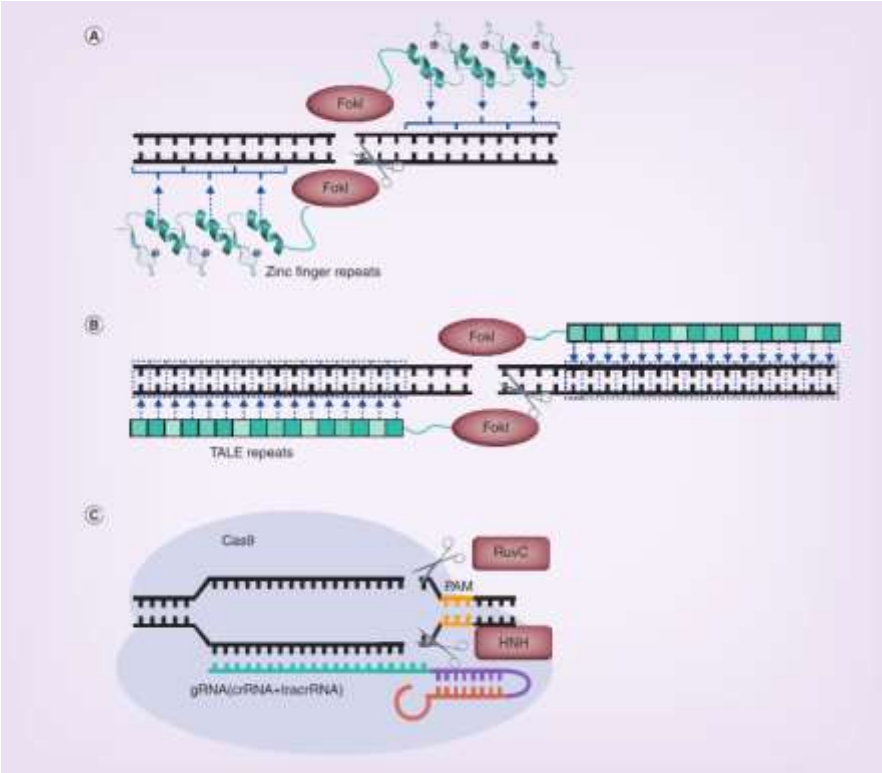


*Figure 41: Genome editing tools evolution* (Chen & Knoepfler 2016)

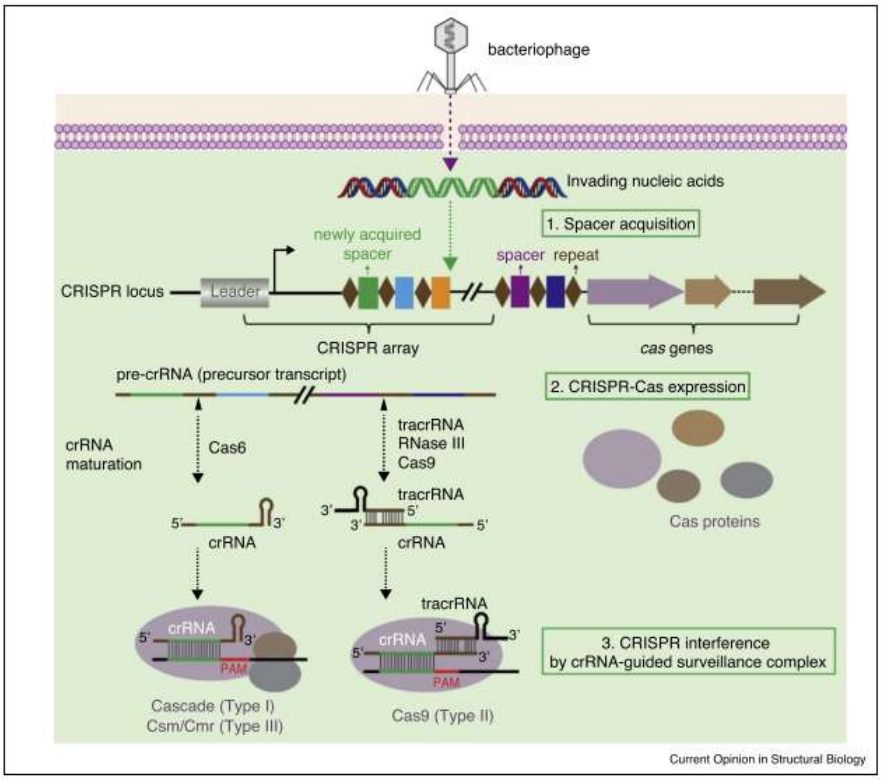


*Figure 42 CRISPR/Cas9 biology* (Jiang & Doudna 2015)

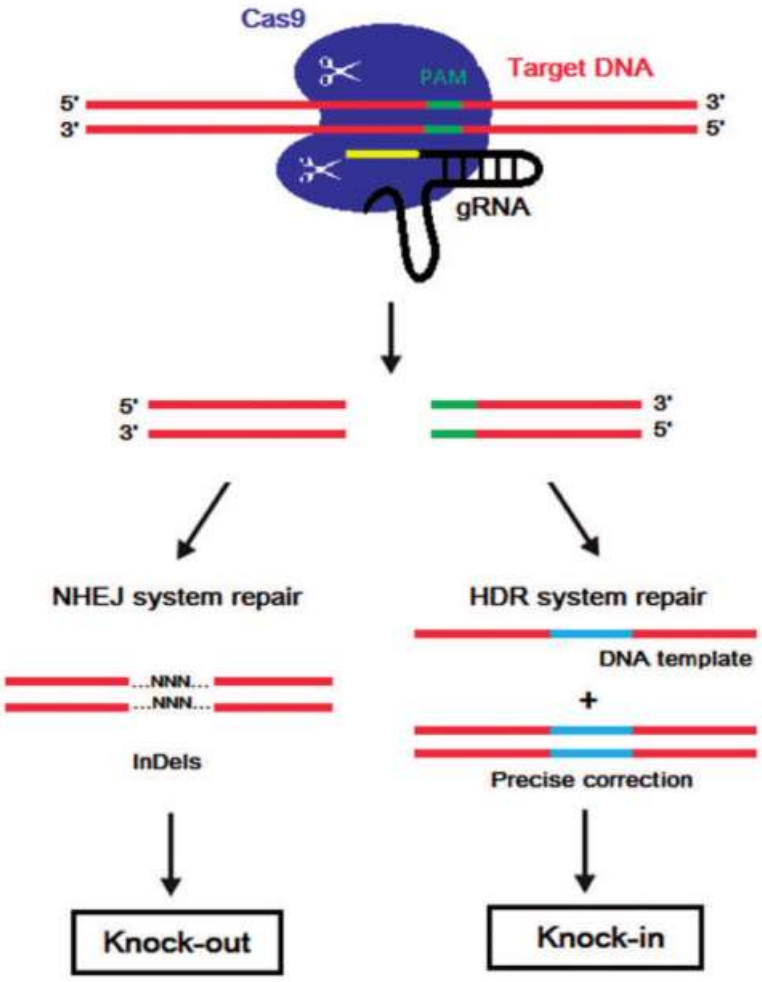


*Figure 43 Genome editing by CRISPR/Cas9* (D'Agostino & D'Aniello 2017)

**Developing elements for CRISPR/Cas9 system**

CRISPR/Cas9 system is based on the activity of a Cas9 protein that produces a double strand break on a target region. The target region is recognized by the single guide RNA (sgRNA) associated to Cas9. An essential element that allows Cas9 activity is the presence of a PAM sequence on the target DNA; Cas9 cuts dsDNA three nucleotides upstream the PAM sequence (Horvath & Barrangou 2010). Without a PAM sequence Cas9 cannot work. Our system is based on a Cas9 whose catalytic site has been modified (D10A): this modified Cas9D10A is turned from an endonuclease to a nickase (that insert a single strand break also called "nick") (Cong et al. 2013; Ran et al. 2013). The presence of a single nick on one DNA strand is immediately repaired, but if two nicks are closed to each other (distance between the nicks is called *offset*) DNA repair system sense these two nicks as a DSB. To obtain these two nicks two sgRNA are needed: a first sgRNA (guide1) that drives the Cas9 to the plus strand and a second sgRNA (guide 2) that drives Cas9 to the minus strand (Figure 45A-B). I used a plasmid, named pX335B that encodes for Cas9D10A that also contains two restriction sites (BbsI and SapI) used for guides cloning (Figure 45A). These restriction sites are downstream to two hU6 promoters to ensure sgRNA expression. This system based on the use of two nickase instead of an endonuclease was developed to reduce the number of off target genes; since the guide is a short oligonucleotide (20 nt) Cas9 could be direct in many sites on many different genes. If two different sgRNA are involved, the DNA regions containing both the sequences are drastically lower. Moreover, if the Cas9D10A is directed in an unwanted region, it will produce a nick that is immediately repaired without causing any genome mutation.

The aim of the targeting that I developed was to reduce the length of the poly-CAG tract in a human induced pluripotent stem cell (hiPSCs) line derived from a SBMA patient. To obtain this modification I needed the Cas9 system and a donor template.

**sgRNA design**: I used an open source http://crispr.mit.edu/ to design the guide. This tool screens the sequence that should be targeted and find all the PAM sequences. Then it designs the sgRNA that should target the sequence. It gives a score to each guide for position among the analysed sequence, 3' stability, GC% etc. This software makes also a second analysis in order to find the best couple of sgRNA for targeting the wanted sequence. It also gives a score to the various sgRNA couple analysed on the basis of offset length, quality of the guides and number of off-target genes. I chose to design a pair of guide to target a region upstream the polyQ and another pair of guides to target a region immediately downstream the polyQ (Figure 45 B-C-D).

I cloned the two pairs of guides in pX335B plasmid, and I created two different plasmids targeting regions upstream or downstream the polyQ.

**Donor template design**: donor template is a long sequence of DNA that acts as template for DNA polymerase that repair the DSB; in this way is obtained a homologous end joining repair (HDR). Since it should mimic sister chromatid invasion (mechanism of DNA repair during mitosis), it must have two long homology arms of at least 500-600 bp, upstream and downstream the DSB (Figure 46). These two homology arms will form a tertiary structure with the target DNA; the region between these two homology arms will act as a template for DNA polymerase that will introduce the wanted correction. I also introduced a selection cassette to facilitate colony screening (Figure 46). Selection cassette is flipped, so that the promoter of the antibiotic resistance will not influence the expression of the downstream exon. I chose to use a selection cassette coding for zeocin resistance. I also mutated the PAM sequence on the donor template so that the remaining Cas9 protein would not target the corrected sequence.

A

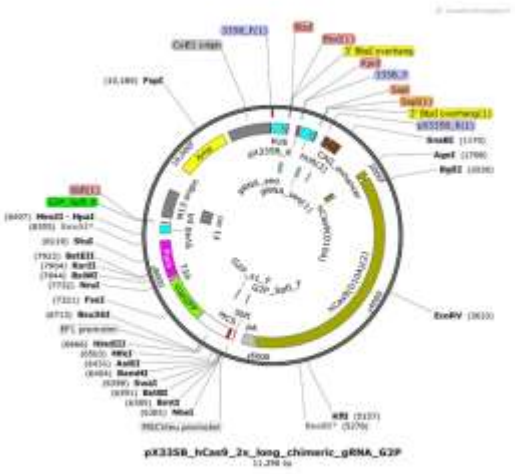


B

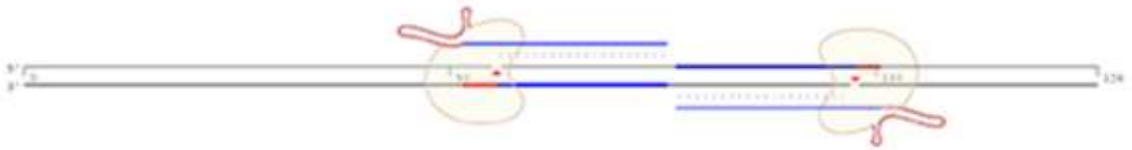

C

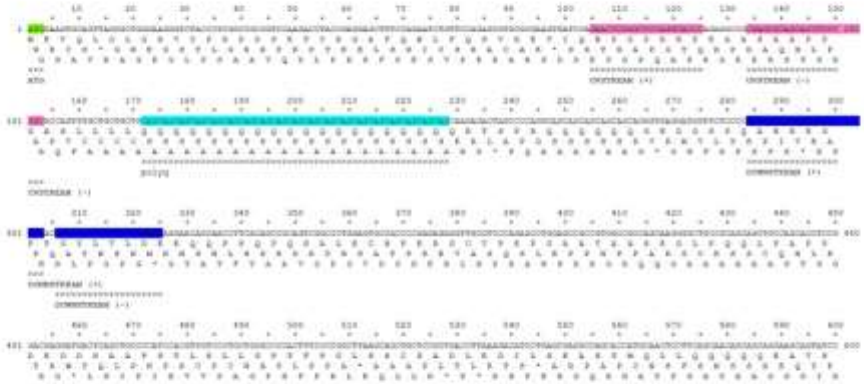

D

| Gene | Number | target sequence on + strand (PAM) | gRNA binds to strand | nicked strand | gRNA sequence 5'->3' | Forward Oligo | Reverse Oligo | Remarks |
|---|---|---|---|---|---|---|---|---|
| | | | | | | CACC | AAAC- (for pX335A, 1 site)<br>AAC- (for pX335B, 2 sites) | |
| AR | | CCAGAACCCGGGCCCAGGCACCC | | + | GGCTGCCTGGGGCCCGGGTTC | CACCgggttcccgggccccaggcacccc | AAACggggcctgggcccgggttcctgg | UPSTREAM |
| AR | | GCCGGGAGGTGCTGCGCTCGCCG | | - | GCCGGGAGAGTGCTGCGCTCG | CACCgccgggaggtgctgcgctcgc | AACCgagcgcagcacctccccggc | |
| AR | | CCCAAGCCCATCGTAGAGGCCC | | + | GGGGCCTCTACGATGGGCTT | CACCgggcctctacgatgggcttt | AAACaagcccatcgtagaggcccc | DOWN STREAM |
| AR | | AAGCTACCTGGTCCTGGATTAGG | | - | AGGCTACCTGGTCCTGGATG | CACCaggctacctggtcctggatg | AACCatccaggaccaggtagcctt | |

*Figure 44: (A) schematic representation of guide expression vector (B) schematic representation of how double nickase works and where guides are giong to target the DNA (C) sequence of exon1 of the hAR gene. In pink are underlined the couple of guide that target upstream the polyQ and in blue the couple of guide that will target downstream the polyQ. polyQ tract is highlighted in light blue and ATG codon in green (D) representation of oligonucleotide design for guides insertion in plasmid vector.*

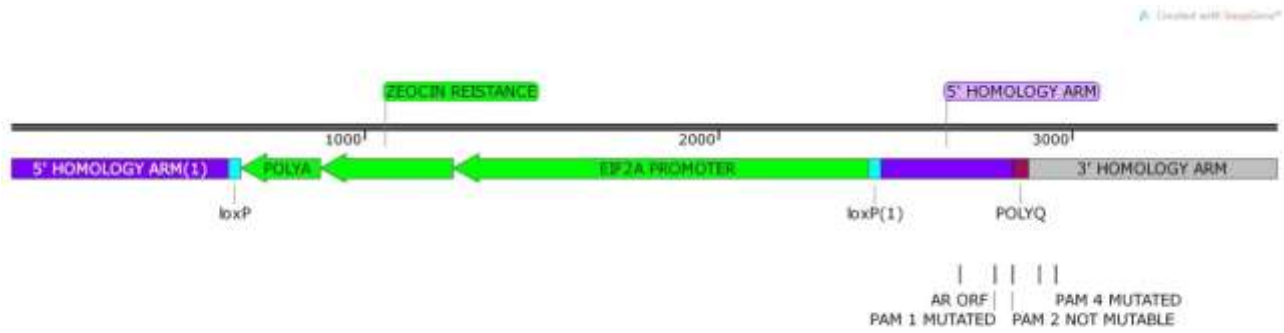


*Figure 45: Schematic representation of donor template*

**Targeting of polyglutamine tract in SBMA derived human induced pluripotent stem cells**

hiPSCs derived from SBMA patients were routinely seeded on Matrigel® Matrix (Corning Incorporated, NY, USA) and cultured in E8 medium (Life Technologies, Thermo Scientific Life Sciences Research, Waltham, MA, USA) supplemented with ROCK-I (Y27632, Tocris Bioscince, Bristol, UK) during splitting and reseeding procedures. Splitting was performed using accutase (Life Technologies, Thermo Scientific Life Sciences Research, Waltham, MA, USA) E8 composition is now known and the eight components are: insulin, selenium, transferrin, L-ascorbic acid, FGF2, and TGFβ in DMEM/F12 (Chen et al. 2011). For thawing, clonal dilution at single cells and picking procedures E8 medium was replaced with mTeSR™1 medium (Stemcell technologies, Vancouver, Canada).

Here I summarized the procedure I followed to target ARpolyQ with CRISPR/Cas9 system (Figure 47A).

Day 0: hiPSCs were seeded as single cell in mTeSR™1 medium with ROCK-I. I seeded 175,000 cells per well (6well-plate).

Day1: cells were transfected with guide-plasmid and donor template (2µg of total DNA; I chose 1:1 ratio guide plasmid vs donor template). Cell were transfected using FuGENE® HD Transfection Reagent (Promega Corporation, Madison, WI, USA), following manufacturer instruction. To target both upstream and downstream two different transfections were performed.

Transfection A: guides to target upstream + donor template

Transfection B: guides to target downstream + donor template

Day 2: cells were treated with puromycin to get rid of not transfected cells (puromycin resistance is present on the pX335B plasmid). Puromycin (Sigma Aldrich, Merck, Darmstadt, Germany) was used 0.5ug/mL overnight.

Day 4-5: when cells recovered from puromycin treatment, they were seeded at clonal dilution as single cells in mTeSR™1 medium. I seeded 500/750 cells per well (6-well plate).

Day 9-10: when few colonies started forming, cells were treated with zeocin 0.75 µg/mL for 4 days.

Day 11-20: colonies were grown and when they reached a proper dimension, colonies were picked. Each picked colony was split in two: the first part was re-plated in 48-well plate with mTeSR™1 supplemented with ROCK-I; the second part was used for DNA extraction and PCR screening

Primers for screening were routinely used in our lab and were designed to amplify a region containing the polyCAG expansion (FW 5'-CCAGAATCTGTTCCAGAGCGTG-3'; RV 5'-TGTTCCCCTGGACTCAGATG-3'). I picked more than one hundred colonies for each transfection and I found two positive clones from transfection B (Figure 46B) with $(CAG)_1$ instead of $(CAG)_{51}$.

Positive colonies were grown, amplified and frozen.

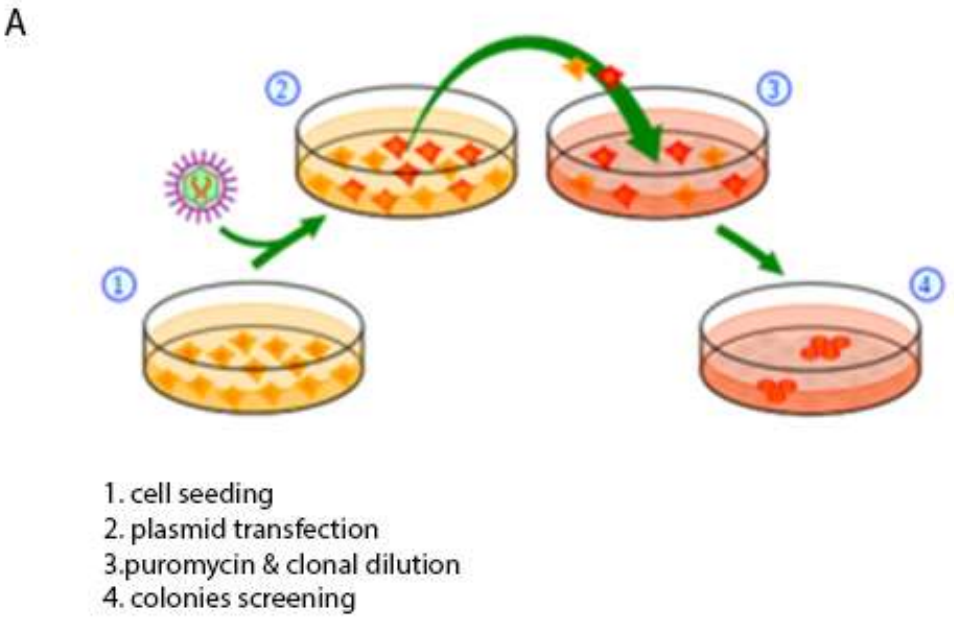


*Figure 46: (A) Protocol for CRISPR/Cas9 gene editing on hiPSCs. (B) PCR on hiPSCs (SB1SG1 1Q)*

## DISCUSSION

CRISPR/Cas9 system has gained importance in the fields of hereditary disease since it allows the generation of isogenic cell line. Isogenic cell line means that two cell line differs only by the presence of a mutation (point mutation, deletion, expansion etc..) while genetic and historical background are the same. CRISPR/Cas9 technique is a genome editing tool easy to use and that gives results with very high efficiency. SBMA is a X-linked hereditary disease caused by a CAG abnormal repetition in the androgen receptor gene. I aimed to obtain from hiPSCs obtained from SBMA patient, an isogenic cell line with normal CAG, using CRISPR/Cas9 system. I obtained two clones that, by PCR, display a shorter (physiological) CAG tract; the obtained cell line will be the control cell line for studying the effects of ARpolyQ in cells. Moreover, differentiating hiPSCs into motor neurons and muscle will let me study ARpolyQ effect directly in affected cell type.

# CONCLUSIONS

My work in these three years focused on the study of the protein quality control system in two neurodegenerative diseases: amyotrophic lateral sclerosis and spinal and bulbar muscular atrophy. I studied the PQC system in muscle cells, to investigate the behavior of these cells in presence of misfolded aggregation prone proteins.

My work is divided in three main parts

i) Studying amyotrophic lateral sclerosis (ALS): I observed that TDP-43 fragments of 35 and 25 kDa aggregate in muscle cells, even if in a slower rate than in motor neurons. To explain this difference, I investigate the involvement of degradative systems in presence of these misfolded aggregation prone proteins. It resulted that proteasome was highly involved in degradation of these toxic species linked to ALS. Even if autophagy seems not involved at basal levels in the degradation of these species, I noted that routing of misfolded proteins to autophagy reverts or slows down the formation of aggregates and reduce the presence of the oligomeric/monomeric proteins. Routing to autophagy was achieved by overexpression of key components of the CASA-complex such as HspB8 and Bag3.

ii) Studying spinal and bulbar muscular atrophy: I studied the effect of trehalose, inducer of autophagy, on muscle cells in presence of ARpolyQ. Since autophagy is highly involved in the degradation of the oligomeric species of ARpolyQ formed in muscle cells. Trehalose was able to reduce the aggregation of ARpolyQ induced by testosterone. Moreover, trehalose in these cells also induces the expression of autophagy-related genes, beneficial for degrading ARpolyQ oligomeric species as demonstrated by the overexpression of one of these factors, such as HspB8.

iii) Generation of a human model to further study SBMA: I generate a cell line bearing a normal CAG tract ($CAG_1$) by editing a hiPSCs line derived from SBMA patient ($CAG_{51}$). For genome editing a used CRISPR/Cas9 system that is and easy and efficient genome editing tool. The two cell line obtained are called isogenic, since the historical and genetic background is the same between the two cell lines, since they differ only for the presence of the polyCAG tract.

# BIBLIOGRAPHY

Adachi, H. et al., 2005. Widespread nuclear and cytoplasmic accumulation of mutant androgen receptor in SBMA patients. *Brain*, 128(3), pp.659–670.

Adams, J. et al., 1998. Potent and selective inhibitors of the proteasome: Dipeptidyl boronic acids. *Bioorganic and Medicinal Chemistry Letters*, 8(4), pp.333–338.

Afroz, T. et al., 2017. Functional and dynamic polymerization of the ALS- linked protein TDP-43 antagonizes its pathologic aggregation. *Nature Communications*, pp.1–14. Available at: https://www.nature.com/articles/s41467-017-00062-0.pdf.

Ajroud-Driss, S. & Siddique, T., 2014. Sporadic and Hereditary Amyotrophic Lateral Sclerosis (ALS). *Biochimica et biophysica acta*, 1852(4), pp.679–684. Available at: http://www.sciencedirect.com/science/article/pii/S0925443914002634.

Akbar, M. et al., 2016. Mitochondrial dysfunction and cell death in neurodegenerative diseases through nitroxidative stress. *Brain Research*, 1637, pp.34–55. Available at: http://dx.doi.org/10.1016/j.brainres.2016.02.016.

Al-Chalabi, A. et al., 2014. Analysis of amyotrophic lateral sclerosis as a multistep process: A population-based modelling study. *The Lancet Neurology*, 13(11), pp.1108–1113. Available at: http://dx.doi.org/10.1016/S1474-4422(14)70219-4.

Al-Chalabi, A. et al., 2012. The genetics and neuropathology of amyotrophic lateral sclerosis. *Acta Neuropathologica*, 124(3), pp.339–352.

Al-Chalabi, A. & Hardiman, O., 2013. The epidemiology of ALS: a conspiracy of genes, environment and time. *Nature Reviews Neurology*, 9(11), pp.617–628. Available at: http://www.nature.com/doifinder/10.1038/nrneurol.2013.203.

Alami, N.H. et al., 2014. Axonal Transport of TDP-43 mRNA Granules Is Impaired by ALS-Causing Mutations. *Neuron*, 81(3), pp.536–543. Available at: http://dx.doi.org/10.1016/j.neuron.2013.12.018.

Alberti, S., Esser, C. & Höhfeld, J., 2003. BAG-1--a nucleotide exchange factor of Hsc70 with multiple cellular functions. *Cell stress & chaperones*, 8(3), pp.225–31. Available at: http://www.pubmedcentral.nih.gov/articlerender.fcgi?artid=514875&tool=pmcentrez&rendertype=abstract.

Allen, S. et al., 2003. Analysis of the cytosolic proteome in a cell culture model of familial amyotrophic lateral sclerosis reveals alterations to the proteasome, antioxidant defenses, and nitric oxide synthetic pathways. *Journal of Biological Chemistry*, 278(8), pp.6371–6383.

Almer, G. et al., 1999. Inducible nitric oxide synthase up-regulation in a transgenic mouse model of familial amyotrophic lateral sclerosis. *Journal of neurochemistry*, 72(6), pp.2415–2425.

Andersen, P.M., 2006. Amyotrophic lateral sclerosis associated with mutations in the CuZn superoxide dismutase gene. *Current Neurology and Neuroscience Reports*, 6(1), pp.37–46.

Appel, S.H. et al., 2011. The microglial-motoneuron dialogue in ALS. *Acta Myologica*, 30(JUNE), pp.4–8.

Arimon, M. et al., 2008. Hsp104 Targets Multiple Intermediates on the Amyloid Pathway and Suppresses the Seeding Capacity of A?? Fibrils and Protofibrils. *Journal of Molecular Biology*, 384(5), pp.1157–1173. Available at: http://dx.doi.org/10.1016/j.jmb.2008.09.063.

Arndt, V. et al., 2005. BAG-2 acts as an inhibitor of the chaperone-associated ubiquitin ligase CHIP. *Mol Biol Cell*, 16(12), pp.5891–5900. Available at: http://www.ncbi.nlm.nih.gov/pubmed/16207813.

Arrigo, A.P., 2017. Mammalian HspB1 (Hsp27) is a molecular sensor linked to the physiology and environment of the cell. *Cell Stress and Chaperones*, 22(4), pp.517–529.

Arvidson, B., 1992. Inorganic mercury is transported from muscular nerve terminals to spinal and brainstem motone urons. *Muscle & Nerve*, 15(10), pp.1089–1094.

Ash, P.E. et al., 2013. Unconventional translation of C9ORF72 GGGGCC expansion generates insoluble polypeptides specific to c9FTD/ALS. *Neuron*, 77(4), pp.639–646. Available at: http://www.ncbi.nlm.nih.gov/pubmed/23415312.

Atkin, J.D. et al., 2014. Mutant SOD1 inhibits ER-Golgi transport in amyotrophic lateral sclerosis. *Journal of Neurochemistry*, 129(1), pp.190–204.

Axe, E.L. et al., 2008. Autophagosome formation from membrane compartments enriched in phosphatidylinositol 3-phosphate and dynamically connected to the endoplasmic reticulum. , 182(4), pp.685–701.

Ayala, Y.M. et al., 2011. TDP-43 regulates its mRNA levels through a negative feedback loop. *EMBO J*, 30(2), pp.277–288. Available at: http://www.ncbi.nlm.nih.gov/pubmed/21131904.

Badadani, M. et al., 2010. VCP associated inclusion body myopathy and paget disease of bone knock-in mouse model exhibits tissue pathology typical of human disease. *PLoS ONE*, 5(10).

Bandyopadhyay, U. et al., 2008. The Chaperone-Mediated Autophagy Receptor Organizes in Dynamic Protein Complexes at the Lysosomal Membrane. , 28(18), pp.5747–5763.

Baniahmad, A., 2016. Inhibition of the Androgen Receptor by Antiandrogens in Spinobulbar Muscle Atrophy. *Journal of Molecular Neuroscience*, 58(3), pp.343–347.

Banno, H. et al., 2012. Pathogenesis and molecular targeted therapy of spinal and bulbar muscular atrophy (SBMA). *Cell and Tissue Research*, 349(1), pp.313–320.

Barber, S. & Shaw, P.J., 2010. Oxidative stress in ALS: Key role in motor neuron injury and therapeutic target. *Free Radical Biology and Medicine*, 48(5), pp.629–641. Available at: http://dx.doi.org/10.1016/j.freeradbiomed.2009.11.018.

Bayraktar, O. et al., 2016. IBMPFD Disease-Causing Mutant VCP/p97 Proteins Are Targets of Autophagic-Lysosomal Degradation. *PloS one*, 11(10), p.e0164864. Available at: http://journals.plos.org/plosone/article?id=10.1371/journal.pone.0164864 [Accessed October 25, 2016].

Beck, J. et al., 2013. Large C9orf72 hexanucleotide repeat expansions are seen in multiple neurodegenerative syndromes and are more frequent than expected in the UK population. *American Journal of Human Genetics*, 92(3), pp.345–353. Available at: http://dx.doi.org/10.1016/j.ajhg.2013.01.011.

Becker, M. et al., 2000. Cytoplasmic localization and the choice of ligand determine aggregate formation by androgen receptor with amplified polyglutamine stretch. *Journal of Cell Biology*, 149(2), pp.255–262.

Beckman, J.S. et al., 2001. Superoxide dismutase and the death of motoneurons in ALS. *Trends in Neurosciences*, 24(11), pp.S15–S20.

Beghi, E. et al., 2010. Amyotrophic lateral sclerosis, physical exercise, trauma and sports: Results of a population-based pilot case-control study. *Amyotrophic Lateral Sclerosis*, 11(3), pp.289–292. Available at: http://www.tandfonline.com/doi/full/10.3109/17482960903384283.

Behl, C., 2011. BAG3 and friends: Co-chaperones in selective autophagy during aging and disease. *Autophagy*, 7(7), pp.795–798.

Behl, C., 2016. Breaking BAG: The Co-Chaperone BAG3 in Health and Disease. *Trends in Pharmacological Sciences*, xx, pp.1–17. Available at: http://linkinghub.elsevier.com/retrieve/pii/S0165614716300189.

Belzil, V. V. et al., 2014. Characterization of DNA hypermethylation in the cerebellum of c9FTD/ALS patients. *Brain Research*, 1584, pp.15–21. Available at: http://dx.doi.org/10.1016/j.brainres.2014.02.015.

Belzil, V. V., Gendron, T.F. & Petrucelli, L., 2013. RNA-mediated toxicity in neurodegenerative disease. *Molecular and Cellular Neuroscience*, 56, pp.406–419. Available at: http://dx.doi.org/10.1016/j.mcn.2012.12.006.

Bendotti, C. & Carrì, M.T., 2004. Lessons from models of SOD1-linked familial ALS. *Trends in Molecular Medicine*, 10(8), pp.393–400.

Bentmann, E. et al., 2012. Requirements for stress granule recruitment of fused in sarcoma (FUS) and TAR DNA-binding protein of 43 kDa (TDP-43). *Journal of Biological Chemistry*, 287(27), pp.23079–23094.

Berchtold, N.C. & Cotman, C.W., 1998. Evolution in the Conceptualization of Dementia and Alzheimer's Disease: Greco-Roman Period to the 1960s. *Neurobiology of Aging*, 19(3), pp.173–189. Available at: http://linkinghub.elsevier.com/retrieve/pii/S0197458098000529.

Bhattacharya, A. et al., 2014. Neuronal cells but not muscle cells are resistant to oxidative stress mediated protein misfolding and cell death: Role of molecular chaperones. *Biochemical and Biophysical Research Communications*, 446(4), pp.1250–1254. Available at: http://dx.doi.org/10.1016/j.bbrc.2014.03.097.

Bjorkoy, G., Lamark, T. & Johansen, T., 2006. p62/SQSTM1: a missing link between protein aggregates and the autophagy machinery. *Autophagy*, 2(2), pp.138–139. Available at: http://www.ncbi.nlm.nih.gov/pubmed/16874037.

van Blitterswijk, M. et al., 2015. Novel clinical associations with specific C9ORF72 transcripts in patients with repeat expansions in C9ORF72. *Acta Neuropathologica*, 130(6), pp.863–876.

Blitterswijk, M. Van et al., 2013. Associations of repeat sizes with clinical and pathological characteristics in C9ORF72 expansion carriers (Xpansize-72): a cross-sectional cohort study. *Lancet Neurology*, 12(10), pp.1–18.

Boch, J. et al., 2009. Breaking the Code of DNA Binding Specificity of TAL-Type III Effectors. *Science*, 326(5959), pp.1509–1512. Available at: http://www.sciencemag.org/cgi/doi/10.1126/science.1178811.

Boillée, S., Vande Velde, C. & Cleveland, D.W.W., 2006. ALS: A Disease of Motor Neurons and Their Nonneuronal Neighbors. *Neuron*, 52(1), pp.39–59.

Bonafede, R. & Mariotti, R., 2017. ALS Pathogenesis and Therapeutic Approaches: The Role of Mesenchymal Stem Cells and Extracellular Vesicles. *Frontiers in Cellular Neuroscience*, 11(March), pp.1–16. Available at: http://journal.frontiersin.org/article/10.3389/fncel.2017.00080/full.

Boncoraglio, A., Minoia, M. & Carra, S., 2012. The family of mammalian small heat shock proteins (HSPBs): Implications in protein deposit diseases and motor neuropathies. *International Journal of Biochemistry and Cell Biology*, 44(10), pp.1657–1669. Available at: http://dx.doi.org/10.1016/j.biocel.2012.03.011.

Borgia, D. et al., 2017. Increased mitophagy in the skeletal muscle of spinal and bulbar muscular atrophy patients.

Bott, L.C. et al., 2016. A small-molecule Nrf1 and Nrf2 activator mitigates polyglutamine toxicity in spinal and bulbar muscular atrophy. *Human Molecular Genetics*, 25(10), pp.1979–1989.

Boutet, S.C. et al., 2007. Regulation of Pax3 by Proteasomal Degradation of Monoubiquitinated Protein in Skeletal Muscle Progenitors. *Cell*, 130(2), pp.349–362.

Brégégère, F., Milner, Y. & Friguet, B., 2006. The ubiquitin-proteasome system at the crossroads of stress-response and ageing pathways: A handle for skin care? *Ageing Research Reviews*, 5(1), pp.60–90.

Brinkmann, A.O., 2001. Molecular basis of androgen insensitivity. *Mol Cell Endocrinol*, 179(1–2), pp.105–109. Available at: http://www.ncbi.nlm.nih.gov/pubmed/11420135%5Cnhttp://ac.els-cdn.com/S030372070100466X/1-s2.0-S030372070100466X-main.pdf?_tid=04ae7b74-e6f0-11e3-b6bc-00000aab0f6c&acdnat=1401340609_d8b1e0b0e0cfb07a3585a2831d4882f6.

Brodsky, J.L. & McCracken, A.A., 1999. ER protein quality control and proteasome-mediated protein degradation. *Seminars in Cell & Developmental Biology*, 10(5), pp.507–513. Available at: http://linkinghub.elsevier.com/retrieve/pii/S108495219990321X.

Brookmeyer, R. et al., 2007. Forecasting the global burden of Alzheimer's disease. *Alzheimer's and Dementia*, 3(3), pp.186–191.

Brooks BR, Miller RG, S.M., 2000. El Escorial revisited: revised criteria for the diagnosis of amyotrophic lateral sclerosis. *Amyotrophic Lateral Scler Other Motor. Neuron Disord*, 1, pp.293–299.

Brown, C.J. et al., 2013. Androgen receptor (AR) gene CAG trinucleotide repeat length associated with body composition measures in non-syndromic obese, non-obese and Prader-Willi syndrome individuals. *Journal of Assisted Reproduction and Genetics*, 18(3), pp.2–9. Available at: http://www.pubmedcentral.nih.gov/articlerender.fcgi?artid=2362888&tool=pmcentrez&rendertype=abstract.

Brown, I.R., 2007. Heat shock proteins and protection of the nervous system. *Ann N Y Acad Sci*, 1113, pp.147–158. Available at: http://www.ncbi.nlm.nih.gov/pubmed/17656567.

Bruno, A.P. et al., 2008. Identification of a synaptosome-associated form of BAG3 protein. *Cell Cycle*, 7(19), pp.3104–3105.

Buchman, V.L. et al., 2013. Simultaneous and independent detection of C9ORF72 alleles with low and high number of GGGGCC repeats using an optimised protocol of Southern blot hybridisation. *Molecular neurodegeneration*, 8(1), p.12. Available at: http://www.pubmedcentral.nih.gov/articlerender.fcgi?artid=3626718&tool=pmcentrez&rendertype=abstract.

Buchner, J. & Li, J., 2013. Structure, Function and Regulation of the Hsp90 Machinery. *Biomedical Journal*, 36(3), p.106. Available at: http://biomedj.cgu.edu.tw/pdfs/2013/36/3/images/BiomedJ_2013_36_3_106_113230.pdf.

Bug, M. & Meyer, H., 2012. Expanding into new markets - VCP/p97 in endocytosis and autophagy. *Journal of Structural Biology*, 179(2), pp.78–82. Available at: http://dx.doi.org/10.1016/j.jsb.2012.03.003.

Bukau, B., Weissman, J. & Horwich, A., 2006. Molecular chaperones and protein quality control. *Cell*, 125(3), pp.443–451. Available at: http://www.ncbi.nlm.nih.gov/pubmed/16678092.

Buratti, E. et al., 2005. TDP-43 binds heterogeneous nuclear ribonucleoprotein A/B through its C-terminal tail: An important region for the inhibition of cystic fibrosis transmembrane conductance regulator exon 9 splicing. *Journal of Biological Chemistry*, 280(45), pp.37572–37584.

Caccamo, A. et al., 2015. Reduced protein turnover mediates functional deficits in transgenic mice expressing the 25 kDa C-terminal fragment of TDP-43. *Human Molecular Genetics*, 24(16), pp.4625–4635.

Cardozo, C.P. et al., 2003. C-terminal Hsp-interacting protein slows androgen receptor synthesis and reduces its rate of degradation. *Archives of Biochemistry and Biophysics*, 410(1), pp.134–140.

Carra, S. et al., 2008. HspB8 chaperone activity toward poly(Q)-containing proteins depends on its association with Bag3, a stimulator of macroautophagy. *J Biol Chem*, 283(3), pp.1437–1444. Available at: http://www.ncbi.nlm.nih.gov/pubmed/18006506.

Carrettiero, D.C. et al., 2009. The Co-chaperone BAG2 Sweeps PHF Insoluble Tau from the Microtubule. , 29(7), pp.2151–2161.

Carroll, D., 2011. Genome engineering with zinc-finger nucleases. *Genetics*, 188(4), pp.773–782.

Caughey, B. & Lansbury, P.T., 2003. PROTOFIBRILS , PORES, FIBRILS, AND NEURODEGENERATION: Separating the Responsible Protein Aggregates from The Innocent Bystanders. *Annual Review of Neuroscience*, 26(1), pp.267–298. Available at: http://www.annualreviews.org/doi/10.1146/annurev.neuro.26.010302.081142.

Chaudhuri, K.R. et al., 1995. The validation of El Escorial criteria for the diagnosis of amyotrophic lateral sclerosis: a clinicopathological study. *J Neurol Sci*, 129 Suppl, pp.11–12. Available at: http://www.ncbi.nlm.nih.gov/pubmed/7595600.

Chauhan, D. et al., 2003. Hsp27 inhibits release of mitochondrial protein Smac in multiple myeloma cells and confers dexamethasone resistance. *Blood*, 102(9), pp.3379–3386.

Che, M.-X. et al., 2011. Aggregation of the 35-kDa fragment of TDP-43 causes formation of cytoplasmic inclusions and alteration of RNA processing. *The FASEB Journal*, 25(7), pp.2344–2353. Available at: http://www.fasebj.org/cgi/doi/10.1096/fj.10-174482.

Chen, G. et al., 2011. Chemically defined conditions for human iPS cell derivation and culture. *Nature Methods*, 8(5), pp.424–429.

Chen, K. & Knoepfler, P.S., 2016. To CRISPR and beyond : the evolution of genome editing in stem cells. *Regenerative Medicine*, 11, pp.801–816.

Chen, Y. et al., 2005. ER-associated protein degradation is a common mechanism underpinning numerous monogenic diseases including Robinow syndrome. *Human Molecular Genetics*, 14(17), pp.2559–2569.

Chen, Y., 2012. Organophosphate-induced brain damage: Mechanisms, neuropsychiatric and neurological consequences, and potential therapeutic strategies. *NeuroToxicology*, 33(3), pp.391–400.

Chondrogianni, N. et al., 2015. Proteasome activation: An innovative promising approach for delaying aging and retarding age-related diseases. *Ageing Research Reviews*, 23(PA), pp.37–55. Available at: http://dx.doi.org/10.1016/j.arr.2014.12.003.

Ciechanover, A., 1994. The ubiquitin-proteasome proteolytic pathway. *Cell*, 79(1), pp.13–21.

Ciechanover, A. & Kwon, Y.T., 2015. Degradation of misfolded proteins in neurodegenerative diseases: therapeutic targets and strategies. *Exp Mol Med*, 47, p.e147. Available at: http://www.ncbi.nlm.nih.gov/pubmed/25766616.

Ciechanover, A. & Kwon, Y.T., 2017. Protein Quality Control by Molecular Chaperones in Neurodegeneration. *Frontiers in Neuroscience*, 11(April), pp.1–18. Available at: http://journal.frontiersin.org/article/10.3389/fnins.2017.00185/full.

Ciura, S. et al., 2013. Loss of function of C9orf72 causes motor deficits in a zebrafish model of amyotrophic lateral sclerosis. *Annals of Neurology*, 74(2), pp.180–187.

Clement, A.M., 2003. Wild-Type Nonneuronal Cells Extend Survival of SOD1 Mutant Motor Neurons in ALS Mice. *Science*, 302(5642), pp.113–117. Available at: http://www.sciencemag.org/cgi/doi/10.1126/science.1086071.

Colombrita, C. et al., 2009. TDP-43 is recruited to stress granules in conditions of oxidative insult. *Journal of Neurochemistry*, 111(4), pp.1051–1061.

Cong, L. et al., 2013. Multiplex Genome Engineering Using CRISPR/VCas Systems. *Science*, 339(6121), pp.819–823.

Connell, P. et al., 2001. The co-chaperone CHIP regulates protein triage decisions mediated by heat-shock proteins. , 3(January), pp.93–96.

Conway, K.A., 2001. Kinetic Stabilization of the alpha -Synuclein Protofibril by a Dopamine-alpha -Synuclein Adduct. *Science*, 294(5545), pp.1346–1349. Available at: http://www.sciencemag.org/cgi/doi/10.1126/science.1063522.

Corduan, A. et al., 2009. Sequential interplay between BAG6 and HSP70 upon heat shock. *Cellular and Molecular Life Sciences*, 66(11–12), pp.1998–2004.

Cortes, C.J. et al., 2014. Muscle expression of mutant androgen receptor accounts for systemic and motor neuron disease phenotypes in spinal and bulbar muscular atrophy. *Neuron*, 82(2), pp.295–307.

Crippa, V. et al., 2013. Differential autophagy power in the spinal cord and muscle of transgenic ALS mice. *Frontiers in cellular neuroscience*, 7(November), p.234. Available at: http://www.pubmedcentral.nih.gov/articlerender.fcgi?artid=3840302&tool=pmcentrez&rendertype=abstract.

Crippa, V., Cicardi, M.E., et al., 2016. The chaperone HSPB8 reduces the accumulation of truncated TDP-43 species in cells and protects against TDP-43-mediated toxicity. *Human molecular genetics*, p.ddw232-. Available at: http://hmg.oxfordjournals.org/content/early/2016/08/17/hmg.ddw232.long [Accessed October 5, 2016].

Crippa, V. et al., 2010. The small heat shock protein B8 (HspB8) promotes autophagic removal of misfolded proteins involved in amyotrophic lateral sclerosis (ALS). *Human Molecular Genetics*, 19(17), pp.3440–3456.

Crippa, V., D'Agostino, V.G., et al., 2016. Transcriptional induction of the heat shock protein B8 mediates the clearance of misfolded proteins responsible for motor neuron diseases. *Scientific reports*, 6(February), p.22827. Available at: http://www.pubmedcentral.nih.gov/articlerender.fcgi?artid=4785366&tool=pmcentrez&rendertype=abstract.

Cristofani, R., Crippa, V., Rusmini, P., et al., 2017. Inhibition of retrograde transport modulates misfolded protein accumulation and clearance in motoneuron diseases. *Autophagy*, 13(8), pp.1280–1303. Available at: http://dx.doi.org/10.1080/15548627.2017.1308985.

Cristofani, R., Crippa, V., Vezzoli, G., et al., 2017. The small heat shock protein B8 (HSPB8) efficiently removes aggregating species of dipeptides produced in C9ORF72-related neurodegenerative diseases. *Cell Stress and Chaperones*, 8. Available at: http://link.springer.com/10.1007/s12192-017-0806-9.

Cruz, S. Da et al., 2013. Elevated PGC-1α Activity Sustains Mitochondrial Biogenesis and Muscle Function without Extending Survival in a Mouse Model of Inherited ALS. , 15(5), pp.778–786.

Cuanalo-Contreras, K., Mukherjee, A. & Soto, C., 2013. Role of protein misfolding and proteostasis deficiency in protein misfolding diseases and aging. *Int J Cell Biol*, 2013, p.638083. Available at: http://www.ncbi.nlm.nih.gov/pubmed/24348562.

Cudkowicz, M.E. et al., 1997. Epidemiology of Mutations in Superoxide Dismutase in Amyotrophic Lateral Sclerosis. *Epidemiology*, pp.210–221.

Cuervo, A.M. & Wong, E., 2014. Chaperone-mediated autophagy: roles in disease and aging. *Cell Research*, 24(1), pp.92–104. Available at: http://www.nature.com/doifinder/10.1038/cr.2013.153.

D'Agostino, Y. & D'Aniello, S., 2017. Molecular basis, applications and challenges of CRISPR/Cas9: a continuously evolving tool for genome editing. *Briefings in Functional Genomics*, p.elw038. Available at: http://bfgp.oxfordjournals.org/lookup/doi/10.1093/bfgp/elw038.

D'Andrea, L.D. & Regan, L., 2003. TPR proteins: The versatile helix. *Trends in Biochemical Sciences*, 28(12), pp.655–662.

Dai, Q. et al., 2005. Regulation of the cytoplasmic quality control protein degradation pathway by BAG2. *The Journal of biological chemistry*, 280(46), pp.38673–38681.

Davidson, Y.S. et al., 2014. Brain distribution of dipeptide repeat proteins in frontotemporal lobar degeneration and motor neurone disease associated with expansions in C9ORF72. *Acta neuropathologica communications*, 2(1), p.70. Available at: http://actaneurocomms.biomedcentral.com/articles/10.1186/2051-5960-2-70.

Davie, C.A., 2008. A review of Parkinson's disease. *British Medical Bulletin*, 86(1), pp.109–127.

Dejager, S. et al., 2002. A comprehensive endocrine description of Kennedy's disease revealing androgen insensitivity linked to CAG repeat length. *Journal of Clinical Endocrinology and Metabolism*, 87(8), pp.3893–3901.

Delesus-Hernandez, M. et al., 2011. Expanded GGGGCC hexanucleotide repeat in noncoding region of C9ORF72 causes chromosome 9p-linked FTD and ALS. *Neuron*, 72(2), pp.245–256. Available at: http://www.ncbi.nlm.nih.gov/pubmed/21944778.

DeLaBarre, B. & Brunger, A.T., 2003. Complete structure of p97/valosin-containing protein reveals communication between nucleotide domains. *Nat Struct Biol*, 10(10), pp.856–863. Available at: http://www.ncbi.nlm.nih.gov/pubmed/12949490.

DeLaBarre, B. & Brunger, A.T., 2005. Nucleotide dependent motion and mechanism of action of p97/VCP. *J Mol Biol*, 347(2), pp.437–452. Available at: http://www.ncbi.nlm.nih.gov/pubmed/15740751.

Demand, J. et al., 2001. Cooperation of a ubiquitin domain protein and an E3 ubiquitin ligase during chaperone/proteasome coupling. *Curr Biol*, 11(20), pp.1569–1577. Available at: http://www.ncbi.nlm.nih.gov/pubmed/11676916.

Deng, D.H.-X. et al., 2011. Differential Involvement of Optineurin in Amyotrophic Lateral Sclerosis With or Without SOD1 Mutations. *Arch Neurol*, 68(8), pp.1057–1061.

Deng, H.-X. et al., 2010. FUS-immunoreactive inclusions are a common feature in sporadic and non-SOD1 familial amyotrophic lateral sclerosis Han-Xiang. , 10(7), pp.552–554.

Deng, H., Gao, K. & Jankovic, J., 2014. The role of FUS gene variants in neurodegenerative diseases. *Nature Reviews Neurology*, 10(6), pp.337–348. Available at: http://www.nature.com/doifinder/10.1038/nrneurol.2014.78.

Deng, H.X. et al., 2011. Mutations in UBQLN2 cause dominant X-linked juvenile and adult-onset ALS and ALS/dementia. *Nature*, 477(7363), pp.211–215. Available at: http://www.ncbi.nlm.nih.gov/pubmed/21857683.

Diaper, D.C. et al., 2013. Loss and gain of Drosophila TDP-43 impair synaptic efficacy and motor control leading to age-related neurodegeneration by loss-of-function phenotypes. *Human Molecular Genetics*, 22(8), pp.1539–1557.

Dick, T.P. et al., 1996. Coordinated dual cleavages induced by the proteasome regulator PA28 lead to dominant MHC ligands. *Cell*, 86(2), pp.253–262.

Dobrowolny, G. et al., 2005. Muscle expression of a local Igf-1 isoform protects motor neurons in an ALS mouse model. *Journal of Cell Biology*, 168(2), pp.193–199.

Dobrowolny, G. et al., 2015. Muscle Expression of SOD1(G93A) Modulates microRNA and mRNA Transcription Pattern Associated with the Myelination Process in the Spinal Cord of Transgenic Mice. *Frontiers in cellular neuroscience*, 9(12), p.463. Available at: http://www.pubmedcentral.nih.gov/articlerender.fcgi?artid=4664730&tool=pmcentrez&rendertype=abstract.

Dobrowolny, G. et al., 2008. Skeletal Muscle Is a Primary Target of SOD1G93A-Mediated Toxicity. *Cell Metabolism*, 8(5), pp.425–436.

Dobson, C.M., 2003. Protein folding and misfolding. *Nature*, 426(6968), pp.884–890. Available at: http://www.ncbi.nlm.nih.gov/pubmed/14685248.

Dobson, C.M., Sali, A. & Karplus, M., 1998. Protein folding: A perspective from theory and experiment. *Angewandte Chemie - International Edition*, 37(7), pp.868–893.

Dols-Icardo, O. et al., 2014. Characterization of the repeat expansion size in C9orf72 in amyotrophic lateral sclerosis and frontotemporal dementia. *Human Molecular Genetics*, 23(3), pp.749–754.

Donnelly, C.J. et al., 2014. RNA Toxicity from the ALS/FTD C9ORF72 Expansion Is Mitigated by Antisense Intervention. , 80(2), pp.415–428.

Doong, H. et al., 2003. CAIR-1/BAG-3 abrogates heat shock protein-70 chaperone complex-mediated protein degradation. Accumulation of poly-ubiquitinated Hsp90 client proteins. *Journal of Biological Chemistry*, 278(31), pp.28490–28500.

Du, K. et al., 2011. TLS and PRMT1 synergistically coactivate transcription at the survivin promoter through TLS arginine methylation. *Biochemical and Biophysical Research Communications*, 404(4), pp.991–996. Available at: http://dx.doi.org/10.1016/j.bbrc.2010.12.097.

Dupuis, L. et al., 2004. Evidence for defective energy homeostasis in amyotrophic lateral sclerosis: Benefit of a high-energy diet in a transgenic mouse model. *Proceedings of the National Academy of Sciences*, 101(30), pp.11159–11164. Available at: http://www.pnas.org/cgi/doi/10.1073/pnas.0402026101.

During, R.L. et al., 2007. Anthrax lethal toxin paralyzes actin-based motility by blocking Hsp27 phosphorylation. *The EMBO journal*, 26(9), pp.2240–50. Available at: http://www.pubmedcentral.nih.gov/articlerender.fcgi?artid=1864983&tool=pmcentrez&rendertype=abstract.

Duyckaerts, C., Potier, M.-C. & Delatour, B., 2007. *Alzheimer disease models and human neuropathology: similarities and differences*, Available at: http://link.springer.com/10.1007/s00401-007-0312-8.

Eisele, F. & Wolf, D.H., 2008. Degradation of misfolded protein in the cytoplasm is mediated by the ubiquitin ligase Ubr1. *FEBS Letters*, 582(30), pp.4143–4146. Available at: http://dx.doi.org/10.1016/j.febslet.2008.11.015.

Elbaz, A. et al., 2016. Epidemiology of Parkinson's disease. *Revue neurologique*, 172(1), pp.14–26.

Ellerby, L.M. et al., 1999. Kennedy's disease: Caspase cleavage of the androgen receptor is a crucial event in cytotoxicity. *Journal of Neurochemistry*, 72(1), pp.185–195.

Fader, C.M. et al., 2009. Biochimica et Biophysica Acta TI-VAMP / VAMP7 and VAMP3 / cellubrevin : two v-SNARE proteins involved in speci fi c steps of the autophagy / multivesicular body pathways. *BBA - Molecular Cell Research*, 1793(12), pp.1901–1916. Available at: http://dx.doi.org/10.1016/j.bbamcr.2009.09.011.

Fang, F. et al., 2010. Association between blood lead and the risk of amyotrophic lateral sclerosis. *American Journal of Epidemiology*, 171(10), pp.1126–1133.

Fang, F. & Ye, W., 2010. SMOKING MAY BE CONSIDERED AN ESTABLISHED RISK FACTOR FOR SPORADIC ALS. *Neurology*, 95(1), pp.1927–1930.

Faravelli, I. et al., 2014. Stem cell transplantation for amyotrophic lateral sclerosis: Therapeutic potential and perspectives on clinical translation. *Cellular and Molecular Life Sciences*, 71(17), pp.3257–3268.

Felzen, V. et al., 2015. Estrogen receptor α regulates non-canonical autophagy that provides stress resistance to neuroblastoma and breast cancer cells and involves BAG3 function. *Cell Death and Disease*, 6(7), p.e1812. Available at: http://www.nature.com/doifinder/10.1038/cddis.2015.181.

Fernandez-Guasti, A. et al., 2000. Sex differences in the distribution of androgen receptors in the human hypothalamus. *Journal of Comparative Neurology*, 425(January), pp.422–435.

Fernández-Rhodes, L.E. et al., 2011. Efficacy and safety of dutasteride in patients with spinal and bulbar muscular atrophy: A randomised placebo-controlled trial. *The Lancet Neurology*, 10(2), pp.140–147.

Fernández-Sáiz, V. & Buchberger, A., 2010. Imbalances in p97 co-factor interactions in human proteinopathy. *EMBO reports*, 11(6), pp.479–485. Available at: http://embor.embopress.org/cgi/doi/10.1038/embor.2010.49.

Ferrari, R. et al., 2011. FTD and ALS: a tale of two diseases. *Curr Alzheimer Res*, 8(3), pp.273–294. Available at: http://www.ncbi.nlm.nih.gov/pubmed/21222600.

Figley, M.D. et al., 2014. Profilin 1 associates with stress granules and ALS-linked mutations alter stress granule dynamics. *The Journal of neuroscience : the official journal of the Society for Neuroscience*, 34(24), pp.8083–97. Available at: http://www.jneurosci.org/content/34/24/8083.short.

Finsterer, J. & Soraru, G., 2016. Onset Manifestations of Spinal and Bulbar Muscular Atrophy (Kennedy???s Disease). *Journal of Molecular Neuroscience*, 58(3), pp.321–329.

Fischbeck, K., 1997. Kennedy Disease. *inherited metabolism disease*, 20(June), pp.152–158.

Fischbeck, K.H., 2001. Polyglutamine expansion neurodegenerative disease. *Brain Research Bulletin*, 56(3–4), pp.161–163.

Fratta, P. et al., 2012. C9orf72 hexanucleotide repeat associated with amyotrophic lateral sclerosis and frontotemporal dementia forms RNA G-quadruplexes. *Scientific Reports*, 2(1), p.1016. Available at: http://www.nature.com/articles/srep01016.

Fratta, P. et al., 2014. Correlation of clinical and molecular features in spinal bulbar muscular atrophy. *Neurology*, 82(23), pp.2077–2084.

Frydman, J., 2001. F OLDING OF N EWLY T RANSLATED P ROTEINS I N V IVO : The Role of Molecular Chaperones.

Fu, M. et al., 2002. Androgen receptor acetylation governs trans activation and MEKK1-induced apoptosis without affecting in vitro sumoylation and trans-repression function. *Molecular and cellular biology*, 22(10), pp.3373–88. Available at: http://www.pubmedcentral.nih.gov/articlerender.fcgi?artid=133781&tool=pmcentrez&rendertype=abstract.

Fuchs, M. et al., 2015. A Role for the Chaperone Complex BAG3-HSPB8 in Actin Dynamics, Spindle Orientation and Proper Chromosome Segregation during Mitosis. *PLoS Genetics*, 11(10), pp.1–32.

Fuentealba, R.A. et al., 2010. Interaction with polyglutamine aggregates reveals a Q/N-rich domain in TDP-43. *Journal of Biological Chemistry*, 285(34), pp.26304–26314.

Furuta, N. et al., 2010. Combinational Soluble N -Ethylmaleimide-sensitive Factor Attachment Protein Receptor Proteins VAMP8 and Vti1b Mediate Fusion of Antimicrobial and Canonical Autophagosomes with Lysosomes. , 21, pp.1001–1010.

Furuya, N. et al., 2005. The Evolutionarily Conserved Domain of Beclin 1 is Required for Vps34 Binding, Autophagy and Tumor Suppressor Function. , (June), pp.46–52.

Gaj, T. et al., 2016. Genome-Editing Technologies : Principles and Applications.

Gallo, V. et al., 2016. Physical activity and risk of Amyotrophic Lateral Sclerosis in a prospective cohort study. *European Journal of Epidemiology*, 31(3), pp.255–266.

Gamerdinger, M., Kaya, A.M., et al., 2011. BAG3 mediates chaperone-based aggresome-targeting and selective autophagy of misfolded proteins. *EMBO Rep*, 12(2), pp.149–156. Available at: http://www.ncbi.nlm.nih.gov/pubmed/21252941.

Gamerdinger, M., Carra, S. & Behl, C., 2011. Emerging roles of molecular chaperones and co-chaperones in selective autophagy: focus on BAG proteins. *J Mol Med (Berl)*, 89(12), pp.1175–1182. Available at: http://www.ncbi.nlm.nih.gov/pubmed/21818581.

Ganley, I.G. et al., 2009. ULK1 ATG13 FIP200 Complex Mediates mTOR Signaling and Is Essential for Autophagy. , 284(18), pp.12297–12305.

Garrido, C. et al., 2001. Heat Shock Proteins: Endogenous Modulators of Apoptotic Cell Death. *Biochemical and Biophysical Research Communications*, 286(3), pp.433–442. Available at: http://linkinghub.elsevier.com/retrieve/pii/S0006291X01954270.

Garrido, C. et al., 2006. Heat shock proteins 27 and 70: anti-apoptotic proteins with tumorigenic properties. *Cell Cycle*, 5(22), pp.2592–2601. Available at: http://www.ncbi.nlm.nih.gov/pubmed/17106261.

Gascon, E. & Gao, F.-B., 2014. The Emerging Roles of MicroRNAs in the Pathogenesis of Frontotemporal Dementia–Amyotrophic Lateral Sclerosis (FTD-ALS) Spectrum Disorders. *Journal of Neurogenetics*, 28(1–2), pp.30–40. Available at: http://www.tandfonline.com/doi/full/10.3109/01677063.2013.876021.

Ge, F. et al., 2010. Identification of novel 14-3-3X interacting proteins by quantitative immunoprecipitation combined with knockdown (QUICK). *Journal of Proteome Research*, 9(11), pp.5848–5858.

Gendron, T.F. et al., 2013. Antisense transcripts of the expanded C9ORF72 hexanucleotide repeat form nuclear RNA foci and undergo repeat-associated non-ATG translation in c9FTD/ALS. *Acta Neuropathol*, 126(6), pp.829–844. Available at: http://www.ncbi.nlm.nih.gov/pubmed/24129584.

Gendron, T.F. et al., 2014. Mechanisms of toxicity in C9FTLD/ALS. *Acta Neuropathologica*, 127(3), pp.359–376.

Gendron, T.F. & Petrucelli, L., 2017. Disease Mechanisms of C9ORF72 Repeat Expansions. , pp.1–22.

Gentilella, A. & Khalili, K., 2011. BAG3 expression in glioblastoma cells promotes accumulation of ubiquitinated clients in a n Hsp70-dependent manner. *Journal of Biological Chemistry*, 286(11), pp.9205–9215.

Georgiou, I. et al., 2001. Preimplantation genetic diagnosis for spinal and bulbar muscular atrophy (SBMA). *Human Genetics*, 108(6), pp.494–498.

Gioeli, D. et al., 2002. Androgen receptor phosphorylation. Regulation and identification of the phosphorylation sites. *Journal of Biological Chemistry*, 277(32), pp.29304–29314.

Giorgetti, E. et al., 2016. Rescue of Metabolic Alterations in AR113Q Skeletal Muscle by Peripheral Androgen Receptor Gene Silencing. *Cell reports*, 17(1), pp.125–36. Available at: http://www.sciencedirect.com/science/article/pii/S2211124716311809 [Accessed October 17, 2016].

Giorgetti, E. et al., 2014. Synergic prodegradative activity of Bicalutamide and trehalose on the mutant Androgen Receptor responsible for Spinal and Bulbar Muscular Atrophy. , pp.1–37.

Giorgetti, E. & Lieberman, A.P., 2016a. Polyglutamine androgen receptor-mediated neuromuscular disease. *Cellular and Molecular Life Sciences*. Available at: http://link.springer.com/10.1007/s00018-016-2275-1.

Giorgetti, E. & Lieberman, A.P., 2016b. Polyglutamine androgen receptor-mediated neuromuscular disease. *Cellular and Molecular Life Sciences*, 73(21), pp.3991–3999.

Glabe, C.G., 2006. Common mechanisms of amyloid oligomer pathogenesis in degenerative disease. *Neurobiology of Aging*, 27(4), pp.570–575.

Glickman, M.H. et al., 1998. A subcomplex of the proteasome regulatory particle required for ubiquitin-conjugate degradation and related to the COP9-signalosome and eIF3. *Cell*, 94(5), pp.615–623. Available at: http://www.ncbi.nlm.nih.gov/pubmed/9741626.

Glickman, M.H. & Ciechanover, A., 2002. The ubiquitin-proteasome proteolytic pathway: destruction for the sake of construction. *Physiol Rev*, 82(2), pp.373–428. Available at: http://www.ncbi.nlm.nih.gov/pubmed/11917093.

Goldstein, L.A. & Sengelaub, D.R., 1990. Timing and duration of DHT treatment alters motoneuron number, morphology, and specificity in a sexually dimorphic rat spinal nucleus. *Society for Neuroscience*, 16, p.0.

Gregory, R.I. et al., 2004. The Microprocessor complex mediates the genesis of microRNAs. *Nature*, 432(7014), pp.235–240. Available at: http://www.nature.com/doifinder/10.1038/nature03120.

Groll, M. et al., 2000. A gated channel into the proteasome core particle. *Nat Struct Biol*, 7(11), pp.1062–1067. Available at: http://www.ncbi.nlm.nih.gov/pubmed/11062564.

Groll, M. & Huber, R., 2004. Inhibitors of the eukaryotic 20S proteasome core particle: A structural approach. *Biochimica et Biophysica Acta - Molecular Cell Research*, 1695(1–3), pp.33–44.

Grune, T. et al., 2004. Decreased proteolysis caused by protein aggregates, inclusion bodies, plaques, lipofuscin, ceroid, and "aggresomes" during oxidative stress, aging, and disease. *International Journal of Biochemistry and Cell Biology*, 36(12), pp.2519–2530.

Grunseich, C., Rinaldi, C. & Fischbeck, K.H., 2014. Spinal and bulbar muscular atrophy: pathogenesis and clinical management. *Oral diseases*, 20(1), pp.6–9. Available at: http://www.pubmedcentral.nih.gov/articlerender.fcgi?artid=4284073&tool=pmcentrez&rendertype=abstract.

Guidetti, D. et al., 2016. Epidemiological Survey of X-Linked Bulbar and Spinal Muscular Atrophy , or Kennedy Disease , in the Province of Reggio Emilia , Italy Author ( s ): D . Guidetti , R . Sabadini , A . Ferlini and I . Torrente Published by : Springer Stable URL : http://www. , 17(6), pp.587–591.

Guo, H. et al., 2003. Increased expression of the glial glutamate transporter EAAT2 modulates excitotoxicity and delays the onset but not the outcome of ALS in mice. *Hum Mol Genet*, 12(19), pp.2519–2532. Available at: http://www.ncbi.nlm.nih.gov/pubmed/12915461.

Guo, Y. et al., 2010. Ultrastructural diversity of inclusions and aggregations in the lumbar spinal cord of SOD1-G93A transgenic mice. *Brain Research*, 1353, pp.234–244. Available at: http://dx.doi.org/10.1016/j.brainres.2010.07.025.

Guyant-Marechal, L. et al., 2006. Valosin-containing protein gene mutations: clinical and neuropathologic features. *Neurology*, 67(4), pp.644–651. Available at: http://www.ncbi.nlm.nih.gov/pubmed/16790606.

Gwinn, D.M. et al., 2009. AMPK phosphorylation of raptor mediates a metabolic checkpoint. , 30(2), pp.214–226.

Haeusler, A.R. et al., 2014. C9orf72 nucleotide repeat structures initiate molecular cascades of disease. *Nature*, 507(7491), pp.195–200. Available at: http://www.ncbi.nlm.nih.gov/pubmed/24598541.

Halter, B. et al., 2010. Oxidative stress in skeletal muscle stimulates early expression of Rad in a mouse model of amyotrophic lateral sclerosis. *Free Radical Biology and Medicine*, 48(7), pp.915–923.

Hampton, R.Y., 2002. ER-associated degradation in protein quality control and cellular regulation. *Curr.Opin.Cell Biol.*, 14(455–674), pp.476–482.

Hao, R. et al., 2013. Proteasomes Activate Aggresome Disassembly and Clearance by Producing Unanchored Ubiquitin Chains. *Molecular Cell*, 51(6), pp.819–828.

Harding, A. et al., 1982. X-linked recessive bulbospinal neuronopathy: a report of ten cases. *Journal of Neurology, Neurosurgery, and Psychiatry*, 45, pp.1012–1019.

Hartl, F.U. & Hayer-Hartl, M., 2002. Molecular chaperones in the cytosol: from nascent chain to folded protein. *Science (New York, N.Y.)*, 295(5561), pp.1852–8. Available at: http://www.ncbi.nlm.nih.gov/pubmed/11884745.

Hartl, U.F., Bracher, A. & Hayer-Hartl, M., 2011. Molecular chaperones in protein folding and proteostasis. *Nature*, 475(1), pp.324–333.

Hasegawa, M. et al., 2008. Phosphorylated TDP-43 in frontotemporal lobar degeneration and amyotrophic lateral sclerosis. *Annals of Neurology*, 64(1), pp.60–70.

Hayashi-Nishino, M. et al., 2009. A subdomain of the endoplasmic reticulum forms a cradle for autophagosome formation. *Nat Cell Biol*, 11(12), pp.1433–1437. Available at: http://www.ncbi.nlm.nih.gov/pubmed/19898463.

He, B. & Wilson, E.M., 2002. The NH2-terminal and carboxyl-terminal interaction in the human androgen receptor. *Molecular Genetics and Metabolism*, 75(4), pp.293–298.

He, C. et al., 2008. Self-Interaction Is Critical for Atg9 Transport and Function at the Phagophore Assembly Site during Autophagy. , 19(December), pp.5506–5516.

Healy, E.F., 2017. A prion-like mechanism for the propagated misfolding of SOD1 from in silico modeling of solvated near-native conformers. *PloS one*, 12(5), p.e0177284. Available at: http://www.ncbi.nlm.nih.gov/pubmed/28472188.

Hebron, M.L. et al., 2013. Parkin ubiquitinates tar-DNA binding protein-43 (TDP-43) and promotes its cytosolic accumulation via interaction with histone deacetylase 6 (HDAC6). *Journal of Biological Chemistry*, 288(6), pp.4103–4115.

Heck, J.W., Cheung, S.K. & Hampton, R.Y., 2010. Cytoplasmic protein quality control degradation mediated by parallel actions of the E3 ubiquitin ligases Ubr1 and San1. *Proceedings of the National Academy of Sciences*, 107(3), pp.1106–1111. Available at: http://www.pnas.org/cgi/doi/10.1073/pnas.0910591107.

Heinemeyer, W. et al., 1997. The active sites of the eukaryotic 20 S proteasome and their involvement in subunit precursor processing. *Journal of Biological Chemistry*, 272(40), pp.25200–25209.

Hershko, A. & Ciechanover, A., 1998. The ubiquitin system. *Annu Rev Biochem*, 67, pp.425–479. Available at: http://www.ncbi.nlm.nih.gov/pubmed/9759494.

Hirano, Y. et al., 2008. Dissecting beta-ring assembly pathway of the mammalian 20S proteasome. *The EMBO journal*, 27(16), pp.2204–13. Available at: http://emboj.embopress.org/content/27/16/2204.abstract.

Hochstrasser, M., 2006. Lingering mysteries of ubiquitin-chain assembly. *Cell*, 124(1), pp.27–34.

Höhfeld, J. & Jentsch, S., 1997. GrpE-like regulation of the Hsc70 chaperone by the anti-apoptotic protein BAG-1. *EMBO Journal*, 16(20), pp.6209–6216.

Horvath, P. & Barrangou, R., 2010. CRISPR/Cas, the Immune System of Bacteria and Archaea. *Science*, 327(5962), pp.167–170. Available at: http://www.sciencemag.org/cgi/doi/10.1126/science.1179555.

Horwitz, J., 1992. Alpha-crystallin can function as a molecular chaperone. *Proceedings of the National Academy of Sciences of the United States of America*, 89(21), pp.10449–53. Available at: http://www.ncbi.nlm.nih.gov/pubmed/1438232%5Cnhttp://www.pubmedcentral.nih.gov/articlerender.fcgi?artid=PMC50356.

Hosokawa, N. et al., 2009. Nutrient-dependent mTORC1 Association with the ULK1 – Atg13 – FIP200 Complex Required for Autophagy. , 20(m), pp.1981–1991.

Hough, R., Pratt, G. & Rechsteiner, M., 1987. Purification of two high molecular weight proteases from rabbit reticulocyte lysate. *Journal of Biological Chemistry*, 262(17), pp.8303–8313.

Howland, D.S. et al., 2002. Focal loss of the glutamate transporter EAAT2 in a transgenic rat model of SOD1 mutant-mediated amyotrophic lateral sclerosis (ALS). *Proceedings of the National Academy of Sciences*, 99(3), pp.1604–1609. Available at: http://www.pnas.org/cgi/doi/10.1073/pnas.032539299.

Huang, E.J. et al., 2010. Extensive FUS-immunoreactive Pathology in Juvenile Amyotrophic Lateral Sclerosis with Basophilic Inclusions Eric. , 70(4), pp.646–656.

Ichimura, Y. et al., 2000. A ubiquitin-like system mediates protein lipidation. , 408(November).

Ignatius, S.O. et al., 1995. Cloning and Characterization of a Novel Cellular Protein, TDP-43, That Binds to Human Immunodeficiency Virus Type 1 TAR DNA Sequence Motifs. *J. Virol.*, 69(6), pp.3584–3596.

Iguchi, Y. et al., 2012. Oxidative stress induced by glutathione depletion reproduces pathological modifications of TDP-43 linked to TDP-43 proteinopathies. *Neurobiology of Disease*, 45(3), pp.862–870. Available at: http://dx.doi.org/10.1016/j.nbd.2011.12.002.

Ikeda, F. & Dikic, I., 2008. Atypical ubiquitin chains: new molecular signals. "Protein Modifications: Beyond the Usual Suspects" Review Series. *EMBO reports*, 9(6), pp.536–542. Available at: http://embor.embopress.org/cgi/doi/10.1038/embor.2008.93.

Ikeda, K. & Iwasaki, Y., 2015. Edaravone, a free radical scavenger, delayed symptomatic and pathological progression of motor neuron disease in the wobbler mouse. *PLoS ONE*, 10(10), pp.1–11.

Ikenaka, K. et al., 2012. Disruption of axonal transport in motor neuron diseases. *International Journal of Molecular Sciences*, 13(1), pp.1225–1238.

Ines Moreno-Gonzalez & soto, claudio, 2012. Potential for Disease Transmission. , 22(5), pp.482–487.

Inoki, K. et al., 2003. TSC2 Mediates Cellular Energy Response to Control Cell Growth and Survival. , 115, pp.577–590.

Inukai, Y. et al., 2008. Abnormal phosphorylation of Ser409/410 of TDP-43 in FTLD-U and ALS. *FEBS Letters*, 582(19), pp.2899–2904.

Itakura, E. et al., 2008. Beclin 1 Forms Two Distinct Phosphatidylinositol 3-Kinase Complexes with Mammalian Atg14 and UVRAG. , 19(December), pp.5360–5372.

Itakura, E. & Mizushima, N., 2010. Characterization of autophagosome formation site by a hierarchical analysis of mammalian Atg proteins. , 6(6), pp.764–776.

Itoh, H. et al., 2002. Mammalian HSP60 is quickly sorted into the mitochondria under conditions of dehydration. *European Journal of Biochemistry*, 269(23), pp.5931–5938.

Iwaki, T. et al., 1994. Sense and antisense modification of glial αB-crystallin production results in alterations of stress fiber formation and thermoresistance. *Journal of Cell Biology*, 125(6), pp.1385–1393.

Jankovic, J., 2008. Parkinson's disease: clinical features and diagnosis. *Journal of Neurology, Neurosurgery & Psychiatry*, 79(4), pp.368–376. Available at: http://jnnp.bmj.com/cgi/doi/10.1136/jnnp.2007.131045.

Janssen, C. et al., 2010. Differential Histone Deacetylase mRNA Expression Patterns in Amyotrophic Lateral Sclerosis. , 69(6), pp.573–581.

Jenster, G., Trapman, J. & Brinkmann, A.O., 1993. Nuclear import of the human androgen receptor. *The Biochemical journal*, 293 ( Pt 3, pp.761–8.

Jiang, F. & Doudna, J.A., 2015. The structural biology of CRISPR-Cas systems. *Current Opinion in Structural Biology*, 30, pp.100–111. Available at: http://dx.doi.org/10.1016/j.sbi.2015.02.002.

Jiang, Y. et al., 1999. Prevention of Constitutive TNF Receptor 1 Signaling by Silencer of Death Domains. , 283(January), pp.543–547.

Jin, L. et al., 2008. Mechanism of Ubiquitin-Chain Formation by the Human Anaphase-Promoting Complex. *Cell*, 133(4), pp.653–665.

Jinek, M. et al., 2012. A Programmable Dual-RNA – Guided. , 337(August), pp.816–822.

Johansen, T. & Lamark, T., 2011. Selective autophagy mediated by autophagic adapter proteins. *Autophagy*, 7(3), pp.279–296. Available at: http://www.ncbi.nlm.nih.gov/pubmed/21189453.

Johnson, J.O. et al., 2010. Exome sequencing reveals VCP mutations as a cause of familial ALS. *Neuron*, 68(5), pp.857–864. Available at: http://www.ncbi.nlm.nih.gov/pubmed/21145000.

Jordan, C.L., Price, R.H. & Handa, R.J., 2002. Androgen receptor messenger RNA and protein in adult rat sciatic nerve: Implications for site of androgen action. *Journal of Neuroscience Research*, 69(4), pp.509–518.

Jovicic, A. & Gitler, A.D., 2014. TDP-43 in ALS: Stay on Target...Almost There. *Neuron*, 81(3), pp.463–465.

Ju, J.S. & Weihl, C.C., 2010. p97/VCP at the intersection of the autophagy and the ubiquitin proteasome system. *Autophagy*, 6(2), pp.283–285.

Jung, C.H. et al., 2009. ULK-Atg13-FIP200 Complexes Mediate mTOR Signaling to the Autophagy Machinery. , 20, pp.1992–2003.

Jung, T., Catalgol, B. & Grune, T., 2009. The proteasomal system. *Molecular Aspects of Medicine*, 30(4), pp.191–296. Available at: http://dx.doi.org/10.1016/j.mam.2009.04.001.

Kalia, S.K. et al., 2004. BAG5 inhibits parkin and enhances dopaminergic neuron degeneration. *Neuron*, 44(6), pp.931–945.

Kampinga, H.H. et al., 2009. Guidelines for the nomenclature of the human heat shock proteins. *Cell Stress and Chaperones*, 14(1), pp.105–111.

Kampinga, H.H. & Bergink, S., 2016. Heat shock proteins as potential targets for protective strategies in neurodegeneration. *The Lancet Neurology*, 15(7), pp.748–759. Available at: http://dx.doi.org/10.1016/S1474-4422(16)00099-5.

Kampinga, H.H. & Craig, E.A., 2010. The HSP70 chaperone machinery: J proteins as drivers of functional specificity. *Nature Reviews Molecular Cell Biology*, 11(8), pp.579–592. Available at: http://www.nature.com/doifinder/10.1038/nrm2941.

Kanouchi, T., Ohkubo, T. & Yokota, T., 2012. Can regional spreading of amyotrophic lateral sclerosis motor symptoms be explained by prion-like propagation? *J Neurol Neurosurg Psychiatry*, 83(7), pp.739–745. Available at: http://www.ncbi.nlm.nih.gov/pubmed/22544947.

Katsuno, M. et al., 2006. Pathogenesis, animal models and therapeutics in Spinal and bulbar muscular atrophy (SBMA). *Experimental Neurology*, 200(1), pp.8–18.

Katsuno, M. et al., 2012. Pathogenesis and therapy of spinal and bulbar muscular atrophy (SBMA). *Progress in Neurobiology*, 99(3), pp.246–256. Available at: http://dx.doi.org/10.1016/j.pneurobio.2012.05.007.

Katsuno, M. et al., 2002. Testosterone reduction prevents phenotypic expression in a transgenic mouse model of spinal and bulbar muscular atrophy. *Neuron*, 35(5), pp.843–854.

Kaur, S.J., McKeown, S.R. & Rashid, S., 2016. Mutant SOD1 mediated pathogenesis of Amyotrophic Lateral Sclerosis. *Gene*, 577(2), pp.109–118. Available at: http://dx.doi.org/10.1016/j.gene.2015.11.049.

Kessler, H. et al., 2005. Dementia of frontal lobe type in Kennedy's disease. *Amyotrophic Lateral Sclerosis and Other Motor Neuron Disorders*, 6(SUPPL. 1), pp.250–253.

Kettern, N. et al., 2011. The Hsc/Hsp70 co-chaperone network controls antigen aggregation and presentation during maturation of professional antigen presenting cells. *PLoS ONE*, 6(1).

Kihara, A. et al., 2001. Two Distinct Vps34 Phosphatidylinositol 3 – Kinase Complexes Function in Autophagy and Carboxypeptidase Y Sorting in Saccharomyces cerevisiae. , 152(3).

Kim, H. et al., 2009. Targeted genome editing in human cells with zinc finger nucleases constructed via modular assembly. *Genome research*, pp.1279–1288. Available at: http://genome.cshlp.org/content/19/7/1279.short.

Kim, J. et al., 1999. Apg7p / Cvt2p Is Required for the Cytoplasm-to- Vacuole Targeting , Macroautophagy , and Peroxisome Degradation Pathways. , 10(May), pp.1337–1351.

Kim, K.K., Kim, R. & Kim, S.H., 1998. Crystal structure of a small heat-shock protein. *Nature*, 394(6693), pp.595–9. Available at: http://www.pubmedcentral.nih.gov/articlerender.fcgi?artid=3384710&tool=pmcentrez&rendertype=abstract.

King, I.N. et al., 2014. The RNA-binding protein TDP-43 selectively disrupts MicroRNA-1/206 incorporation into the RNA-induced silencing complex. *Journal of Biological Chemistry*, 289(20), pp.14263–14271.

Kirisako, T. et al., 1999. Formation Process of Autophagosome Is Traced with Apg8 / Aut7p in Yeast. , 147(2), pp.435–446.

Kirisako, T. et al., 2000. The Reversible Modification Regulates the Membrane-Binding State of Apg8 / Aut7 Essential for Autophagy and the Cytoplasm to Vacuole Targeting Pathway. , 151(2), pp.263–275.

Klionsky, D.J. et al., 2003. Letter to the Editor A Unified Nomenclature for Perhaps the most striking advantage of working with. , 5, pp.539–545.

Ko, H.S. et al., 2004. Ubiquilin interacts with ubiquitylated proteins and proteasome through its ubiquitin-associated and ubiquitin-like domains. *FEBS Lett*, 566(1–3), pp.110–114. Available at: http://www.ncbi.nlm.nih.gov/pubmed/15147878.

Köhler, A. et al., 2001. The axial channel of the proteasome core particle is gated by the Rpt2 ATPase and controls both substrate entry and product release. *Molecular Cell*, 7(6), pp.1143–1152.

Kong, J. & Xu, Z., 2000. Overexpression of neurofilament subunit NF-L and NF-H extends survival of a mouse model for amyotrophic lateral sclerosis. *Neuroscience Letters*, 281(1), pp.72–74.

Koppers, M. et al., 2012. VCP mutations in familial and sporadic amyotrophic lateral sclerosis. *Neurobiol Aging*, 33(4), p.837 e7-13. Available at: http://www.ncbi.nlm.nih.gov/pubmed/22078486.

Koval, E.D. et al., 2013. Method for widespread microRNA-155 inhibition prolongs survival in ALS-model mice. *Human Molecular Genetics*, 22(20), pp.4127–4135.

Kuhlenbäumer, G. et al., 2001. Thirty-seven CAG repeats in the androgen receptor gene in two healthy individuals. *Journal of Neurology*, 248(1), pp.23–26.

Lackie, R.E. et al., 2017. The Hsp70/Hsp90 chaperone machinery in neurodegenerative diseases. *Frontiers in Neuroscience*, 11(May), p.254. Available at: http://journal.frontiersin.org/article/10.3389/fnins.2017.00254/full.

Lagier-Tourenne, C. et al., 2013. Divergent roles of ALS-linked proteins FUS/TLS and TDP-43 intersect in processing long pre-mRNAs. , 15(11), pp.1488–1497.

Lambert, H. et al., 1999. CELL BIOLOGY AND METABOLISM : HSP27 Multimerization Mediated by Interactions at the Amino Terminus HSP27 Multimerization Mediated by Phosphorylation-sensitive Intermolecular Interactions at the Amino Terminus *. *The Journal of biological chemistry*, 274(14), pp.9378–9385.

Laufen, T. et al., 1999. Mechanism of regulation of Hsp70 chaperones by DnaJ cochaperones. *Proceedings of the National Academy of Sciences*, 96(10), pp.5452–5457. Available at: http://www.pnas.org/cgi/doi/10.1073/pnas.96.10.5452.

Lee, D.Y. & Brown, E.J., 2012. Ubiquilins in the crosstalk among proteolytic pathways. *Biological Chemistry*, 393(6), pp.441–447.

Lee, I.H. & Finkel, T., 2009. Regulation of Autophagy by the p300 Acetyltransferase * □ , 284(10), pp.6322–6328.

Li, M. et al., 2014. Mutations in the HFE gene and sporadic amyotrophic lateral sclerosis risk: a meta-analysis of observational studies. *Brazilian journal of medical and biological research = Revista brasileira de pesquisas médicas e biológicas / Sociedade Brasileira de Biofísica ... [et al.]*, 47(3), pp.215–22. Available at: http://www.pubmedcentral.nih.gov/articlerender.fcgi?artid=3982942&tool=pmcentrez&rendertype=abstract.

Li, W.W., Li, J. & Bao, J.K., 2012. Microautophagy: Lesser-known self-eating. *Cellular and Molecular Life Sciences*, 69(7), pp.1125–1136.

Li, Y.R. et al., 2013. Stress granules as crucibles of ALS pathogenesis. *Journal of Cell Biology*, 201(3), pp.361–372.

Liang, C. et al., 2006. Autophagic and tumour suppressor activity of a novel Beclin1-binding protein UVRAG. , 8(7).

Liang, C. et al., 2008. Beclin1-binding UVRAG targets the class C Vps complex to coordinate autophagosome maturation and endocytic trafficking. , 10(7).

Liang, X.H. et al., 1999. Induction of autophagy and inhibition of tumorigenesis by beclin 1. , 402(December), pp.1–5.

Liao, Q. et al., 2001. The anti-apoptotic protein (BAG)-3 is overexpressed in pancreatic cancer and induced by heat stress in pancreatic cancer cell lines. *FEBS Lett. 503*, 503, pp.151–157.

Lieberman, A.P. et al., 2014. Peripheral Androgen Receptor Gene Suppression Rescues Disease in Mouse Models of Spinal and Bulbar Muscular Atrophy. *Cell Reports*, 7(3), pp.774–784.

Lin, C.L.G. et al., 1998. Aberrant RNA processing in a neurodegenerative disease: The cause for absent EAAT2, a glutamate transporter, in amyotrophic lateral sclerosis. *Neuron*, 20(3), pp.589–602.

Lin, Y. et al., 2015. Formation and Maturation of Phase-Separated Liquid Droplets by RNA-Binding Proteins. *Molecular Cell*, 60(2), pp.208–219.

Lindquist, S., 2009. Protein folding sculpting evolutionary change. *Cold Spring Harbor Symposia on Quantitative Biology*, 74, pp.103–108.

Ling Song and Michael Rape, 2011. Regulated Degradation of Spindle Assembly Factors by the Anaphase-Promoting Complex. , 38(3), pp.369–382.

Link, C.D. et al., 2008. The alpha amyloid peptide can act as a modular aggregation domain. *Neurobiology of Disease*, 32(3), pp.420–425. Available at: http://dx.doi.org/10.1016/j.nbd.2008.08.003.

Liu-Yesucevitz, L. et al., 2014. ALS-Linked Mutations Enlarge TDP-43-Enriched Neuronal RNA Granules in the Dendritic Arbor. *Journal of Neuroscience*, 34(12), pp.4167–4174. Available at: http://www.jneurosci.org/cgi/doi/10.1523/JNEUROSCI.2350-13.2014.

Liu, C.W. et al., 2002. Conformational remodeling of proteasomal substrates by PA700, the 19 S regulatory complex of the 26 S proteasome. *Journal of Biological Chemistry*, 277(30), pp.26815–26820.

Liu, G.Z., Wang, H. & Wang, Z., 2003. Identification of a highly conserved domain in the androgen receptor that suppresses the DNA-binding domain-DNA interactions. *Journal of Biological Chemistry*, 278(17), pp.14956–14960.

Liu, J. et al., 2004. Toxicity of familial ALS-linked SOD1 mutants from selective recruitment to spinal mitochondria. *Neuron*, 43(1), pp.5–17. Available at: http://www.ncbi.nlm.nih.gov/pubmed/15233913.

Liu, X. et al., 2015. Chaperone-mediated autophagy and neurodegeneration: connections, mechanisms, and therapeutic implications. *Neuroscience Bulletin*, 31(4), pp.407–415.

Logroscino, G. et al., 2010. Incidence of amyotrophic lateral sclerosis in Europe. *Journal of Neurology, Neurosurgery & Psychiatry*, 81(4), pp.385–390. Available at: http://jnnp.bmj.com/cgi/doi/10.1136/jnnp.2009.183525.

Loidl, G. et al., 1999. Bivalency as a principle for proteasome inhibition. *Proceedings of the National Academy of Sciences of the United States of America*, 96(10), pp.5418–5422.

Luciani, F. et al., 2005. A Mathematical Model of Protein Degradation by the Proteasome. *Biophysical Journal*, 88(4), pp.2422–2432. Available at: http://linkinghub.elsevier.com/retrieve/pii/S0006349505732999.

Luders, J., Demand, J. & Hohfeld, J., 2000. The Ubiquitin-related BAG-1 Provides a Link between the Molecular Chaperones Hsc70 / Hsp70 and the Proteasome * . , 275(7), pp.4613–4617.

MacKenzie, I.R. et al., 2013. Dipeptide repeat protein pathology in C9ORF72 mutation cases: Clinico-pathological correlations. *Acta Neuropathologica*, 126(6), pp.859–879.

Mackenzie, I.R.A. et al., 2007. Pathological TDP-43 distinguishes sporadic amyotrophic lateral sclerosis from amyotrophic lateral sclerosis with SOD1 mutations. *Annals of Neurology*, 61(5), pp.427–434.

Mackenzie, I.R.A. et al., 2015. Quantitative analysis and clinico-pathological correlations of different dipeptide repeat protein pathologies in C9ORF72 mutation carriers. *Acta Neuropathologica*, 130(6), pp.845–861.

Mackenzie, I.R. & Rademakers, R., 2008. The role of transactive response DNA-binding protein-43 in amyotrophic lateral sclerosis and frontotemporal dementia. *Current Opinion in Neurology*, 21(6), pp.693–700. Available at: http://content.wkhealth.com/linkback/openurl?sid=WKPTLP:landingpage&an=00019052-200812000-00015.

Mackenzie, I.R., Rademakers, R. & Neumann, M., 2010. TDP-43 and FUS in amyotrophic lateral sclerosis and frontotemporal dementia. *Lancet Neurol*, 9(10), pp.995–1007. Available at: http://www.ncbi.nlm.nih.gov/pubmed/20864052.

Maekawa, S. et al., 2009. TDP-43 is consistently co-localized with ubiquitinated inclusions in sporadic and Guam amyotrophic lateral sclerosis but not in familial amyotrophic lateral sclerosis with and without SOD1 mutations. *Neuropathology*, 29(6), pp.672–683. Available at: http://www.ncbi.nlm.nih.gov/pubmed/19496940.

Majcher, V. et al., 2015a. Autophagy receptor defects and ALS-FTLD. *Molecular and Cellular Neuroscience*, 66(Part A), pp.43–52.

Majcher, V. et al., 2015b. Autophagy receptor defects and ALS-FTLD. *Molecular and Cellular Neuroscience*, 66(PA), pp.43–52.

Majounie, E. et al., 2012. Frequency of the C9orf72 hexanucleotide repeat expansion in patients with amyotrophic lateral sclerosis and frontotemporal dementia: A cross-sectional study. *The Lancet Neurology*, 11(4), pp.323–330. Available at: http://dx.doi.org/10.1016/S1474-4422(12)70043-1.

Mariotti, C. et al., 2000. Phenotypic manifestations associated with CAG-repeat expansion in the androgen receptor gene in male patients and heterozygous females: A clinical and molecular study of 30 families. *Neuromuscular Disorders*, 10(6), pp.391–397.

Maruyama, H. et al., 2010. Mutations of optineurin in amyotrophic lateral sclerosis. *Nature*, 465(7295), pp.223–226. Available at: http://www.nature.com/doifinder/10.1038/nature08971.

Masseret, E. et al., 2013. Dietary BMAA exposure in an amyotrophic lateral sclerosis cluster from southern France. *PLoS ONE*, 8(12), pp.1–9.

Mastrianni, J.A. & Roos, R.P., 2000. The prion diseases. *Seminars in neurology*, 20(3), pp.337–352.

Matias, P.M. et al., 2000. Structural evidence for ligand specificity in the binding domain of the human androgen receptor: Implications for pathogenic gene mutations. *Journal of Biological Chemistry*, 275(34), pp.26164–26171.

Matsumoto, A., 1997. Hormonally induced neuronal plasticity in the adult motoneurons. *Brain Research Bulletin*, 44(4), pp.539–547.

Mayer, M.P. & Bukau, B., 2005. Hsp70 chaperones: cellular functions and molecular mechanism. *Cell Mol Life Sci*, 62(6), pp.670–684. Available at: http://www.ncbi.nlm.nih.gov/pubmed/15770419.

McCarty, J.S. et al., 1995. The Role of ATP in the Functional Cycle of the DnaK Chaperone System. *Journal of Molecular Biology*, 249(1), pp.126–137. Available at: http://linkinghub.elsevier.com/retrieve/pii/S0022283685702847.

Mercer, C.A. et al., 2009. interacts with ULK1 and is essential for A novel , human Atg13 binding protein , Atg101 , interacts with ULK1 and is essential for macroautophagy. , 8627(October).

Merry, D.E., 2001. Molecular pathogenesis of spinal and bulbar muscular atrophy. *Brain Research Bulletin*, 56(3–4), pp.203–207.

Meyer, H. & Weihl, C.C., 2014. The VCP/p97 system at a glance: connecting cellular function to disease pathogenesis. *Journal of cell science*, 127(Pt 18), pp.3877–83. Available at: http://www.ncbi.nlm.nih.gov/pubmed/25146396.

Milioto, C. et al., 2017. Beta-agonist stimulation ameliorates the phenotype of spinal and bulbar muscular atrophy mice and patient-derived myotubes. *Scientific Reports*, 7(January), p.41046. Available at: http://www.nature.com/articles/srep41046.

Miller, R.G. et al., 2012. Riluzole for amyotrophic lateral sclerosis (ALS)/ motor neuron disease (MND). *Cochrane Database of Systematic Reviews*, 3(3), pp.191–206.

Minamiyama, M. et al., 2004. Sodium butyrate ameliorates phenotypic expression in a transgenic mouse model of spinal and bulbar muscular atrophy. *Human Molecular Genetics*, 13(11), pp.1183–1192.

Minoia, M. et al., 2014. BAG3 induces the sequestration of proteasomal clients into cytoplasmic puncta: Implications for a proteasome-to-autophagy switch. *Autophagy*, 10(9), pp.1603–1621.

Mioshi, E. et al., 2014. Neuropsychiatric changes precede classic motor symptoms in ALS and do not affect survival. *Neurology*, 82(2), pp.149–154.

Miyazaki, Y. et al., 2012. Viral delivery of miR-196a ameliorates the SBMA phenotype via the silencing of CELF2. *Nature Medicine*, 18(7), pp.1136–1141. Available at: http://www.nature.com/doifinder/10.1038/nm.2791.

Mizushima, N. et al., 1998. A protein conjugation system essential for autophagy. , 395(July), pp.395–398.

Mizushima, N., 2007. FIP200, a ULK-interacting protein, is required for autophagosome formation in mammalian cells. , 9, pp.497–510.

Mizushima, N. et al., 2004. In Vivo Analysis of Autophagy in Response to Nutrient Starvation Using Transgenic Mice Expressing a Fluorescent Autophagosome Marker. , 15(March), pp.1101–1111.

Mizushima, N. et al., 2003. Mouse Apg16L , a novel WD-repeat protein , targets to the autophagic isolation membrane with the Apg12- Apg5 conjugate.

Mizushima, N., 2010. The role of the Atg1/ULK1 complex in autophagy regulation. *Curr Opin Cell Biol*, 22(2), pp.132–139. Available at: http://www.ncbi.nlm.nih.gov/pubmed/20056399.

Mojica, F.J.M. et al., 2009. Short motif sequences determine the targets of the prokaryotic CRISPR defence system. *Microbiology*, 155(3), pp.733–740.

Molliex, A. et al., 2015. Phase Separation by Low Complexity Domains Promotes Stress Granule Assembly and Drives Pathological Fibrillization. *Cell*, 163(1), pp.123–133. Available at: http://dx.doi.org/10.1016/j.cell.2015.09.015.

Monastyrska, I. et al., 2010. Multiple roles of the cytoskeleton in autophagy. , 84(3), pp.431–448.

Mori, K. et al., 2013. The C9orf72 GGGGCC repeat is translated into aggregating dipeptide-repeat proteins in FTLD/ALS. *Science*, 339(6125), pp.1335–1338. Available at: http://www.ncbi.nlm.nih.gov/pubmed/23393093.

Morris, H.R. et al., 2012. Recent advances in the genetics of the ALS-FTLD complex. *Current Neurology and Neuroscience Reports*, 12(3), pp.243–250.

Mosser, D.D., Ho, S. & Glover, J.R., 2004. Saccharomyces cerevisiae Hsp104 enhances the chaperone capacity of human cells and inhibits heat stress-induced proapoptotic signaling. *Biochemistry*, 43(25), pp.8107–8115.

Naeve, G.S. et al., 1997. Neuritin: A gene induced by neural activity and neurotrophins that promotes neuritogenesis. *Neurobiology*, 94(March), pp.2648–2653.

NAGAI, Y. et al., 1999. Polyglutamine Domain Proteins with Expanded Repeats Bind Neurofilament, Altering the Neurofilament Network. *Annals of the New York Academy of Sciences*, 893(1 OXIDATIVE/ENE), pp.192–201. Available at: http://doi.wiley.com/10.1111/j.1749-6632.1999.tb07826.x.

Nandi, D. et al., 2006. The ubiquitin-proteasome system. *Journal of Biosciences*, 31(1), pp.137–155.

Nedelsky, N.B. et al., 2012. Native functions of the androgen receptor are essential to pathogenesis in a Drosophila model of spinobulbar muscular atrophy. , 67(6), pp.936–952.

Neumann, M. et al., 2010. Phosphorylation of S409/410 of TDP-43 is a consistent feature in all sporadic and familial forms of TDP-43 proteinopathies. , 117(2), pp.137–149.

Neumann, M. et al., 2006. Ubiquitinated TDP-43 in frontotemporal lobar degeneration and amyotrophic lateral sclerosis. *Science*, 314(5796), pp.130–133. Available at: http://www.ncbi.nlm.nih.gov/pubmed/17023659.

Neuschmid-Kaspar, F. et al., 1996. CAG-repeat expansion in androgen receptor in Kennedy's disease is not a loss of function mutation. *Molecular and Cellular Endocrinology*, 117(2), pp.149–156.

Noda, N.N. & Mizushima, N., 2016. Atg101 : Not Just an Accessory Subunit in the Autophagy-initiation Complex. , 20, pp.13–20.

Nolan, M., Talbot, K. & Ansorge, O., 2016. Pathogenesis of FUS-associated ALS and FTD: insights from rodent models. *Acta Neuropathologica Communications*, 4(1), p.99. Available at: http://actaneurocomms.biomedcentral.com/articles/10.1186/s40478-016-0358-8.

Nonaka, T. et al., 2013. Prion-like Properties of Pathological TDP-43 Aggregates from Diseased Brains. *Cell Reports*, 4(1), pp.124–134. Available at: http://dx.doi.org/10.1016/j.celrep.2013.06.007.

Novak, M.J.U. & Tabrizi, S.J., 2010. Huntington's disease. *Bmj*, 340(jun30 4), pp.c3109–c3109. Available at: http://www.bmj.com/cgi/doi/10.1136/bmj.c3109.

Oddo, S. et al., 2003. Triple-transgenic model of Alzheimer's Disease with plaques and tangles: Intracellular Aβ and synaptic dysfunction. *Neuron*, 39(3), pp.409–421.

Ohsumi, Y., 2013. Historical landmarks of autophagy research. *Nature Publishing Group*, 24(1), pp.9–23. Available at: http://dx.doi.org/10.1038/cr.2013.169.

Ohsumi, Y., 2001. MOLECULAR DISSECTION OF AUTOPHAGY : TWO UBIQUITIN-LIKE SYSTEMS. , 2(March), pp.1–6.

Olzscha, H. et al., 2011. Amyloid-like aggregates sequester numerous metastable proteins with essential cellular functions. *Cell*, 144(1), pp.67–78. Available at: http://dx.doi.org/10.1016/j.cell.2010.11.050.

Orr, C.R. et al., 2010. An interdomain interaction of the androgen receptor is required for its aggregation and toxicity in spinal and bulbar muscular atrophy. *Journal of Biological Chemistry*, 285(46), pp.35567–35577.

Osterloh, P. et al., 2006. Proteasomes shape the repertoire of T cells participating in antigen-specific immune responses. *Proceedings of the National Academy of Sciences of the United States of America*, 103(13), pp.5042–5047. Available at: http://www.pubmedcentral.nih.gov/articlerender.fcgi?artid=1458791&tool=pmcentrez&rendertype=abstract.

Pansarasa, O. et al., 2014. Amyotrophic lateral sclerosis and skeletal muscle: An update. *Molecular Neurobiology*, 49(2), pp.984–990.

Papadopoulos, C. et al., 2016. VCP/p97 cooperates with YOD1, UBXD1 and PLAA to drive clearance of ruptured lysosomes by autophagy. *The EMBO journal*, p.e201695148. Available at: http://emboj.embopress.org/content/early/2016/10/17/embj.201695148.abstract [Accessed October 25, 2016].

Parakh, S. & Atkin, J.D., 2016. Protein Folding Alterations in Amyotrophic Lateral Sclerosis. *Brain Research*, pp.1–17. Available at: http://linkinghub.elsevier.com/retrieve/pii/S0006899316302037.

Pardo, C.A. et al., 1995. Superoxide dismutase is an abundant component in cell bodies, dendrites, and axons of motor neurons and in a subset of other neurons. *Proceedings of the National Academy of Sciences*, 92(4), pp.954–958. Available at: http://www.pnas.org/cgi/doi/10.1073/pnas.92.4.954.

Parisi, C. et al., 2013. Dysregulated microRNAs in amyotrophic lateral sclerosis microglia modulate genes linked to neuroinflammation. *Cell Death and Disease*, 4(12), p.e959. Available at: http://www.nature.com/doifinder/10.1038/cddis.2013.491.

Park, K.H.J. & Vincent, I., 2009. Presymptomatic biochemical changes in hindlimb muscle of G93A human Cu/Zn superoxide dismutase 1 transgenic mouse model of amyotrophic lateral sclerosis. *Amyotrophic Lateral Sclerosis*, 1782, pp.462–468.

Parzych, K.R. & Klionsky, D.J., 2014. An Overview of Autophagy: Morphology, Mechanism, and Regulation. *Antioxidants & Redox Signaling*, 20(3), pp.460–473. Available at: http://online.liebertpub.com/doi/abs/10.1089/ars.2013.5371.

Pasinelli, P. et al., 2004. Amyotrophic lateral sclerosis-associated SOD1 mutant proteins bind and aggregate with Bcl-2 in spinal cord mitochondria. *Neuron*, 43(1), pp.19–30. Available at: http://www.ncbi.nlm.nih.gov/pubmed/15233914.

Patel, A. et al., 2015. A Liquid-to-Solid Phase Transition of the ALS Protein FUS Accelerated by Disease Mutation. *Cell*, 162(5), pp.1066–1077. Available at: http://dx.doi.org/10.1016/j.cell.2015.07.047.

Pearl, L.H. & Prodromou, C., 2006. Structure and Mechanism of the Hsp90 Molecular Chaperone Machinery. *Annual Review of Biochemistry*, 75(1), pp.271–294. Available at: http://www.annualreviews.org/doi/10.1146/annurev.biochem.75.103004.142738.

Perutz, M.F. et al., 2002. Amyloid fibers are water-filled nanotubes. *Proceedings of the National Academy of Sciences*, 99(8), pp.5591–5595. Available at: http://www.pnas.org/cgi/doi/10.1073/pnas.042681399.

Pesiridis, G.S., Lee, V.M.Y. & Trojanowski, J.Q., 2009. Mutations in TDP-43 link glycine-rich domain functions to amyotrophic lateral sclerosis. *Human Molecular Genetics*, 18(R2), pp.156–162.

Peters, O.M., Ghasemi, M. & Brown, R.H., 2015. Emerging mechanisms of molecular pathology in ALS. *Journal of Clinical Investigation*, 125(5), pp.1767–1779.

Picard, D., 2002. Heat-shock protein 90, a chaperone for folding and regulation. *Cellular and molecular life sciences : CMLS*, 59, pp.1640–1648.

Poletti, A., 2004. The polyglutamine tract of androgen receptor: From functions to dysfunctions in motor neurons. *Frontiers in Neuroendocrinology*, 25(1), pp.1–26.

Polymenidou, M. et al., 2011. Long pre-mRNA depletion and RNA missplicing contribute to neuronal vulnerability from loss of TDP-43. *Nat Neurosci*, 14(4), pp.459–468. Available at: http://www.ncbi.nlm.nih.gov/pubmed/21358643.

Polymenidou, M. & Cleveland, D.W., 2012. Prion-like spread of protein aggregates in neurodegeneration. *J Exp Med*, 209(5), pp.889–893. Available at: http://www.ncbi.nlm.nih.gov/pubmed/22566400.

Poukka, H. et al., 2000. Covalent modification of the androgen receptor by small ubiquitin-like modifier 1 (SUMO-1). *Proceedings of the National Academy of Sciences of the United States of America*, 97(26), pp.14145–14150.

Prasad, R., Shinichi, K. & Ng*, D.T.W., 1992. Characterization of the membrane binding and fusion events during nuclear envelope assembly using purified components. *Journal of Cell Biology*, 116(2), pp.295–306.

Prodromou, C. et al., 1997. Identification and structural characterization of the ATP/ADP-binding site in the Hsp90 molecular chaperone. *Cell*, 90(1), pp.65–75.

Prodromou, C. et al., 1999. Regulation of Hsp90 ATPase activity by tetratricopeptide repeat (TPR)-domain co-chaperones. *The EMBO Journal*, 18(3), pp.754–762. Available at: http://emboj.embopress.org/cgi/doi/10.1093/emboj/18.3.754.

Proudfoot, M. et al., 2014. Early dipeptide repeat pathology in a frontotemporal dementia kindred with C9ORF72 mutation and intellectual disability. *Acta Neuropathologica*, 127(3), pp.451–458.

Prusiner, S.B., 1998. Prions. *Proc Natl Acad Sci U S A*, 95(23), pp.13363–13383. Available at: http://www.ncbi.nlm.nih.gov/pubmed/9811807.

Puls, I. et al., 2003. Mutant dynactin in motor neuron disease. *Nat Genet*, 33(4), pp.455–456. Available at: http://www.ncbi.nlm.nih.gov/pubmed/12627231.

Querin, G. et al., 2016. Non-neural phenotype of spinal and bulbar muscular atrophy: results from a large cohort of Italian patients. *Journal of Neurology, Neurosurgery & Psychiatry*, 87(8), pp.810–816. Available at: http://jnnp.bmj.com/lookup/doi/10.1136/jnnp-2015-311305.

Querin, G., Sorarù, G. & Pradat, P.-F., 2017. Kennedy disease (X-linked recessive bulbospinal neuronopathy): A comprehensive review from pathophysiology to therapy. *Revue Neurologique*, pp.1–12. Available at: http://www.ncbi.nlm.nih.gov/pubmed/28473226.

Ran, F.A. et al., 2013. Double nicking by RNA-guided CRISPR Cas9 for enhanced genome editing specificity. *Cell*, 154(6), pp.1380–1389.

Ranford, J.C., Coates, a R. & Henderson, B., 2000. Chaperonins are cell-signalling proteins: the unfolding biology of molecular chaperones. *Expert reviews in molecular medicine*, 2(8), pp.1–17.

Ratner, H.K., Sampson, T.R. & Weiss, D.S., 2016. Overview of CRISPR–Cas9 Biology. *Cold Spring Harbor Protocols*, 2016(12), p.pdb.top088849. Available at: http://www.cshprotocols.org/lookup/doi/10.1101/pdb.top088849.

Ravikumar, B. et al., 2011. Plasma membrane contributes to the formation of pre- autophagosomal structures. , 12(8), pp.747–757.

Ravits, J.M. & La Spada, A.R., 2009. Als motor phenotype heterogeneity, focality, and spread: Deconstructing motor neuron degenerationsymbol. *Neurology*, 73(10), p.1.

Rea, S.L. et al., 2013. New insights into the role of sequestosome 1/p62 mutant proteins in the pathogenesis of paget's disease of bone. *Endocrine Reviews*, 34(4), pp.501–524.

Rea, S.L. et al., 2014. SQSTM1 mutations - Bridging Paget disease of bone and ALS/FTLD. *Experimental Cell Research*, 325(1), pp.27–37.

Reggiori, F. et al., 2004. The Atg1-Atg13 Complex Regulates Atg9 and Atg23 Retrieval Transport from the Pre-Autophagosomal Structure. , 6, pp.79–90.

Renton, A.E. et al., 2011. A hexanucleotide repeat expansion in C9ORF72 is the cause of chromosome 9p21-linked ALS-FTD. *Neuron*, 72(2), pp.257–268.

van Rheenen, W. et al., 2013. H63D polymorphism in HFE is not associated with amyotrophic lateral sclerosis. *Neurobiology of Aging*, 34(5), p.1517.e5-1517.e7. Available at: http://dx.doi.org/10.1016/j.neurobiolaging.2012.07.020.

Rippon, G.A. et al., 2006. An Observational Study of Cognitive Impairment in Amyotrophic Lateral Sclerosis. *Archives of Neurology*, 63(3), p.345. Available at: http://archneur.jamanetwork.com/article.aspx?doi=10.1001/archneur.63.3.345.

Robberecht, W. & Philips, T., 2013. The changing scene of amyotrophic lateral sclerosis. *Nat Rev Neurosci*, 14(4), pp.248–264. Available at: http://www.ncbi.nlm.nih.gov/pubmed/23463272.

Rodríguez-Navarro, J.A. et al., 2010. Trehalose ameliorates dopaminergic and tau pathology in parkin deleted/tau overexpressing mice through autophagy activation. *Neurobiology of Disease*, 39(3), pp.423–438. Available at: http://dx.doi.org/10.1016/j.nbd.2010.05.014.

Rosati, A. et al., 2007. Apoptosis inhibition in cancer cells: A novel molecular pathway that involves BAG3 protein. *The International Journal of Biochemistry & Cell Biology*, 39(7), pp.1337–1342.

Rosen, D.R. et al., 1993. Mutations in Cu/Zn superoxide dismutase gene are associated with familial amyotrophic lateral sclerosis. *Nature*, 362(6415), pp.59–62. Available at: http://www.ncbi.nlm.nih.gov/pubmed/8446170.

Rowinska-Zyrek, M., Salerno, M. & Kozlowski, H., 2015. Neurodegenerative diseases - Understanding their molecular bases and progress in the development of potential treatments. *Coordination Chemistry Reviews*, 284, pp.298–312. Available at: http://dx.doi.org/10.1016/j.ccr.2014.03.026.

Rüdiger, S. et al., 1997. Substrate specificity of the DnaK chaperone determined by screening cellulose-bound peptide libraries. *EMBO Journal*, 16(7), pp.1501–1507.

Rusmini, P. et al., 2011. 17-AAG increases autophagic removal of mutant androgen receptor in spinal and bulbar muscular atrophy. *Neurobiology of Disease*, 41(1), pp.83–95. Available at: http://dx.doi.org/10.1016/j.nbd.2010.08.023.

Rusmini, P. et al., 2015. Aberrant Autophagic Response in The Muscle of A Knock-in Mouse Model of Spinal and Bulbar Muscular Atrophy. *Scientific reports*, 5(October), p.15174. Available at: http://www.pubmedcentral.nih.gov/articlerender.fcgi?artid=4614888&tool=pmcentrez&rendertype=abstract.

Rusmini, P. et al., 2013. Clearance of the mutant androgen receptor in motoneuronal models of spinal and bulbar muscular atrophy. *Neurobiol Aging*, 34(11), pp.2585–2603. Available at: http://www.ncbi.nlm.nih.gov/pubmed/23810450.

Rusmini, P. et al., 2013. Clearance of the mutant androgen receptor in motoneuronal models of spinal and bulbar muscular atrophy. *Neurobiology of Aging*, 34(11), pp.2585–2603. Available at: http://dx.doi.org/10.1016/j.neurobiolaging.2013.05.026.

Rusmini, P. et al., 2016. The Role of the Protein Quality Control System in SBMA. *Journal of Molecular Neuroscience*, 58(3), pp.348–364.

Rutherford, N.J. et al., 2008. Novel mutations in TARDBP (TDP-43) in patients with familial amyotrophic lateral sclerosis. *PLoS Genet*, 4(9), p.e1000193. Available at: http://www.ncbi.nlm.nih.gov/pubmed/18802454.

Sau, D. et al., 2007. Mutation of SOD1 in ALS: a gain of a loss of function. *Hum Mol Genet*, 16(13), pp.1604–1618. Available at: http://www.ncbi.nlm.nih.gov/pubmed/17504823.

Schmitz, A. & Herzog, V., 2004. Endoplasmic reticulum-associated degradation : exceptions to the rule. , 83, pp.501–509.

Scotter, E.L., Chen, H.J. & Shaw, C.E., 2015. TDP-43 Proteinopathy and ALS: Insights into Disease Mechanisms and Therapeutic Targets. *Neurotherapeutics*, 12(2), pp.352–363.

Shaid, S. et al., 2013. Ubiquitination and selective autophagy. *Cell Death and Differentiation*, 20(1), pp.21–30. Available at: http://www.nature.com/doifinder/10.1038/cdd.2012.72.

Sharma, S. et al., 2017. αB-crystallin is a sensor for assembly intermediates and for the subunit topology of desmin intermediate filaments. *Cell Stress and Chaperones*, 22(4), pp.613–626.

Shaw, B.F. & Valentine, J.S., 2007. How do ALS-associated mutations in superoxide dismutase 1 promote aggregation of the protein? *Trends in Biochemical Sciences*, 32(2), pp.78–85.

Shefner, J. et al., 1999. Mice lacking cytosolic copper/zinc superoxide dismutase display a distinctive motor axonopathy. *Neurology*.

Sheikh, S. et al., 2013. Neurodegenerative Diseases: Multifactorial Conformational Diseases and Their Therapeutic Interventions. *Journal of Neurodegenerative Diseases*, 2013, pp.1–8. Available at: http://www.hindawi.com/journals/jnd/2013/563481/.

Shelkovnikova, T.A. et al., 2013. Recruitment into stress granules prevents irreversible aggregation of FUS protein mislocalized to the cytoplasm. *Cell Cycle*, 12(19), pp.3194–3202.

Sherman, M.Y. & Gabai, V.L., 2015. Hsp70 in cancer: back to the future. *Oncogene*, 34(32), pp.4153–4161. Available at: http://www.nature.com/doifinder/10.1038/onc.2014.349.

Shintani, T. et al., 1999. Apg10p , a novel protein-conjugating enzyme essential for autophagy in yeast. , 18(19), pp.5234–5241.

Simeoni, S., 2000. Motoneuronal cell death is not correlated with aggregate formation of androgen receptors containing an elongated polyglutamine tract. *Human Molecular Genetics*, 9(1), pp.133–144. Available at: http://hmg.oxfordjournals.org/content/9/1/133.long.

Smith, R.A. et al., 2006. Antisense oligonucleotide therapy for neurodegenerative disease 12. *Journal of Clinical Investigation*, 116(8), pp.2290–2296.

Sondermann, H., 2001. Structure of a Bag/Hsc70 Complex: Convergent Functional Evolution of Hsp70 Nucleotide Exchange Factors. *Science*, 291(5508), pp.1553–1557. Available at: http://www.sciencemag.org/cgi/doi/10.1126/science.1057268.

Song, L., Craney, A. & Rape, M., 2014. Microtubule-Dependent Regulation of Mitotic Protein Degradation. *Molecular Cell*, 53(2), pp.179–192.

Soo, K.Y. et al., 2015a. Rab1-dependent ER–Golgi transport dysfunction is a common pathogenic mechanism in SOD1, TDP-43 and FUS-associated ALS. *Acta Neuropathologica*, 130(5), pp.679–697.

Soo, K.Y. et al., 2015b. Rab1-dependent ER???Golgi transport dysfunction is a common pathogenic mechanism in SOD1, TDP-43 and FUS-associated ALS. *Acta Neuropathologica*, 130(5), pp.679–697.

Soo, K.Y. & Atkin, J.D., 2015. Autophagy dysregulation by mutant fused in sarcoma--implications for amyotrophic lateral sclerosis. *Cell Death Dis*, 6, p.e1945. Available at: http://www.ncbi.nlm.nih.gov/pubmed/26512956.

Sooyeon, Lee; Sato, Y. & Ralph, N., 2013. Lysosomal proteolysis inhibition selectively disrupts axonal transport of degradative organelles and causes an Alzheimer's- like axonal dystrophy. , 70(4), pp.646–656.

Soto, C., 2001. Protein misfolding and disease; protein refolding and therapy. *FEBS letters*, 498(2–3), pp.204–207.

Soto, C., 2003. Unfolding the role of protein misfolding in neurodegenerative diseases. *Nature Reviews Neuroscience*, 4(1), pp.49–60. Available at: http://www.nature.com/doifinder/10.1038/nrn1007.

Soto, C., Estrada, L. & Castilla, J., 2006. Amyloids, prions and the inherent infectious nature of misfolded protein aggregates. *Trends in Biochemical Sciences*, 31(3), pp.150–155.

Soto, C. & Estrada, L.D., 2008. Protein Misfolding and Neurodegeneration. *Archives of Neurology*, 65(2), pp.184–189. Available at: http://archneur.jamanetwork.com/article.aspx?doi=10.1001/archneurol.2007.56.

La Spada AR et al., 1991. Androgen receptor gene mutations in X-linked spinal and bulbar muscular atrophy. *Letters to Nature*, 353, pp.737–740.

Spence, J.J. et al., 1995. A ubiquitin mutant with specific defects in DNA repair and multiubiquitination. *Molecular and cellular biology*, 15(3), pp.1265–1273. Available at: http://mcb.asm.org/content/15/3/1265.long%5Cnpapers3://publication/uuid/CA0CA8E8-5387-4746-A311-017BE4C6C726%5Cnhttp://eutils.ncbi.nlm.nih.gov/entrez/eutils/elink.fcgi?dbfrom=pubmed&id=7862120&retmode=ref&cmd=prlinks%5Cnpapers3://publication/uuid/02E2EA3D-B1FC-.

Spies, T., Bresnahan, M. & Strominger, J.L., 1989. Human major histocompatibility complex contains a minimum of 19 genes between the complement cluster and HLA-B. *Proceedings of the National Academy of Sciences of the United States of America*, 86(22), pp.8955–8. Available at: http://www.pubmedcentral.nih.gov/articlerender.fcgi?artid=298409&tool=pmcentrez&rendertype=abstract.

Spillantini, M.G. et al., 1998. alpha-Synuclein in filamentous inclusions of Lewy bodies from Parkinson's disease and dementia with lewy bodies. *Proceedings of the National Academy of Sciences of the United States of America*, 95(11), pp.6469–73. Available at: http://www.pubmedcentral.nih.gov/articlerender.fcgi?artid=27806&tool=pmcentrez&rendertype=abstract.

Sreedharan, J. et al., 2008. TDP-43 mutations in familial and sporadic amyotrophic lateral sclerosis. *Science*, 319(5870), pp.1668–1672. Available at: http://www.ncbi.nlm.nih.gov/pubmed/18309045.

Stenoien, D.L. et al., 1999. Polyglutamine-expanded androgen receptors form aggregates that sequester heat shock proteins, proteasome components and SRC-1, and are suppressed by the HDJ-2 chaperone. *Human molecular genetics*, 8(5), pp.731–741.

Stephan, J.S. et al., 2010. The Tor and cAMP-dependent protein kinase signaling pathways coordinately control autophagy in Saccharomyces cerevisiae. , 8627(October 2017).

Strong, M.J. & Yang, W., 2011. The frontotemporal syndromes of ALS. Clinicopathological correlates. *Journal of Molecular Neuroscience*, 45(3), pp.648–655.

Sun, Y., 2003. Targeting E3 ubiquitin ligases for cancer therapy. *Cancer Biology and Therapy*, 2(6), pp.623–629.

Sundaramoorthy, V., Sultana, J.M. & Atkin, J.D., 2015. Golgi fragmentation in amyotrophic lateral sclerosis, an overview of possible triggers and consequences. *Frontiers in Neuroscience*, 9(OCT), pp.1–11.

Sweeney, P. et al., 2017. Protein misfolding in neurodegenerative diseases: implications and strategies. *Translational Neurodegeneration*, 6(1), p.6. Available at: http://translationalneurodegeneration.biomedcentral.com/articles/10.1186/s40035-017-0077-5.

Swinnen, B. & Robberecht, W., 2014. The phenotypic variability of amyotrophic lateral sclerosis. *Nature Reviews Neurology*, 10(11), pp.661–670. Available at: http://dx.doi.org/10.1038/nrneurol.2014.184%255Cnpapers2://publication/doi/10.1038/nrneurol.2014.184.

Szabo, A. et al., 1994. The ATP hydrolysis-dependent reaction cycle of the Escherichia coli Hsp70 system DnaK, DnaJ, and GrpE. *Proceedings of the National Academy of Sciences*, 91(22), pp.10345–10349. Available at: http://www.pnas.org/cgi/doi/10.1073/pnas.91.22.10345.

Taipale, M., Jarosz, D.F. & Lindquist, S., 2010. HSP90 at the hub of protein homeostasis: emerging mechanistic insights. *Nature Reviews Molecular Cell Biology*, 11(7), pp.515–528. Available at: http://www.nature.com/doifinder/10.1038/nrm2918.

Takayama, S. et al., 1997. BAG-1 modulates the chaperone activity of Hsp70 / Hsc70. *EMBO Journal*, 16(16), pp.4887–4896.

Takayama, S., Xie, Z. & Reed, J.C., 1999. An evolutionarily conserved family of Hsp70/Hsc70 molecular chaperone regulators. *Journal of Biological Chemistry*, 274(2), pp.781–786.

Takeshige, K. et al., 1992. Autophagy in Yeast Demonstrated with Proteinase-deficient Mutants and Conditions for its Induction. , 119(2), pp.3–8.

Takeuchi, J. & Toh-e, A., 2001. Genetic dissection of the yeast 26S proteasome: Cell cycle defects caused by the ??rpn mutation. *Biochimie*, 83(3–4), pp.333–340.

Tan, A.Y. et al., 2012. TLS/FUS (translocated in liposarcoma/fused in sarcoma) regulates target gene transcription via single-stranded DNA response elements. *Proceedings of the National Academy of Sciences of the United States of America*, 109(16), pp.6030–6035.

Tanaka, K., 2009. The proteasome: overview of structure and functions. *Proceedings of the Japan Academy. Series B, Physical and biological sciences*, 85(1), pp.12–36. Available at: http://www.pubmedcentral.nih.gov/articlerender.fcgi?artid=3524306&tool=pmcentrez&rendertype=abstract.

Tanaka, K. & Matsuda, N., 2014. Proteostasis and neurodegeneration: The roles of proteasomal degradation and autophagy. *Biochimica et Biophysica Acta - Molecular Cell Research*, 1843(1), pp.197–204. Available at: http://dx.doi.org/10.1016/j.bbamcr.2013.03.012.

Tateno, M. et al., 2009. Mutant SOD1 impairs axonal transport of choline acetyltransferase and acetylcholine release by sequestering KAP3. *Human Molecular Genetics*, 18(5), pp.942–955.

Taylor, J.P., Brown, R.H. & Cleveland, D.W., 2016. Decoding ALS: from genes to mechanism. *Nature*, 539(7628), pp.197–206. Available at: http://www.nature.com/doifinder/10.1038/nature20413.

Taylor, J.P., Hardy, J. & Fischbeck, K.H., 2002. Toxic Proteins in Neurodegenerative Disease. *Source: Science, New Series*, 296(5575), pp.1991–1995. Available at: http://www.jstor.org/stable/3076994%255Cnhttp://www.jstor.org/stable/3076994?seq=1&cid=pdf-reference#references_tab_contents%255Cnhttp://about.jstor.org/terms.

Thress, K. et al., 1998. Scythe: A novel reaper-binding apoptotic regulator. *EMBO Journal*, 17(21), pp.6135–6143.

Thrower, J.S. et al., 2000. Recognition of the polyubiquitin proteolytic signal. *EMBO J*, 19(1), pp.94–102. Available at: http://www.ncbi.nlm.nih.gov/pubmed/10619848.

Todd, T.W. & Petrucelli, L., 2016. Insights into the pathogenic mechanisms of Chromosome 9 open reading frame 72 (C9orf72) repeat expansions. *Journal of Neurochemistry*, p.n/a-n/a. Available at: http://dx.doi.org/10.1111/jnc.13623.

Tokui, K. et al., 2009. 17-DMAG ameliorates polyglutamine-mediated motor neuron degeneration through well-preserved proteasome function in an SBMA model mouse. *Human Molecular Genetics*, 18(5), pp.898–910.

Tooze, S.A. & Dikic, I., 2016. Autophagy Captures the Nobel Prize. *Cell*, 167(6), pp.1433–1435.

Tremolizzo, L. et al., 2014. Whole-blood global DNA methylation is increased in amyotrophic lateral sclerosis independently of age of onset. *Amyotrophic Lateral Sclerosis and Frontotemporal Degeneration*, 15(1–2), pp.98–105. Available at: http://www.tandfonline.com/doi/full/10.3109/21678421.2013.851247.

Trojsi, F., Monsurrò, M.R. & Tedeschi, G., 2013. Exposure to environmental toxicants and pathogenesis of amyotrophic lateral sclerosis: State of the art and research perspectives. *International Journal of Molecular Sciences*, 14(8), pp.15286–15311.

Tsay, H.J. & Schmidt, J., 1989. Skeletal muscle denervation activates acetylcholine receptor genes. *Journal of Cell Biology*, 108(4), pp.1523–1526.

Turner, B.J. & Talbot, K., 2008. Transgenics, toxicity and therapeutics in rodent models of mutant SOD1-mediated familial ALS. *Progress in Neurobiology*, 85(1), pp.94–134.

Tutar, L. & Tutar, Y., 2010. Heat Shock Proteins: An Overview. *Current Pharmaceutical Biotechnology*, 11(2), pp.216–222. Available at: http://www.eurekaselect.com/openurl/content.php?genre=article&issn=1389-2010&volume=11&issue=2&spage=216.

Upadhya, S.C. & Hegde, A.N., 2007. Role of the ubiquitin proteasome system in Alzheimer's disease. *BMC Biochemistry*, 8(Suppl 1), p.S12. Available at: http://www.biomedcentral.com/1471-2091/8/S1/S12.

Valentine, J.S. & Hart, P.J., 2003. Misfolded CuZnSOD and amyotrophic lateral sclerosis. *Proceedings of the National Academy of Sciences of the United States of America*, 100(7), pp.3617–3622.

Valle, C. et al., 2014. Tissue-specific deregulation of selected HDACs characterizes ALS progression in mouse models: pharmacological characterization of SIRT1 and SIRT2 pathways. *Cell Death and Disease*, 5(6), p.e1296. Available at: http://www.nature.com/doifinder/10.1038/cddis.2014.247.

Vance, C. et al., 2009. Mutations in FUS, an RNA processing protein, cause familial amyotrophic lateral sclerosis type 6. *Science*, 323(5918), pp.1208–1211. Available at: http://www.ncbi.nlm.nih.gov/pubmed/19251628.

Vega, A. & Bell, A., 1967. α-Amino-β-methylaminopropionic acid, a new amino acid from seeds of Cycas circinalis. *Phytochemistry*, 6(5), pp.759–762.

Verhoef, L.G.G.C. et al., 2002. Aggregate formation inhibits proteasomal degradation of polyglutamine proteins. *Human molecular genetics*, 11(22), pp.2689–2700. Available at: http://www.hmg.oupjournals.org/cgi/doi/10.1093/hmg/11.22.2689.

Vinceti, M. et al., 2010. The relation between amyotrophic lateral sclerosis and inorganic selenium in drinking water: a population-based case-control study. *Environmental Health*, 9(1), p.77. Available at: http://www.ehjournal.net/content/9/1/77%5Cnpapers://dc5b7a66-c191-4125-90d3-2536c98d4438/Paper/p10380.

Waibel, S. et al., 2004. Rasagiline alone and in combination with riluzole prolongs survival in an ALS mouse model. *Journal of Neurology*, 251(9), pp.1080–1084.

Walcott, J.L. & Merry, D.E., 2002. Ligand promotes intranuclear inclusions in a novel cell model of spinal and bulbar muscular atrophy. *Journal of Biological Chemistry*, 277(52), pp.50855–50859.

Walker, F.O., 2007. Huntington's disease. *Lancet*, 369(9557), pp.218–228.

Walker, M., Kublin, J.G. & Zunt, J.R., 2009. The Crystal Structures of the Eukaryotic Chaperonin CCT Reveal Its Functional Partitioning. , 42(1), pp.115–125.

Wang, W. et al., 2017. Response and Repair in Neurons. , 16(10), pp.1383–1391.

Watanabe, M. et al., 2001. Histological evidence of protein aggregation in mutant SOD1 transgenic mice and in amyotrophic lateral sclerosis neural tissues. *Neurobiol Dis*, 8(6), pp.933–941. Available at: http://www.ncbi.nlm.nih.gov/pubmed/11741389.

Watts, G.D. et al., 2004. Inclusion body myopathy associated with Paget disease of bone and frontotemporal dementia is caused by mutant valosin-containing protein. *Nat Genet*, 36(4), pp.377–381. Available at: http://www.ncbi.nlm.nih.gov/pubmed/15034582.

Weidberg, H. et al., 2010. LC3 and GATE-16 / GABARAP subfamilies are both essential yet act differently in autophagosome biogenesis. *The EMBO Journal*, 29(11), pp.1792–1802. Available at: http://dx.doi.org/10.1038/emboj.2010.74.

Whitesell, L. & Lindquist, S.L., 2005. HSP90 and the chaperoning of cancer. *Nature Reviews Cancer*, 5(10), pp.761–772. Available at: http://www.nature.com/doifinder/10.1038/nrc1716.

Wiles, M. V. et al., 2015. CRISPR/Cas9-mediated genome editing and guide RNA design. *Mammalian Genome*, 26(9–10), pp.501–510.

Wilkinson, K.D., Urban, M.K. & Haas, A.L., 1980. Ubiquitin is the ATP-dependent proteolysis factor I of rabbit reticulocytes. *Journal of Biological Chemistry*, 255(16), pp.7529–7532.

Williams, A.H. et al., 2009a. MicroRNA-206 Delays ALS Progression and Promotes Regeneration of Neuromuscular Synapses in Mice. , 326(5959), pp.1549–1554.

Williams, A.H. et al., 2009b. Neuromuscular Synapses in Mice. *Science*, 358(December), pp.1549–1554.

Williams, K.L. et al., 2012. UBQLN2/ubiquilin 2 mutation and pathology in familial amyotrophic lateral sclerosis. *Neurobiology of Aging*, 33(10), p.2527.e3-2527.e10. Available at: http://dx.doi.org/10.1016/j.neurobiolaging.2012.05.008.

Williamson, T.L. & Cleveland, D.W., 1999. Slowing of axonal transport is a very early event in the toxicity of ALS-linked SOD1 mutants to motor neurons. *Nature neuroscience*, 2(1), pp.50–56.

Wilis, A.M. et al., 2009. A large-scale international meta-analysis of paraoxonase gene polymorphisms in sporadic ALS. *Neurology*, 73(1), pp.16–24.

Winton, M.J. et al., 2008. Disturbance of nuclear and cytoplasmic TAR DNA-binding protein (TDP-43) induces disease-like redistribution, sequestration, and aggregate formation. *Journal of Biological Chemistry*, 283(19), pp.13302–13309.

Wong, C.I. et al., 1993. Steroid requirement for androgen receptor dimerization and DNA binding: Modulation by intramolecular interactions between the NH2-terminal and steroid-binding domains. *Journal of Biological Chemistry*, 268(25), pp.19004–19012.

Wong, M. & Martin, L.J., 2010. Skeletal muscle-restricted expression of human SOD1 causes motor neuron degeneration in transgenic mice. *Human Molecular Genetics*, 19(11), pp.2284–2302.

Wu, C.H. et al., 2012. Mutations in the profilin 1 gene cause familial amyotrophic lateral sclerosis. *Nature*, 488(7412), pp.499–503. Available at: http://www.ncbi.nlm.nih.gov/pubmed/22801503.

Xiao, S., McLean, J. & Robertson, J., 2006. Neuronal intermediate filaments and ALS: A new look at an old question. *Biochimica et Biophysica Acta - Molecular Basis of Disease*, 1762(11–12), pp.1001–1012.

Xu, Z., 2012. Does a loss of TDP-43 function cause neurodegeneration? *Molecular Neurodegeneration*, 7(1), p.27. Available at: ???

Yamashita, S. et al., 2014. Concomitant accumulation of ??-synuclein and TDP-43 in a patient with corticobasal degeneration. *Journal of Neurology*, 261(11), pp.2209–2217.

Yang, Z. et al., 2007. ASC-J9 ameliorates spinal and bulbar muscular atrophy phenotype via degradation of androgen receptor. *Nature medicine*, 13(3), pp.348–353.

Yau, R. & Rape, M., 2016. The increasing complexity of the ubiquitin code. *Nature Cell Biology*, 18(6), pp.579–586. Available at: http://www.nature.com/doifinder/10.1038/ncb3358.

Yerbury, J.J. et al., 2016. Walking the tightrope: Proteostasis and neurodegenerative disease. *Journal of Neurochemistry*.

Young, J.C., Barral, J.M. & Hartl, F.U., 2003. More than folding: Localized functions of cytosolic chaperones. *Trends in Biochemical Sciences*, 28(10), pp.541–547.

Yu, W., 1989. Administration of testosterone attenuates neuronal loss following axotomy in the brain-stem motor nuclei of female rats. *J. Neurosci.*, 9(11), pp.3908–3914. Available at: http://www.jneurosci.org/content/9/11/3908.short.

Yuan, A. et al., 2006. -Internexin Is Structurally and Functionally Associated with the Neurofilament Triplet Proteins in the Mature CNS. *Journal of Neuroscience*, 26(39), pp.10006–10019. Available at: http://www.jneurosci.org/cgi/doi/10.1523/JNEUROSCI.2580-06.2006.

Zhang, X. et al., 2011. Rapamycin treatment augments motor neuron degeneration in SOD1 G93A mouse model of amyotrophic lateral sclerosis. *Autophagy*, 7(4), pp.412–425.

Zhang, Y.-J. et al., 2009. Aberrant cleavage of TDP-43 enhances aggregation and cellular toxicity. *Pnas*, 106(18), pp.7607–7612.

Zhang, Y.-J. et al., 2007. Progranulin Mediates Caspase-Dependent Cleavage of TAR DNA Binding Protein-43. *Journal of Neuroscience*, 27(39), pp.10530–10534. Available at: http://www.jneurosci.org/cgi/doi/10.1523/JNEUROSCI.3421-07.2007.

Zhao, W., Beersù, D.R. & Appel, S.H., 2009. Immune-mediated Mechanisms in the Pathoprogression of Amyotrophic Lateral Sclerosis Weihua. , 42(1), pp.115–125.

Zhifen, Y. & Klionsky, D.J., 2010. *An Overview of the Molecular Mechanism of Autophagy Zhifen*,

Zu, T. et al., 2010. Non-ATG – initiated translation directed by microsatellite expansions. *Pnas*, 108(1), pp.260–265.

Zuehlke, A. & Johnson, J.L., 2011. Proteins. *Molecular Biology*, 93(3), pp.211–217.

Zufiría, M. et al., 2016. ALS: A bucket of genes, environment, metabolism and unknown ingredients. *Progress in Neurobiology*, 142, pp.104–129.